UNIVERSITAT POLITÈCNICA DE CATALUNYA

Ph.D. Program:

AUTOMATIC CONTROL, ROBOTICS AND COMPUTER VISION

Ph.D. Thesis

Solving Robotic Kinematic Problems: Singularities and Inverse Kinematics

Isiah Zaplana Agut

Thesis Advisor: Luis Basañez Villaluenga

November 2017

Solving Robotic Kinematic Problems: Singularities and Inverse Kinematics

Submitted in partial fulfillment of the requirements for the degree of Ph.D. in

Automatic Control, Robotics and Computer Vision

Supervised by

Luis Basañez Villaluenga

Institut d'Organització i Control de Sistemes Industrials

Universitat Politècnica de Catalunya

November 2017

A mi familia de Cartagena,
Barcelona y, especialmente,
a mi padre,
que no llegó a ver el final

There's a Road
Calling you to stray.
Step by step
Pulling you away.

Under Moon and Star
Take the Road
No matter how far.

Where it leads
No-one ever knows
Don't look back
Follow where it goes.
Far beyond the Sun
Take the Road
Wherever it runs.

The Road goes on
Ever ever on
Hill by hill
Mile by mile
Field by field
Stile by stile.
The Road goes on
Ever ever on

The Road goes on
Adapted from
the work of *J.R.R. Tolkien*

Acknowledgements/Agradecimientos

Me gustaría agradecer a la Agencia Estatal de Investigación del Ministerio de Economía y Competitividad (MINECO) por la beca predoctoral *Formación de personal investigador (FPI)* con referencia *BES-2012-059884* que me fue concedida y sin la cual hubiera sido imposible haber realizado el doctorado y por la beca *Ayudas a la movilidad predoctoral para la realización de estancias breves en centros de I+D 2016* con referencia *EEBB-I-17-12281* con la que pude estar tres meses en el *Signal Processing and Communications Laboratory (SigProC)* de la Universidad de Cambridge. También agradecer a los proyectos de la *Comisión Interministerial de Ciencia y Tecnología (CICYT)* DPI2011-22471, DPI2013-40882-P, DPI2014-57757-R y DPI2016-80077-R dentro de los cuales se elaboraron los resultados contenidos en esta memoria.

Me gustaría comenzar dando las gracias al profesor Luis Basañez. Él fue quien me dio la oportunidad de hacer el doctorado en su grupo de investigación y ha sabido, con infinita paciencia, dirigirme en la buena dirección durante estos cuatro años. También quiero agradecerle que me diera la libertad para elegir los temas en los que centrar mi investigación, y que, aunque a veces estos se alejaban un poco de la temática del grupo, siempre estuviera allí para darme oportunos comentarios sobre como enfocar los distintos problemas que iban surgiendo. Finalmente, me gustaría agradecerle todo aquello que me enseñó y que no tiene relación directa con la robótica: cómo ser preciso al redactar un artículo, cómo realizar transparencias y exposiciones que capten la atención del público, etc.

A Jan Rosell, por permitirme introducirme de nuevo en el mundo de la docencia (que siempre me ha apasionado) y por compartir mi entusiasmo por la innovación docente, implicándose al cien por cien desde el primer momento cuando surgió la idea de introducir una nueva metodología docente en la asignatura que compartíamos. Me gustaría agradecerle también que haya hecho de oyente paciente, consejero y personal coach en mis momentos de frustración a lo largo de esta etapa.

A Raúl Suárez, al que agradezco que siempre esté allí para hablar de cualquier cosa. Su disponibilidad en los momentos de apuros, sobretodo para echar una mano en temas relacionados con la gestión ha sido siempre decisiva para hacer las cosas bien. Su experiencia en el mundo universitario me ha ayudado en no pocas ocasiones.

A Carlos Alberto Lopez Franco, por venir al IOC a darnos una charla sobre las aplicaciones del

álgebra geométrica a diversos campos de la ingeniería, entre ellos la robótica, que permitió abrir una nueva línea de investigación que ha sido a partes iguales fascinante y fructífera.

A Leo y su familia, por ayudarme a sobrevivir los primeros días en Barcelona, por ayudarme cuando mi padre enfermó (tanto a nivel práctico como a nivel emocional) y por escucharme siempre con paciencia infinita las mil peticiones que le he hecho en estos cuatro años.

A mis compañeros del IOC: Abiud, Ali, Andres, Diab, Fernando, GM, Henry, Jose, Josep, Nestor y Orestes, y a los que pasaron por el IOC: Alex, Carlos A., Carlos R., Marcos, Niliana, Noe y Shiva. Gracias por las conversaciones a la hora de comer, por las risas, por hablar de futbol, cine, series y de casi cualquier cosa que uno pueda imaginar. To my officemates, I would like to thank their patience, understanding and help during these four years.

To Joan Lasenby, who gave me the opportunity of collaborating with her and kindly invited me to the Engineering Department of Cambridge University for three months. She introduced me to the beauty world of geometric algebra which still fascinates me (especially the rotors, that are everywhere). Her enthusiasm and passion for the research encourage me and her kindness and closeness allowed me to enjoy the experience, to take advantage of the opportunity and to learn a lot.

To the members of the Signal Processing and Communications Laboratory of Cambridge University: Oliver, Stuart, Jianwei, Kuan, Marina, Alex, Jos, Phill and Richard. Thanks for making me feel comfortable and for inviting me to the coffee talks where I learned from how to survive in the Pyrenees to how I can decomposed a picture in different colors.

To my housemates in Cambridge: Lisa, Valeria, Dalila, Jonny, Afka and Sanjie. Thanks for being friendly and making me feel comfortable in our little world.

Al mini-grupo de españoles que se creó en Cambridge: Alex, Natalia, Ronces and Max. Gracias por compartir esos buenos momentos en los que podía volver a hablar en español y quejarme a gusto del infernal tiempo de Reino Unido.

A mis amigos de Valencia, tanto los compis de piso: Carme, Irene, Carlos, Maria y Bernat como los del grupo predoctoral: Carme, Quique, Marina, Abel, Elena, Thais, Isa, Juanmi y todos los demás. Gracias por hacerme sentir tan a gusto en Valencia, ciudad que me enamoró y por tan buenos momentos en el piso, en el Castillo de las Tapas, en las Fallas y en cualquier lugar donde al final terminábamos pasando un rato.

A mis compañeros de carrera, especialmente a Jose (Jope), Ester, Espin y Antonio. Gracias por los buenos momentos pasados en el aula, las risas, las horas de estudio, las frecuentes visitas a la cantina de la facultad de veterinaria y por, aún estando cada uno en una punta de España (y Francia) seguimos encontrando un hueco para vernos siempre que podemos. Incluyo en este grupo a Antoñito, un agregado almeriense al que siempre he considerado mi hermano (mangabro) y que siempre busca un hueco para que coincidamos.

A Javi y su familia, que desde que la amistad se fraguó en la Escuela de Idiomas de Murcia, se ha convertido en mi amigo y en parte de mi familia, estando allí en una epoca especialmente difícil y ayudándome siempre que lo he necesitado. Con él se cumple la frase: *Un verdadero amigo es aquel que entra cuando todos los demás se van*.

A mi familia de Barcelona, especialmente a Laura, Silvia y Raúl , por haberme aceptado tan rápidamente como a uno más de la familia y haberme abierto las puertas de su casa. Por apoyarme en todo momento y por estar siempre allí tanto en lo bueno como en lo malo.

A mi hermana, Denise, por la experiencia de crecer a su lado, porque a pesar de la distancia nos sentimos como si siguiéramos viviendo bajo el mismo techo y porque, gracias a ella, nunca he tirado la toalla.

A mi abuela, porque aunque aún no sabe exactamente a que me dedico, siempre ha creído en mí y constantemente me ha recordado lo importante que es esforzarse por ser un buen profesional y persistir en las metas que uno tiene.

A mis padres, José Ramón y Elisa, por inculcarme desde niño la pasión por la lectura, el deseo de saber más y el don de la curiosidad. Siempre me apoyaron en todas mis decisiones, celebrando mis logros y animándome a seguir intentándolo cuando fracasaba.

Final y especialmente, a Raúl, por mil cosas: paciencia infinita, apoyo incondicional, comprensión, ánimo, etc. Por escucharme cuando verbalizaba las trabas que encontraba al trabajar en un problema, por aguantarme cuando me tocaba escribir un artículo (ya es difícil de normal...), por soportarme y animarme cuando estaba frustrado y desanimado y, en definitiva, por estar allí en el día a día. Puedo decir sin duda que no hubiera podido concluir este proyecto sin él, y, por tanto, este trabajo es tanto mío como suyo.

Abstract

Kinematics is a branch of classical mechanics that describes the motion of points, bodies, and systems of bodies without considering the forces that cause such motion. For serial robot manipulators, kinematics consists of describing the open chain geometry as well as the position, velocity and/or acceleration of each one of its components. Rigid serial robot manipulators are designed as a sequence of rigid bodies, called links, connected by motor-actuated pairs, called joints, that provide relative motion between consecutive links. Two kinematic problems of special relevance for serial robots are:

I *Singularities:* are the configurations where the robot loses at least one degree of freedom (DOF). This is equivalent to:

(a) The robot cannot translate or rotate its end-effector in at least one direction.

(b) Unbounded joint velocities are required to generate finite linear and angular velocities.

Either if it is real-time teleoperation or off-line path planning, singularities must be addressed to make the robot exhibit a good performance for a given task. The objective is not only to identify the singularities and their associated singular directions but to design strategies to avoid or handle them.

II *Inverse kinematic problem:* Given a particular position and orientation of the end-effector, also known as the end-effector pose, the inverse kinematics consists of finding the configurations that provide such desired pose. The importance of the inverse kinematics relies on its role in the programming and control of serial robots. Besides, since for each given pose the inverse kinematics has up to sixteen different solutions, the objective is to find a closed-form method for solving this problem, since closed-form methods allow to obtain all the solutions in a compact form.

The main goal of this dissertation is to contribute to the solution of both problems. In particular, with respect to the singularity problem, a novel scheme for the identification of the singularities and their associated singular directions is introduced. Moreover, geometric algebra is used to simplify such identification and to provide a distance function in the configuration space of the robot that allows the definition of algorithms for avoiding them.

With respect to the inverse kinematics, redundant robots are reduced to non-redundant ones by selecting a set of joints, denoted *redundant joints*, and by parameterizing their joint variables. This selection is made through a workspace analysis which also provides an upper bound for the number of different closed-form solutions. Once these joints have been identified, several closed-form methods developed for non-redundant manipulators can be applied to obtain the analytical expressions of all the solutions. One of these methods is a novel strategy developed using again the conformal model of the spatial geometric algebra.

To sum up, this dissertation provides a rigorous analysis of the two above-mentioned kinematic problems as well as novel strategies for solving them. To illustrate the different results introduced in this memory, examples are given at the end of each chapter.

Contents

List of Figures

List of Tables

Notation and Acronyms

Notation

$\exists$	There exists
$\forall$	For any
$\Rightarrow$	Implies that
$\in$	Belongs to
$\subset$	Subset
$\equiv$	Equivalent
$\cup$	Set union
$\cap$	Set intersection
$\mathbb{R}$	All real numbers $\in (-\infty, \infty)$
$\mathbb{R}^+$	All real numbers $\in [0, \infty)$
$SO(n)$	Special orthogonal group of an n-dimensional Euclidean space
$SE(n)$	Special Euclidean group of an n-dimensional Euclidean space
$\mathcal{G}_n$	Geometric algebra of an n-dimensional Euclidean space
$\mathcal{G}_n^+$	Even subalgebra of $\mathcal{G}_n$
$\mathcal{G}_n^-$	Odd subalgebra of $\mathcal{G}_n$
$\mathcal{G}_{n+1,1}$	Conformal model of $\mathcal{G}_n$
n	Number of DOF or signature of a generic geometric algebra $\mathcal{G}$ or basis null vector of any conformal geometric algebra
$\overline{n}$	basis null vector of any conformal geometric algebra
$\mathcal{R}$	An arbitrary serial robot
$\mathcal{R}_i$	Joint i of $\mathcal{R}$
$\{\boldsymbol{o}_i, \boldsymbol{x}_i, \boldsymbol{y}_i, \boldsymbol{z}_i\}$	Frame attached to $\mathcal{R}_i$ (origin and the three coordinate axes)
A_i^{i-1}	Homogeneous matrix relating the frames attached to $\mathcal{R}_i$ and $\mathcal{R}_{i-1}$
T_i^j	Matrix product $A_{j+1}^j \cdots A_i^{i-1}$
$\mathbf{q} \in \mathbb{R}^n$	Robot's configuration
$\dot{\mathbf{q}} \in \mathbb{R}^n$	Joint velocity vector
$\mathbf{p} \in \mathbb{R}^3$	Robot's end-effector position relative to the world reference frame

$R \in SO(3)$	Robot's end-effector orientation relative to the world reference frame
$\mathbf{x} \in \mathbb{R}^6$	Robot's end effector pose (position and orientation)
$\mathbf{v} \in \mathbb{R}^3$	Robot's end-effector linear velocity vector
$\boldsymbol{\omega} \in \mathbb{R}^3$	Robot's end-effector angular velocity vector
J_G	Geometric Jacobian
J_A	Analytical Jacobian
$\mathcal{W}$	Robot's workspace
$\mathcal{SW}$	Section of $\mathcal{W}$ obtained after fixing the first revolute joint of $\mathcal{R}$
$\boldsymbol{\tau} \in \mathbb{R}^n$	Joint torques vector
Δ	Difference operator or Matrix whose columns are the eigenvectors of a given matrix
$\lambda_i(A)$	i-th eigenvalue of matrix A
$\times$	Cross or vector product
$\cdot$	Scalar or interior product
$\wedge$	Wedge or exterior product
$\|\cdot\|$	Norm (either the Euclidean norm or the multivector norm)
a, b, ...	Real numbers or scalars
$\boldsymbol{a}$, $\boldsymbol{b}$, ...	Vectors
A, B, ...	Matrices or multivectors of $\mathcal{G}_n$ or null vectors of the conformal model of $\mathcal{G}_n$
A_r, B_r, ...	r-vectors of $\mathcal{G}_n$

General Acronyms

BMM	Barcelona Mobile Manipulator
CDF	Cartesian degrees of freedom
CGA	Conformal geometric algebra
DOF	Degrees of freedom
GA	Geometric algebra
GDM	Globally degenerated manipulator
SVD	Singular value decomposition

Latin abbreviations

etc.	-et cetera-	and the rest
et al.	-et alii-	and others
i.e.	-id est-	that is

Chapter 1

Introduction

1.1 Context and motivation

Kinematics is a branch of classical mechanics that describes the motion of points, bodies, and systems of bodies without considering the forces that cause such motion. Its study allows a better understanding of the behavior of systems of rigid bodies as well as important properties related to the motion of such systems like, for example, its position, velocity and acceleration. An example of a system such that are the rigid serial robot manipulators, i.e., a sequence of rigid bodies, called *links*, connected by motor-actuated kinematic pairs, called *joints*, that provide relative motion between consecutive joints. At the end of the last link, a tool or device, called *end-effector*, is placed.

For industrial serial robots, the kinematics allows, given the position of each joint (also known as the *configuration*), to determine the position and orientation (also known as the *pose*) of the end-effector. This is referred as the *forward kinematics* of the robot. In addition, the kinematics also allows to formulate the inverse problem, i.e., the *inverse kinematics*. Since industrial robots are robotic systems used for manufacturing (that includes welding, painting, assembly, pick and place for printed circuit boards, packaging and labeling), the inverse kinematics becomes a key problem. For any of the above-mentioned tasks, a spatial trajectory, made up of points, is given to the robot. Such trajectory should be followed by the end-effector making each one of these points become a target pose of the end-effector. That is the definition of the inverse kinematics problem and it still has open aspects.

Moreover, for industrial redundant robots, i.e., robots with more joints that the ones required for a given task, the inverse kinematics has an infinite number of different solutions which allows the definition of secondary tasks. The objective is to select, from the set of all solutions, those that satisfy certain conditions like not to be close to an obstacle or to a joint limit, etc. Therefore,

for redundant robots, the inverse kinematics consists of finding, instead of just one solution, all of them, so the redundancy can be exploited. However, the majority of the contributions related to the inverse kinematics of redundant robots develop numerical strategies that only return one particular solution. Despite some of these numerical methods include a particular secondary task for exploiting the redundancy, these approaches are not the most suitable for solving the problem because:

- They have a high computational cost and execution time in comparison with other methods.
- It might be necessary to use different secondary tasks at different times which would imply the design of a new numerical algorithm to solve the inverse kinematics for each new secondary task.

Therefore, for a good performance of an arbitrary industrial robot in the execution of its tasks, an efficient method for solving the inverse kinematics that provides all the associated solutions is required.

On the other hand, another key problem of robot kinematics is the *singularity problem*. Singularities (or, equivalently, kinematic singularities) are those configurations where the end-effector cannot be translated or rotated around at least one direction. Therefore, the singularities affect the motion capabilities of the industrial robot by limiting such motion in certain directions. Furthermore, at singularities, finite linear and angular velocities of the end-effector require infinite joint velocities which make impossible to command the robot. The singularity problem can be split into two subproblems:

- Identification of singularities and their associated singular directions.
- Handling or avoiding the singularities.

With respect to the first subproblem, the identification of both singularities and singular directions is important because it allows the design of control schemes or numerical algorithms for handling them. Such identification is made through the determinant of the matrix that relates the joint velocity vector with the Cartesian velocity vector (the vector of linear and angular velocities), also known as the *geometric Jacobian matrix*. However, for redundant robots, this matrix is non-square so the determinant cannot be computed. Although there are alternative methods to identify the singularities of redundant robots, they are not computationally efficient.

Regarding the second subproblem, the majority of the methods developed in the literature generate trajectories that avoid the singular directions once they have been identified. However, due to the lack of a good definition of the distance to a singularity, these trajectories are usually generated far from the singularities which limits the effective workspace of the robot. Therefore, this is another open problem of great importance.

1.2 Objectives

The main objective is to contribute significantly to the solution of the two kinematic problems introduced in section 1.1, i.e., the inverse kinematics for redundant serial robots and the singularity identification and handling for arbitrary rigid serial manipulators. To reach that goal, the main objective is split into the following particular objectives.

1. **Inverse Kinematics:**
    - Characterization of globally degenerated robots in terms of the Jacobian matrix.
    - Development of a method to analyse both quantitative and qualitatively the workspace of arbitrary redundant manipulators.
    - Definition of the concept *redundant joint* based on the above-mentioned criteria.
    - Proposal of a method for the identification of redundant joints according to the proposed definition.
    - Design of algorithms to solve analytically the inverse kinematics of redundant robots through the parametrization of their redundant joints.
    - Development of closed-form methods for the inverse kinematics of 6 and 7 DOF robots using conformal geometric algebra.
2. **Singularity Problem:**
    - Proposal of a method for the identification of singularities using geometric algebra.
    - Proposal of a practical and easy to implement definition for the distance to a singularity.

1.3 Outline of the thesis

The present work is organized in seven chapters and three appendices. A brief description of their content is given:

- **Chapter 1** describes the motivation and objectives of this dissertation.
- **Chapter 2** discusses the state of the art in the topics of inverse kinematics and singularities of serial robot manipulators.
- **Chapter 3** characterizes globally degenerated 6 DOF robots in terms of the rank-deficiency of the Jacobian matrix. Besides, such characterization is extended to robots with less than 6 DOF.

- **Chapter 4** develops a workspace analysis as well as its application to the definition and identification of redundant joints. Furthermore, solves the inverse kinematics of several well-known redundant robots.
- **Chapter 5** develops a closed-form method for solving the inverse kinematics of 6 and 7 DOF serial robots using conformal geometric algebra. This method complements strategy developed in chapter 4.
- **Chapter 6** proposes a method for the identification of singularities using geometric algebra. Furthermore, it defines a distance function in configuration space that restricted to singularities allows the design of algorithms for avoiding them.
- **Chapter 7** summarizes the contributions of this dissertation, states the future research lines and lists the publications derived from this research.
- **Appendix A** presents an overview of the mathematical concepts and results used throughout this work.
- **Appendix B** presents an overview of the kinematics of serial robots as well as a basic kinematic analysis of three industrial robots of 7 DOF.
- **Appendix C** lists the most used trigonometric equations need for the resolution of the inverse kinematics of non-redundant serial robots.

Chapter 2

State of the Art

In this chapter some of the most important works found in the kinematics literature are outlined. First section focuses on the inverse kinematics, while the second section focuses on the singularity identification and handling. In each section, the main contributions of each work are highlighted and the open problems are pointed out.

As introduced in chapter 1, two of the most robotic kinematic poblems are the inverse kinematics and the singularity identification and handling for serial robots. These two problems have received great attention during the past decades. More recently, due to the necessity of closed-form solutions and efficient numerical methods, many authors have brought new insights to both topics.

This chapter intends to provide an overview of the main contributions developed to the resolution of both problems.

2.1 Inverse kinematics of serial manipulators

As defined in section B.2, the inverse kinematics has as goal obtaining the configurations that provide the desired position and orientation of the end-effector. Non-redundant manipulators have up to sixteen different configurations for the same particular end-effector pose (Pieper, 1968), while redundant manipulators has an infinite number of configurations leading to the same end-effector pose (Siciliano et al., 2008; Spong et al., 2006). The methods to solve the inverse kinematics for serial robots are categorized in two groups:

a) Analytical or closed-form methods: All the solutions are expressed as functions in terms of the pose matrix elements.

b) Numerical methods: Starting with an initial configuration $\boldsymbol{q}_0$, an iterative process returns a good approximation $\widetilde{\boldsymbol{q}}$ of one of the solutions.

2.1.1 Closed-form methods

The importance of the inverse kinematics relies on its role in the programming and manipulation of serial robots. Its solutions, generated using either closed-form methods, where all the solutions are obtained, or numerical methods, where particular solutions are calculated, play an important role in the design of control and path-planning algorithms.

Closed-form methods strongly depend on the robot structure and, therefore, cannot be applied to arbitrary robots. However, they are computationally efficient and give all the solutions for a given pose. In his PhD thesis, Pieper (1968) develops a procedure to obtain the solutions for the inverse kinematics of serial robots with three consecutive joints whose axes intersect at a single point. If the joint variable associated with joint i is denoted by q_i (as stated in section B.2), then the method consists of transforming each $\cos(q_i)$ and $\sin(q_i)$ into $\tan(q_i/2)$. Then, the change of variables $t_i = \tan(q_i/2)$ is performed and, as a result, the inverse kinematic solutions are given as the solutions of a set of polynomials. For an arbitrary serial robot with spherical wrist, at least one of these polynomials has degree four which makes the problem, in general, difficult to solve. Later, Paul (1981) establishes a more rigorous and generic method based on the manipulation of the homogeneous transformation matrices A_i^{i-1} (defined in B.14) that can be applied to manipulators of other kind. In particular, this method consists of the derivation of the following set of matrix equations (see appendix B):

$$\left(A_{i-1}^{i-2}\right)^{-1} \cdots \left(A_1^0\right)^{-1} \cdot T = A_i^{i-1} \cdots A_n^{n-1} \quad \text{for } i = 2, \ldots, n \tag{2.1}$$

where T denotes the matrix representation of the end-effector's pose. The objective is to isolate those non-linear equations that contain just one joint variable. Since T has twelve non-null terms, a maximum of $12n$ non-linear equations needs to be formulated and solved. Besides, in some cases, a combination of two or more non-linear equations are needed to obtain the value of a single joint variable, which makes this approach difficult to apply.

For anthropomorphic redundant robots, i.e., robots of 7 DOF where the joints are divided into three groups: the shoulder – with the first three joints, the elbow – with the fourth joint – and the wrist – with the three last joints, most of the approaches are based on the definition of the *arm angle parameter* φ, a parameter defined using the geometrical relation between the shoulder, the elbow and the wrist. With this parameter, the inverse kinematics is solved geometrically. Particular instances for φ are determined based on secondary tasks such as avoiding joint limits, obstacles or offsets (Lau and Wai, 2002; Shimizu et al., 2008; Jung et al., 2011; Yu et al., 2012) or obtaining human-like solutions (Xia et al., 2014). As mentioned before, these methods are restricted to anthropomorphic manipulators with spherical wrist.

Regarding the approaches based on the use of geometric strategies, in (Judd and Van Til, 1985; Singh and Claassens, 2010; Wei et al., 2014; Liu et al., 2015; Qingmei et al., 2015) different geometric methods are introduced. Most of them are focused on particular non-redundant serial robots or particular redundant manipulators of 7 DOF and, therefore, they cannot be extended to arbitrary robots.

In (Ivlev and Gräser, 1997, 1998) a closed-form method based on the definition of imaginary links is presented. Given a desired pose, represented by T, if T is equated to the symbolic pose matrix T_n^0 (as defined in equation (B.13)), a non-linear system of twelve equations and n variables is obtained. Hence, for a six or seven DOF robot, the system obtained has more equations than variables. Then, the idea of these methods consists of defining extra joints connected by imaginary links so the extended manipulator has twelve DOF and the associated non-linear system of equations has the same number of equations and variables. Finally, the system can be solved either analytically or numerically. However, in the majority of the cases, a non-linear system of twelve equations cannot be solved analytically and needs to be solved numerically.

Finally, other approaches include the use of Lagrange multipliers (Chang, 1987), the development of an analytical strategy in rate domain (Huang and Jiang, 2013) or heuristic strategies (Pozna et al., 2016).

2.1.2 Numerical methods

Numerical methods usually work with any kind of robot, but they suffer from several drawbacks like, for example, high computational cost and execution time, existence of local minima and numerical errors. Moreover, only one of the sixteen (infinite) possible solutions is obtained for non-redundant (redundant) manipulators.

The most extended numerical approaches are the *Jacobian-based methods*, in which the relation (B.20) is inverted and solved iteratively starting with an initial condition $\boldsymbol{q}_0$:

$$\boldsymbol{q}_{i+1} = \boldsymbol{q}_i + J_G^{-1}(\boldsymbol{q}_i)\boldsymbol{e}_i \tag{2.2}$$

where $\boldsymbol{e}_i$ denotes the vector of errors, i.e., the position and orientation errors between the pose associated with $\boldsymbol{q}_i$ and the target pose. Inverting the Jacobian matrix is not always possible. For redundant manipulators, J_G is a non-square matrix while for non-redundant manipulators, $\det(J_G(\boldsymbol{q}))$ vanishes at singularities (as shown in (B.22)). To handle these two situations, J_G^{-1} is replaced by a generalized inverse. The most well-known ones are the pseudoinverse $J_G^{\dagger}$ (that can be calculated using the identity (A.21)), the transpose J_G^T and the damped least-squares $J_G^T(J_G J_G^T + \lambda^2 I)^{-1}$ with damping factor $\lambda \in \mathbb{R}$ (Baillieul, 1986; Buss, 2009; Buss and Kim, 2005; Hsu et al., 1988; Kircanski and Petrovic, 1991; Lau and Wai, 2002; Nenchev, 1989; Pozna et al., 2016; Sung et al., 1996; Wang et al., 2012; Wampler, 1986). Other Jacobian-based methods include the use of the augmented Jacobian (Fratu et al., 2010), the so-called $\{1\}$-inverse (Lovass-Nagy and Schilling, 1987) or other generalized inverses based on the pseudoinverse

$J_G^{\dagger}$ (Manocha and Canny, 1994; Aspragathos and Dimitros, 1998). As stated before, the main drawbacks of using generalized inverses are the high computational cost, execution time and tracking error.

However, for 6 DOF serial robots, all these methods fail in the presence of singularities (with the exception of the damped least-squares if an appropriated damping factor λ is chosen). In this situation, some methods also modify the Jacobian matrix but in another way. For example, in (Hueso et al., 2009), $J_G(\boldsymbol{q})^{-1}$ is replaced by a modified Jacobian matrix obtained from J_G by adding a weighted diagonal matrix. If the initial conditions are properly chosen, this method has quadratic convergence. Buhmiler et al. (2010) propose the so-called quasi-Newton's method. This method is a two-step algorithm with quadratic convergence under good initial conditions. However, it only works for the singularities where only one degree of freedom is lost. Finally, in (Waziri Yusuf et al., 2011) $J_G(\boldsymbol{q})$ is replaced by a diagonal matrix where its diagonal elements are calculated using variational techniques. The objective is to bypass the singular configuration. However, this method suffers from a high computational cost.

Other methods are focused on the use of numerical algorithms based on local optimization (De Luca and Oriolo, 1991a,b; De Luca et al., 2006). In (Wang et al., 2012) a quadratic minimization algorithm is developed, while in (Ahuactzin and Gupta, 1999; Burdick, 1989) a solution trajectory is generated by exploring the feasible directions of the end-effector from its current position at each step.

Finally, other approaches include the use of conformal geometry algebra (Kim et al., 2015a,b), Crank-Nicholson methods (Drexler, 2016) and reachability maps (Vahrenkamp et al., 2015).

2.2 Singularities of serial manipulators

As stated in section B.2, kinematic singularities are those configurations in which the end-effector cannot move through certain directions or, equivalently, where unbounded joint velocities are required to generate a given end-effector velocity vector $\dot{\boldsymbol{x}}$. Hollerbach (1985) and Gottlieb (1986) independently demonstrate that every serial robot of $n > 2$ DOF has kinematic singularities, even the redundant ones. Since only the kinematics singularities are going to be considered throughout this work, from now on and, unless other is specified, the term singularities will refer to kinematic singularities.

Handling the singularities consists of two steps:

- Identification of singular configurations and their associated singular directions.
- Design of efficient algorithms to handle these singularities.

2.2.1 Identification and classification of singularities

There are several ways of classifying general singularities. The main one, according to (Oetomo, 2004; Siciliano and Khatib, 2008; Burdick, 1989), is:

- *Kinematic singularities*: are those singularities that correspond to the mechanical limitations of the serial robot $\mathcal{R}$.
- *Representation singularities*: are those singularities associated with minimal representations of the orientation.
- *Algorithmic singularities*: are those configurations where the main task of positioning and orientating the end-effector contradicts a secondary task (such as avoiding joint limits, singularities or obstacles).

In turn, kinematic singularities can be divided into the following two groups:

- *Position singularities*: are the singularities where only the joints that contribute to the position of the end-effector are involved.
- *Orientation singularities*: are the singularities where only the joints that contribute to the orientation of the end-effector are involved.

As seen in section B.2, singularities are identified through equations (B.22). However, if $\mathcal{R}$ has revolute joints, several elements of J_G are non-linear expressions and, as a result, it becomes difficult to compute these equations. Tchoń and Muszyński (1997) present a mathematical study of the singularities of non-redundant robots, while in (Shamir, 1990) a similar study is performed of redundant manipulators. Xu et al. (2016) develop an strategy for the identification of the singularities of arbitrary serial robots of 6 DOF. On the other hand, in (Bruyninckx, 2010; Angeles, 2007; Murray et al., 1994; Oetomo, 2004; Cheng et al., 1997, 1998; Oetomo and Lim, 2001; Vaezi et al., 2011; Oetomo and Ang Jr, 2009) a simplification for manipulators with spherical wrist is proposed. Since the origin of the end-effector frame is placed at the wrist center point, a zero block appears in J_G:

$$J_G(\boldsymbol{q}) = \begin{pmatrix} J_{11}(\boldsymbol{q}) & \mathbf{0}_{3\times 3} \\ J_{21}(\boldsymbol{q}) & J_{22}(\boldsymbol{q}) \end{pmatrix} \tag{2.3}$$

where $J_{11}(\boldsymbol{q})$ and $J_{21}(\boldsymbol{q})$ are two submatrices of order $3 \times (n-3)$, while $J_{22}(\boldsymbol{q})$ has order 3.

Thus, the singularities of $\mathcal{R}$ can be decoupled into position and orientation singularities. Its identification can be summarized as follows:

- *Non-redundant case:* the solutions of $\det(J_{11}(\boldsymbol{q})) = 0$ determine the position singularities while the solutions of $\det(J_{22}(\boldsymbol{q})) = 0$, the orientation singularities.

- *Redundant Case:*
  - Position singularities: are those $\boldsymbol{q} \in \mathcal{C}$ such that $\rho(J_{11}(\boldsymbol{q})) < 3$.
  - Orientation singularities: are those $\boldsymbol{q} \in \mathcal{C}$ such that:

$$\left.\begin{aligned} \rho(J_{22}(\boldsymbol{q})) &< 3 \\ \rho(J_{21}(\boldsymbol{q})) &< 3 \\ \rho(J_{21}|J_{22}(\boldsymbol{q})) &< 3 \end{aligned}\right\} \tag{2.4}$$

    where $J_{21}|J_{22}$ denotes the juxtaposition of the submatrices J_{21} and J_{22}, while $\rho(\cdot)$ denotes the rank of the corresponding matrix.

Once the singularities have been identified, their associated singular directions can be found by representing the Jacobian J_G in a different frame in which J_G has a zero row. In this situation, for a non-null joint velocity vector $\dot{\boldsymbol{q}}$, a component of the end-effector velocity vector $\dot{\boldsymbol{x}}$ is zero and, thus, the corresponding component of the linear or angular velocity vector is zero. Hence, the end-effector of $\mathcal{R}$ cannot be translated or rotated around the corresponding axis of the frame in which J_G is now represented (Cheng et al., 1998, 1997; Oetomo and Lim, 2001; Oetomo, 2004; Oetomo and Ang Jr, 2009; Vaezi et al., 2011). There are two main methods for finding out these frames:

(1) Let denote by $\{1\}, \ldots, \{n\}$ the joint frames of $\mathcal{R}$. Then, a first attempt consists of representing J_G in each one of these joint frames (using identity (B.23)). If one of the first three rows of $J_G^{\{i\}}$ is a zero row, then the corresponding component of the linear velocity vector is zero and, thus, the end-effector cannot be translated along the corresponding axis of $\{i\}$, while if the zero row is one of the last three, then the corresponding component of the angular velocity vector is zero and, therefore, the end-effector cannot be rotated around the corresponding axis of $\{i\}$.

(2) Given a singularity $\boldsymbol{q} \in \mathcal{C}$, since $J_G(\boldsymbol{q})$ is a constant matrix, the singular value decomposition (as defined in identity (A.20)) can be applied to $J_G(\boldsymbol{q})$:

$$J_G(\boldsymbol{q}) = U \Sigma V^T$$

Recall that Σ is a diagonal matrix that has as many zeros in its diagonal as degrees of freedom $\mathcal{R}$ loses. Thus, for each lost degree of freedom there is a zero row in ΣV^T and, since

$$U^T J_G(\boldsymbol{q}) = \Sigma V^T \tag{2.5}$$

there is also a zero row in $U^T J_G(\boldsymbol{q})$. Since U is an orthogonal matrix, $U^T J_G(\boldsymbol{q})$ can be seen as the representation of the Jacobian matrix $J_G(\boldsymbol{q})$ in a different frame. In the literature, this frame is known as the *singular frame* $\mathcal{S}$. Therefore, as in the preceding situation, the singular direction is aligned with the axes of $\mathcal{S}$.

2.2.2 Handling of singularities

Handling singularities has become an important part of robot kinematics research due to the necessity of robust and efficient algorithms for a good performance of the different tasks that modern robots must execute. The different methods recently developed can be classified into three groups (Oetomo, 2004; Yong et al., 2013):

- Methods that handle singularities without workspace division.
- Methods that handle singularities with workspace division (singular and non-singular regions).
- Methods that handle singularities using the redundancy of $\mathcal{R}$.

Methods without workspace division

These methods usually modify either the Jacobian matrix J_G or the end-effector trajectory through a continuous function to avoid the vanishing of $\det(J_G(\boldsymbol{q}))$ at singularities. Such function is defined in the whole workspace $\mathcal{W}$.

Regarding the contributions where the Jacobian matrix is modified, in (Nakamura and Hanafusa, 1986) the SR-inverse method is introduced. This method uses a generalized pseudoinverse matrix with less computational cost than the regular pseudoinverse. In addition, such method is able to avoid the singular directions. However, its computational cost is still high with respect to other methods and has tracking errors. Kircanski (1993) uses the singular value decomposition to obtain the matrix Σ for a given singularity $\boldsymbol{q} \in \mathcal{C}$. Then, the zero elements of its diagonal are replaced by non-zero functions so the new Jacobian matrix is not singular at $\boldsymbol{q}$. Moreover, the singular direction associated with $\boldsymbol{q}$ is eliminated from the workspace. Using a similar idea, Oetomo et al. (2002) add imaginary joints in order to obtain a virtual redundancy. Then, extra columns are added to J_G and, at a singularity, despite the loss of some degrees of freedom, the new Jacobian matrix still has full-rank. In (Huang et al., 2016), three methods that modify the Jacobian matrix are presented: non-redundancy singularity avoidance (NRSA), redundancy singularity avoidance (RSA) and point-to-point singularity avoidance (PTPSA). All of them exhibit a good performance but are restricted to particular manipulators.

Other approaches modify the trajectory. For example, Schinstock (1998) extends the damped least-squares method for improving the robustness in the presence of singularities. However, the accuracy of this method decreases at some singular configurations and, hence, the end-effector does not follow the trajectory in all its points. In (Kieffer, 1994; O'Neil et al., 1997) the end-effector trajectory $\phi(t)$ is reparametrized to $\phi(\lambda(t))$ so the reparametrization and its higher derivatives exhibit a good behavior close to singularities. This idea is extended by Lloyd (1998) considering arbitrary trajectories within the workspace.

Finally, in (Hijazi et al., 2016) the singularities are studied before designing the robot. Although a robot without singularities cannot be designed, some singularities can be avoided at the design stage.

The main drawback of all these methods is the high computational cost and, in some cases, the tracking error associated with them.

Methods with workspace division

These methods usually divide the workspace in two regions: the *singular region* S and the *non-singular region* NS. If $\boldsymbol{q}_1, \ldots, \boldsymbol{q}_r$ denote the singularities of $\mathcal{R}$, then:

$$\mathrm{S} = \bigcup_{i=1}^{r} f(\mathcal{U}_i) \tag{2.6}$$

where f denotes the forward kinematics function (B.15) and each $\mathcal{U}_i$ is an open neighborhood of $\boldsymbol{q}_i \in \mathcal{C}$. Conversely, $\mathrm{NS} = \mathcal{W} \setminus \mathrm{S}$. Robust control algorithms dealing with the singularities are designed to work only in S, while general control algorithms are used in NS. The transition between control schemes must be continuous.

Some contributions propose numerical algorithms that work inside S. They are based on the use of several generalized inverses. Aboaf and Paul (1987) handle the wrist singularity by eliminating its associated singular direction. The value of the corresponding component of the velocity vector $\dot{\boldsymbol{x}}$ is bounded in the eliminated direction to guarantee the accuracy in the position while minimizing the orientation error. However, this strategy cannot be extended to other kinematic singularities. On the other hand, Chiaverini and Egeland (1990) identify the singular directions of 6 DOF serial robots and eliminate them. Inside the singular region S, the Jacobian matrix becomes a non-square matrix so the pseudoinverse is used to generate the joint velocities. One of the main drawbacks of this method is the high computational cost associated with the use of the pseudoinverse. In (Cheng et al., 1997), a similar strategy is followed. Once the singular directions have been removed, a combination of a generalized inverse together with an optimization method (the singularity isolation plus QP compact method) is used to generate the motion in the eliminated directions.

Other works are focused on the design of control algorithms based on the gradient projection method. In (Chang and Khatib, 1995; Oetomo and Lim, 2001; Oetomo, 2004; Oetomo and Ang Jr, 2009), the singularities and their associated singular directions are identified. Then, a control algorithm is designed and implemented inside the singular region S for making the end-effector escape from there. Such control algorithm is based on the gradient projection method and generates a null torque vector that is projected onto the null space of J_G (Khatib, 1987). Such projection creates an internal motion that allows the end-effector to escape from the singularity. In Cheng et al. (1998), the same strategy is extended for redundant robots of 7 DOF. The gradient projection method is applied with different performance measures as, for example, manipulability, lower energy consumption, etc. Nenchev and Uchiyama (1995) give a

new classification of singularities according to its geometrical and differential behavior. A path planning algorithm based on the velocities generated by the null space of J_G is introduced to achieve trajectories that move arbitrarily close to some of these singularities.

Regarding the contributions based on the use of self-motions, in (Seng et al., 1995; O'Neil et al., 1997) a study about the escapability from singular configurations is presented. Escapability is defined as the ability of a serial robot $\mathcal{R}$ of reconfiguring itself from a singular pose to a non-singular one via self-motion. However, at a singularity, the self-motion generated (if it exists) might or might not assist the end-effector of $\mathcal{R}$ in escaping from a singularity. A detailed study of when the self-motion can be used is found in (Bedrossian, 1990; Bedrossian and Flueckiger, 1991).

Finally, Bohigas (2013) introduces a division of the configuration space $\mathcal{C}$. The singular region S is redefined as:

$$\mathrm{S} = \bigcup_{i \in \mathcal{I}} \mathcal{V}_i \tag{2.7}$$

where $\mathcal{V}_i$ is an open neighborhood of $\boldsymbol{q}_i \in \mathcal{C}$. Then, all the trajectories are generated in $\mathcal{C} \setminus \mathrm{S}$. However, the computational cost of this strategy is very high because a discretization of $\mathcal{C} \setminus \mathrm{S}$ is required for generating such trajectories.

Methods using redundancy

It is well-known that redundancy can be used to perform secondary tasks such as avoiding obstacles, singularities or joint limits. In this context, the idea of these methods is to use the redundancy through a cost function and an optimization process to generate alternative trajectories to achieve a target pose avoiding singularities. Since the serial robot $\mathcal{R}$ is redundant, there are infinite possible trajectories to achieve any given pose of the end-effector.

In particular, most of the contributions in this field develop strategies for solving the inverse kinematics of redundant robots. Then, the redundancy is exploited by using an optimization algorithm. Because of that, this topic is widely covered in section 2.1. Several examples of these strategies are (Cheng et al., 1998; De Luca and Oriolo, 1991a; Taki and Nenchev, 2014).

Finally, in (Fang and Tsai, 2003) an identification of the singularities is made by using the screw theory. Then, the singular directions are isolated and eliminated to allow the computation of feasible directions leading to non-singular trajectories. On the other hand, Chevallereau (1996) also proposes the identification of feasible directions using, instead of the screw theory, artificial constraints defined over the trajectory.

2.3 Open problems

Summarizing all the contributions explored in the preceding sections, the following open problems can be listed:

- Development of a general closed-form method for solving the inverse kinematics of redundant serial robots.
- Development of a general method for solving the inverse kinematics of non-redundant serial robots without spherical wrist.
- Development of computationally efficient strategies for the identification of the singularities and their associated singular directions.
- Design of robust and efficient numerical algorithms or control schemes for avoiding or handling the singularities.

Chapter 3

Characterization of Globally Degenerated Robots

What has been affirmed without proof
can also be denied without proof
Euclid

In this chapter an analytical and easy to implement characterization of globally degenerated serial robots based on Heiss's theorem is presented. Besides, the concept of globally degeneration is extended to manipulators with less than 6 DOF and the relations between non globally degenerated manipulators and their kinematic subchains are studied. Finally, several examples are introduced to illustrate the utility of such characterization.

3.1 Problem Statement

As stated in section 1.2, one of the thesis objectives is to develop an easy to implement strategy for identifying the serial robots that have limited motion in the whole workspace. This characterization is especially useful for the identification of the redundant joints (as it will be seen in chapter 4), which is a crucial point in the resolution of the inverse kinematic problem for redundant serial robots.

Given a serial robot $\mathcal{R}$, its number of *Cartesian degrees of freedom* (CDF) is defined as the number of independent translations and rotations the end-effector of $\mathcal{R}$ can perform in the Cartesian

space. If the manipulator's end-effector moves in the three dimensional space, the number of CDF is 6 at the most.

According to Schrake et al. (1990), a serial robot of 6 DOF is said to be *globally degenerated* when its number of CDF is strictly lower than 6 for any possible configuration. Obviously, a manipulator is said to be *locally degenerated* when its number of CDF is strictly lower than 6 only for some configurations. Due to the existence of orientation singularities, any serial manipulator with at least 3 revolute joints is locally degenerated (Gottlieb, 1986; Hollerbach, 1985).

By its definition it is clear that globally degenerated manipulators have limited their motion in the whole workspace. However, it is not obvious how these manipulators can be identified. In his PhD thesis, Pieper (1968) shows some kinematic structures that are globally degenerated. Theorem 3.1.1, proposed in (Heiss, 1985), provides a geometric characterization of when a manipulator is globally degenerated, based on its kinematic structure. Despite informal, this characterization has shown to be useful.

Theorem 3.1.1 (Heiss, 1985)**.** *A serial manipulator of 6 DOF is globally degenerated if and only if at least one of the following statements holds:*

(a) It possesses three coplanar prismatic joints.

(b) It possesses more than three revolute joints with parallel axes.

(c) It possesses four revolute joints whose axes intersect at a single point.

(d) It possesses two groups of three revolute joints whose axes intersect at a single point.

(e) It possesses two revolute joints with coincident axes.

(f) It possesses six revolute joints, three of them whose axes intersect at a single point and the rest with parallel axes.

(g) It possesses two prismatic joints with parallel axes.

(h) Number of prismatic joints + number of revolute joints with parallel axes − 1 > 3.

Due to its geometrical nature, it is difficult to formulate this theorem as an algorithm. Besides, some special geometric structures cannot be identified by an algorithm based on the above criteria, like, for example, structures with two consecutive joints – one revolute and one prismatic – with parallel axes (Schrake et al., 1991).

For that reasons, Schrake et al. (1990) propose a different approach. Given that the determinant of the Jacobian matrix vanishes at singularities, they extend this idea and establish that a manipulator is globally degenerated if, and only if, the determinant of the Jacobian matrix vanishes in the whole workspace. However, these authors do not prove its assumption. In the next section two different approaches for the mathematical characterization of globally degenerated manipulators are presented.

3.2 Characterization of globally degenerated manipulators based on Heiss theorem

Following the idea introduced in (Schrake et al., 1991), a characterization of the geometric structures that make a serial robot to be globally degenerated is proposed. This result is especially useful because it allows to construct a computational algorithm for its easy practical use. Before presenting and proving this theorem, an auxiliary lemma is required:

Lemma 3.2.1. *Let $M \in \mathcal{M}_3(\mathbb{R})$. Its determinant, $\det(M)$, vanishes if, and only if, one of the columns (rows) is zero, two columns (rows) are proportional or there exists a linear combination between the three columns (rows).*

Proof. It follows inmediatly from the properties of determinants (as depicted in section A.1). □

Statements $(a)-(h)$ of theorem 3.1.1 are denoted as *Heiss's Criteria*. A serial robot fulfills Heiss's Criteria if its kinematic structure meets at least one of the mentioned statements.

Theorem 3.2.2. *A serial manipulator of 6 DOF fulfills Heiss's Criteria if, and only if,* $\det(J_G(\boldsymbol{q})) = 0$ *for every* $\boldsymbol{q} \in \mathcal{C}$.

Proof.
$\boxed{\Longrightarrow}$

(a) *It possesses three coplanar prismatic joints.*

If the axes of these three coplanar prismatic joints are denoted by $\boldsymbol{z}_i, \boldsymbol{z}_j$ and $\boldsymbol{z}_k$, there exists $\lambda_1, \lambda_2 \in \mathbb{R}$ such that:

$$\boldsymbol{z}_j = \lambda_1 \boldsymbol{z}_i + \lambda_2 \boldsymbol{z}_k$$

This implies that $\det(J_G(\boldsymbol{q}))$ vanishes for any $\boldsymbol{q} \in \mathcal{C}$.

(b) *It possesses more than three revolute joints with parallel axes.*

It is enough to consider the case of four revolute joints with parallel axes. In order to preserve the parallelism, the joint axes should be consecutive or to have one o more prismatic joints between two of them. In both cases, three of the four columns associated with the parallel revolute joints are subtracted to the other one, obtaining an equivalent matrix with a zero block. Since exchanging the columns of a matrix does not modify the absolute value of its determinant, an equivalent matrix is obtained such as the four revolute joints with parallel axes are the last ones:

$$J_G(\boldsymbol{q}) = \left[\begin{array}{c|c} \bigstar & A_1 \\ \hline A_2 & 0 \end{array}\right],$$

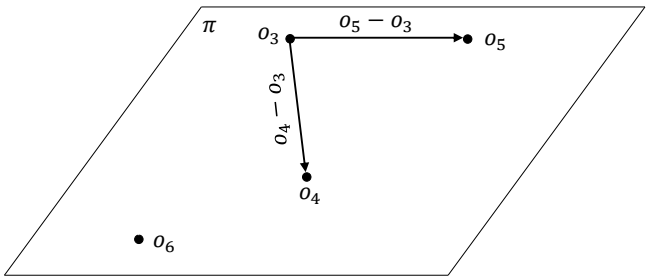

Figure 3.1: Three revolute joints with parallel axes

where the equivalent matrix is denoted as the original one for simplicity.

So, $\det(J_G(\boldsymbol{q})) = -\det(A_1)\det(A_2)$, where

$$A_1 = [\boldsymbol{z}_3 \times (\boldsymbol{o}_3 - \boldsymbol{o}_4) \quad \boldsymbol{z}_3 \times (\boldsymbol{o}_3 - \boldsymbol{o}_5) \quad \boldsymbol{z}_3 \times (\boldsymbol{o}_3 - \boldsymbol{o}_6)]$$
$$A_2 = [\boldsymbol{z}_1 \quad \boldsymbol{z}_2 \quad \boldsymbol{z}_3]$$

where $\boldsymbol{z}_i$ and $\boldsymbol{o}_i$ are defined in section B.2 and operation $\times$, in definition A.3.2. If there is a prismatic joint, $\det(A_2)$ clearly vanishes. If not, $\boldsymbol{o}_3, \boldsymbol{o}_4, \boldsymbol{o}_5$ and $\boldsymbol{o}_6$ are located in the same plane π. Due to the rotational nature of these joints, π is defined by two vectors of the form $\boldsymbol{o}_3 - \boldsymbol{o}_j$ with $j = 4, 5$ or 6 (figure 3.1). This implies that there exists $\lambda_1, \lambda_2 \in \mathbb{R}$ such that:

$$(\boldsymbol{o}_3 - \boldsymbol{o}_6) = \lambda_1(\boldsymbol{o}_3 - \boldsymbol{o}_5) + \lambda_2(\boldsymbol{o}_3 - \boldsymbol{o}_4).$$

Hence,

$$\begin{aligned}
\det(A_1) &= \det([\boldsymbol{z}_3 \times (\boldsymbol{o}_3 - \boldsymbol{o}_4) \quad \boldsymbol{z}_3 \times (\boldsymbol{o}_3 - \boldsymbol{o}_5) \quad \boldsymbol{z}_3 \times (\boldsymbol{o}_3 - \boldsymbol{o}_6)]) = \\
&= \det([\boldsymbol{z}_3 \times (\boldsymbol{o}_3 - \boldsymbol{o}_4) \quad \boldsymbol{z}_3 \times (\boldsymbol{o}_3 - \boldsymbol{o}_5) \quad \boldsymbol{z}_3 \times (\lambda_1(\boldsymbol{o}_3 - \boldsymbol{o}_5) + \lambda_2(\boldsymbol{o}_3 - \boldsymbol{o}_4))]) = \\
&= \lambda_1 \det([\boldsymbol{z}_3 \times (\boldsymbol{o}_3 - \boldsymbol{o}_4) \quad \boldsymbol{z}_3 \times (\boldsymbol{o}_3 - \boldsymbol{o}_5) \quad \boldsymbol{z}_3 \times (\boldsymbol{o}_3 - \boldsymbol{o}_5)]) + \\
&+ \lambda_2 \det([\boldsymbol{z}_3 \times (\boldsymbol{o}_3 - \boldsymbol{o}_4) \quad \boldsymbol{z}_3 \times (\boldsymbol{o}_3 - \boldsymbol{o}_5) \quad \boldsymbol{z}_3 \times (\boldsymbol{o}_3 - \boldsymbol{o}_4)])
\end{aligned}$$

where every term vanishes.

(c) *It possesses four revolute joints whose axes intersect at a single point.*

Let denote the axes of these joints as $\boldsymbol{z}_i, \boldsymbol{z}_{i+1}, \boldsymbol{z}_{i+2}$ and $\boldsymbol{z}_{i+3}$ and let consider that the origins of their frames are placed at the intersection point. Since there are four axes, one of them should be a combination of the other three. For instance, $\boldsymbol{z}_i = \lambda_1\boldsymbol{z}_{i+1} + \lambda_2\boldsymbol{z}_{i+2} + \lambda_3\boldsymbol{z}_{i+3}$ with $\lambda_i \in \mathbb{R}$. The columns of $J_G(\boldsymbol{q})$ associated to these joints are:

$$(\lambda_1\boldsymbol{z}_{i+1} + \lambda_2\boldsymbol{z}_{i+2} + \lambda_3\boldsymbol{z}_{i+3}) \times (\boldsymbol{o}_6 - \boldsymbol{o}_i)$$

$$\lambda_1\boldsymbol{z}_{i+1} + \lambda_2\boldsymbol{z}_{i+2} + \lambda_3\boldsymbol{z}_{i+3}$$

and

$$\boldsymbol{z}_{i+1} \times (\boldsymbol{o}_6 - \boldsymbol{o}_i) \qquad \boldsymbol{z}_{i+2} \times (\boldsymbol{o}_6 - \boldsymbol{o}_i) \qquad \boldsymbol{z}_{i+3} \times (\boldsymbol{o}_6 - \boldsymbol{o}_i)$$

$$\boldsymbol{z}_{i+1} \qquad \boldsymbol{z}_{i+2} \qquad \boldsymbol{z}_{i+3}$$

Again, by the linearity of the cross product, $\det(J_G(\boldsymbol{q}))$ vanishes.

(d) *It possesses two groups of three revolute joints whose axes intersect at a single point.*

Let consider that the origin of the world frame is placed at the intersection point of the first group of joint axes. Analogously, let place the origin of the end-effector's frame $\boldsymbol{o}_6$ at the intersection point of the second group. Therefore, $\det(J_G(\boldsymbol{q})) = \det(A_1)\det(A_2)$, where

$$A_1 = [\boldsymbol{z}_1 \times \boldsymbol{o}_6 \quad \boldsymbol{z}_2 \times \boldsymbol{o}_6 \quad \boldsymbol{z}_3 \times \boldsymbol{o}_6]$$
$$A_2 = [\boldsymbol{z}_4 \quad \boldsymbol{z}_5 \quad \boldsymbol{z}_6]$$

Now, $\{\boldsymbol{z}_1, \boldsymbol{z}_2, \boldsymbol{z}_3\}$ and $\{\boldsymbol{z}_4, \boldsymbol{z}_5, \boldsymbol{z}_6\}$ are two sets of linearly independent vectors almost for every configuration. If there exists $\boldsymbol{q} \in \mathcal{C}$ such that any of the two sets become linearly dependent, $\boldsymbol{q}$ is a singular configuration. Excluded that situation, and, since each set can be considered as a basis of $\mathbb{R}^3$, there exist $\lambda_1, \lambda_2, \lambda_3 \in \mathbb{R}$ such that:

$$\boldsymbol{o}_6 = \lambda_1 \boldsymbol{z}_1 + \lambda_2 \boldsymbol{z}_2 + \lambda_3 \boldsymbol{z}_3.$$

Then, $\det(A_1)$ vanishes due to the linearity and anticommutativity of the cross product.

(e) *It possesses two revolute joints with coincident axes.*

Let denote the common axis by $\boldsymbol{z}_i$. Besides, the origins of the two joint frames can be settled together. Then, $J_G(\boldsymbol{q})$ will have two identical columns and, as a consequence, its determinant will vanish.

(f) *It possesses six revolute joints, three of them whose axes intersect at a single point and the rest with parallel axes.*

Consider just the case where the last three joints intersect at a single point. Then,

$$\det(J_G(\boldsymbol{q})) = \det(A_1)\det(A_2)$$

where

$$A_1 = [\boldsymbol{z}_1 \times (\boldsymbol{o}_6 - \boldsymbol{o}_1) \quad \boldsymbol{z}_1 \times (\boldsymbol{o}_6 - \boldsymbol{o}_2) \quad \boldsymbol{z}_1 \times (\boldsymbol{o}_6 - \boldsymbol{o}_3)]$$
$$A_2 = [\boldsymbol{z}_4 \quad \boldsymbol{z}_5 \quad \boldsymbol{z}_6]$$

The last three joints do not change the position of $\boldsymbol{o}_6$ and the first three joints axes are parallel, so the frames of the three first joints can be placed such that their origins are collinear (figure 3.2). Then, $\boldsymbol{o}_1, \boldsymbol{o}_2, \boldsymbol{o}_3$ and $\boldsymbol{o}_6$ define a plane π, i.e., there exist $\lambda_1, \lambda_2 \in \mathbb{R}$ such that:

$$\boldsymbol{o}_6 - \boldsymbol{o}_3 = \lambda_1(\boldsymbol{o}_6 - \boldsymbol{o}_1) + \lambda_2(\boldsymbol{o}_6 - \boldsymbol{o}_2)$$

Therefore, by the properties of the cross product, $\det(A_1)$ vanishes.

If the joint axes intersecting at a single point are not the last three, the columns of $J_G(\boldsymbol{q})$ can be exchanged in order to be in the precedent case. This modification will not affect the value of the determinant but its sign.

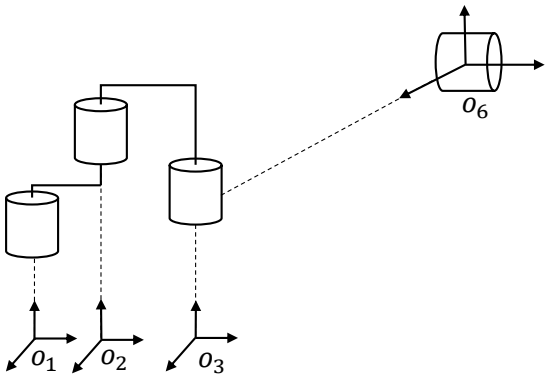

Figure 3.2: Plane generated by points $\boldsymbol{o}_1, \boldsymbol{o}_2, \boldsymbol{o}_3$ and $\boldsymbol{o}_6$

(g) *It possesses two prismatic joints with parallel axes.*

As in statement *(e)*, $J_G(\boldsymbol{q})$ has two identical columns and therefore, its determinant vanishes.

(h) *Number of prismatic joints + number of revolute joints with parallel axes − 1 > 3.*

Let m denote the number of revolute joints with parallel axes. Only the case $m \leq 3$ is considered since when $m > 3$, statement (b) holds. Two different cases should be treated:

1) $m \leq 2$ and there are at least three prismatic joints with axes $\boldsymbol{z}_i, \boldsymbol{z}_j$ and $\boldsymbol{z}_k$. Due to the presence of prismatic joints, there is a zero block in $J_G(\boldsymbol{q})$. Therefore, $\det(J_G(\boldsymbol{q})) = \det(A_1)\det(A_2)$ where

$$\begin{aligned} A_1 &= [\boldsymbol{z}_i \quad \boldsymbol{z}_j \quad \boldsymbol{z}_k] \\ A_2 &= [\boldsymbol{z}_\ell \quad \boldsymbol{z}_r \quad 0] \end{aligned}$$

if $m = 1$, and

$$\begin{aligned} A_1 &= [\boldsymbol{z}_i \quad \boldsymbol{z}_j \quad \boldsymbol{z}_k] \\ A_2 &= [\boldsymbol{z}_\ell \quad \boldsymbol{z}_\ell \quad \boldsymbol{z}_r] \end{aligned}$$

if $m = 2$. In both cases, $\det(A_2)$ clearly vanishes.

2) $m = 3$ and there are at least two prismatic joints with axes $\boldsymbol{z}_i$ and $\boldsymbol{z}_j$. There is not a zero block in $J_G(\boldsymbol{q})$ but, since $m = 3$ a such block can be obtained by simple manipulation over $J_G(\boldsymbol{q})$. It is enough with subtracting two of the three columns associated with the frames attached to the parallel revolute joints. Hence, $\det(J_G(\boldsymbol{q})) = \det(A_1)\det(A_2)$ where:

$$\begin{aligned} A_1 &= [\boldsymbol{z}_\ell \times (\boldsymbol{o}_6 - \boldsymbol{o}_\ell) \quad \boldsymbol{z}_i \quad \boldsymbol{z}_j] \\ A_2 &= [\boldsymbol{z}_\ell \quad \boldsymbol{z}_\ell \quad \boldsymbol{z}_r] \end{aligned} \tag{3.1}$$

As in the precedent case, $\det(A_2)$ vanishes.

$\boxed{\Longleftarrow}$

In order to proof the necessity part of the theorem, $J_G(\boldsymbol{q})$ is split into four order 3 submatrices:

$$J_G(\boldsymbol{q}) = \begin{pmatrix} A_1 & A_2 \\ A_3 & A_4 \end{pmatrix}$$

where A_1 and A_2 are the matrices that relates the contribution of the joints velocity vector to the end-effector linear velocity and A_3 and A_4 are the matrices relating the contribution of the joints velocity vector to the end-effector angular velocity.

The following cases that makes $\det(J_G(\boldsymbol{q})) = 0$ should be distinguished:

(α) A_i is a zero block for some $i = 1, 2, 3$ or 4.

(α.1) A_1 cannot be a zero block because $\boldsymbol{o}_6 \neq \boldsymbol{o}_1$.

(α.2) A_2 is a zero block only when the last three joint axes intersect at a single point. In that situation, $\det(J_G(\boldsymbol{q})) = \det(A_1)\det(A_4)$.
Clearly, since the last three joints have axes intersecting at a single point, $\det(A_4)$ does not vanish globally. Hence, $\det(A_1)$ vanishes. Now, using lemma 3.2.1, the different combinations for the columns of A_1 are studied:

(α.2.1) A_1 has a zero column. If the third one is not zero, then the other two cannot be zero, because $\boldsymbol{o}_6 \neq \boldsymbol{o}_1$ and $\boldsymbol{o}_6 \neq \boldsymbol{o}_2$. If the third column is zero, it means that there is another revolute joint whose axis intersects the other three at the same point. Then, statement (c) holds.

(α.2.2) A_1 has two proportional columns. These columns correspond to: two prismatic joints or two revolute joints or a prismatic joint with a revolute one.
The first case agrees with statement (g). For the second one, let consider that the columns are $\boldsymbol{z}_1 \times (\boldsymbol{o}_6 - \boldsymbol{o}_1)$ and $\boldsymbol{z}_2 \times (\boldsymbol{o}_6 - \boldsymbol{o}_2)$. Since they are proportional:

$$\boldsymbol{z}_1 \perp (\boldsymbol{z}_2 \times (\boldsymbol{o}_6 - \boldsymbol{o}_2)) \Longrightarrow \begin{cases} \boldsymbol{z}_1 = \boldsymbol{z}_2 & \text{or} \\ \boldsymbol{z}_1 = (\boldsymbol{o}_6 - \boldsymbol{o}_2) & \text{or} \\ \boldsymbol{z}_1 = \lambda_1 \boldsymbol{z}_2 + \mu_1(\boldsymbol{o}_6 - \boldsymbol{o}_2) \end{cases} \tag{3.2}$$

Analogously,

$$\boldsymbol{z}_2 \perp (\boldsymbol{z}_1 \times (\boldsymbol{o}_6 - \boldsymbol{o}_1)) \Longrightarrow \begin{cases} \boldsymbol{z}_2 = \boldsymbol{z}_1 & \text{or} \\ \boldsymbol{z}_2 = (\boldsymbol{o}_6 - \boldsymbol{o}_1) & \text{or} \\ \boldsymbol{z}_2 = \lambda_2 \boldsymbol{z}_1 + \mu_2(\boldsymbol{o}_6 - \boldsymbol{o}_1) \end{cases} \tag{3.3}$$

Let suppose that $\boldsymbol{z}_1 \neq \boldsymbol{z}_2$, $\boldsymbol{z}_1 \neq \lambda_1 \boldsymbol{z}_2 + \mu_1(\boldsymbol{o}_6 - \boldsymbol{o}_2)$ and $\boldsymbol{z}_2 \neq \lambda_2 \boldsymbol{z}_1 + \mu_2(\boldsymbol{o}_6 - \boldsymbol{o}_1)$. Then:

$$\begin{aligned} \boldsymbol{z}_1 \times (\boldsymbol{o}_6 - \boldsymbol{o}_1) = \boldsymbol{z}_2 \times (\boldsymbol{o}_6 - \boldsymbol{o}_2) &\Longrightarrow \\ \boldsymbol{z}_1 \times \boldsymbol{z}_2 = \boldsymbol{z}_2 \times \boldsymbol{z}_1 &\Longrightarrow \\ \boldsymbol{z}_1 \times \boldsymbol{z}_2 = -\boldsymbol{z}_1 \times \boldsymbol{z}_2 &\Longrightarrow \\ \boldsymbol{z}_1 \times \boldsymbol{z}_2 = 0 & \end{aligned} \tag{3.4}$$

which leads to a contradiction with $\boldsymbol{z}_1 \neq \boldsymbol{z}_2$. Hence,

$$\begin{cases} \boldsymbol{z}_1 = \boldsymbol{z}_2 \quad \text{or} \\ \boldsymbol{z}_1 = \lambda_1 \boldsymbol{z}_2 + \mu_1(\boldsymbol{o}_6 - \boldsymbol{o}_2) \quad \text{or} \\ \boldsymbol{z}_2 = \lambda_2 \boldsymbol{z}_1 + \mu_2(\boldsymbol{o}_6 - \boldsymbol{o}_1) \end{cases} \tag{3.5}$$

Now, let suppose that $\boldsymbol{z}_1 \neq \lambda_1 \boldsymbol{z}_2 + \mu_1(\boldsymbol{o}_6 - \boldsymbol{o}_2)$ and $\boldsymbol{z}_2 \neq \lambda_2 \boldsymbol{z}_1 + \mu_2(\boldsymbol{o}_6 - \boldsymbol{o}_1)$. Then:

$$\begin{gathered} \boldsymbol{z}_1 \times (\boldsymbol{o}_6 - \boldsymbol{o}_1) = \boldsymbol{z}_2 \times (\boldsymbol{o}_6 - \boldsymbol{o}_2) \Longrightarrow \\ \boldsymbol{z}_1 \times (\boldsymbol{o}_6 - \boldsymbol{o}_1) = \boldsymbol{z}_1 \times (\boldsymbol{o}_6 - \boldsymbol{o}_2) \Longrightarrow \\ \boldsymbol{z}_1 \times (\boldsymbol{o}_2 - \boldsymbol{o}_1) = 0 \end{gathered} \tag{3.6}$$

which implies two possibilities. The first one is $(\boldsymbol{o}_2 - \boldsymbol{o}_1) = 0$, which means that the two joint axes are coincident. Hence, statement (e) holds. The second possibility cannot hold because, since $\boldsymbol{z}_1 = \boldsymbol{z}_2$, $\boldsymbol{z}_1 \neq \boldsymbol{o}_2 - \boldsymbol{o}_1$.

Finally, let suppose that $\boldsymbol{z}_1 = \lambda_1 \boldsymbol{z}_2 + \mu_1(\boldsymbol{o}_6 - \boldsymbol{o}_2)$ and $\boldsymbol{z}_2 = \lambda_2 \boldsymbol{z}_1 + \mu_2(\boldsymbol{o}_6 - \boldsymbol{o}_1)$. Then:

$$\left.\begin{aligned} \boldsymbol{z}_1 = \lambda_1 \boldsymbol{z}_2 + \mu_1(\boldsymbol{o}_6 - \boldsymbol{o}_2) \\ \boldsymbol{z}_2 = \lambda_2 \boldsymbol{z}_1 + \mu_2(\boldsymbol{o}_6 - \boldsymbol{o}_1) \end{aligned}\right\}$$

and by substituting the expressions of $\boldsymbol{z}_1$ and $\boldsymbol{z}_2$ in the precedent identities, the following is obtained:

$$\left.\begin{aligned} \boldsymbol{z}_1 = a_1(\boldsymbol{o}_6 - \boldsymbol{o}_1) + a_2(\boldsymbol{o}_6 - \boldsymbol{o}_2) \\ \boldsymbol{z}_2 = a_3(\boldsymbol{o}_6 - \boldsymbol{o}_2) + a_4(\boldsymbol{o}_6 - \boldsymbol{o}_1) \end{aligned}\right\} \tag{3.7}$$

where

$$\begin{aligned} a_1 &= \lambda_1\mu_2/(1 - \lambda_1\lambda_2) \\ a_2 &= \mu_1/(1 - \lambda_1\lambda_2) \\ a_3 &= \lambda_2\mu_1/(1 - \lambda_1\lambda_2) \\ a_4 &= \mu_2/(1 - \lambda_1\lambda_2) \end{aligned} \tag{3.8}$$

where $1 - \lambda_1\lambda_2 \neq 0$ because, if $\lambda_1\lambda_2 = 1$, then $(\boldsymbol{o}_6 - \boldsymbol{o}_1) = (\boldsymbol{o}_6 - \boldsymbol{o}_2) = 0$. If the proportional columns of A_1 are the first two, there is a contradiction, while if they are the last two, $\boldsymbol{z}_1$ and $\boldsymbol{z}_2$ intersect with the last three joint axes at a single point, and then statement (c) holds. Equation (3.7) implies that $\boldsymbol{z}_1$ and $\boldsymbol{z}_2$ belong to the plane defined by $(\boldsymbol{o}_6 - \boldsymbol{o}_1)$ and $(\boldsymbol{o}_6 - \boldsymbol{o}_2)$. Since $\boldsymbol{z}_1$ and $\boldsymbol{z}_2$ are not parallel, they intersect at a single point. Thus, $\boldsymbol{o}_2 = \boldsymbol{o}_1$ and:

$$\left.\begin{aligned} \boldsymbol{z}_1 = K(\boldsymbol{o}_6 - \boldsymbol{o}_1) \\ \boldsymbol{z}_2 = K'(\boldsymbol{o}_6 - \boldsymbol{o}_1) \end{aligned}\right\}$$

where

$$\begin{aligned} K &= \frac{\lambda_1\mu_2 + \mu_1}{1 - \lambda_1\lambda_2} \\ K' &= \frac{\lambda_2\mu_1 + \mu_2}{1 - \lambda_1\lambda_2} \end{aligned} \tag{3.9}$$

If either K or K' vanishes, then either $\boldsymbol{z}_1 = \lambda_1\lambda_2\boldsymbol{z}_1$ or $\boldsymbol{z}_2 = \lambda_1\lambda_2\boldsymbol{z}_2$ – with $\lambda_1\lambda_2 \neq 1$, which is a contradiction. Therefore $\boldsymbol{z}_2 = (K'/K)\boldsymbol{z}_1$. Now,

- If $K'/K = 1$, there is a contradiction with $\boldsymbol{z}_1 \neq \boldsymbol{z}_2$.
- If $K'/K \neq 1$, there is a contradiction because $\boldsymbol{z}_1, \boldsymbol{z}_2$ are unit vectors.

Finally, the case of a prismatic joint proportional to a revolute one is not possible. Let consider that the two columns are $\boldsymbol{z}_1$ and $\boldsymbol{z}_2 \times (\boldsymbol{o}_6 - \boldsymbol{o}_2)$. If they are proportional, $\boldsymbol{z}_1 \perp \boldsymbol{z}_2$ and $\boldsymbol{z}_1 \perp (\boldsymbol{o}_6 - \boldsymbol{o}_2)$. This is not possible because, due its rotational nature, $\boldsymbol{z}_2$ moves $\boldsymbol{o}_6$ in the Cartesian space, making the vector $\boldsymbol{o}_6 - \boldsymbol{o}_2$ not be orthogonal to $\boldsymbol{z}_1$.

(α.2.3) There is a linear combination between the columns of A_1. The possibilities are: three prismatic joints or three revolute joints or two prismatic joints with a revolute one or two revolute joints with a prismatic one.

First case (three prismatic joints) corresponds to statement (a), while for the second case (three revolute joints), there exist $\lambda_1, \lambda_2, \lambda_3 \in \mathbb{R} \setminus \{0\}$ such that:

$$\lambda_1\boldsymbol{z}_1 \times (\boldsymbol{o}_6 - \boldsymbol{o}_1) + \lambda_2\boldsymbol{z}_2 \times (\boldsymbol{o}_6 - \boldsymbol{o}_2) + \lambda_3\boldsymbol{z}_3 \times (\boldsymbol{o}_6 - \boldsymbol{o}_3) = 0 \tag{3.10}$$

Different cases should be distinguished:

- $\boldsymbol{z}_1 = \boldsymbol{z}_2$ or $\boldsymbol{z}_1 = \boldsymbol{z}_3$ or $\boldsymbol{z}_2 = \boldsymbol{z}_3$. Let suppose, without loss of generality, that $\boldsymbol{z}_1 = \boldsymbol{z}_2$. Then, by the linearity of the cross product:

  $$\boldsymbol{z}_1 \times (\lambda_1(\boldsymbol{o}_6 - \boldsymbol{o}_1) + \lambda_2(\boldsymbol{o}_6 - \boldsymbol{o}_2)) + \lambda_3\boldsymbol{z}_3 \times (\boldsymbol{o}_6 - \boldsymbol{o}_3) = 0,$$

  where $\lambda_1(\boldsymbol{o}_6 - \boldsymbol{o}_1) + \lambda_2(\boldsymbol{o}_6 - \boldsymbol{o}_2)$ can be seen as a position vector of the form $\boldsymbol{o}_6 - \boldsymbol{o}$ for certain $\boldsymbol{o} \in \mathbb{R}^3$. As a consequence, this case is analogous to the case of two proportional columns corresponding to two revolute joints, that corresponds to statement (e).
- $\boldsymbol{z}_1 = \boldsymbol{z}_2 = \boldsymbol{z}_3$. This identity corresponds to three parallel revolute joint axes, that agrees with statement (f).
- $\boldsymbol{o}_1 = \boldsymbol{o}_2$ or $\boldsymbol{o}_1 = \boldsymbol{o}_3$ or $\boldsymbol{o}_2 = \boldsymbol{o}_3$. Reasoning as before, it can be deduced that this case is analogous to the case of two proportional columns corresponding to two revolute joints, i.e., statement (e).
- $\boldsymbol{o}_1 = \boldsymbol{o}_2 = \boldsymbol{o}_3$. This identity correspond to three revolute joints whose axes intersect at a single point. Then, statement (d) holds.
- $\boldsymbol{z}_1 \neq \boldsymbol{z}_2 \neq \boldsymbol{z}_3$ and $\boldsymbol{o}_1 \neq \boldsymbol{o}_2 \neq \boldsymbol{o}_3$. Due to the rotational nature of these joints, there is no linear combination between $\boldsymbol{z}_1, \boldsymbol{z}_2, \boldsymbol{z}_3$. Therefore, they conform a linearly independent set of vectors that spans $\mathbb{R}^3$ and, thus:

  $$\left.\begin{aligned} \boldsymbol{o}_6 - \boldsymbol{o}_1 &= a_{11}\boldsymbol{z}_1 + a_{12}\boldsymbol{z}_2 + a_{13}\boldsymbol{z}_3 \\ \boldsymbol{o}_6 - \boldsymbol{o}_2 &= a_{21}\boldsymbol{z}_1 + a_{22}\boldsymbol{z}_2 + a_{23}\boldsymbol{z}_3 \\ \boldsymbol{o}_6 - \boldsymbol{o}_3 &= a_{31}\boldsymbol{z}_1 + a_{32}\boldsymbol{z}_2 + a_{33}\boldsymbol{z}_3 \end{aligned}\right\}$$

  where $a_{ij} \in \mathbb{R}$.

  By the linearity of the cross product, (3.10) changes into:

$$(\lambda_1 a_{12} - \lambda_2 a_{21})\boldsymbol{z}_1 \times \boldsymbol{z}_2 + (\lambda_1 a_{13} - \lambda_3 a_{31})\boldsymbol{z}_1 \times \boldsymbol{z}_3 + (\lambda_2 a_{23} - \lambda_3 a_{32})\boldsymbol{z}_2 \times \boldsymbol{z}_3 = 0$$

that is equivalent to:

$$\boldsymbol{z}_1 \times ((\lambda_1 a_{12} - \lambda_2 a_{21})\boldsymbol{z}_2 + (\lambda_1 a_{13} - \lambda_3 a_{31})\boldsymbol{z}_3) + (\lambda_2 a_{23} - \lambda_3 a_{32})\boldsymbol{z}_2 \times \boldsymbol{z}_3 = 0$$

which implies that $\boldsymbol{z}_1 \perp \boldsymbol{z}_2 \times \boldsymbol{z}_3$. This is impossible due to the rotational nature of their associated joints.

For the case of two prismatic joints with a revolute one, let consider that the columns of A_1 are $\boldsymbol{z}_1$, $\boldsymbol{z}_2$ and $\boldsymbol{z}_3 \times (\boldsymbol{o}_6 - \boldsymbol{o}_3)$. Let suppose, without loss of generality, that there exist $\lambda_1, \lambda_2, \lambda_3 \in \mathbb{R}$ such that

$$\lambda_1 \boldsymbol{z}_1 + \lambda_2 \boldsymbol{z}_2 + \lambda_3 \boldsymbol{z}_3 \times (\boldsymbol{o}_6 - \boldsymbol{o}_3) = 0 \tag{3.11}$$

As a consequence,

$$(\boldsymbol{o}_6 - \boldsymbol{o}_3) \perp (\lambda_1 \boldsymbol{z}_1 + \lambda_2 \boldsymbol{z}_2) \tag{3.12}$$

Since $\boldsymbol{z}_3$ moves $\boldsymbol{o}_6$ in Cartesian space, $(\boldsymbol{o}_6 - \boldsymbol{o}_3)$ cannot be orthogonal to $(\lambda_1 \boldsymbol{z}_1 + \lambda_2 \boldsymbol{z}_2)$.
Finally, for the case of two revolute joints with a prismatic one, let consider that the columns of A_1 are $\boldsymbol{z}_1$, $\boldsymbol{z}_2 \times (\boldsymbol{o}_6 - \boldsymbol{o}_2)$ and $\boldsymbol{z}_3 \times (\boldsymbol{o}_6 - \boldsymbol{o}_3)$. Let suppose that there exist $\lambda_1, \lambda_2 \in \mathbb{R}$ such that

$$\boldsymbol{z}_1 = \lambda_1 \boldsymbol{z}_2 \times (\boldsymbol{o}_6 - \boldsymbol{o}_2) + \lambda_2 \boldsymbol{z}_3 \times (\boldsymbol{o}_6 - \boldsymbol{o}_3) \tag{3.13}$$

Since $\boldsymbol{z}_2 \times (\boldsymbol{o}_6 - \boldsymbol{o}_2)$ and $\boldsymbol{z}_3 \times (\boldsymbol{o}_6 - \boldsymbol{o}_3)$ belong to the same plane and are not parallel, they intersect at a single point. Their normal planes, π_2 and π_3, intersect at a single line, $\pi_2 \cap \pi_3$. The joint axes $\boldsymbol{z}_2$ and $\boldsymbol{z}_3$ belong to π_2 and π_3 respectively and are not parallel because if they were parallel, $\boldsymbol{z}_1 \perp \boldsymbol{z}_2$ and $\boldsymbol{z}_1 \perp (\boldsymbol{o}_6 - \boldsymbol{o}_2) \times (\boldsymbol{o}_6 - \boldsymbol{o}_3)$, and these two conditions cannot hold simultaneously due to the rotational nature of the joints. Now,

- $\boldsymbol{z}_2$ and $\boldsymbol{z}_3$ intersect at a single point (that belongs to the line $\pi_2 \cap \pi_3$) or
- $\boldsymbol{z}_2$ ($\boldsymbol{z}_3$) is parallel to $\pi_2 \cap \pi_3$ and $\boldsymbol{z}_3$ ($\boldsymbol{z}_2$) intersects $\pi_2 \cap \pi_3$.

The second possibility can be reduced to the first one by redefining π_3 as the normal plane to $\boldsymbol{z}_3$ such that $\boldsymbol{z}_2 = \pi_2 \cap \pi_3$. As $\boldsymbol{z}_2$ and $\boldsymbol{z}_3$ intersect at a single point, $\boldsymbol{o}_2 = \boldsymbol{o}_3$ (figure 3.3) and identity (3.13) remains as:

$$\boldsymbol{z}_1 = \lambda_1 \boldsymbol{z}_2 \times (\boldsymbol{o}_6 - \boldsymbol{o}_2) + \lambda_2 \boldsymbol{z}_3 \times (\boldsymbol{o}_6 - \boldsymbol{o}_2),$$

which implies

$$\boldsymbol{z}_1 = (\lambda_1 \boldsymbol{z}_2 + \lambda_2 \boldsymbol{z}_3) \times (\boldsymbol{o}_6 - \boldsymbol{o}_2) \Longrightarrow \begin{cases} \boldsymbol{z}_1 \perp (\lambda_1 \boldsymbol{z}_2 + \lambda_2 \boldsymbol{z}_3) \\ \boldsymbol{z}_1 \perp (\boldsymbol{o}_6 - \boldsymbol{o}_2) \end{cases} \tag{3.14}$$

which is impossible.

(α.3) A_3 is a zero block only when the first three joints are prismatic. In that situation, $\det(J_G(\boldsymbol{q})) = \det(A_1)\det(A_4)$.

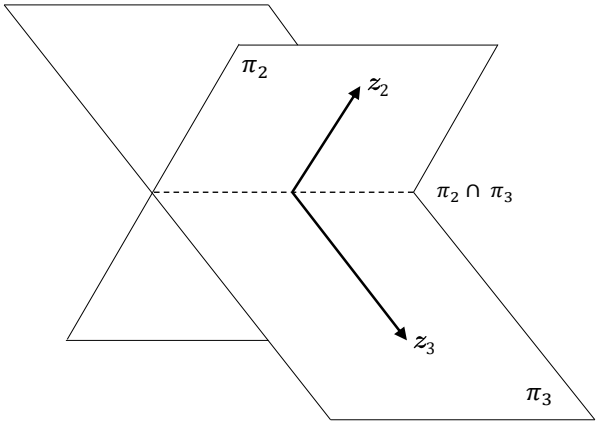

Figure 3.3: Intersection of planes π_2 and π_3

(α.3.1) A_1 has null determinant only when two columns are proportional, that is related to two prismatic joints with parallel axes – statement (g) – or when there is a linear combination between the three columns, that is related to three coplanar prismatic joints – statement (a).

(α.3.2) A_4 has null determinant only when there is a zero column or when two columns are proportional. The first situation corresponds to four prismatic joints, that agrees with statement (h). The second situation corresponds to two revolute joints with parallel or coincident axes, that agrees with statements (h) and (e), respectively. If the axes are not pairwise parallel, there is no linear combination between the three columns due to the rotational nature of the associated revolute joints.

(α.4) A_4 is a zero block only when the last three joints are prismatic. This case is completely analogous to the precedent one.

(β) $A_1|A_2$ or $A_3|A_4$ do not contain a zero block but elementary operations can be made over them to obtain one.
Since they do not contain zero blocks, the robot has no more than two prismatic joints.

(β.1) No elementary operations can modify $A_1|A_2$ to obtain a zero block due to the presence of at least four revolute joints.

(β.2) Since the columns of $A_3|A_4$ are either zero columns (for prismatic joints) or revolute joint axes (for revolute joints), there cannot be a linear combination between the non zero columns, as it has been reasoned before. Then, $A_3|A_4$ can be modify to obtain a zero block in the following cases:

(β.2.1) There are two zero columns and two equal columns. This case corresponds to two prismatic joints and two revolute joints with parallel axes. Let suppose that the prismatic joint axes are $\boldsymbol{z}_5$ and $\boldsymbol{z}_6$ and the parallel revolute joint axes are $\boldsymbol{z}_3$ and $\boldsymbol{z}_4$. Then,

$$\det(J_G(\boldsymbol{q})) = \det(A_2)\det(A_3),$$

with:

$$\begin{aligned} A_2 &= [\boldsymbol{z}_3 \times (\boldsymbol{o}_3 - \boldsymbol{o}_4) \quad \boldsymbol{z}_5 \quad \boldsymbol{z}_6] \\ A_3 &= [\boldsymbol{z}_1 \quad \boldsymbol{z}_2 \quad \boldsymbol{z}_3] \end{aligned} \tag{3.15}$$

Lemma 3.2.1 is applied to both A_2 and A_3. For A_3, the proportionality of two columns is translated into the parallelism of two revolute joints. Hence, statement (h) holds. There cannot be a linear combination between the columns of A_3 due to the rotational nature of their associated joints.

For A_2, if $\boldsymbol{z}_5$ and $\boldsymbol{z}_6$ are proportional, statement (g) holds. The rest of cases described in lemma 3.2.1 are not possible for this submatrix.

(β.2.2) There are a zero column and three equal columns. This case corresponds to a prismatic joint and three revolute ones with parallel axes. Let assume that the prismatic joint axis is $\boldsymbol{z}_6$ and the parallel revolute joint axes are $\boldsymbol{z}_1, \boldsymbol{z}_2$ and $\boldsymbol{z}_3$. Therefore,

$$\det(J_G(\boldsymbol{q})) = \det(A_2)\det(A_3),$$

with:

$$\begin{aligned} A_2 &= [\boldsymbol{z}_3 \times (\boldsymbol{o}_3 - \boldsymbol{o}_4) \quad \boldsymbol{z}_3 \times (\boldsymbol{o}_3 - \boldsymbol{o}_5) \quad \boldsymbol{z}_6] \\ A_3 &= [\boldsymbol{z}_1 \quad \boldsymbol{z}_2 \quad \boldsymbol{z}_3] \end{aligned} \tag{3.16}$$

A_2 only vanishes when the two revolute joint axes are proportional. This happens only if $\boldsymbol{o}_4 = \boldsymbol{o}_5$, that corresponds to statement (e).
A_3 has null determinant in the same situations that the precedent case. The case of proportional columns also corresponds to statement (b).

(β.2.3) There are at least four equal columns. This case corresponds to at least four parallel revolute joints, which agrees with statement (b).

(γ) There is not a zero block in $J_G(\boldsymbol{q})$ and no elementary operations allow to obtain one.
Due to the structure of the Jacobian matrix, only the following situations are possible: there are two prismatic joints with parallel axes, that correspond to statement (g) and there are two revolute joints with coincident axes which correspond to statement (e).

□

Combining this theorem with Heiss's theorem, it can be deduced:

Corollary 3.2.3. *A serial robot of 6 DOF is globally degenerated if, and only if,* $\det(J_G(\boldsymbol{q})) = 0$ *for every* $\boldsymbol{q} \in \mathcal{C}$.

Nevertheless, this corollary can be obtained without considering theorem 3.1.1. For that purpose, the following set of definitions and results are required (Munkres, 2000):

Definition 3.2.4. Let (X, τ) be a topological space. $Y \subset X$ is said to be a *connected* subset of X if there is no two disjoint open sets $A, B \in \tau$ such that $Y = A \cup B$.

Definition 3.2.5. Let (X, τ) be a topological space. $Y \subset X$ is said to be *path-connected* if for any two distinct points $x_1, x_2 \in Y$ there exists a continuous path $\alpha : [0, 1] \to Y$ such that $\alpha(0) = x_1$ and $\alpha(1) = x_2$.

Theorem 3.2.6. *Let (X, τ) be a topological space. If a subset $Y \subset X$ is path-connected then is connected.*

Theorem 3.2.7 (Edwards (1973))**.** *Let $f : \mathcal{D} \subset \mathbb{R}^n \to \mathbb{R}$ be a differentiable function with connected domain $\mathcal{D}$. If all partial derivatives $\left(\frac{\partial f}{\partial x_i}\right)_{1 \leq i \leq n}$ vanish in $\mathcal{D}$, then f is constant in its domain.*

Now, some properties can be easily proven:

Proposition 3.2.8. *The configuration space $\mathcal{C}$ of any serial manipulator is connected.*

Proof.
The configuration space $\mathcal{C}$ is a subset of ($\mathbb{R}^n$,τ) where τ denotes the topology induced by the metric (since $\mathbb{R}^n$ is an Euclidean space, its metric is just the distance d_2 (A.23)).

Since the range of each joint variable is an interval of $\mathbb{R}$, $\mathcal{C}$ can be seen as an n-dimensional hypercube inside $\mathbb{R}^n$. Therefore, $\mathcal{C}$ is path-connected and, by theorem 3.2.6, $\mathcal{C}$ is also connected. □

Lemma 3.2.9. $\det(J_A(\boldsymbol{q})) = 0$ *if and only if* $\det(J_G(\boldsymbol{q})) = 0$.

Proof.
Since representation singularities are not associated with any mechanical limitation of the serial robot $\mathcal{R}$, they are not going to be considered. Hence, by proposition B.2.8, there exists a relation between $J_G(\boldsymbol{q})$ and $J_A(\boldsymbol{q})$ that can be established easily:

$$J_G(\boldsymbol{q}) = T(\boldsymbol{x}) J_A(\boldsymbol{q}), \tag{3.17}$$

where, since the representation singularities are not considered, $T(\boldsymbol{x})$ is not singular.

As a consequence:

$$\det(J_G(\boldsymbol{q})) = \det(T(\boldsymbol{x}) J_A(\boldsymbol{q})) = \det(T(\boldsymbol{x})) \det(J_A(\boldsymbol{q}))$$

which gives the desirable result. □

Now, corollary 3.2.3 can be proven without theorem 3.1.1.

Proof.
$\boxed{\Longrightarrow}$

Let consider the six-dimensional vector $\boldsymbol{x}$ that describes the end-effector pose in the operational space $\mathcal{X}$ (as defined in section B.2):

$$\boldsymbol{x}(\boldsymbol{q}) = (p_x(\boldsymbol{q})\ p_y(\boldsymbol{q})\ p_z(\boldsymbol{q})\ \phi(\boldsymbol{q})\ \theta(\boldsymbol{q})\ \psi(\boldsymbol{q})),$$

where $(p_x(\boldsymbol{q}), p_y(\boldsymbol{q}), p_z(\boldsymbol{q}))$ is the position vector that describes the end-effector position and $(\phi(\boldsymbol{q}), \theta(\boldsymbol{q}), \psi(\boldsymbol{q}))$ is a set of Euler angles describing the end-effector orientation.

If the manipulator is globally degenerated, then its number of CDF is 5 at the most. Hence, either one translation/rotation cannot be executed or it is not an independent translation/rotation (i.e., it can be expressed as a function of the others translations and rotations). Suppose that one of the translations cannot be executed or it is not independent (the case of a rotation is completely analogous).

Therefore, the corresponding component of the position vector is constant or a function of the other components. For the first case, $p_i(\boldsymbol{q}) \equiv K$ for $i = x, y$ or z. When the analytic Jacobian J_A is calculated, a zero row will appear in one of the first three rows for any given configuration:

$$J_A(\boldsymbol{q}) = \begin{pmatrix} \frac{\partial p_x}{\partial q_1} & \cdots & \frac{\partial p_x}{\partial q_6} \\ 0 & \cdots & 0 \\ \vdots & \vdots & \vdots \\ \frac{\partial \psi}{\partial q_1} & \cdots & \frac{\partial \psi}{\partial q_6} \end{pmatrix}$$

For the second case, let suppose that $p_i(\boldsymbol{q}) = f(p_k(\boldsymbol{q}), p_\ell(\boldsymbol{q}))$ where f is a differentiable function and $\{i, k, \ell\}$ is a permutation of the set of indexes $\{x, y, z\}$. If f also depends on other components, the reasoning is completely analogous. Now, by applying the chain rule, the following is obtained:

$$\frac{\partial p_i}{\partial q_j} = \frac{\partial f}{\partial p_k} \cdot \frac{\partial p_k}{\partial q_j} + \frac{\partial f}{\partial p_\ell} \cdot \frac{\partial p_\ell}{\partial q_j}$$

Hence, the analytical Jacobian is:

$$J_A(\boldsymbol{q}) = \begin{pmatrix} \frac{\partial p_x}{\partial q_1} & \cdots & \frac{\partial p_x}{\partial q_6} \\ \vdots & \vdots & \vdots \\ \frac{\partial p_i}{\partial q_1} & \cdots & \frac{\partial p_i}{\partial q_6} \\ \vdots & \vdots & \vdots \\ \frac{\partial \psi}{\partial q_1} & \cdots & \frac{\partial \psi}{\partial q_6} \end{pmatrix} = \begin{pmatrix} \frac{\partial p_x}{\partial q_1} & \cdots & \frac{\partial p_x}{\partial q_6} \\ \vdots & \vdots & \vdots \\ \boxed{\frac{\partial f}{\partial p_k} \cdot \frac{\partial p_k}{\partial q_j} + \frac{\partial f}{\partial p_\ell} \cdot \frac{\partial p_\ell}{\partial q_1} \quad \cdots \quad \frac{\partial f}{\partial p_k} \cdot \frac{\partial p_k}{\partial q_j} + \frac{\partial f}{\partial p_\ell} \cdot \frac{\partial p_\ell}{\partial q_6}} \\ \vdots & \vdots & \vdots \\ \frac{\partial \psi}{\partial q_1} & \cdots & \frac{\partial \psi}{\partial q_6} \end{pmatrix}$$

where, clearly, the boxed row is a combination of other rows for any given configuration.

Therefore, in both cases $\det(J_A(\boldsymbol{q})) = 0$ and, by lemma 3.2.9, also $\det(J_G(\boldsymbol{q}))$ vanishes globally.

$\boxed{\Longleftarrow}$

By lemma 3.2.9, $\det(J_A(\boldsymbol{q})) = 0$. Now, two different situations can arise: $J_A(\boldsymbol{q})$ has a zero row or no row of $J_A(\boldsymbol{q})$ is null.

For the first case, let suppose that the zero row is one of the first three rows (again, the other cases are completely analogous). Then, $\frac{\partial p_i}{\partial q_j} \equiv 0$ for every $j = 1, \ldots, 6$.

Since $\mathcal{C}$ is connected, $p_i(\boldsymbol{q}) \equiv K$ for a constant $K \in \mathbb{R}$ by theorem 3.2.7. Hence, a component of the end-effector's position does not change in the whole workspace. Therefore, the number of CDF is 5 at the most and the manipulator is globally degenerated.

Conversely, if every row of $J_A(\boldsymbol{q})$ is non-null, then there exists a relation between the rows of $J_A(\boldsymbol{q})$ – given by a differentiable function f. This relation is translated into a relation between the components of the linear and angular velocity vectors that, in turn, defines a relation between the position and orientation components of the pose vector $\boldsymbol{x}(\boldsymbol{q})$. Therefore, such component is not independent and, as a result, the number of CDF is 5 at the most. □

3.3 Globally degenerated manipulators with less than 6 DOF

The concept of being globally degenerated used in this chapter has only been associated with serial manipulators of 6 DOF. Freund and Weber (1985) consider that every serial robot with less than 6 DOF is globally degenerated by definition, but if the Cartesian degrees of freedom are considered, the concept can be adapted to robots with less than 6 DOF in order to extend the results presented in the previous section.

Definition 3.3.1. A serial robot $\mathcal{R}$ of n DOF, with $n < 6$, is said to be *globally degenerated* if its number of Cartesian degrees of freedom (CDF) is strictly lower than n. At least one of the independent translations and rotations its end-effector could perform cannot be executed or is a function of the other independent translations and rotations.

The first objective is to obtain a characterization in the line of corollary 3.2.3. For that purpose, an auxiliary lemma is requested:

Lemma 3.3.2. *$\rho(J_A(\boldsymbol{q})) = n$ if, and only if, $\rho(J_G(\boldsymbol{q})) = n$.*

Proof.
The proof is completely analogous to the proof of lemma 3.2.9. □

Theorem 3.3.3. *A serial robot $\mathcal{R}$ of n DOF, with $n < 6$, is globally degenerated if and only if $\rho(J_G(\boldsymbol{q})) < n$ for every $\boldsymbol{q} \in \mathcal{C}$.*

Proof.
$\boxed{\Longrightarrow}$

One of the n translations or rotations is either a function of the other components or cannot be executed by the end-effector. In both cases, elementary operations can be made in $J_A(\boldsymbol{q})$ to obtain a zero row. Besides, since $n < 6$, elementary operations can be made in $J_A(\boldsymbol{q})$ to obtain an additional set of $6 - n$ zero rows.

Since there are $(6 - n) + 1$ zero rows, the rank of J_A is $6 - ((6 - n) + 1) = n - 1$ at most, which is strictly lower than n. Using lemma 3.3.2, it can be deduced that $\rho(J_G(\boldsymbol{q}))$ is also strictly lower than n.

$\boxed{\Longleftarrow}$

If $\rho(J_G(\boldsymbol{q})) < n$ then, by lemma 3.3.2, $\rho(J_A(\boldsymbol{q})) < n$. As a result, elementary operations can be done in order to obtain more than $6 - n$ zero rows in J_A. This implies that there are more than $6-n$ components of the linear and angle variation velocity vectors that are zero. Exactly $6-n$ of these zero rows correspond to the DOF that the manipulator does not have. The remaining zero rows correspond, by theorem 3.2.7, either to a constant component of the end-effector's pose or to a function of these components. Therefore, an independent translation or rotation cannot be produced and the manipulator is globally degenerated by definition. □

Now, the relation between non-globally degenerated robots and their kinematics subchains is presented:

Theorem 3.3.4. *A serial manipulator $\mathcal{R}$ of 6 DOF that is not globally degenerated has not a globally degenerated subchain of 5 DOF.*

Proof.
Since $\mathcal{R}$ is not globally degenerated, $\det(J_G(\boldsymbol{q})) \neq 0$ for every $\boldsymbol{q} \in \mathcal{C}$.

Suppose now, by reductio ad absurdum, that there exists a subchain of 5 DOF that is globally degenerated. By theorem 3.3.3, the corresponding submatrix of $J_G(\boldsymbol{q})$, $N(\boldsymbol{q})$, has rank strictly lower than 5. Since $N(\boldsymbol{q})$ has order 6×5, this implies that all its minors of order 5 have null determinant. Elementary operations can be done over each one of these minors to obtain a zero row. These zero rows are also in $N(\boldsymbol{q})$ and, therefore, in $J_G(\boldsymbol{q})$. As there is not a common row in

all the minors, there must be at least two different zero rows, that are in both $N(\boldsymbol{q})$ and $J_G(\boldsymbol{q})$.

$$J_G(\boldsymbol{q}) = \overset{\overset{N(\boldsymbol{q})}{\overbrace{\quad\quad\quad\quad\quad}}}{\begin{pmatrix} \bullet & \bullet & \bullet & \bullet & \bullet & \bigstar \\ \bullet & \bullet & \bullet & \bullet & \bullet & \bigstar \\ \bullet & \bullet & \bullet & \bullet & \bullet & \bigstar \\ 0 & 0 & 0 & 0 & 0 & \bigstar \\ \bullet & \bullet & \bullet & \bullet & \bullet & \bigstar \\ 0 & 0 & 0 & 0 & 0 & \bigstar \\ \bullet & \bullet & \bullet & \bullet & \bullet & \bigstar \end{pmatrix}}$$

With independence of the value that takes $\bigstar$ in these two zero rows, it is clear that they are proportional, which implies that $\rho(J_G(\boldsymbol{q})) < 6$. That gives the desired contradiction. □

Corollary 3.3.5. *A non-globally degenerated serial robot $\mathcal{R}$ of n DOF, with $n \leq 6$, has not a globally degenerated subchain of m DOF, with $m < n$.*

3.4 Application to some redundant robots

To show the advantages of the results presented in this chapter, some examples are developed in this section. All the robots selected are redundant. As stated in section 3.1, the purpose of using redundant manipulators is to provide an application of the results developed in this chapter to the identification of the redundant joints. An interesting goal is to be able to identify those joints that, once fixed at some position, leave a globally degenerated subchain. These joints are important because, due to the losing of motion associated with them, they are not expendable, because the manipulability of the robot will decrease if their joint variables are fixed at some value. Clearly, these joints are not good candidates for being redundant joints. In addition, these examples allow to appreciate the benefits, in terms of efficiency and computing time, of using corollary 3.2.3 instead of theorem 3.1.1. For the computations of these examples, MATLAB R2015a and Maple18 have been used.

3.4.1 Kuka LWR 4+

As state in section B.3.1, Kuka LWR 4+ is an anthropomorphic arm with seven degrees of freedom (figure B.3a). For computing the globally degenerated subchains just the D-H parameters are required (table B.1). Once $J_G(\boldsymbol{q})$ is derived, an iterative algorithm computes the determinant of the submatrices obtained by fixing one of the columns in each iteration.

From the seven different subchains that can be obtained from the original chain, just one is globally degenerated. This subchain is the result of fixing the fourth joint and verifies the Heiss's criteria. The six non-fixed revolute joints form two groups whose axes intersect at a single point, which corresponds with statement (d). While joints 1,2,3,5,6 and 7 may be dispensable, joint 4

is not expendable. However, since Kuka LWR 4+ has a spherical wrist, the last three joints are also of special importance for kinematics, as explained in chapter 2.

3.4.2 Stäubli TX90 mounted on a translational motion unit

Stäubli TX90 is an industrial manipulator with six degrees of freedom and spherical wrist. This robot has been mounted on a linear track, that can be seen as an additional prismatic joint (figure B.4a and table B.2). As in the precedent example, once $J_G(\boldsymbol{q})$ is calculated, the iterative algorithm is applied in order to find out the globally degenerated kinematic subchains. No one of the seven obtained subchains is globally degenerated. That means that adding a prismatic joint at the beginning of Stäubli TX90 does not affect its number of Cartesian degrees of freedom.

Moreover, due to the properties of determinants, if the prismatic joint is placed between any two joints of the original robot, the result will be the same. That means that for every redundant manipulator that results from the addition of a prismatic joint to the Stäubli TX90 there will not be globally degenerated subchains. Therefore, the characterization introduced in this chapter allows an easy study of a family of redundant manipulators, while it will be highly difficult if done using theorem 3.1.1 (the study should cover eight different redundant manipulators with seven kinematic subchains each one).

3.4.3 Barcelona Mobile Manipulator

The Barcelona Mobile Manipulator (BMM) is an omnidirectional mobile platform with spherical wheels carrying a standard arm manipulator (figure B.7).

Since BMM has ten degrees of freedom, there exists $C(10, 6) = 210$ different kinematic subchains of 6 DOF. Applying the iterative algorithm, 24 globally degenerated subchains are obtained. Each one of these globally degenerated subchains corresponds to one of the eight statements of the Heiss's criteria. For example, if the first three joints are considered as the ones that correspond to the three degrees of freedom of the platform, the set of joints $\{1, 2, 3, 8, 9, 10\}$ gives rise to a globally degenerated manipulator that corresponds to statement (d) of theorem 3.1.1.

Studying the 210 different subchains and comparing each one of them to the Heiss's geometric criteria is expensive in terms of time and computation, while using the characterization provided in this chapter has proven to be faster and easier.

Chapter 4

Inverse Kinematics of Redundant Manipulators

Problems worthy of attack prove their worth by fighting back

Piet Hein

In this chapter, a novel strategy to solve the inverse kinematics of redundant robots is presented. In this strategy, redundant manipulators are reduced to non-redundant ones by selecting a set of joints, denoted *redundant joints*, and parametrizing its joint variables. This selection is made through a workspace analysis which also provides an upper bound for the number of different families of solutions of the inverse kinematics for a given end-effector pose. Once the redundant joints have been identified, several closed-form methods developed for non-redundant manipulators can be applied to obtain the analytical solutions. Finally, particular instances for the parametrized joints variables are determined depending on the task to be executed. Different criteria and optimization functions can be defined for that purpose.

4.1 Problem statement

As stated in section 2.1.1, the importance of the inverse kinematic problem relies on its role in the programming and control of serial robots. Besides, this problem becomes of great significance for redundant manipulators because, existing an infinite number of solutions for a

particular end-effector pose, several manipulability measures can be defined for selecting one of them. Among all the methods presented in section 2.1, closed-form methods are the most suitable for redundant robots as they allow to obtain the set of all solutions with a small computational cost. In this chapter, a novel method for deriving all the solutions for the inverse kinematics of redundant serial robots is proposed. These solutions are given as m-parameter families of functions depending on the end-effector' pose (recall that m denotes the rotational degrees of redundancy, as defined in B.2.5). Redundant robots are reduced to non-redundant ones through the parametrization of a set of joint variables, called *redundant joints*. The selection of such joints is crucial and is performed using global rank-deficiency conditions of the Jacobian matrix and an analysis of the workspace properties such as shape, area and volume. Once the redundant robot has been reduced to a non-redundant one, several closed-form methods developed for non-redundant robots can be applied.

First mentions of redundant joints are found in (Hollerbach, 1985; Judd and Van Til, 1985; Luh and Gu, 1985; Stanisic and Pennock, 1985; Schwartz and Doty, 1988; Cheng et al., 2010; Tokarz and Kieltyka, 2010). In these papers, a redundant manipulator is designed from a known non-redundant one. In this context, the authors assume that the added joint is the redundant one. Hemami (1988) derives several families of solutions for an anthropomorphic manipulator by fixing the different joint variables at an arbitrary value. Following that idea, in (Schrake et al., 1990, 1991) the authors develop a criterion based on Heiss theorem 3.1.1 for discarding some of these joints as redundant joints. Heiss theorem 3.1.1 provides a geometrical characterization of globally degenerated non-redundant robots. However, since this characterization cannot be implemented easily, in chapter 3 an easy to implement characterization of globally degenerated manipulators is implemented. Such characterization (depicted as corollary 3.2.3) is based on the global rank-deficiency of J_G. The criterion developed in (Schrake et al., 1990) consists of discarding as redundant those joints that, once their joint variables are fixed at some value, leave a globally degenerated non-redundant manipulator.

As shown in section 3.4, if this criterion is applied to anthropomorphic manipulators, just the fourth joint should be discarded as an option for being the redundant joint. Then, with the remaining joints, the idea collected in (Hemami, 1988) is applied for obtaining the different families of solutions for the anthropomorphic manipulator. The main drawback of these approaches relies on the high number of solution families obtained for each pose. While Hemami (1988) develops four one-parameter families of solutions for a 7 DOF anthropomorphic manipulator, the approach followed by Schrake et al. (1990) computes up to six one-parameter families of solutions for the same manipulator. The use of either of these solution families depends on the task executed. If, instead of considering a 7 DOF redundant manipulator, a 8 DOF robot is considered, there will be up to $C(8,2) = 28$ 2-parameter families of solutions. In general, for an n DOF redundant manipulator there will be up to $C(n,r)$ r-parameter families of solutions (where r denotes the number of degrees of redundancy (as defined in B.2.5)). This large set of solutions increases the difficulties for selecting one of them for each particular pose.

On the other hand, Lee and Bejczy (1991) proposed a selection of redundant joints based on the null space range of each joint, while Podhorodeski et al. (1991) base their selection on the null space of the Jacobian matrix. These approaches turn to be impractical due to their

computational cost. Besides, their implementation become extremely difficult for robots with more than one degree of redundancy. The approaches collected in (Diankov, 2010; Heiss, 1993; Kauschke, 1996; Lau and Wai, 2002; Tatum et al., 2015) are focused on developing strong and general closed-form methods for non-redundant manipulators. In these works redundant joints are selected arbitrarily. Finally, (Jung et al., 2011; Qingmei et al., 2015; Shimizu et al., 2008; Yu et al., 2012) are recent examples of the arm angle parameter use. This parameter, usually denoted by φ, is defined for anthropomorphic manipulators attending to the relation between the shoulder (the three first joints), the elbow (the fourth joint) and the wrist (the three last joints). Therefore, φ can be regarded as a joint variable, and thus, it can be considered as defining the redundant joint. Clearly, this approach is restricted to manipulators of this kind.

The approach given in (Schrake et al., 1990, 1991) is the most interesting and easy to implement. However, as it has been shown above, this approach is not easily generalized for n DOF redundant manipulators. Besides, it does not represent a method for selecting the redundant joints but to discard some of them as candidates. For all these reasons the strategy proposed in this chapter includes such criterion but also presents a workspace analysis with two main objectives: the first objective is to prove that it is enough with a maximum of 2^m m-parameter families of solutions. This number is always much smaller than $C(n, r)$. Besides, each one of these solution families corresponds to a set of m redundant joints. Therefore, this analysis also defines a procedure for identifying the redundant joints. The second objective is to define a criterion for selecting, given a particular pose T, which one of these 2^m families of solutions is the best one to solve the inverse kinematics for T.

Since the crucial point relies on the workspace analysis that is going to be introduced in the following sections, a good representation of such workspace is required. Many authors have dealt with the problem of representing effectively the serial robots workspace: Dong et al. (2013) develop an strategy for the identification of the workspace area of planar serial manipulators, while in (Gupta and Roth, 1982; Lee and Yang, 1983; Yang and Lee, 1983) an iterative process that only works for serial robots with revolute joints is defined. Such method attains the analytical equations of the workspace defining the end-effector as a three dimensional point that is rotated from the n-th joint to the first one. Then, a cross section is obtained by taking $q_1 = 0$. On the other hand, in (Haug et al., 2000; Goyal and Sethi, 2010; Porges et al., 2013) different methods are developed to obtain the boundary surfaces of the workspace of an arbitrary serial robot. Following a similar idea, in (Abdel-Malek and Othman, 1999; Abdel-Malek et al., 1999) the authors define the interior and exterior boundaries of serial manipulators workspace using the singular surfaces achieved from the Jacobian matrix. Then, the total volume of the workspace is calculated using the Divergence Theorem.

4.2 Number of closed-form families of solutions

As mentioned in the preceding section, some authors develop up to four or six families of solutions for the same 7 DOF manipulator. In this section, an upper bound for the number of

different families of solutions is given. It will be proven that is enough with a maximum of 2^m m-parameter families of solutions for an n DOF manipulator.

For simplicity, the following notation will be used in this chapter:

- p denotes the number of prismatic joints of $\mathcal{R}$.
- $\mathcal{W}$ denotes the workspace of $\mathcal{R}$, generated only by its revolute joints.
- $\mathcal{W}_i$ denotes the volume of $\mathcal{W}$ once the joint variable q_i is fixed at some value, i.e, the i-th joint is fixed at some particular position.

The idea is to prove that, given $\mathcal{W}$, one of the two following statement holds:

$$\text{There exists } 2 \leq i \leq n \text{ such that } \mathcal{W}_i = \mathcal{W} \tag{4.1}$$

$$\text{There exist } 2 \leq j \neq k \leq n \text{ such that } \mathcal{W}_j \cup \mathcal{W}_k = \mathcal{W} \tag{4.2}$$

For $n = 7$ (or, equivalently, $m = 1$), if statement (4.1) holds, since $\mathcal{W}_i$ is obtained when the joint i is fixed, the redundant manipulator $\mathcal{R}$ has been reduced to a non-redundant one. The solutions for the inverse kinematics will form a single one-parameter family of solutions depending on q_i. However, if statement (4.2) holds, there will be two different non-redundant reduced manipulators. Therefore, two different one-parameter families of solutions will be obtained (one depending on q_j and the other on q_k).

If, conversely, $n > 7$ (or, equivalently $m > 1$) the process is repeated with $\mathcal{W}_i$ or with $\mathcal{W}_j, \mathcal{W}_k$. The reasoning is exactly the same, since $\mathcal{W}_i, \mathcal{W}_j$ or $\mathcal{W}_k$ can be seen as the workspace of a manipulator of $n - 1$ DOF. The maximum number of subregions of the original workspace that can be obtained for each rotational degree of redundancy is two. So, given the recursiveness of the procedure, the maximum number of subregions of $\mathcal{W}$ will be 2^m. As each one generates a family of solutions, there will be up to 2^m m-parameter families of solutions. By the same reason, the minimum number of different m-parameter families of solutions will be one. Therefore, for any given manipulator $\mathcal{R}$ with n DOF and m rotational degrees of redundancy the number r of different solution families verifies:

$$1 \leq r \leq 2^m.$$

Therefore, it only remains to prove that, for any redundant robot $\mathcal{R}$, either statement (4.1) or statement (4.2) holds.

First of all, since the effect of the prismatic joints in the workspace of $\mathcal{R}$ is just the translation of the volume generated by the following joints and since, given a pose, it is easy to obtain the values of the prismatic joint variables, i.e., the solution of the inverse kinematics for these joints, their joint variables can be fixed at particular instances for allowing the study of $\mathcal{W}$.

Let denote by $\mathcal{R}_{j_1}, \mathcal{R}_{j_2}, \ldots, \mathcal{R}_{j_p}$ the prismatic joints of $\mathcal{R}$. Then, each of their joint variables $d_{j_1}, d_{j_2}, \ldots, d_{j_p}$ move within $[d_{j_{i\text{Low}}}, d_{j_{i\text{Up}}}]$. As $\mathcal{W}$ is generated only by the revolute joints of

$\mathcal{R}$, each d_{j_i} can be fixed at a particular value, selected, for instance, to make $\mathcal{W}$ as compact as possible. Although the values of the prismatic joint variables are, in general, positive, depending on where the world frame is placed, different cases can arise. Such cases are treated as follows:

- $0 \in [d_{j_{i\text{Low}}}, d_{j_{i\text{Up}}}] \Longrightarrow d_{j_i} = 0$.
- $[d_{j_{i\text{Low}}}, d_{j_{i\text{Up}}}] \subset \mathbb{R}^+ \setminus \{0\} \Longrightarrow d_{j_i} = d_{j_{i\text{Low}}}$.
- $[d_{j_{i\text{Low}}}, d_{j_{i\text{Up}}}] \subset \mathbb{R}^- \setminus \{0\} \Longrightarrow d_{j_i} = d_{j_{i\text{Up}}}$.

Since only the revolute joints of $\mathcal{R}$ are going to be considered, let $\boldsymbol{z}_i$ be the first revolute joint of $\mathcal{R}$. Then, $\mathcal{W}$ is a revolving figure around the axis $\boldsymbol{z}_i$ and, as a result, the study of $\mathcal{W}$ can be performed over a $\boldsymbol{x}_i$–$\boldsymbol{z}_i$ cross section of it. For a redundant robot, such cross section is obtained by fixing q_i at a particular value. Besides, it is also necessary to fix other joints like, in particular, all the rotational joints whose axes are not orthogonal to $\boldsymbol{z}_i$. To prove this remark, let suppose that there exists $\boldsymbol{z}_j$ such that $\boldsymbol{z}_j$ and $\boldsymbol{z}_i$ are not mutually orthogonal. If $\boldsymbol{z}_j$ is not fixed, then its rotational action generates a volume that escapes from the section obtained by setting $q_i = k$ (figure 4.1a). Thus, the cross section area is generated by the joints whose axes are orthogonal to $\boldsymbol{z}_i$, while the rest are fixed at particular values. Let s denote the number of joints whose axes are orthogonal to $\boldsymbol{z}_i$. Different cases should be treated:

$\boxed{s = \{0, 1, 2\}}$

There are no joint axes, one joint axis or two joint axes orthogonal to $\boldsymbol{z}_i$. Since $\mathcal{R}$ is redundant, at least there are three, two or one more joints whose variables are fixed – as they are not orthogonal to $\boldsymbol{z}_i$. Two different situations arise: one of the other joint axes is contained in the cross section plane or intersects it. Both cases are treated analogously. Let denote by $\mathcal{SW}$ the cross section area obtained by setting $q_i = k$. Since $s < 3$, there is at least one fixed joint whose axis, $\boldsymbol{z}_j$, intersects $\mathcal{SW}$ not orthogonally. Then, $\mathcal{SW} \subset \mathcal{W}_j$ for some value of q_j. Moreover, if an analogous cross section $\mathcal{SW}_j$ is taken from $\mathcal{W}_j$, then

$$\mathcal{SW}_j = \mathcal{SW} \tag{4.3}$$

Since $\mathcal{W}$ is of revolution around $\boldsymbol{z}_i$, rotating q_i turns (4.3) into $\mathcal{W}_j = \mathcal{W}$ which gives the desirable result.

$\boxed{s \geq 3}$

From $s = 3$, induction over s can be used for completing the proof. Again, two different situations can arise:

- There exists a joint whose axis, $\boldsymbol{z}_k$, is contained in the cross section obtained by setting $q_i = k$ or intersects it (not orthogonally).
- The only revolute joints contributing to position the end-effector are i and the s joints whose axes are orthogonal to $\boldsymbol{z}_i$.

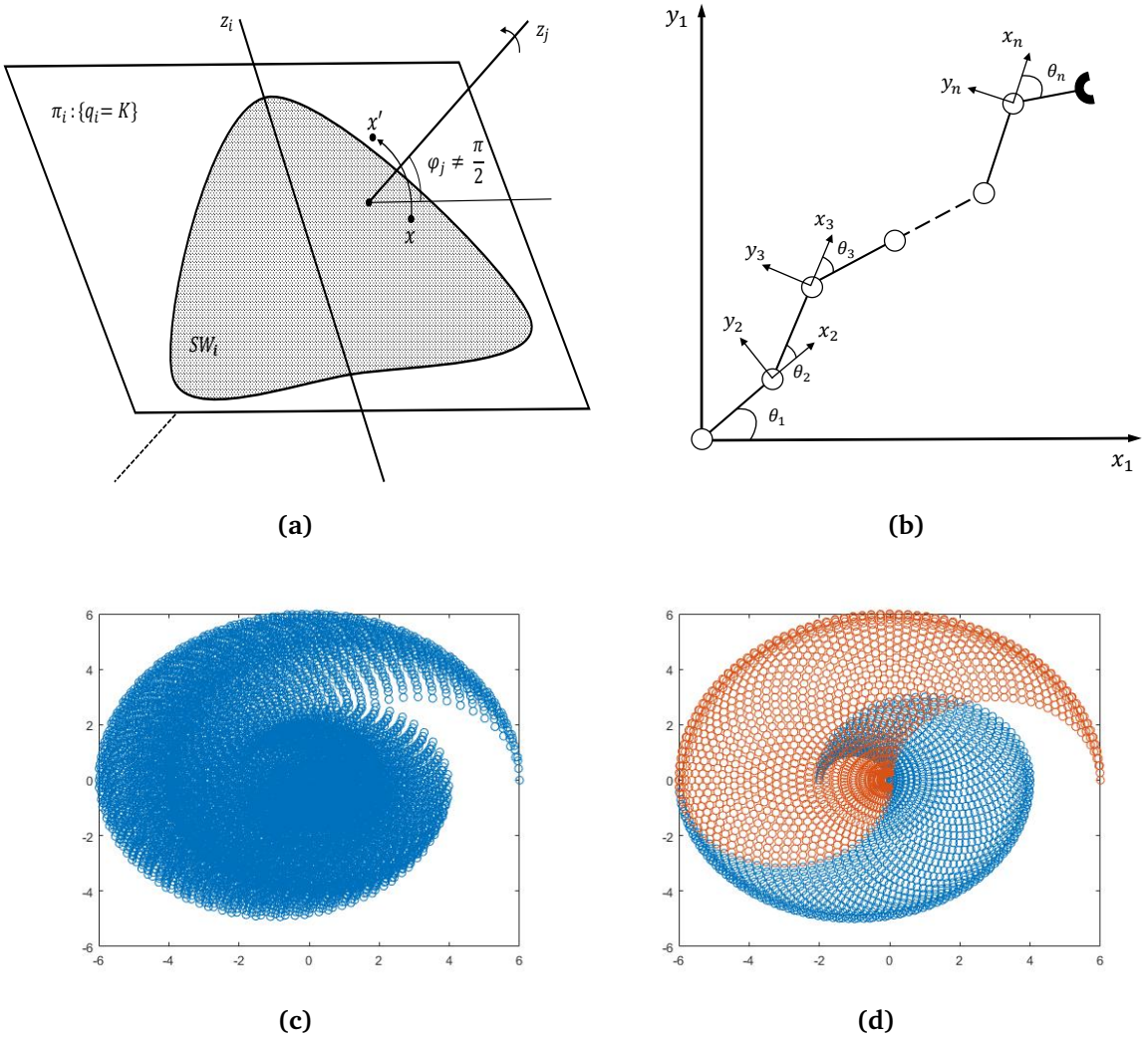

Figure 4.1: (a) Cross section $\mathcal{SW}_i$ of $\mathcal{W}$ for a given value of q_i where an arbitrary point $\boldsymbol{x} \in \mathcal{SW}_i$ under the action of $\boldsymbol{z}_j$ is transformed into $\boldsymbol{x}' \notin \mathcal{SW}_i$; (b) Schematic representation of a planar manipulator; (c) Workspace of the three-link manipulator and (d) Workspace regions after fixing the first two joints.

For the first situation, the previous reasoning can be used to prove that $\mathcal{W}_k = \mathcal{W}$. For the second, it is clear that $\mathcal{SW}$ is generated by the s joints whose axes are orthogonal to $\boldsymbol{z}_i$ (and, as a result, normal to $\mathcal{SW}$). In particular, if $i_1, \ldots, i_s$ denote these joints and $\mathcal{SW}_{i_j}$ denote the plane section of $\mathcal{SW}$ obtained when the joint i_j is fixed, then

$$\mathcal{SW}_{i_1} \cup \mathcal{SW}_{i_2} \cup \cdots \cup \mathcal{SW}_{i_s} = \mathcal{SW} \tag{4.4}$$

It is sufficient with proving that:

$$\exists i_j, i_k \quad : \quad \mathcal{SW}_{i_j} \cup \mathcal{SW}_{i_k} = \mathcal{SW} \tag{4.5}$$

If so, rotating q_i gives that

$$\mathcal{W}_j \cup \mathcal{W}_k = \mathcal{W},$$

which would complete the proof.

To prove (4.5), let notice that $\mathcal{SW}$ can be seen as the workspace of a s-link planar manipulator (figure 4.1b). Thus, (4.5) is equivalent to prove that the workspace of a s-link planar manipulator can be split in two subregions associated with two fixed joints. This proof will be performed using induction over s.

For $s = 3$, a 3-link planar manipulator is obtained. Figure 4.1c depicts the workspace of an example of a manipulator of this kind. In general, the end effector position vector of a 3-link planar manipulator is:

$$\mathbf{p} = \begin{pmatrix} a_1c_1 + a_2c_{12} + a_3c_{123} \\ a_1s_1 + a_2s_{12} + a_3s_{123} \\ 0 \end{pmatrix},$$

where a_i is the length of link i and $c_1 = \cos(q_{i_1}), s_1 = \sin(q_{i_1}), c_{12} = \cos(q_{i_1} + q_{i_2}), s_{12} = \sin(q_{i_1} + q_{i_2})$ and $c_{123} = \cos(q_{i_1} + q_{i_2} + q_{i_3}), s_{123} = \sin(q_{i_1} + q_{i_2} + q_{i_3})$. Figure 4.1d shows that it is enough with putting together $\mathcal{SW}_{i_1}$ and $\mathcal{SW}_{i_2}$ for obtaining $\mathcal{SW}$. To prove that this is a general result let suppose, by contradiction, that

$$\mathcal{SW}_{i_1} \cup \mathcal{SW}_{i_2} \neq \mathcal{SW}$$

for all the constant values $q_{i_1} = k_1$ and $q_{i_2} = k_2$ of joints i_1 and i_2. Then, there exists $\boldsymbol{x} \in \mathcal{SW}$ such that $\boldsymbol{x} \notin \mathcal{SW}_{i_1}$ and $\boldsymbol{x} \notin \mathcal{SW}_{i_2}$ for all $q_{i_1} = k_1$ and $q_{i_2} = k_2$. Now, by (4.4) $\boldsymbol{x} \in \mathcal{SW}_{i_3}$ for some constant value $q_{i_3} = k_3$. Since the position vector for the 3-link planar manipulator depends on q_{i_1}, q_{i_2} and q_{i_3}, if q_{i_1} (or q_{i_2}) is considered as a parameter, i.e., its value varies in its range, then q_{i_2} (or q_{i_1}) has a particular value for $\boldsymbol{x}$. Then, $\boldsymbol{x} \in \mathcal{SW}_{i_2}$ (or $\boldsymbol{x} \in \mathcal{SW}_{i_1}$), which is a contradiction.

Now, let suppose that the statement holds for s. As in the case of $s = 3$ it is enough to prove that

$$\mathcal{SW}_{i_1}(s+1) \cup \mathcal{SW}_{i_2}(s+1) = \mathcal{SW}(s+1)$$

where the notation $(s+1)$ highlights that the sections belong to a $(s+1)$-link manipulator. Let suppose, again by contradiction, that

$$\mathcal{SW}_{i_1}(s+1) \cup \mathcal{SW}_{i_2}(s+1) \neq \mathcal{SW}(s+1)$$

for all the constant values $q_{i_1} = k_1$ and $q_{i_2} = k_2$. Then, there exists $\boldsymbol{x} \in \mathcal{SW}(s+1)$ such that $\boldsymbol{x} \notin \mathcal{SW}_{i_1}(s+1)$ and $\boldsymbol{x} \notin \mathcal{SW}_{i_2}(s+1)$ for all $q_{i_1} = k_1$ and $q_{i_2} = k_2$. Now, again by (4.4), $\boldsymbol{x} \in \mathcal{SW}_{i_\ell}(s+1)$ for some $3 \leq \ell \leq s+1$ and some constant value $q_{i_\ell} = k_\ell$. Since $\mathcal{SW}_{i_\ell}(s+1)$ can be seen as the workspace of a s-link planar manipulator, the hypothesis of induction implies that $\boldsymbol{x} \in \mathcal{SW}_{i_1}(s)$ or $\boldsymbol{x} \in \mathcal{SW}_{i_2}(s)$ for some constant values $q_{i_1} = k_1$ and $q_{i_2} = k_2$. But now, it is clear that, for the same constant values k_1, k_2:

$$\mathcal{SW}_{i_1}(s) \subset \mathcal{SW}_{i_1}(s+1)$$
$$\mathcal{SW}_{i_2}(s) \subset \mathcal{SW}_{i_2}(s+1)$$

These relations are true for every extension of a s-link planar manipulator to a $(s+1)$-link planar manipulator. In particular, they are true if the extension of the s-link planar manipulator is made to obtain the $(s+1)$-link planar manipulator of the beginning of this part of the proof. Then, $\boldsymbol{x} \in \mathcal{SW}_{i_1}(s+1)$ or $\boldsymbol{x} \in \mathcal{SW}_{i_2}(s+1)$ for the constant values $q_{i_1} = k_1$ and $q_{i_2} = k_2$. This gives the desirable contradiction.

Given that there could be many other joints fixed at some position, this result is not useful for the identification of the redundant joints but to prove the upper bound in the number of different families of solutions. Next section displays the criteria for efficiently selecting the redundant joints.

4.3 Identification of redundant joints

Once it has been proven that there is a maximum of 2^m families of solutions, the criteria for the identification of which joints are the redundant ones are presented. These criteria are based on the global rank-deficiency of the Jacobian matrix and the workspace analysis introduced in the previous section.

If $\mathcal{R}_1, \ldots, \mathcal{R}_n$ denote the joints of a redundant robot $\mathcal{R}$ of n DOF, then not every $\mathcal{R}_i$ is candidate for being a redundant joint. First, a list of conditions for discarding some of these joints is shown. If $\mathcal{R}_i$ meets any condition of the following list it will be discarded as candidate. The workspace analysis is performed over the remaining joints.

List 4.3.1.

- *$\mathcal{R}_i$ is a prismatic joint.*
- *$\mathcal{R}_i$ is one the three joints that conforms a spherical wrist.*
- *$\mathcal{R}_i$ leaves a globally degenerated manipulator when its joint variable is fixed at some value.*

Corollary 3.2.3 provides a simple and easy to implement way of testing the third condition of the list 4.3.1. Algorithm 1 returns, given the geometric Jacobian matrix of $\mathcal{R}$, the joints $\mathcal{R}_{i_1}, \ldots, \mathcal{R}_{i_m}$ that leave a globally degenerated subchain.

Once the joints meeting any condition of the list 4.3.1 are discarded, a workspace analysis is performed over the remaining joints in order to choose the redundant ones. For the sake of simplicity, the analysis is described in detail for the case of one rotational degree of redundancy. After that, it is generalized. The analysis consists of two main steps:

I As explained before, the prismatic joint variables $d_{j_1}, d_{j_2}, \ldots, d_{j_p}$ are fixed (they cannot be the redundant joints). Once they have been fixed, the manipulator is made up of revolute

Algorithm 1 Globally Degeneracy Criterion

Require: $6 \times n$ Jacobian matrix J
Ensure: Integers $i_1, \ldots, i_m$
1: **procedure** GLOBALLY DEGENERACY TEST
2: **for** $1 \leq i \leq n$ **do**
3: $M \leftarrow J[1:6; 1:(i-1), (i+1):n]$
4: **if** M square **then**
5: det $\leftarrow \det(M)$
6: **if** det $==$ 0 **then**
7: return i
8: **else** go to step 2
9: **else** Globally Degeneracy Test$\leftarrow M$

joints. Now, Algorithm 2 generates the swept volume of $\mathcal{W}$ and $\mathcal{W}_1, \ldots, \mathcal{W}_m$. As shown in the precedent section, either there exists i such that $\mathcal{W}_i = \mathcal{W}$ or there exist $j \neq k$ such that $\mathcal{W}_j \cup \mathcal{W}_k = \mathcal{W}$. Graphical visualization allows to deduce which one of these two situations happen for every redundant manipulator $\mathcal{R}$. If it seems that the two situations hold with different joints, then only the case $\mathcal{W}_i = \mathcal{W}$ will be considered since it is the most simple and leads to a single family of solutions.

II To confirm what it has been observed through the graphical visualization, the $\boldsymbol{x}$–$\boldsymbol{z}$ cross section of $\mathcal{W}$ is compared with the $\boldsymbol{x}$–$\boldsymbol{z}$ cross sections of either $\mathcal{W}_i$ or $\mathcal{W}_j$ and $\mathcal{W}_k$. Since $\mathcal{W}$ is a revolving figure around the axis of the first revolute joint, q, the $\boldsymbol{x}$–$\boldsymbol{z}$ cross section can be obtained by setting $q = 0$. This cross section can be obtained through a discretization of the joint variables that are not fixed. Apart from comparing the cross sections, a quantitative analysis based on the area can be performed. As $\mathcal{R}$ is made up of revolute joints, its cross section is composed of circle sectors. Therefore, for a given cross section, the area can be obtained analytically using the expression:

$$A = \sum_i \pi r_i^2 \frac{\alpha_i}{360^\circ} \tag{4.6}$$

where r_i denotes the radius of each circle sector and α_i, its angle in degrees.

However, for some geometric structures it could be difficult to find out the radius or angle of a particular circle sector. For those cases, given a discretization of the cross section, the following numerical expression for the area can be used (Lee and Yang, 1983):

$$A = \sum_{x_{\min}}^{x_{\max}} (z_{\max}(x) - z_{\min}(x))\Delta_x \tag{4.7}$$

where $x_{\min}$ and $x_{\max}$ denote the extreme values of the cross section abscissa, while $z_{\min}$ and $z_{\max}$ denote the extreme values of the ordinate. However, (4.7) works only for convex cross sections without voids. Otherwise, (4.7) changes into the following one:

$$A = \sum_{x_{\min}}^{x_{\max}} (z_{\max}(x) - z_{1\max}(x) - \cdots + z_{\mathrm{L}\max}(x) - z_{\min}(x))\Delta_x \tag{4.8}$$

Algorithm 2 3D Workspace Generation

Require: D-H parameters DH, Forward Kinematics function FK
Ensure: Workspaces $\mathcal{W}, \mathcal{W}_1, \ldots, \mathcal{W}_m$

```
procedure WORKSPACE GENERATION
    cont← 0
    for 1 ≤ i ≤ #DOF do
        if joint i is revolute then
            Δ_i ← discretization q_i
            cont ← cont+1
            if joint i does not meet 4.3.1 then
                I ← i
        else d_i ← 0
    T ←FK(DH)
    P ← Position vector(T)
    W ← P(Δ_1, ..., Δ_cont)
    for i ∈ I do
        q_i ← 0
        T_i ←FK(DH)
        P_i ← Position vector(T_i)
        W_i ← P(Δ_1, ..., Δ_{i-1}, Δ_{i+1}, ..., Δ_cont)
```

where $z_{1\max}(x), \ldots, z_{\mathrm{Lmax}}(x)$ denote the local extreme values of z for each x. When, from the graphical visualization, some $\mathcal{W}_i$ looks equal to $\mathcal{W}$, the areas of both cross sections have to match. On the other hand, if it looks that $\mathcal{W}_j \cup \mathcal{W}_k = \mathcal{W}$ for some $\mathcal{W}_j$ and $\mathcal{W}_k$, then the addition of the area of each cross section have to match the area of $\mathcal{SW}$. As it could happen that $\mathcal{W}_j \cap \mathcal{W}_k \neq \emptyset$, the addition of both areas might not match the area of $\mathcal{SW}$. In this case, given a discretization of each cross section, the area – obtained using either (4.6), (4.7) or (4.8) – of the region conformed by the points that belong to both cross sections has to be subtracted from the addition of the cross sections area of $\mathcal{W}_j, \mathcal{W}_k$. This value has to match the area of $\mathcal{SW}$.

If $\mathcal{W}_i = \mathcal{W}$ for some i, there is only one one-parameter family of solutions. Besides, the redundant joint is the i-th joint. If, however, $\mathcal{W}_j \cup \mathcal{W}_k = \mathcal{W}$ for some $j \neq k$, then there are two families of solutions: one with the j-th joint as the redundant joint and the other with the k-th joint as the redundant joint. Therefore, they are two one-parameter families of solutions.

Finally, in order to summarize the procedure, let consider a serial robot $\mathcal{R}$ of n DOF and m rotational degrees of redundancy. Then, for obtaining the 2^m m-parameter families of solutions, it is proceeded as follows:

- First, the joints meeting any point of the list 4.3.1 are discarded. With the remaining joints the workspace analysis explained before is applied to $\mathcal{W}$. Then, ore or two redundant joint are selected and, therefore, up to two sets of one redundant joint can be defined. If $m = 1$,

each set leads to a one-parameter family of solutions.

- If, conversely, $m > 1$, the process is repeated with the serial robot if $n-1$ DOF obtained from $\mathcal{R}$ after parameterizing the redundant joint (recall that if only one redundant joint has been obtained in the previous step, then only one reduced manipulator of $n-1$ DOF is obtained (with workspace $\mathcal{W}_i$). If, conversely, two different redundant joints have been obtained, then two different reduced $n-1$ DOF robots are derived (one with workspace $\mathcal{W}_j$ and the other with workspace $\mathcal{W}_k$)). The joints meeting any point of the list 4.3.1 are discarded and the workspace analysis is repeated for either $\mathcal{W}_i$ or $\mathcal{W}_j$ and $\mathcal{W}_k$. Then, one or two new redundant joints are obtained for each new workspace and, therefore, there are up to four sets of two redundant joints each that leads to a maximum of four two-parameter families of solutions.
- Again, the process is repeated in the same way until each set of redundant joints have exactly m joints. There are up to 2^m of these sets and each one of them leads to a m-parameter family of solutions.

4.4 Closed-form families of solutions for the inverse kinematics

Once the redundant joints have been identified and parametrized, a non-redundant reduced manipulator is achieved. If m denotes the number of rotational degrees of redundancy, a maximum of 2^m sets of m redundant joints can be obtained and, therefore, there exists a partition of $\mathcal{W}$ in a maximum of 2^m parts where each one of them has associated one of these 2^m sets of redundant joints. Denote the elements of such partition by $\overline{\mathcal{W}_1}, \ldots, \overline{\mathcal{W}_{2^m}}$. For every given pose $T \in \mathcal{W}$ there exists $1 \leq i \leq 2^m$ such that $T \in \overline{\mathcal{W}_i}$. Thus, the non-redundant reduced manipulator is the one obtained after parametrizing the joints of the i-th set. Therefore, this criterion allows to decide which solution family should be used for any given pose T.

Now, several closed-form methods can be applied attending to the different classes of robots. For manipulators with three consecutive joints whose axes are either parallel or intersect at a single point, Pieper method (Pieper, 1968) works properly. However, for some of these robots, the solutions provided by Pieper method are given as the solutions of a four-degree polynomial. Although the real roots of a four-degree polynomial can be obtained, this solution is not computationally efficient. Because of that, next chapter introduces a novel strategy to solve the inverse kinematics of serial robots of this kind using geometric algebra, that provides a framework for an elegant and compact formulation and resolution of the inverse kinematics. For the rest of manipulators, different approaches can be followed: Paul method (Paul, 1981) is the most formal and generic one. It consists of the manipulation of a set of equations obtained from the elements of the following set of matrix identities

$$\left(A_{i-1}^{i-2}\right)^{-1} \cdots \left(A_1^0\right)^{-1} \cdot T_n^0 = A_i^{i-1} \cdots A_n^{n-1} \quad \text{for } i = 2, \ldots, n \tag{4.9}$$

The objective is to isolate the joint variables in some of the equations in order to solve them. Its only drawback is the high number of combinations required for obtaining a solution. Besides,

there exists no guarantee that Paul method can solve the inverse kinematics for all kind of robots. For un-resoluble manipulators, different geometric approaches have been developed in literature.

One interesting technique, followed by several authors, relies on the combination between closed-form and numerical methods. In particular, the approach followed by Lin and Min (2015) uses a geometric method for obtaining the first three joint variables and a numerical one for the last three. On the other hand, in (Kucuck and Bingul, 2005; Kucuk and Bingul, 2014) the inverse kinematics of several robots is solved using a combination of pure analytical and numerical methods, while Wu et al. (2015) assign a particular instance to q_6. Later, such value is corrected through a numerical method. Finally, Pan et al. (2012) consider a variation of the original manipulator. Such variation has three joint axes intersecting at a single point. Then, a closed-form method can be employed for solving the inverse kinematics of the modified manipulator. The solution for the original robot is obtained numerically using as initial condition one of the sixteen solutions achieved with the closed-form method. The advantages of this last method will be shown in an illustrative example in next section, where it will be extended for redundant robots.

The instances for the parametrized joint variables depend on the imposed constraints. From avoiding obstacles, singularities or joint limits to obtaining the most efficient solution in terms of velocity or energy, the different constraints are usually modeled with cost functions and the solution is obtained through an optimization process. In particular, given the kinematic relation $\boldsymbol{x} = f(\boldsymbol{q})$ (as defined in section B.2), the optimization problem can be defined as:

$$\left.\begin{array}{ll} \underset{\boldsymbol{q}}{\text{maximize}} & g(\boldsymbol{q}) \\ \text{subject to} & f(\boldsymbol{q}) = \boldsymbol{x} \end{array}\right\} \tag{4.10}$$

More precisely, since only the redundant joints acts as variables in the optimization process, (4.10) turns to:

$$\left.\begin{array}{ll} \underset{\boldsymbol{q}_r}{\text{maximize}} & g(\boldsymbol{q}_0) \\ \text{subject to} & f(\boldsymbol{q}) = \boldsymbol{x} \end{array}\right\} \tag{4.11}$$

where $\boldsymbol{q}_r = (q_{r1}, \ldots, q_{rm})$ is the vector of redundant joint variables.

Examples of cost functions $g(\boldsymbol{q})$ are (Siciliano et al., 2008):

- For avoiding singularities:
$$g(\boldsymbol{q}) = \sqrt{\det(J_G(\boldsymbol{q}) J_G^T(\boldsymbol{q}))}$$
- For avoiding joint limits:
$$g(\boldsymbol{q}) = -\frac{1}{2n} \sum_{i=1}^{n} \left(\frac{q_i - \overline{q_i}}{q_{iM} - q_{im}} \right)$$
where q_{iM} (q_{im}) denotes the maximum (minimum) joint limit and $\overline{q}_i$, the middle value of the joint range.

- For avoiding obstacles:

$$g(\boldsymbol{q}) = \|\boldsymbol{p}(\boldsymbol{q}) - \boldsymbol{o}\|$$

where $\boldsymbol{p}(\boldsymbol{q})$ denotes the position vector of the end-effector of $\mathcal{R}$ and $\boldsymbol{o}$ is a suitable point on the obstacle.

4.5 Application to some redundant robots

To show the advantages of the proposed method, three examples are developed in this section. Two of them are 7 DOF robots while the other is a 8 DOF manipulator. Besides, the second example contains a prismatic joint at the beginning of the kinematic chain. All the cases have a single one-parameter family of solutions. The different computations have been carried out using MATLAB R2015a.

4.5.1 Kuka LWR 4+

As stated in section B.3.1, Kuka LWR 4+ is an anthropomorphic arm with seven degrees of freedom (figure B.3a) and, as a consequence, it has just one rotational degree of redundancy. To identify the redundant joint, the joints meeting the criteria 4.3.1 are discarded as candidates. For Kuka LWR 4+, the last three joints conform a spherical wrist. Therefore, these joints are discarded. The application of corollary 3.2.3 through Algorithm 1 gives that the fourth joint leaves a globally degenerated subchain if it is fixed. Then, it cannot be the redundant joint and, therefore, the candidates are the first, the second and the third joint.

For these joints the workspace analysis presented in the preceding section is performed. Without loss of generality, the fixed values assigned to the joint variables are zero. A discretization of the workspace volume for each subchain is generated using Algorithm 2. The workspace of the Kuka LWR 4+ is depicted in figure 4.2a while the rest (figures 4.2b, 4.2c and 4.2d) show the workspace volume of each subchain. From graphical visualization it is evident that the workspace shape of the subchain resulting from fixing the third joint ($\mathcal{W}_3$) coincides with the Kuka LWR 4+ whole workspace ($\mathcal{W}$). Since $\mathcal{W}$ and $\mathcal{W}_3$ are of revolution around $\boldsymbol{z}_1$, the $\boldsymbol{x}$–$\boldsymbol{z}$ cross section of both workspaces are obtained by setting $q_1 = 0$ and compared. The area of each cross section is obtained using the identity (4.6): 0.3101 m^2 for both $\mathcal{W}$ and $\mathcal{W}_3$. This confirms that the workspace remains invariant if the third joint is fixed. Therefore, the redundant joint for the Kuka LWR 4+ is the third one.

Once the redundant joint has been selected, and since the Kuka LWR 4+ possesses a spherical wrist, Paul closed-form method can be applied for deriving the analytical expressions of each q_i in terms of the pose matrix elements. Given:

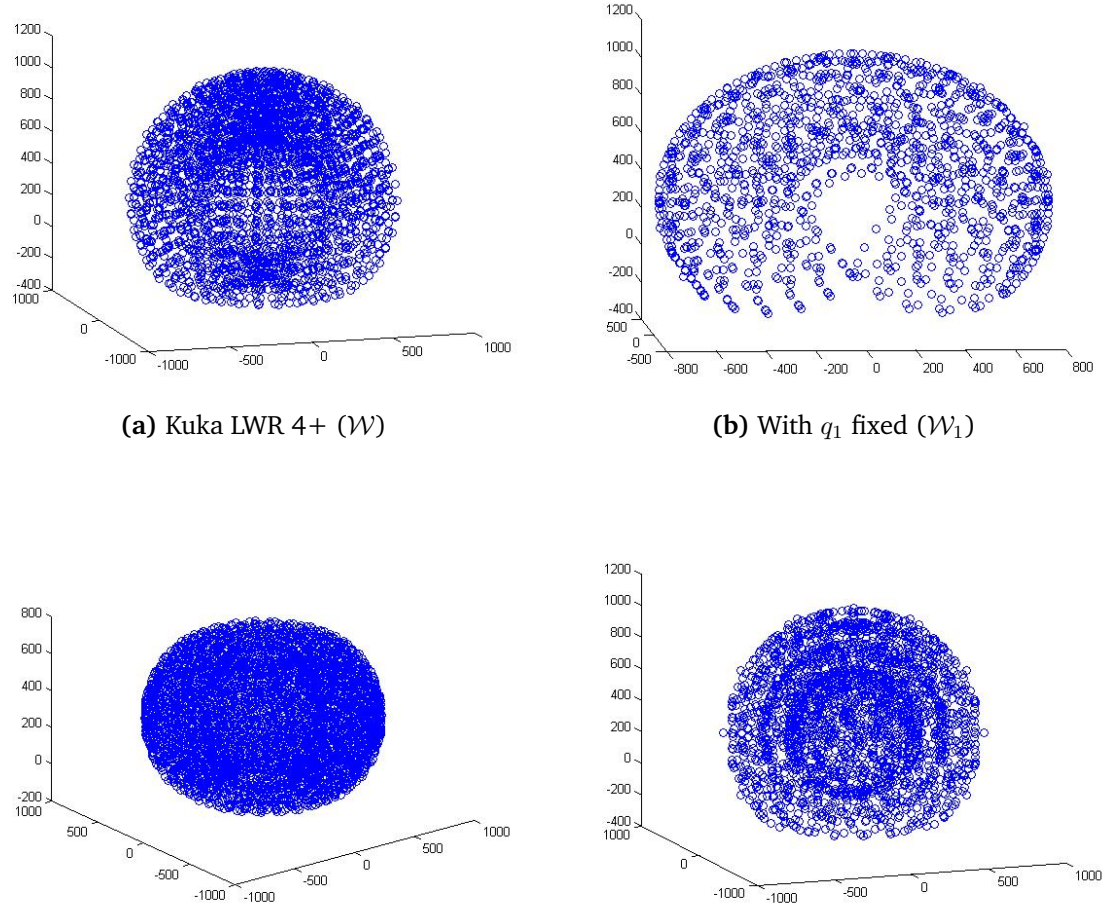

(a) Kuka LWR 4+ ($\mathcal{W}$)

(b) With q_1 fixed ($\mathcal{W}_1$)

(c) With q_2 fixed ($\mathcal{W}_2$)

(d) With q_3 fixed ($\mathcal{W}_3$)

Figure 4.2: Comparison between Kuka LWR 4+ workspace and its subschains workspace

$$T = \begin{pmatrix} n_x & o_x & a_x & p_x \\ n_y & o_y & a_y & p_y \\ n_z & o_z & a_z & p_z \\ 0 & 0 & 0 & 1 \end{pmatrix},$$

the resolution can be split in two different problems: the position problem, in which from $\boldsymbol{p} = (p_x, p_y, p_z)$ it is possible to obtain q_1, q_2 and q_4 and the orientation problem, in which from

$$R = \begin{pmatrix} n_x & o_x & a_x \\ n_y & o_y & a_y \\ n_z & o_z & a_z \end{pmatrix}$$

q_5, q_6 and q_7 are obtained.

For the position problem, (4.9) is used to obtain the following identity:

$$\left(A_1^0\right)^{-1} \cdot T_7^0 = A_2 \cdots A_7$$

Now, the fourth column of each matrix is taken:

$$\begin{cases} p_x c_1 + p_y s_1 = c_2(400 + 390c_4) + 390 s_2 c_3 s_4 \\ -p_x s_1 + p_y c_1 = 390 s_3 s_4 \\ p_z - 310 = -390 c_2 c_3 s_4 + s_2(390 c_4 + 400) \end{cases} \tag{4.12}$$

where, again, $c_i = \cos(q_i)$ and $s_i = \sin(q_i)$.

Squaring each equation of 4.12 and adding gives:

$$p_x^2 + p_y^2 + (p_z - 310)^2 = 400^2 + 390^2 + 2 \cdot 400 \cdot 390 c_4 \Longrightarrow c_4 = \frac{p_x^2 + p_y^2 + (p_z - 310)^2 - 312100}{312000}$$

Therefore, through the prototype equation (C.2), the analytical expression for q_4 is derived:

$$q_4 = \operatorname{atan2}(\pm\sqrt{1 - a^2}, a)$$

where:

$$a = \left(\frac{p_x^2 + p_y^2 + (p_z - 310)^2 - 312100}{312000}\right)$$

Once the expression for q_4 is known, the expression for q_1 can be deduced from the following identity:

$$-p_x s_1 + p_y c_1 = 390 s_3 s_4$$

through the prototype equation (C.5):

$$q_1 = \operatorname{atan2}\left(390 s_3 s_4, \pm\sqrt{p_x^2 + p_y^2 - 390^2 s_3^2 s_4^2}\right) - \operatorname{atan2}(p_y, p_x)$$

Now, the expression for q_2 can be obtained from the following identity using again the prototype equation (C.5):

$$p_z - 310 = -390 c_2 c_3 s_4 + s_2(390 c_4 + 400) \Longrightarrow q_2 = \operatorname{atan2}\left(c, \pm\sqrt{a^2 + b^2 - c^2}\right) - \operatorname{atan2}(a, b)$$

with:

$$\begin{aligned} a &= (390 c_4 + 400) \\ b &= -390 c_3 s_4 \\ c &= p_z - 310 \end{aligned}$$

Once the position problem has been solved, it is possible to solve the orientation problem. If R_i denotes the matrix that defines the relative orientation of A_i^{i-1}, then:

$$R_1 \cdot R_2 \cdots R_7 = R$$

And, therefore,

$$R_5 \cdot R_6 \cdot R_7 = \underbrace{R_4^{-1} \cdot R_3^{-1} \cdot R_2^{-1} \cdot R_1^{-1} \cdot R}_{\text{Numerical matrix } M}$$

or, analogously:

$$\begin{pmatrix} c_5c_6c_7 - s_5s_7 & -c_7s_5 - c_5c_6s_7 & -c_5s_6 \\ c_7s_6 & -s_6s_7 & c_6 \\ -c_5s_7 - c_6c_7s_5 & c_6s_5s_7 - c_5c_7 & s_5s_6 \end{pmatrix} = M = \begin{pmatrix} m_{11} & m_{12} & m_{13} \\ m_{21} & m_{22} & m_{23} \\ m_{31} & m_{32} & m_{33} \end{pmatrix}$$

from where, using the prototype equations (C.2) and (C.3), the following expressions can be obtained:

$$\begin{aligned} q_6 &= \operatorname{atan2}\left(\pm\sqrt{m_{13}^2 + m_{33}^2}, m_{23}\right) \\ q_5 &= \operatorname{atan2}(m_{33}/\sin(q_6), -m_{13}/\sin(q_6)) \\ q_7 &= \operatorname{atan2}(-m_{22}/\sin(q_6), m_{21}/\sin(q_6)) \end{aligned}$$

that completes the solution of the orientation problem. Since q_1 and q_2 depend on q_3, this solution is a one-parameter family of solutions.

4.5.2 Extended Stäubli TX90 mounted on a translational motion unit

As stated in section B.3.2, the Stäubli TX90 is an industrial manipulator with six degrees of freedom and spherical wrist. This manipulator has been mounted on a linear track, that can be considered as an additional prismatic joint. Besides, it has been extended by adding an extra revolute joint whose axis is parallel to the axes of the third and fourth joints (figure 4.3). Despite the manipulator has 8 DOF, $m = 1$ due to the presence of a prismatic joint. Furthermore, as in the precedent example, the three last joints are discarded for being the redundant ones since they conform a spherical wrist. After fixing the joint variable of the first joint – the prismatic one, Algorithm 1 is applied in order to find out whether any other joint should be discarded or not as a candidate. From the seven different kinematic subchains, the one obtained after fixing the second joint – the first revolute joint – is a globally degenerated subchain. Therefore, only the third, the fourth and the fifth joints are the candidates for being the redundant joint.

For these joints the workspace analysis is performed using Algorithm 2. The prismatic joint variable is set to zero (its motion lies within the range $[0, 2]$). The extended Stäubli TX90 workspace is depicted in figure 4.4a while the workspaces of the subchains are depicted in figures 4.4b, 4.4c and 4.4d. In this case, as in the precedent example, there exists i such that $\mathcal{W}_i = \mathcal{W}$. It is clear, from direct visualization, that $\mathcal{W}_5 = \mathcal{W}$. Furthermore, the workspaces dimensions also show that $\mathcal{W}_5 = \mathcal{W}$. Indeed, the dimensions of $\mathcal{W}$ are $3m \times 4m \times 3m$, while the dimensions fo the workspaces after the parametrization of the candidates are:

- $\mathcal{W}_3$: $1.8m \times 2m \times 2m$ (figure 4.4b).

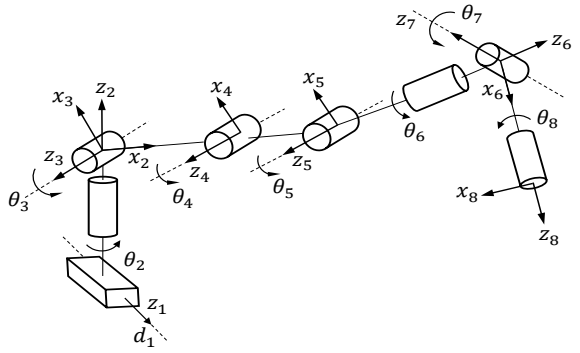

Figure 4.3: Schematic representation of extended Stäubli TX90 mounted on a translational motion unit

- $\mathcal{W}_4$: $2m \times 2m \times 2m$ (figure 4.4c).
- $\mathcal{W}_5$: $3m \times 3m \times 4m$ (figure 4.4d).

Again, setting $q_2 = 0$ returns the $\boldsymbol{x}$–$\boldsymbol{z}$ cross section of $\mathcal{W}$ and $\mathcal{W}_5$. Moreover, if (4.8) is used to calculate the cross section areas of $\mathcal{W}$ and $\mathcal{W}_5$, the resulting value is the same (up to some discretization error):

$$A_{\mathcal{W}} = 2.560m^2 \quad A_{\mathcal{W}_5} = 2.555m^2$$

This confirms that the redundant joint for the extended Stäubli TX90 is the fifth one from which it can be obtained the one-parameter family of solutions.

As in the case of the Kuka LWR 4+, the presence of a spherical wrist allows to decomposed the problem into the position and orientation problems. For both, Paul method can be used to obtain the closed-form solutions. For this example, q_5 will work as the parameter of the family of solutions.

For the position problem, a geometric method can be used to calculate d_1. The position vector $\boldsymbol{p}$ is projected onto the $\boldsymbol{x}$–$\boldsymbol{y}$ plane of the reference frame (attached to the base of the robot). If the projection is denoted by $\pi(\boldsymbol{p})$, then $d_1 = \min\{\|d_1 - \pi(\boldsymbol{p})\|\}$. For the remaining joint variables, the following identity is used:

$$\left(A_2^0\right)^{-1} \cdot T_8^0 = A_3 \cdots A_8 \tag{4.13}$$

The position vector from both sides of (4.13) is:

$$\begin{cases} p_x c_2 + p_y s_2 = 425 s_3 + 300 c_{34} + 425 c_{345} + 50 & (4.14) \\ p_y c_2 - p_x s_2 = 50 & (4.15) \\ p_z - 478 = 425 c_3 + 300 s_{34} + 425 s_{345} & (4.16) \end{cases}$$

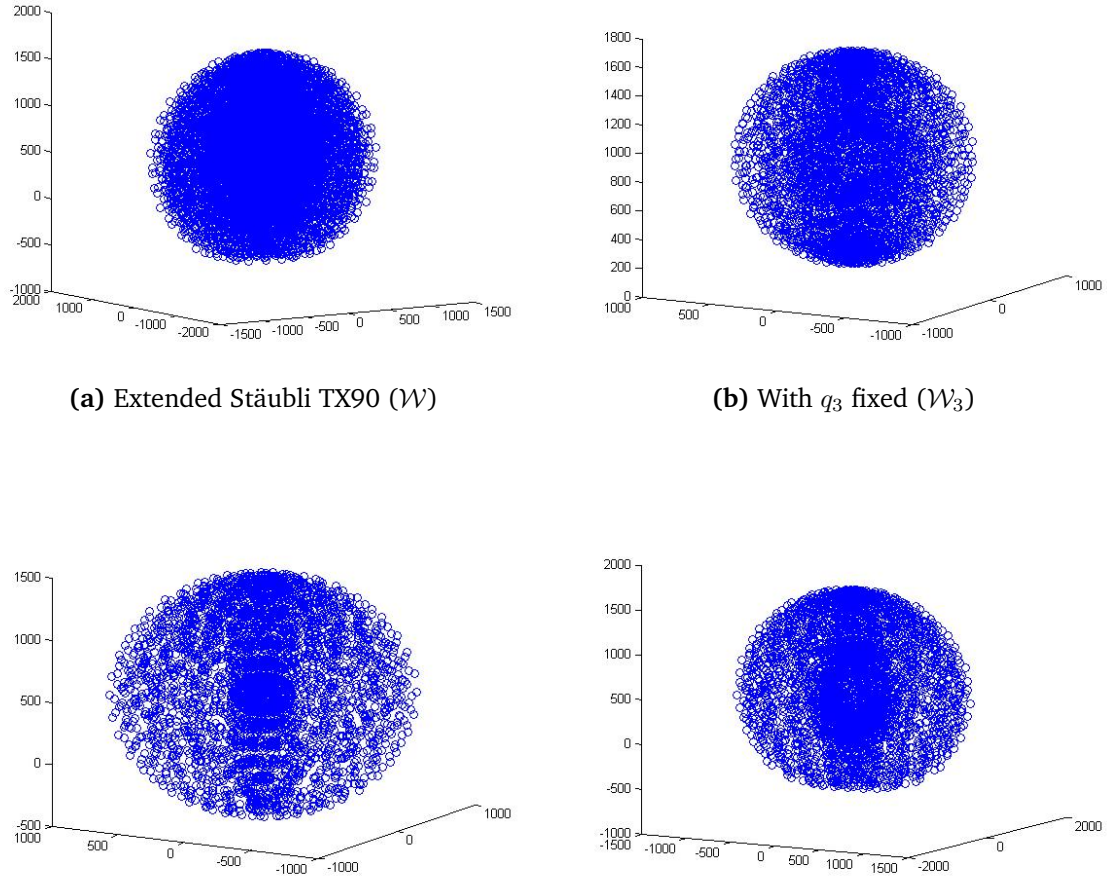

(a) Extended Stäubli TX90 ($\mathcal{W}$)

(b) With q_3 fixed ($\mathcal{W}_3$)

(c) With q_4 fixed ($\mathcal{W}_4$)

(d) With q_5 fixed ($\mathcal{W}_5$)

Figure 4.4: Comparison between Extended Stäubli TX90 workspace and its subchains workspace

Equation (4.15) can be solved using the prototype equation (C.5). Thus, the analytical expression for q_2 is:

$$q_2 = \text{atan2}\left(50, \pm\sqrt{p_x^2 + p_y^2 - 50^2}\right) - \text{atan2}(p_y, p_x)$$

Now, equations (4.14) and (4.16) are squared and added. Once the terms have been regrouped, the expression obtained is:

$$\alpha = 451250 - 255000s_4 - 361250s_{45} + 255000c_5 \tag{4.17}$$

where $\alpha = (p_x c_2 + p_y s_2 - 50)^2 + (p_z - 478)^2$.

Since q_5 is the redundant joint and it is parametrized at some value, (4.17) is simplified to:

$$451250 + 255000c_5 - \alpha = (255000 + 361250c_5)s_4 + 361250s_5c_4$$

Again, by using the prototype equation (C.5), the analytical expression for q_4 is:

$$q_4 = \text{atan2}\left(c, \pm\sqrt{a^2 + b^2 - c^2}\right) - \text{atan2}(a, b),$$

with:

$$\begin{aligned} a &= 361250 s_5 \\ b &= (255000 + 361250 c_5) \\ c &= 451250 + 255000 c_5 - \alpha \end{aligned}$$

Finally, since the expression for q_4 is known and q_5 is parametrized at some value, (4.16) is equivalent to:

$$p_z - 478 = (300 + 300 s_4 + 425 s_{45}) c_3 + (300 c_4 + 425 c_{45}) s_3,$$

which can be solve using the prototype equation (C.5):

$$q_3 = \text{atan2}\left(c, \pm\sqrt{a^2 + b^2 - c^2}\right) - \text{atan2}(a, b),$$

with:

$$\begin{aligned} a &= 300 + 300 s_4 + 425 s_{45} \\ b &= 300 c_4 + 425 c_{45} \\ c &= p_z - 478 \end{aligned}$$

which completes the position problem. The orientation problem is solved analogously to the case of the Kuka LWR 4+.

4.5.3 ABB Yumi

As introduced in section B.3.3, the ABB Yumi is a manipulator that possesses two anthropomorphic arms of 7 DOF each one of them connected to a fixed torso (figure B.5 and picture B.6). No one of these two arms have three consecutive joints whose axes intersect at a single point.

To solve the inverse kinematics for this robot, the mixed strategy introduced by Pan et al. (2012) is extended for redundant manipulators. Furthermore, this extension considers a variation of the original manipulator that has, apart from spherical wrist, spherical shoulder, i.e., the first three joint axes also intersect at a single point. This modified manipulator is similar to the Kuka LWR 4+ (only the link lengths are different). Thus, the redundant joint will be the same – the third one.

In this case, Pieper method is used to solve the inverse position problem to illustrate how this method is also a good strategy for some particular classes of robots with a spherical wrist. If the modified manipulator had not had a spherical shoulder, a four-degree equation would have appeared.

Closed-form method

Given a pose matrix T, the position vector $\boldsymbol{p} = (p_x, p_y, p_z)$ and the rotation matrix

$$R = \begin{pmatrix} n_x & o_x & a_x \\ n_y & o_y & a_y \\ n_z & o_z & a_z \end{pmatrix}$$

are considered as inputs of the position and orientation problems respectively. For the position problem:

$$\boldsymbol{p} = T_4^0 \cdot \begin{pmatrix} -40.5 \\ 265 \\ 0 \\ 1 \end{pmatrix}$$

where $T_4^0 = A_1^0 \cdots A_4^3$. Now, the following notation is going to be used:

$$\boldsymbol{p} = \begin{bmatrix} g_1(q_2, q_3, q_4)\cos(q1) + g_2(q_2, q_3, q_4)\sin(q1) \\ g_1(q_2, q_3, q_4)\sin(q1) - g_2(q_2, q_3, q_4)\cos(q1) \\ g_3(q_2, q_3, q_4) \end{bmatrix} \tag{4.18}$$

$$A_3^2 \cdot A_4^3 \cdot \begin{pmatrix} -40.5 \\ 265 \\ 0 \\ 1 \end{pmatrix} = \begin{pmatrix} f_1(q_3, q_4) \\ f_2(q_3, q_4) \\ f_3(q_3, q_4) \\ 1 \end{pmatrix} \tag{4.19}$$

with:

$$\begin{aligned} g_1(q_2, q_3, q_4) &= \cos(q_2) f_1(q_3, q_4) - \sin(q_2) f_2(q_3, q_4) \\ g_2(q_2, q_3, q_4) &= f_3(q_3, q_4) \\ g_3(q_2, q_3, q_4) &= \sin(q_2) f_1(q_3, q_4) + \cos(q_2) f_2(q_3, q_4) + 166 \end{aligned}$$

Therefore,

$$\begin{aligned} & p_x^2 + p_y^2 + (p_z - 166)^2 = \\ & = g_1(q_2, q_3, q_4)^2 + g_2(q_2, q_3, q_4)^2 + (g_1(q_2, q_3, q_4) - 166)^2 = \\ & = f_1(q_3, q_4)^2 + f_2(q_3, q_4)^2 + f_2(q_3, q_4)^2 \qquad (4.20) \\ & p_z = \sin(q_2) f_1(q_3, q_4) + \cos(q_2) f_2(q_3, q_4) + 166 \qquad (4.21) \end{aligned}$$

Now, (4.20) is equal to $\alpha\cos(q_4) - \beta\sin(q_4) + 136757.75$. Hence:

$$q_4 = \operatorname{atan2}\left(\gamma, \pm\sqrt{\alpha^2 + \beta^2 - \gamma^2}\right) - \operatorname{atan2}(\alpha, \beta),$$

where:

$$\begin{aligned} \alpha &= 130014.5 \\ \beta &= -41836.5 \\ \gamma &= p_x^2 + p_y^2 + (p_z - 166)^2 - 136757.75 \end{aligned}$$

On the other hand, (4.21) is equal to:

$$\begin{aligned}&251.5\cos(q_2)+265\cos(q_2)\cos(q_4)+40.5\cos(q_3)\sin(q_2)\\&-40.5\cos(q_2)\sin(q_4)-40.5\cos(q_3)\cos(q_4)\sin(q_2)\\&-265\cos(q_3)\sin(q_2)\sin(q_4)+166\end{aligned}$$

where q_3 denotes the joint variable of the redundant joint and q_4 is already known. Therefore:

$$q_2=\operatorname{atan2}\left(c,\pm\sqrt{a^2+b^2-c^2}\right)-\operatorname{atan2}(a,b),$$

where:

$$\begin{aligned}a&=251.5+265\cos(q_4)-40.5\sin(q_4)\\b&=40.5\cos(q_3)-40.5\cos(q_3)\cos(q_4)-265\cos(q_3)\sin(q_4)\\c&=p_z-166\end{aligned}$$

Finally, since the two first rows of (4.18) only depend on the already known joint variables, either of these can be used to obtain the expression for q_1:

$$q_1=\operatorname{atan2}\left(c,\pm\sqrt{a^2+b^2-c^2}\right)-\operatorname{atan2}(a,b),$$

where:

$$\begin{aligned}a&=g_1(q_2,q_3,q_4)\\b&=g_2(q_2,q_3,q_4)\\c&=p_x\end{aligned}\quad.$$

To obtain all these expressions, the prototype equation (C.5) has been used.

With respect to the orientation problem, the joint variables q_5, q_6 and q_7 can be obtained similarly to the orientation joint variables of the Kuka LWR 4+:

$$\begin{aligned}q_6&=\operatorname{atan2}\left(\pm\sqrt{m_{13}^2+m_{33}^2},m_{23}\right)\\q_5&=\operatorname{atan2}(m_{33}/\sin(q_6),-m_{13}/\sin(q_6))\\q_7&=\operatorname{atan2}(-m_{22}/\sin(q_6),m_{21}/\sin(q_6))\end{aligned}$$

which completes the closed-form solution of the modified manipulator.

Numerical method

Once the one-parameter family of solutions has been obtained for the modified robot, the solution for the original robot is calculated through a numerical method that uses one of the elements of the solution family as initial condition. In this case, the numerical method used is the pseudoinverse, a Jacobian-based method that, starting with an initial condition $\boldsymbol{q}_0$ and a target pose T_d, approximates the solution through the following iteration:

$$\boldsymbol{q}_{i+1}=\boldsymbol{q}_i+J_G^{\dagger}(\boldsymbol{q}_i)\begin{bmatrix}\boldsymbol{e}_P\\\boldsymbol{e}_O\end{bmatrix}$$

where $J_G^{\dagger}(\boldsymbol{q})$ denotes the right Moore-Penrose pseudoinverse matrix of $J_G(\boldsymbol{q})$ (as defined in (A.14)); $\boldsymbol{e}_P$ denotes the position error and $\boldsymbol{e}_O$, the orientation one.

Such errors are calculated in each iteration as follows:

- The target pose T_d is decomposed into the target position $\boldsymbol{p}_d$ and the target orientation R_d. The last one is expressed as a unit quaternion $\boldsymbol{q}_d = \{\alpha_d, \boldsymbol{\varepsilon}_d\}$ where α_d and $\boldsymbol{\varepsilon}_d$ represent its scalar and vector part respectively.
- For each $\boldsymbol{q}_i$, the forward kinematics allows to obtain the associated end-effector pose T_e. Again, from T_e, the position vector $\boldsymbol{p}_e$ and the unit quaternion $\boldsymbol{q}_e = \{\alpha_e, \boldsymbol{\varepsilon}_e\}$ are extracted.
- The position error is:
$$\boldsymbol{e}_P = \boldsymbol{p}_d - \boldsymbol{p}_e$$
- The orientation error is:
$$\boldsymbol{e}_O = \alpha_e \boldsymbol{\varepsilon}_d - \alpha_d \boldsymbol{\varepsilon}_e - \begin{pmatrix} 0 & -e_z & e_y \\ e_z & 0 & -e_x \\ -e_y & e_x & 0 \end{pmatrix} \boldsymbol{\varepsilon}_e,$$
with $\boldsymbol{\varepsilon}_d = (e_x, e_y, e_z)$.

Validation

In order to show the performance of the generalized mixed method proposed in this chapter, a validation has been made using MATLAB R2015a. A random pose has been generated and its corresponding one-parameter family of solutions has been obtained for the modified manipulator. Then, one element of such family has been used as initial condition for the pseudoinverse method. This solution has been compared with those obtained by the purely numerical method of the pseudoinverse.

Figures 4.7a and 4.7b represent the position and orientation errors, while figures 4.5a, 4.5b, 4.5c, 4.5d, 4.5e, 4.5f and 4.6a show how each joint variable converges to a solution for the original robot. In these figures, the blue line represents the behaviour under the mixed approach whereas the red line shows the behaviour but under the purely numerical method of the pseudoinverse (with a random initial condition). As observed, the proposed method needs a smaller number of iterations. Besides, since both approaches use the pseudoinverse, reducing the number of iterations means a shorter execution time and a lower computational cost. If another numerical method is used to improve the convergence time, it could also be used in the mixed approach, which implies that this method will still have a shorter execution time and a lower computational cost.

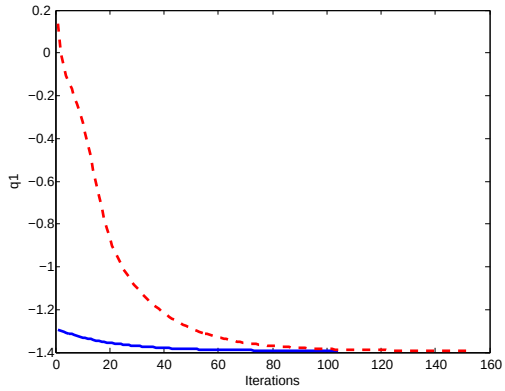

(a) Joint trajectory q_1

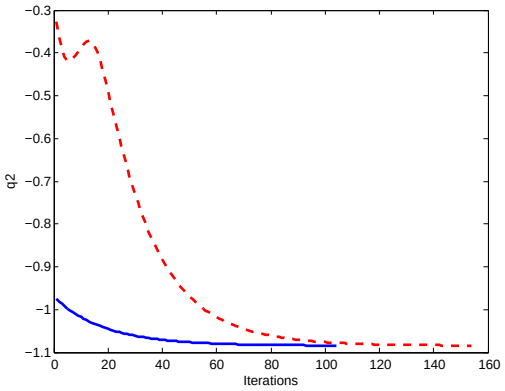

(b) Joint trajectory q_2

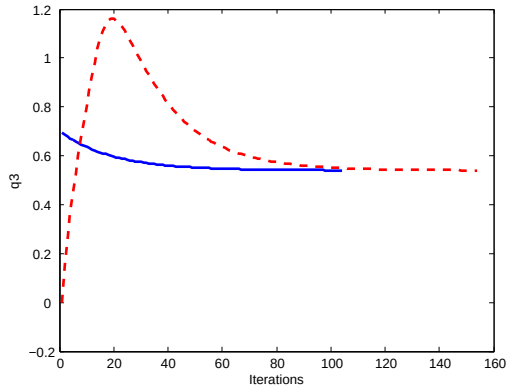

(c) Joint trajectory q_3

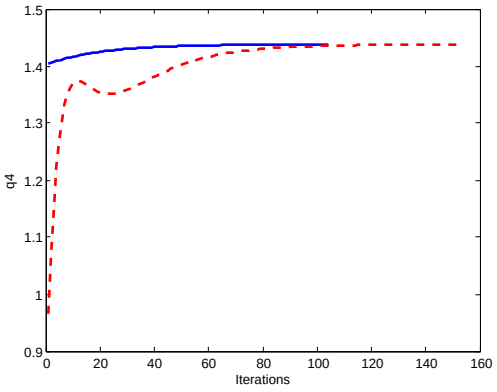

(d) Joint trajectory q_4

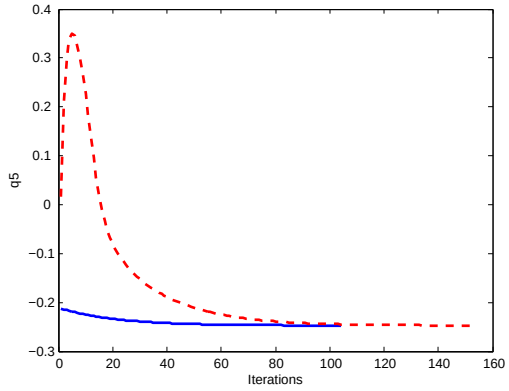

(e) Joint trajectory q_5

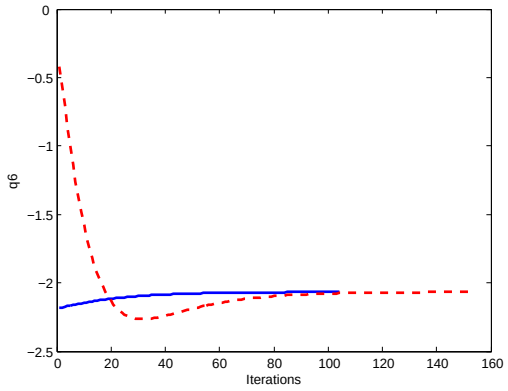

(f) Joint trajectory q_6

Figure 4.5: Joint trajectories

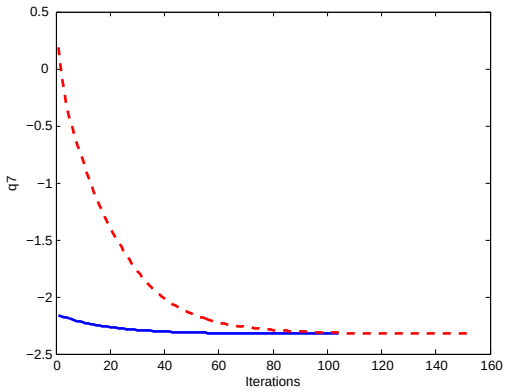

(a) Joint trajectory q_7

Figure 4.6: Joint trajectories (cont.)

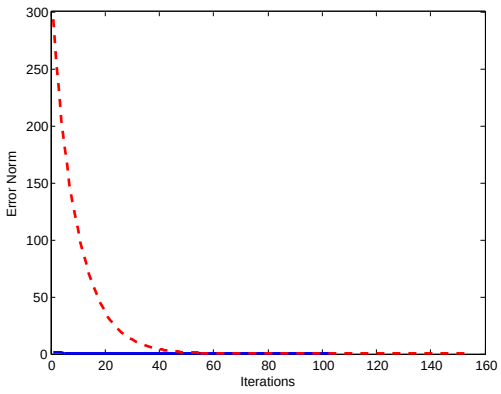

(a) Position error

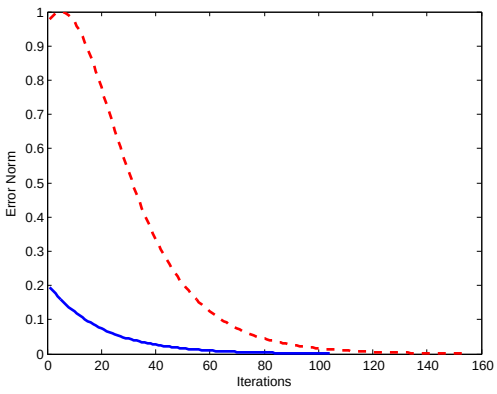

(b) Orientation error

Figure 4.7: Position and orientation errors

Chapter 5

Conformal Geometry Algebra applied to the Inverse Kinematics

There is no royal road to geometry
Euclid

This chapter addresses the inverse kinematics of serial robots with spherical wrist using the conformal model of the spatial geometric algebra. The formulation presented here allows a compact description of robot kinematics and provides a framework for the development of geometric solutions for the inverse kinematics. The position problem is solved geometrically, while the orientation problem is solved algebraically. Finally, the inverse kinematics of 7 DOF redundant manipulators with spherical wrist is solved by extending the geometric solutions obtained for non-redundant robots.

5.1 Problem Statement

As mentioned in sections 2.1.1 and 4.4, some closed-form methods are usually difficult to formulate and solve for non-redundant robots even with spherical wrist. For example, Pieper method allows to obtain the solutions of the inverse kinematics as the solutions of a set of polynomials and, for a general serial robot with spherical wrist, at least one of these polynomials has four-degree which is, in general, difficult to solve.

On the other hand, Paul method consists of the manipulation of the homogeneous matrices of

the relation (B.13) as follows:

$$\left(A_{i-1}^{i-2}\right)^{-1} \cdots \left(A_1^0\right)^{-1} \cdot T_n^0 = A_i^{i-1} \cdots A_n^{n-1} \quad \text{for } i = 2, \ldots, n \tag{5.1}$$

where, as stated in sections 2.1.1 and 4.4, the objective is to isolate those non-linear equations that contain just one joint variable. However, even if the equations containing just one variable are found, solve them analytically is, in general, difficult.

Conversely, geometric methods are usually defined for particular robots. Besides, the formulation and implementation of such methods is difficult. If, for example, the circle intersection of a plane with a sphere is considered, then a system of two equations (one of them non-linear) must be solved. In this context, geometric algebra turns to be very useful. As stated in sections A.3 and A.4 of appendix A, geometric algebra and, in particular, the conformal model of the spatial geometric algebra provide a framework for modeling the kinematics and dynamics of rigid bodies that avoids the use of matrices. In addition, the geometric entities such as points, lines, planes or spheres can be represented with elements of the algebra.

Regarding the contributions using this framework, in (Bayro-Corrochano and Kähler, 2001; Selig, 2001) analogous versions to the Paul and Pieper methods are introduced. In both works, an easy and compact formulation of the problem is presented using the language provided by geometric algebra. However, they have the same drawbacks as the original methods. The approach presented in (Aristidou and Lasenby, 2011) develops a fast and heuristic method that solves the inverse kinematics of arbitrary redundant serial robots. Nevertheless, since it is a numerical method, only one solution is obtained, and the inverse orientation problem is not treated. Similarly, Hildenbrand et al. (2008) only solve the inverse position problem for an anthropomorphic manipulator. There, different geometric entities are defined according to the geometry of the robot. These entities, and the relations between them, are described easily using the conformal model of the spatial geometric algebra. The angles between such entities correspond to the joint variables.

Other approaches are focused on the development of geometric strategies for particular robots. For example, Hrdina et al. (2017) develop the kinematic model of a planar redundant manipulator, while in (Kim et al., 2015a) the inverse kinematics and the singularity problem are formulated and solved using conformal geometric algebra for a class of parallel robots. A 5 DOF serial robot is considered in (Zamora and Bayro-Corrochano, 2004), where the geometric strategy followed is the same as in (Hildenbrand et al., 2008). The work in (Campos-Macías et al., 2017) is devoted to the development of a solution of a 6 DOF humanoid leg. Tørdal et al. (2017) solve geometrically the inverse position problem of the 6 DOF Comau Smart-5 NJ-110, while in (Kleppe and Egeland, 2016) particular solutions of the inverse kinematics of UR5 and Agilus KR6 R900 are given. All of these works extend the strategies introduced in (Hildenbrand et al., 2008; Zamora and Bayro-Corrochano, 2004).

In this chapter, an approach to solve the inverse kinematics of arbitrary 6 or 7 DOF serial robots with spherical wrist is presented. This approach is not focused on a particular robot but applies to an entire class of manipulators. The inverse position problem is solved geometrically

by extending the contributions of (Hildenbrand et al., 2008; Tørdal et al., 2017; Zamora and Bayro-Corrochano, 2004), while a novel method is developed for solving the inverse orientation problem. This method involves splitting the rotor that defines the orientation into three rotors, so that each one of these new rotors contains just one joint variable. The main advantage of the strategy presented here lies in the fact that this approach is still a closed-form method, i.e., all the solutions are obtained as analytical expressions in terms of the end-effector pose. Besides, due to the simplicity of the problem formulation, such expressions are obtained easily.

5.2 Forward Kinematics using Conformal Geometric Algebra

The conformal model of the three-dimensional geometric algebra $\mathcal{G}_{4,1}$ provides an elegant and compact way of describing the forward kinematics. While the classical approach is based on the homogeneous transformation matrices constructed using the D-H parameters, this approach uses only rotors.

Since n denotes the null vector representation of the point at the infinity in $\mathcal{G}_{4,1}$ (as defined in (A.55)), throughout the rest of this chapter m will denote either the number of degrees of freedom of an arbitrary serial robot or the dimension of $\mathbb{R}^m$.

As stated in section B.2, the orthonormal frame attached to each joint is described with respect to the preceding one. The i-th joint frame is constructed from the $(i-1)$-th joint frame by the successive application of rigid motions, i.e., translations and rotations. Since both are described in $\mathcal{G}_{4,1}$ by rotors, for each joint i, the following rotors are defined:

$$\begin{aligned} T_{d_i} &= 1 + \frac{d_i n \boldsymbol{e}_3}{2} \\ R_{\theta_i} &= \cos\left(\frac{\theta_i}{2}\right) - \sin\left(\frac{\theta_i}{2}\right) e_{12} \\ T_{a_i} &= 1 + \frac{a_i n \boldsymbol{e}_1}{2} \\ R_{\alpha_i} &= \cos\left(\frac{\alpha_i}{2}\right) - \sin\left(\frac{\alpha_i}{2}\right) e_{23} \end{aligned} \tag{5.2}$$

where $\{\boldsymbol{e}_1, \boldsymbol{e}_2, \boldsymbol{e}_3\}$ denotes the orthonormal basis of $\mathbb{R}^3$ and $\{e_{12}, e_{23}, e_{13}\}$ denote the basis bivectors of $\mathcal{G}_3$. Then, two main rotors can be constructed with the previous ones:

$$\begin{aligned} M_{\theta_i} &= T_{d_i} R_{\theta_i} \\ M_{\alpha_i} &= T_{a_i} R_{\alpha_i} \end{aligned} \tag{5.3}$$

Notice that rotor M_{θ_i} contains both joint variables while M_{α_i} is a constant rotor. Although rotors are usually denoted by R, some authors denote the rotors that define a translation followed by a rotation by M (known as a *motor*) because of its connections with the screw theory (Bayro-Corrochano and Kähler, 2000).

Given a geometric entity X, each one of these rotors acts in the same way as a general rotor (as depicted in identity (A.63)):

$$X' = M_{\theta_i} X \widetilde{M}_{\theta_i} = T_{d_i} R_{\theta_i} X \widetilde{R}_{\theta_i} \widetilde{T}_{d_i} \tag{5.4}$$

Analogously to the classical approach, where the product of the homogeneous transformation matrices defines the forward kinematics (as shown in equation (B.13)), the successive multiplication of rotors given by:

$$\begin{aligned} X' &= M_{\theta_1} M_{\alpha_1} \cdots M_{\theta_m} M_{\alpha_m} X \widetilde{M}_{\alpha_m} \widetilde{M}_{\theta_m} \cdots \widetilde{M}_{\alpha_1} \widetilde{M}_{\theta_1} = \\ &= M_1 \cdots M_m X \widetilde{M}_m \cdots \widetilde{M}_1 = \prod_{i=1}^{m} M_i X \prod_{i=1}^{m} \widetilde{M}_{m-i+1} \end{aligned} \tag{5.5}$$

with $M_i = M_{\theta_i} M_{\alpha_i}$, defines the forward kinematics of serial robots. This statement can be easily proven: equation (5.5) is valid for points (that represents the end-effector position) and lines (that represents the end-effector orientation).

5.3 Representation of the pose in conformal geometric algebra

If the desired end-effector pose is represented as:

$$T = \begin{pmatrix} R & \boldsymbol{p} \\ 0 & 1 \end{pmatrix}$$

then it is possible to construct a rotor M that also describes such pose. This can be done by transforming the homogeneous transformation matrix defined by the world frame,

$$T_0 = \begin{pmatrix} I_3 & 0 \\ 0 & 1 \end{pmatrix}$$

into the matrix defined by the end-effector pose, T. First, the position vector $\boldsymbol{p}$ defines the following translation:

$$T_{\boldsymbol{p}} = 1 + \|\boldsymbol{p}\| \frac{n\boldsymbol{p}}{2} \tag{5.6}$$

Now, to obtain the rotor that connects the orientations determined by the rotations matrices R and I_3, the following procedure is introduced. Both rotation matrices can be seen as two sets of vectors in the three-dimensional space $\{\boldsymbol{e}_1, \boldsymbol{e}_2, \boldsymbol{e}_3\}$ and $\{\boldsymbol{f}_1, \boldsymbol{f}_2, \boldsymbol{f}_3\}$, respectively. Here the vectors of each basis are orthonormal, but, in general, this is not a requirement. Since rotors define rotations, there is always a rotor relating both sets of vectors, so the following identity holds:

$$\boldsymbol{f}_k = R \boldsymbol{e}_k \widetilde{R} \quad \text{for } k = 1, 2, 3 \tag{5.7}$$

The objective is to seek a simple expression for rotor R. For that, some preliminary results are needed. Associated with any arbitrary frame $\{\boldsymbol{e}_1, \ldots, \boldsymbol{e}_m\}$ there exists a *reciprocal frame* $\{\boldsymbol{e}^1, \ldots, \boldsymbol{e}^m\}$ defined by the property:

$$\boldsymbol{e}^i \cdot \boldsymbol{e}_j = \delta_{ij} \quad \forall i, j = 1, \ldots, m \tag{5.8}$$

where δ_{ij} denotes the Kronecker δ. The reciprocal frame $\{\boldsymbol{e}^1, \ldots, \boldsymbol{e}^m\}$ is constructed as follows:

$$\boldsymbol{e}^k = (-1)^{k-1}(\boldsymbol{e}_1 \wedge \cdots \wedge \boldsymbol{e}_{k-1} \wedge \boldsymbol{e}_{k+1} \wedge \cdots \wedge \boldsymbol{e}_m)E_m^{-1} \tag{5.9}$$

where E_m denotes the volume element $\boldsymbol{e}_1 \wedge \cdots \wedge \boldsymbol{e}_m$. Clearly, if $\{\boldsymbol{e}_1, \ldots, \boldsymbol{e}_m\}$ is an orthonormal frame, then E_m is the pseudoescalar of $\mathcal{G}_m$, I. Two important properties of reciprocal frames are the following:

$$\sum_{k=1}^{m} \boldsymbol{e}_k \boldsymbol{e}^k = m \tag{5.10}$$

and, given an r-vector A_r,

$$\sum_{k=1}^{m} \boldsymbol{e}_k A_r \boldsymbol{e}^k = (-1)^r(m-2r)A_r \tag{5.11}$$

The proof of these two properties is found in (Doran and Lasenby, 2003). Now, in the three-dimensional space the rotor R can be written as

$$R = \alpha - \beta B \tag{5.12}$$

where B is a bivector and

$$\alpha = \cos\left(\frac{\theta}{2}\right) \quad \beta = \sin\left(\frac{\theta}{2}\right)$$

Its reverse is

$$\widetilde{R} = \alpha + \beta B \tag{5.13}$$

Therefore, it is found that:

$$\begin{aligned} \sum_{k=1}^{3} \boldsymbol{e}_k \widetilde{R} \boldsymbol{e}^k = \sum_{k=1}^{3} \boldsymbol{e}_k(\alpha + \beta B)\boldsymbol{e}^k = \alpha \sum_{k=1}^{3} \boldsymbol{e}_k \boldsymbol{e}^k + \beta \sum_{k=1}^{3} \boldsymbol{e}_k B \boldsymbol{e}^k \overset{(1)}{=} \\ = 3\alpha + (-1)^2(3-4)\beta B = 3\alpha - \beta B = \\ = 3\alpha + \alpha - \alpha - \beta B = 4\alpha - \widetilde{R} \end{aligned} \tag{5.14}$$

where identity (1) is the result of the application of equations (5.10) and (5.11). Now, merging (5.7) and (5.14), the following expression is obtained:

$$\sum_{k=1}^{3} \boldsymbol{f}_k \boldsymbol{e}^k = \sum_{k=1}^{3} R \boldsymbol{e}_k \widetilde{R} \boldsymbol{e}^k = 4\alpha R - 1 \tag{5.15}$$

It follows that:

$$R \propto 1 + \sum_{k=1}^{3} \boldsymbol{f}_k \boldsymbol{e}^k$$

where $\propto$ denotes that the left term is a scalar multiple of the right term. Therefore, the following formula is established:

$$R = \frac{1 + \boldsymbol{f}_1 \boldsymbol{e}^1 + \boldsymbol{f}_2 \boldsymbol{e}^2 + \boldsymbol{f}_3 \boldsymbol{e}^3}{|1 + \boldsymbol{f}_1 \boldsymbol{e}^1 + \boldsymbol{f}_2 \boldsymbol{e}^2 + \boldsymbol{f}_3 \boldsymbol{e}^3|} \tag{5.16}$$

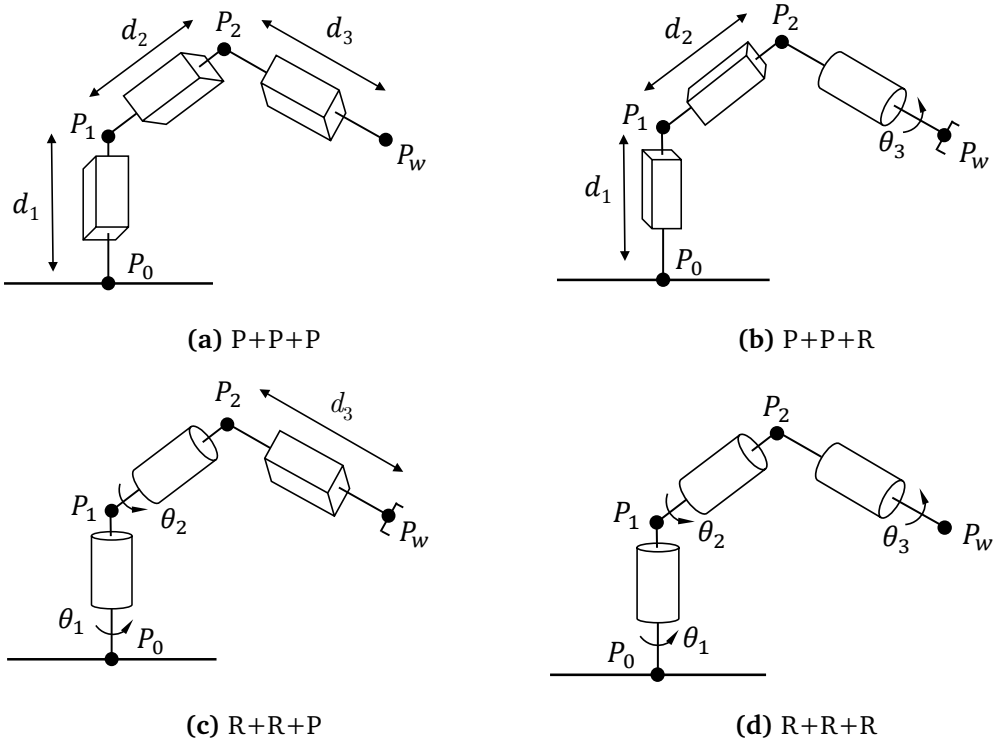

(a) P+P+P **(b)** P+P+R

(c) R+R+P **(d)** R+R+R

Figure 5.1: Different combinations of the joints conforming the position part of a serial robot $\mathcal{R}$

Finally, the rotor M describing the transformation between T_0 and T is the product of rotors (5.6) and (5.16):

$$M = T_{\boldsymbol{p}} R \tag{5.17}$$

As stated in section B.2, for a 6 DOF robot with spherical wrist, the target position $\boldsymbol{p}$ can be moved to the wrist center point $\boldsymbol{p}_w$ by a fixed transformation. Then, the new target position is $\boldsymbol{p}_w$ and thus, it can be assured that the first three joints contribute to the position and orientation while the last three only contribute to the orientation. This allows to decouple the inverse kinematics into the inverse position and the inverse orientation problems.

5.4 Non-redundant robots with spherical wrist

In this section, the inverse position and the inverse orientation problems for a 6 DOF serial robot with spherical wrist is solved. Again, for the position problem different geometric strategies are defined depending on the nature and disposition of the joints along the kinematic chain. For the orientation problem, the rotor R is split into three different rotors from where the joint variables can be obtained.

5.4.1 Solution of the position problem

Four different combinations of prismatic and revolute joints that constitute the position part of the robot are analysed (figure 5.1). For each one of them, a geometric strategy is developed to solve the inverse position problem. This strategy consists of defining auxiliary points at each joint to recover the corresponding joint variables as the angle or displacement between two geometric entities defined by such points. For each case, the point at the origin, $\overline{n}$, is denoted by P_0 and is placed at the base of the robot. Similarly, the target position $\boldsymbol{p}_w$ is expressed as a null vector, P_w, obtained through the Hestenes' embedding (A.59). Finally, depending on the information available, for a given geometric entity it could be convenient to use its primal representation O or its dual representation O^*. Clearly, a geometric entity described with one of these two representations can be expressed in the other representation only by using the dual operator (A.44):

$$O^* = IO \tag{5.18}$$

Therefore, both representations can be used indistinctly.

Three prismatic joints (PPP)

A scheme of the position part of a serial robot $\mathcal{R}$ with three prismatic joints is depicted in figure 5.1a. First of all, the case without offsets between consecutive joints is considered, i.e., the axes of each pair of consecutive joints intersect. Given the first translation axis $\boldsymbol{z}_1$, two of the rotors introduced in (5.2) can be used to obtain the joint axes $\boldsymbol{z}_2$ and $\boldsymbol{z}_3$ as follows:

$$\begin{aligned} \boldsymbol{z}_2 &= R_{\theta_2} R_{\alpha_2} \boldsymbol{z}_1 \widetilde{R}_{\alpha_2} \widetilde{R}_{\theta_2} \\ \boldsymbol{z}_3 &= R_{\theta_3} R_{\alpha_3} \boldsymbol{z}_2 \widetilde{R}_{\alpha_3} \widetilde{R}_{\theta_3} \end{aligned} \tag{5.19}$$

where, since the joints are prismatic, R_{θ_i} is a constant rotor for $i = 1, 2$.

The joint axis $\boldsymbol{z}_3$ together with the target position $\boldsymbol{p}_w$ defines a line ℓ_3 whose dual representation is:

$$\ell_3^* = \boldsymbol{z}_3 e_{123} + (\boldsymbol{z}_3 \times \boldsymbol{p}_w) \wedge n \tag{5.20}$$

Here, the cross product can be expressed in terms of the outer product. Given two vectors $\boldsymbol{a}, \boldsymbol{b} \in \mathbb{R}^3$, the following holds:

$$\boldsymbol{a} \times \boldsymbol{b} = -(\boldsymbol{a} \wedge \boldsymbol{b}) e_{123} \tag{5.21}$$

Therefore:

$$\boldsymbol{z}_3 \times \boldsymbol{p}_w = -(\boldsymbol{z}_3 \wedge \boldsymbol{p}_w) e_{123} \tag{5.22}$$

and, thus, ℓ_3^* changes into:

$$\ell_3^* = \boldsymbol{z}_3 e_{123} - (\boldsymbol{z}_3 \wedge \boldsymbol{p}_w) e_{123} n \tag{5.23}$$

Now, a plane containing the joint axes $\boldsymbol{z}_1$ and $\boldsymbol{z}_2$ and passing through the point P_0 is also defined:

$$\pi_1^* = \boldsymbol{z}_1 \times \boldsymbol{z}_2 \tag{5.24}$$

Again, this representation changes into (5.21):

$$\pi_1^* = -(\boldsymbol{z}_1 \wedge \boldsymbol{z}_2)e_{123} \tag{5.25}$$

Since the end-effector position is not restricted to a fixed plane, there are not parallel prismatic joint axes. Moreover, $\ell_3 \notin \pi_1$ and, thus, its intersection is non-empty:

$$B = \ell_3 \vee \pi_1 \tag{5.26}$$

where $B \neq 0$ is a bivector (equation (A.75)). Hence, it represents a pair of points in conformal geometric algebra. However, since the intersection between a line and a plane is a single point, the bivector B is of the form:

$$B = P_2 \wedge n,$$

for a null vector P_2, that can be extracted from B through identity (A.68). With this point, the following lines are defined:

$$\begin{aligned} \ell_1^* &= \boldsymbol{z}_1 e_{123} - (\boldsymbol{z}_1 \wedge \overline{n})e_{123}n \\ \ell_2^* &= \boldsymbol{z}_2 e_{123} - (\boldsymbol{z}_2 \wedge \boldsymbol{p}_2)e_{123}n \end{aligned} \tag{5.27}$$

where $\boldsymbol{p}_2$ is the vector whose null vector is P_2. Given a null vector X, the associated real vector $\boldsymbol{x} \in \mathbb{R}^3$ is recovered through the formula:

$$\boldsymbol{x} = -\frac{2X}{X \cdot n} \tag{5.28}$$

that is, the inverse of the Hestenes' embedding (as defined in A.59). In addition, $\ell_1 \wedge \pi_1 = 0$ and $\ell_2 \wedge \pi_1 = 0$ and, since the joint axes $\boldsymbol{z}_1$ and $\boldsymbol{z}_2$ are not parallel, they have non-empty intersection:

$$P_1 = \ell_1 \vee \ell_2 \tag{5.29}$$

where point P_1 is calculated as in (A.83).

Finally, with the null vectors P_0, P_1, P_2 and P_w, the joint variables are recovered using the extended Euclidean distance (A.61):

$$\begin{aligned} d_1 &= d(P_0, P_1) \\ d_2 &= d(P_1, P_2) \\ d_3 &= d(P_2, P_w) \end{aligned} \tag{5.30}$$

Now, the case where there is an offset between two consecutive joints is studied. Let suppose, without loss of generality, that there exists an offset of length a between the first two joints (the other cases are analogous). Since the plane π_1 is defined with the joint axes $\boldsymbol{z}_1$ and $\boldsymbol{z}_2$ and offsets do not change the direction of the joint axes, P_2 is obtained from equation (5.26) as in the case without offsets. With P_2, ℓ_2 is determined as in (5.27).

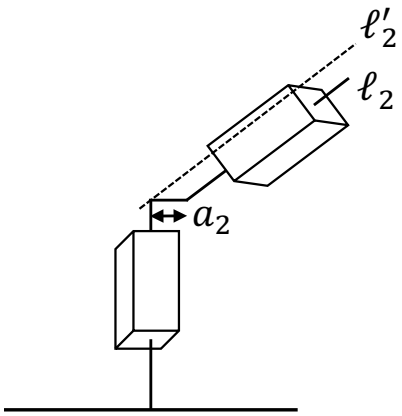

Figure 5.2: An example of a simple offset between the first two joint axes

Offsets between consecutive joints are always modeled by the four D-H parameters: a, α, θ and d. If joint i is revolute (prismatic), then θ_i (d_i) is a joint variable and, therefore, it is decomposed into $\theta_i = \widehat{\theta}_i + \overline{\theta}_i$ ($d_i = \widehat{d}_i + \overline{d}_i$) where $\widehat{\theta}_i$ ($\widehat{d}_i$) is a constant value, usually zero, that describes the component of the offset aligned with the joint axis, while $\overline{\theta}_i$ ($\overline{d}_i$) corresponds to the real joint variable and can be renamed as the original one (i.e., from now on, $\overline{\theta}_i$ and $\overline{d}_i$ are denoted by θ_i and d_i). Hence, an offset between the joints $i-1$ and i can be described by $(a_i, \alpha_i, \widehat{\theta}_i, d_i)$ if joint i is revolute or $(a_i, \alpha_i, \theta_i, \widehat{d}_i)$ if it is prismatic. In either of these two cases, the offset can be compensated simply by applying a sequence of rotors to the proper geometric entity.

In this particular case, since the first two joints are prismatic, the quad $(a_2, \alpha_2, \theta_2, \widehat{d}_2)$ determines the offset. Then, ℓ_2 is transformed as follows:

$$\begin{aligned} \ell'_2 &= T_{\widehat{d}_2}\, \ell_2\, \widetilde{T}_{\widehat{d}_2} & \qquad \ell'''_2 &= T_{a_2}\, \ell''_2\, \widetilde{T}_{a_2} \\ \ell''_2 &= R_{\theta_2}\, \ell'_2\, \widetilde{R}_{\theta_2} & \qquad \ell^{iv}_2 &= R_{\alpha_2}\, \ell'''_2\, \widetilde{R}_{\alpha_2} \end{aligned} \tag{5.31}$$

Since lines ℓ_1 and ℓ^{iv}_2 belong to the same plane, they have non-empty intersection and P_1 can be obtained as in (5.29) using, instead of ℓ_2, ℓ^{iv}_2. This completes the solution for this case.

In practice, most serial robots have simple offsets between their joints. Indeed, they usually involved just a translation of length a_i in the direction $\boldsymbol{e}_1$ of the joint frame $i-1$ (figure 5.2). However, even in the most general case, conformal geometric algebra allows an efficient treatment of them.

Two prismatic joints and one revolute (PPR)

The position part of a serial robot $\mathcal{R}$ with two prismatic joints and one revolute is depicted in figure 5.1b. There are different combinations of two prismatic joints with one revolute but

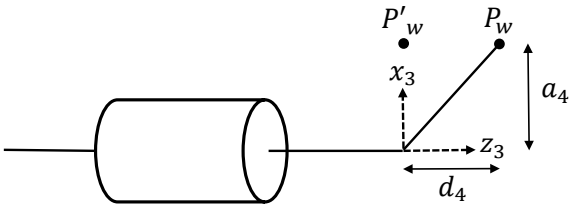

Figure 5.3: Translation of P_w to compensate the offset placed at the end of the third link

many of them are treated in a similar way. Only the most relevant cases are fully developed here. Again, the case without offsets is studied first.

Let suppose that the first two joints of $\mathcal{R}$ are prismatic, while its third joint is revolute. As in the precedent case, given $\boldsymbol{z}_1$, the joint axes $\boldsymbol{z}_2$ and $\boldsymbol{z}_3$ can be calculated as in (5.19). In this case, since the value of θ_3 does not affect the position and direction of $\boldsymbol{z}_3$, R_{θ_3} can be taken as the identity rotor, i.e., $R_{\theta_3} = 1$. Now, the plane π_1 that contains P_0 and the joint axes $\boldsymbol{z}_1$ and $\boldsymbol{z}_2$ is defined as in (5.24). Since the end-effector position is not restricted to a fixed plane, there exists an offset at the end of the third link, i.e., between the third link and the set of joints that conforms the spherical wrist. Besides, $\boldsymbol{z}_3$ cannot be orthogonal to π_1 (if it was, P_w would belong to a fixed plane parallel to π_1).

Since the last three joints of $\mathcal{R}$ do not contribute to the position of the end-effector, they are not considered in the inverse position problem. Therefore, this offset can be seen as a displacement defined in the $\boldsymbol{x}$–$\boldsymbol{z}$ plane of the third joint frame that can be decomposed into a displacement of a_4 in the $\boldsymbol{x}_3$ direction and a displacement of d_4 in the $\boldsymbol{z}_3$ direction (where a_4 and d_4 are two of the four D-H parameters). Then, it is possible to translate P_w to compensate at least one of the components of such offset (figure 5.3):

$$P'_w = T_{\boldsymbol{z}_3} P_w \widetilde{T}_{\boldsymbol{z}_3} \tag{5.32}$$

where

$$T_{\boldsymbol{z}_3} = 1 - d_4 \frac{n\boldsymbol{z}_3}{2} \tag{5.33}$$

Now, the point P_2 belongs to the intersection of two planes with one sphere. One of such planes is π_1, while the other is defined as follows:

$$\pi_2^* = \boldsymbol{z}_3 + d(P_0, P'_w)n \tag{5.34}$$

Additionally, the sphere is:

$$S_1^* = P'_w - \frac{1}{2}(a_3^2 + d_4^2)n \tag{5.35}$$

where a_3 denotes the length of the third link. In this case, since the radius and center of S_1 are already known, the dual representation of S_1 has been chosen. Plane π_2 is translated in the $\boldsymbol{z}_3$ direction:

$$(\pi_2^*)' = T_{\boldsymbol{z}_3} \pi_2^* \widetilde{T}_{\boldsymbol{z}_3} \tag{5.36}$$

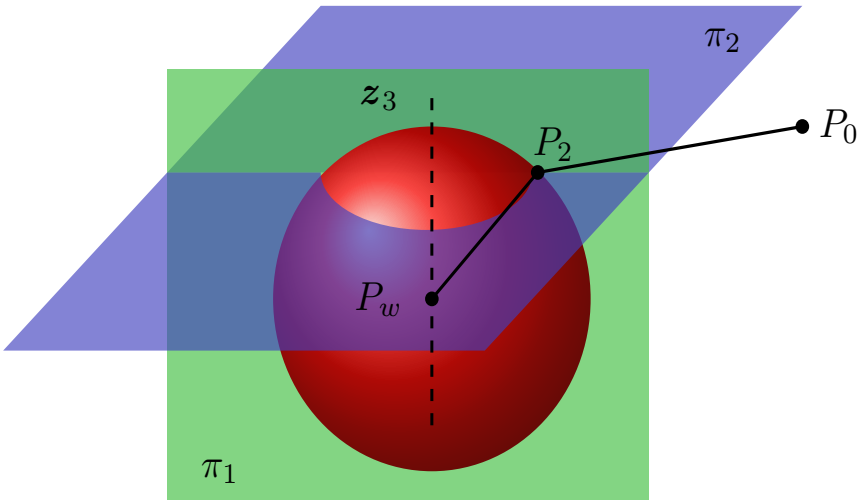

Figure 5.4: P_2 as the intersection of two planes and one sphere

where

$$T_{z_3} = 1 - a_3 \frac{n z_3}{2} \tag{5.37}$$

The intersection of these geometric entities is graphically depicted in figure 5.4 and is given by the expression:

$$B_2 = \pi_1 \vee \pi_2' \vee S_1 \tag{5.38}$$

where B_2 is a bivector (equation (A.75)). This bivector represents a pair of points in the conformal geometric algebra $\mathcal{G}_{4,1}$. Therefore:

$$B_2 = Q_1 \wedge Q_2 \tag{5.39}$$

for some null points Q_1 and Q_2. These points are extracted from (5.39) using (A.67). Clearly, if Q_1 and Q_2 belong to the workspace $\mathcal{W}$ of $\mathcal{R}$, then there are two possible points P_2, namely $P_{21} = Q_1$ and $P_{22} = Q_2$. Each one of these two points defines a line: ℓ_{21}^* (ℓ_{22}^*) if point P_{21} (P_{22}) is used. These lines, as well as line ℓ_1^*, are defined as in (5.27). The intersection

$$P_{1i} = \ell_{2i} \vee \ell_1 \quad \text{for } i = 1, 2 \tag{5.40}$$

returns two distinct points, P_{11} and P_{12}, calculated using (A.83).

Finally, each pair of points P_{1i} and P_{2i} (for $i = 1, 2$) defines an extra plane that can be used to determine the joint variable θ_3:

$$\begin{aligned} \pi_{31} &= P_{11} \wedge P_{21} \wedge P_w' \wedge n \\ \pi_{32} &= P_{12} \wedge P_{22} \wedge P_w' \wedge n \end{aligned} \tag{5.41}$$

Then, by means of the identities (A.61) and (A.90), the joint variables d_1, d_2 and θ_3 can be derived easily. Clearly, since two different expressions have been obtained for P_{2i}, P_{1i} and π_{3i}, two different set of joint variables are achieved:

$$\begin{aligned} d_{11} &= d(P_0, P_{11}) & d_{12} &= d(P_0, P_{12}) \\ d_{21} &= d(P_{11}, P_{21}) & d_{22} &= d(P_{11}, P_{22}) \\ \theta_{31} &= \angle(\pi_1, \pi_{31}) & \theta_{32} &= \angle(\pi_1, \pi_{32}) \end{aligned} \tag{5.42}$$

As stated in section 2.1, serial manipulators of 6 DOF have up to sixteen different solutions for a given end-effector pose T. In particular, 6 DOF serial robots with spherical wrist have up to eight distinct solutions associated with T. Since the orientation problem always has two different solutions for each solution of the position problem, there is a maximum of four distinct solutions for the position problem. This maximum is reached when the three joints that constitute the position part of the robot are revolute. Therefore, this case shows how the geometric strategy introduced in this chapter gives all the solutions for the inverse kinematics. However, from now on, in order to simplify the notation for the remaining cases, just one of the two points that can be extracted from a given bivector will be considered and, thus, only one solution will be developed.

Offsets between consecutive joints are treated analogously as in the previous case. The main difference relies on the geometric entity considered. For instance, if the offset is located between the second and the third joint, then P_2 is extracted from:

$$\pi_1 \vee \pi_2 \vee S_1'$$

where S_1' denotes the sphere S_1 after applying the rotors associated with the D-H parameters that models the offset (in the same way as in the previous case). Since the remaining geometric reasoning does not change, the other points are obtained as in the case without offsets. Moreover, this situation highlights another advantage of conformal geometric algebra: rotors can be applied to any geometric entity which simplifies the formulation and the solution of the problem.

Another relevant case is when the first joint is prismatic, the second joint is revolute and the third joint is also prismatic. This case is solved in a similar way, but it is interested to point out some details. The joint axes $\boldsymbol{z}_2, \boldsymbol{z}_3$ and the plane π_1 are obtained as in (5.19) and (5.24). Now, the following line is defined:

$$\ell_3^* = \boldsymbol{z}_3 e_{123} - (\boldsymbol{z}_3 \wedge \boldsymbol{p}_w) e_{123} n \tag{5.43}$$

Since the position of the end-effector is not restricted to a fixed plane, $\boldsymbol{z}_3 \notin \pi_1$ and, thus, $\ell_3 \vee \pi_1$ is non-empty. From the intersection bivector the point P_2 can be extracted using (A.67). Finally, point P_1 is obtained as the translation of P_2 along the axis $\boldsymbol{z}_2$:

$$P_1 = T_{\boldsymbol{z}_2} P_2 \widetilde{T}_{\boldsymbol{z}_2} \tag{5.44}$$

where

$$T_{\boldsymbol{z}_2} = 1 + a_2 \frac{n \boldsymbol{z}_2}{2} \tag{5.45}$$

The joint variables d_1 and d_3 are determined as in (5.30), while θ_2 is the angle between π_1 and ℓ_3.

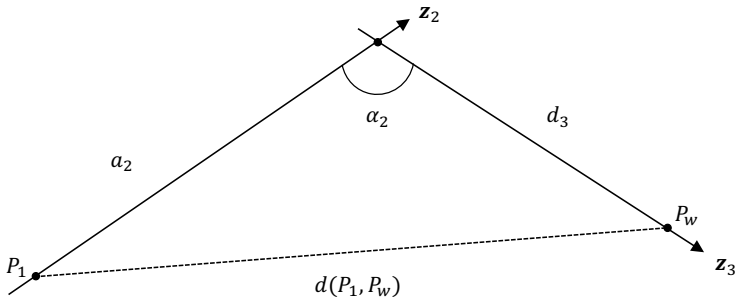

Figure 5.5: Triangle defined by z_2 and z_3

Two revolute joints and one prismatic (RRP)

A scheme of the position part of a serial robot $\mathcal{R}$ with two revolute joints and one prismatic is depicted in figure 5.1c. As in the precedent case, there are different subcases that can be treated similarly. Because of that, only the most relevant cases are developed here.

First, let consider the case where the first two joints are revolute while the third one is prismatic. In addition, there are no offsets between consecutive joints. The point P_1 is obtained as the the translation of P_0 along z_1 an amount equal to the length of the first link (described by the D-H parameters d_1 or a_1):

$$P_1 = T_{e_3} P_0 \widetilde{T}_{e_3} \tag{5.46}$$

with

$$T_{e_3} = 1 + a\frac{n e_3}{2} \tag{5.47}$$

where $a = a_1$ or $a = d_1$.

The remaining part of $\mathcal{R}$ is restricted to the plane determined by the joint axes z_2 and z_3. Furthermore, given the D-H parameters a_2 or d_2 for the length of the second link and α_2 for the angle between the joint axes z_2 and z_3, a triangle is defined (figure 5.5). Using the law of cosines, d_3 can be easily obtained from:

$$d(P_1, P_w)^2 = a_2^2 + d_3^2 - 2a_2 d_3 \cos(\alpha_2) \tag{5.48}$$

Now, equation (5.48) has two distinct positive solutions if, and only if:

$$a_2 \sin(\alpha_2) < d(P_1, P_w) < a_2.$$

In this context, such situation never holds and, thus, the positive solution for d_3 is taken. Notice that d_3 is the distance between P_2 and P_w. If there is a fixed offset aligned with z_3 (the translational axis), then d_3 can be decomposed as $d_3 = \widehat{d}_3 + d_3$ where $\widehat{d}_3$ denotes the length of such offset, while d_3 denotes the real joint variable. In either of these two cases, the joint variable d_3 can be obtained from (5.48).

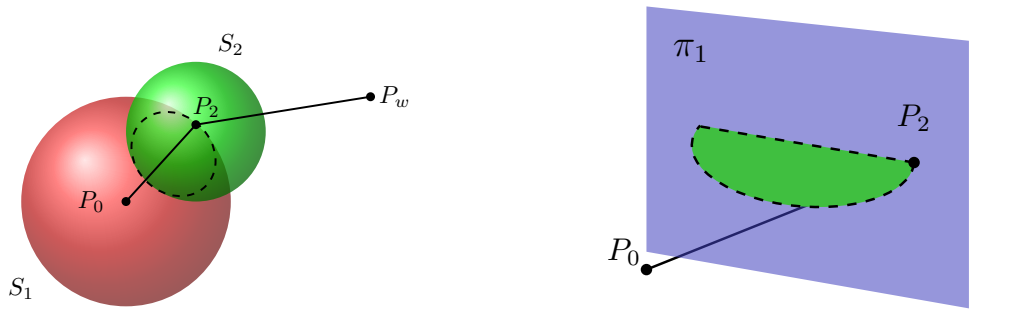

(a) P_2 in the intersection of two spheres **(b)** P_2 in the intersection of a circle and a plane

Figure 5.6: Computation of P_2

Finally, in order to obtain P_2, two distinct spheres and one plane need to be defined:

$$\begin{aligned} S_1^* &= P_1 - \frac{1}{2}a_2^2 n \\ S_2^* &= P_w - \frac{1}{2}d_3^2 n \\ \pi_1 &= P_0 \wedge P_1 \wedge P_w \wedge n \end{aligned} \tag{5.49}$$

Then, the intersection of these geometric entities is computed (figures 5.6a and 5.6b):

$$B_2 = S_1 \vee S_2 \vee \pi_1 \tag{5.50}$$

where P_2 is one of the points extracted from the bivector B_2 by means of (A.67).

Since d_3 has already been calculated, the points P_0, P_1 and P_2 can be used to obtain the remaining joint variables, namely θ_1 and θ_2. The following auxiliary geometric entities are defined for that purpose:

- If the revolute joints are parallel:

$$\begin{aligned} \ell_1 &= P_1 \wedge P_2 \wedge n \\ \ell_2 &= P_2 \wedge P_w \wedge n \end{aligned} \tag{5.51}$$

- If the revolute joints are not parallel:

$$\begin{aligned} \ell_1 &= P_0 \wedge P_1 \wedge n \\ \pi_2 &= P_1 \wedge P_2 \wedge P_w \wedge n \end{aligned} \tag{5.52}$$

Now, for the parallel case, the joint variables are:

$$\theta_1 = \angle(\boldsymbol{e}_1, \pi_1) \tag{5.53}$$

$$\theta_2 = \angle(\ell_1, \ell_2) \tag{5.54}$$

while for the other case, they are:

$$\theta_1 = \angle(\boldsymbol{e}_1, \pi_1) \tag{5.55}$$
$$\theta_2 = \angle(\ell_1, \pi_2) \tag{5.56}$$

Offsets are treated analogously as in the precedent cases. Two different situations arise:

- If the offset is placed between the second and the third joints and is modeled by the quad $(a_3, \alpha_3, \theta_3, \widehat{d_3})$, then the geometric entity that is translated and rotated is the sphere S_2.
- If the offset is placed between the first and the second joints and is modeled by the quad $(a_3, \alpha_3, \widehat{\theta_3}, d_3)$, then the geometric entity that is translated and rotated is the point P_0.

Once these geometric entities have been transformed, the remaining steps are the same as the ones developed in the case without offset.

Finally, let consider another subcase: the first joint is revolute, the second joint is prismatic and the third joint is again revolute. The points P_0 and P_1 are obtained as in the precedent case. To calculate the point P_2, the geometric reasoning used for the case where there are two prismatic joints followed by one revolute is applied. Therefore, the planes π_1, π_2, π_3 and the sphere S_1 are defined as in (5.24),(5.34),(5.35) and (5.41). Finally, the joint variables are obtained as in the above-mentioned case.

Three revolute joints (RRR)

A scheme of the position part of a serial robot $\mathcal{R}$ with three revolute joints is depicted in figure 5.1d. First, the case without offsets is analysed.

It only remains to find the intermediate points P_1 and P_2. As in the precedent case, the point P_0 is translated in the direction of $\boldsymbol{z}_1$:

$$P_1 = T_{\boldsymbol{e}_3} P_0 \widetilde{T}_{\boldsymbol{e}_3} \tag{5.57}$$

where

$$T_{\boldsymbol{e}_3} = 1 + a\frac{n\boldsymbol{e}_3}{2} \quad \text{with } a = a_1 \text{ or } d_1 \tag{5.58}$$

Once the point P_1 has been obtained, the point P_2 is established by intersecting two spheres and one plane as depicted in figures 5.6a and 5.6b. Let P_0, P_1 and P_w be the points defining such plane:

$$\pi_1 = P_0 \wedge P_1 \wedge P_w \wedge n \tag{5.59}$$

On the other side, if a_2 and a_3 denote the lengths of the second and third links respectively, the two spheres are defined as:

$$S_1^* = P_1 - \frac{1}{2}a_2^2 n \tag{5.60}$$

$$S_2^* = P_w - \frac{1}{2}a_3^2 n \tag{5.61}$$

The intersection of these three geometric entities is a bivector:

$$B_2 = S_1 \vee S_2 \vee \pi_1 \tag{5.62}$$

where, as in the precedent cases, two different points P_2 can be extracted from B_2 by (A.67)

Now, it only remains to find the joint variables. Two distinct cases are considered: two joint axes are parallel or no joint axes are parallel. The case where the three joint axes are parallel is not considered because it will mean that the inverse position problem is a two-dimensional problem instead of a three-dimensional one. Let suppose that the two parallel joint axes are the last two (the other cases are analogous). Then, the geometric entities required for calculating the joint variables are defined in terms of the already obtained points:

$$\ell_1 = P_0 \wedge P_1 \wedge n \tag{5.63}$$
$$\ell_2 = P_1 \wedge P_2 \wedge n \tag{5.64}$$
$$\ell_3 = P_2 \wedge P_w \wedge n \tag{5.65}$$

Using the geometric entities (5.59),(5.63-5.65) and the identity (A.90), the joint variables are determined as follows:

$$\theta_1 = \angle(\boldsymbol{e}_1, \pi_1) \tag{5.66}$$
$$\theta_2 = \angle(\ell_1, \ell_2) \tag{5.67}$$
$$\theta_3 = \angle(\ell_2, \ell_3) \tag{5.68}$$

For the case of no parallel joint axes, the geometric entities are:

$$\begin{aligned} \pi_2 &= P_0 \wedge P_1 \wedge P_2 \wedge n \\ \ell_1 &= P_2 \wedge P_w \wedge n \\ \pi_3 &= P_1 \wedge P_2 \wedge P_w \wedge n \end{aligned} \tag{5.69}$$

and the joint variables:

$$\theta_1 = \angle(\boldsymbol{e}_1, \pi_1) \tag{5.70}$$
$$\theta_2 = \angle(\pi_2, \ell_1) \tag{5.71}$$
$$\theta_3 = \angle(\pi_2, \pi_3) \tag{5.72}$$

Finally, the offsets are treated by transforming the proper geometric entity. For instance, if the offset is placed between the first and the second joint, then P_0 is transformed into P_0' according to the rotors defined by the quad $(a_2, \alpha_2, \widehat{\theta}_2, d_2)$ that models such offset. The point P_1 is obtained from identity (5.57) using P_0' instead of P_0, while the remaining steps are the same as the ones in the case without offsets. If, conversely, the offset is placed between the second and the third joint, then the transformation described by the quad that models the offset is applied to S_2. Therefore, the point P_2 is extracted from the intersection bivector $\pi_1 \vee S_1 \vee S_2'$, where S_2' denotes the transformed sphere. Again, the remaining steps are the same as the ones in the case without offsets.

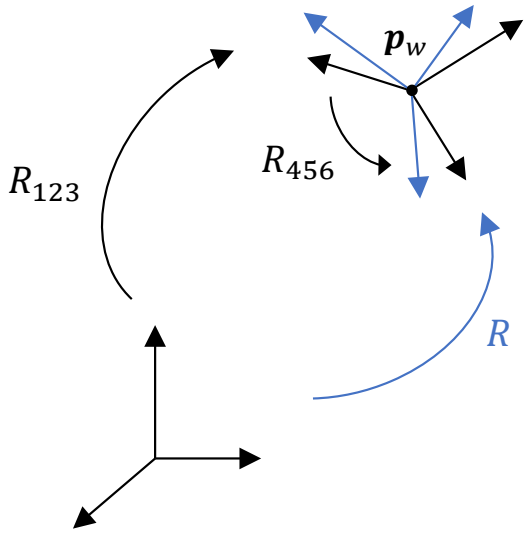

Figure 5.7: Relation between the orientations

5.4.2 Solution of the orientation problem

Since the inverse position problem has been solved, the joint variables q_1, q_2, q_3 are known. Therefore, it only remains to find q_4, q_5 and q_6. With q_1, q_2, q_3, the rotor defining the orientation of the wrist center point $\boldsymbol{p}_w$ under the effect of these joints can be calculated. Let denote by R_{123} such rotor. In addition, recall that R denotes the rotor that relates the orientation of the world frame with the orientation of the end-effector (5.16). Then, the rotor that defines the rotation between R_{123} and R can be obtained from the formula:

$$R = R_{123}R_{456} \tag{5.73}$$

where rotor R_{456} only depends on q_4, q_5 and q_6 (figure 5.7). Since these joints are revolute, q_4, q_5 and q_6 correspond to θ_4, θ_5 and θ_6, respectively.

The idea is to split R_{456} into three different rotors as follows:

$$R_{456} = R_4R_5R_6 \tag{5.74}$$

where $R_i = \cos(\theta_i/2) - \sin(\theta_i/2)B_i$ with angle of rotation θ_i and bivector B_i. The angle extracted from each one of these rotors will correspond to one of the desired joint variables. If the identity

(5.74) is expanded, the following expression is obtained:

$$\begin{aligned}
&R_{456} = R_4 R_5 R_6 = \\
&= \left(\cos\left(\frac{\theta_4}{2}\right) - \sin\left(\frac{\theta_4}{2}\right) B_4\right)\left(\cos\left(\frac{\theta_5}{2}\right) - \sin\left(\frac{\theta_5}{2}\right) B_5\right)\left(\cos\left(\frac{\theta_6}{2}\right) - \sin\left(\frac{\theta_6}{2}\right) B_6\right) = \\
&= \cos\left(\frac{\theta_4}{2}\right)\cos\left(\frac{\theta_5}{2}\right)\cos\left(\frac{\theta_6}{2}\right) - \cos\left(\frac{\theta_4}{2}\right)\cos\left(\frac{\theta_6}{2}\right)\sin\left(\frac{\theta_5}{2}\right) B_5 - \\
&- \cos\left(\frac{\theta_5}{2}\right)\cos\left(\frac{\theta_6}{2}\right)\sin\left(\frac{\theta_4}{2}\right) B_4 - \cos\left(\frac{\theta_4}{2}\right)\cos\left(\frac{\theta_5}{2}\right)\sin\left(\frac{\theta_6}{2}\right) B_6 + \\
&+ \cos\left(\frac{\theta_6}{2}\right)\sin\left(\frac{\theta_4}{2}\right)\sin\left(\frac{\theta_5}{2}\right) B_4 B_5 + \cos\left(\frac{\theta_4}{2}\right)\sin\left(\frac{\theta_5}{2}\right)\sin\left(\frac{\theta_6}{2}\right) B_5 B_6 + \\
&+ \cos\left(\frac{\theta_5}{2}\right)\sin\left(\frac{\theta_4}{2}\right)\sin\left(\frac{\theta_6}{2}\right) B_4 B_6 - \sin\left(\frac{\theta_4}{2}\right)\sin\left(\frac{\theta_5}{2}\right)\sin\left(\frac{\theta_6}{2}\right) B_4 B_5 B_6
\end{aligned} \tag{5.75}$$

where, besides, R_{456} can be expressed as follows:

$$R_{456} = \cos\left(\frac{\theta}{2}\right) - \sin\left(\frac{\theta}{2}\right) B_{456} \tag{5.76}$$

for an angle θ and a bivector B_{456}. As it can be observed, working directly with equation (5.75) is highly difficult, so an alternative path is required.

Theorem 5.4.1. *Let R denote an arbitrary rotor in the conformal geometric algebra $\mathcal{G}_{4,1}$. Then, $RH(\boldsymbol{x})\widetilde{R} = H(R\boldsymbol{x}\widetilde{R})$ for every $\boldsymbol{x} \in \mathbb{R}^3$ where $H(\cdot)$ denotes the Hestenes' embedding (A.59).*

Proof. It is easy to see that, for the special two null vector, it holds:

$$\begin{aligned}
Rn\widetilde{R} &= n \\
R\overline{n}\widetilde{R} &= \overline{n}
\end{aligned} \tag{5.77}$$

Then:

$$\begin{aligned}
RH(\boldsymbol{x})\widetilde{R} &= R\frac{1}{2}\left(\boldsymbol{x}^2 n + 2\boldsymbol{x} - \overline{n}\right)\widetilde{R} = \\
&= \frac{1}{2}\left(\boldsymbol{x}^2 Rn\widetilde{R} + 2R\boldsymbol{x}\widetilde{R} - R\overline{n}\widetilde{R}\right) = \\
&= \frac{1}{2}\left(\boldsymbol{x}^2 n + 2R\boldsymbol{x}\widetilde{R} - \overline{n}\right) = \\
&= H(R\boldsymbol{x}\widetilde{R})
\end{aligned} \tag{5.78}$$

Thus, $RH(\boldsymbol{x})\widetilde{R} = H(R\boldsymbol{x}\widetilde{R})$ for every $\boldsymbol{x} \in \mathbb{R}^3$. □

This implies that rotations can be defined in $\mathcal{G}_{4,1}$ using the bivectors of $\mathcal{G}_3$ and, therefore, B_{456} can be expressed as a linear combination with respect to the basis bivectors of $\mathcal{G}_3$:

$$B_{456} = \beta_1 e_{23} + \beta_2 e_{13} + \beta_3 e_{12} \tag{5.79}$$

for some $\beta_1, \beta_2, \beta_3 \in \mathbb{R}$. Therefore, equation (5.76) can be rewritten as:

$$R_{456} = \cos\left(\frac{\theta}{2}\right) - \sin\left(\frac{\theta}{2}\right)\beta_1 e_{23} - \sin\left(\frac{\theta}{2}\right)\beta_2 e_{13} - \sin\left(\frac{\theta}{2}\right)\beta_3 e_{12} \tag{5.80}$$

As it happens with the Euler angles, different conventions can be adopted. Depending on the convention used, a particular set of equations is obtained. For instance, by setting

$$B_4 = e_{12} \quad B_5 = e_{13} \quad B_6 = e_{12} \tag{5.81}$$

that corresponds to the Euler angles convention ZYZ, the following relations hold:

$$\begin{aligned} B_4 B_5 &= -e_{23} \\ B_5 B_6 &= e_{23} \\ B_4 B_6 &= -1 \\ B_4 B_5 B_6 &= B_5 \end{aligned} \tag{5.82}$$

Hence, by regrouping the terms of (5.75) and equating them to (5.80), the following set of equations is obtained:

$$\begin{aligned} \beta_1' &= \cos\left(\frac{\theta_4}{2}\right)\sin\left(\frac{\theta_5}{2}\right)\sin\left(\frac{\theta_6}{2}\right) - \cos\left(\frac{\theta_6}{2}\right)\sin\left(\frac{\theta_4}{2}\right)\sin\left(\frac{\theta_5}{2}\right) \\ \beta_2' &= -\cos\left(\frac{\theta_4}{2}\right)\cos\left(\frac{\theta_6}{2}\right)\sin\left(\frac{\theta_5}{2}\right) - \sin\left(\frac{\theta_4}{2}\right)\sin\left(\frac{\theta_5}{2}\right)\sin\left(\frac{\theta_6}{2}\right) \\ \beta_3' &= -\cos\left(\frac{\theta_5}{2}\right)\cos\left(\frac{\theta_6}{2}\right)\sin\left(\frac{\theta_4}{2}\right) - \cos\left(\frac{\theta_4}{2}\right)\cos\left(\frac{\theta_5}{2}\right)\sin\left(\frac{\theta_6}{2}\right) \end{aligned} \tag{5.83}$$

where:

$$\beta_i' = -\sin\left(\frac{\theta}{2}\right)\beta_i \quad \text{for} i = 1, 2, 3$$

The system of equations (5.83) can be simplified as follows:

$$\beta_1' = \sin\left(\frac{\theta_6 - \theta_4}{2}\right)\sin\left(\frac{\theta_5}{2}\right) \tag{5.84}$$

$$\beta_2' = -\cos\left(\frac{\theta_6 - \theta_4}{2}\right)\sin\left(\frac{\theta_5}{2}\right) \tag{5.85}$$

$$\beta_3' = -\sin\left(\frac{\theta_6 + \theta_4}{2}\right)\cos\left(\frac{\theta_5}{2}\right) \tag{5.86}$$

So, by squaring and adding (5.84) and (5.85), the following is obtained:

$$\begin{aligned} (\beta_1')^2 + (\beta_2')^2 &= \sin^2\left(\frac{\theta_6 - \theta_4}{2}\right)\sin^2\left(\frac{\theta_5}{2}\right) + \cos^2\left(\frac{\theta_6 - \theta_4}{2}\right)\sin^2\left(\frac{\theta_5}{2}\right) = \\ &= \sin^2\left(\frac{\theta_5}{2}\right) \end{aligned} \tag{5.87}$$

where the solutions of this trigonometric equation are:

$$\theta_5 = \frac{\sin^{-1}\left(\pm\sqrt{(\beta'_1)^2 + (\beta'_2)^2}\right)}{2} \tag{5.88}$$

Finally, if $\sin(\theta_5/2) \neq 0$, then:

$$\beta''_1 = \frac{\beta'_1}{\sin(\theta_5/2)} \quad \beta''_2 = \frac{-\beta'_2}{\sin(\theta_5/2)} \quad \beta''_3 = \frac{-\beta'_3}{\cos(\theta_5/2)} \tag{5.89}$$

and, therefore:

$$\begin{aligned} \beta''_1 &= \sin\left(\frac{\theta_6 - \theta_4}{2}\right) \\ \beta''_3 &= \sin\left(\frac{\theta_6 + \theta_4}{2}\right) \end{aligned} \Longrightarrow \begin{aligned} \frac{\theta_6 - \theta_4}{2} &= \sin^{-1}(\beta''_1) \\ \frac{\theta_6 + \theta_4}{2} &= \sin^{-1}(\beta''_3) \end{aligned} \tag{5.90}$$

that is solved easily as follows:

$$\begin{aligned} \theta_6 &= \sin^{-1}(\beta''_1) + \sin^{-1}(\beta''_3) \\ \theta_4 &= \sin^{-1}(\beta''_3) - \sin^{-1}(\beta''_1) \end{aligned} \tag{5.91}$$

This completes the resolution of the inverse orientation problem.

5.5 Redundant robots with spherical wrist

As stated in section 2.1, there are an infinite number of solutions for the inverse kinematics of redundant serial robots. In chapter 4, redundant robots are reduced to non-redundant ones by the parametrization of the so-called *redundant joints*. Once the analytical solutions for the inverse kinematics have been obtained, particular instances for the parametrized joints are given. Hence, for each instance, a set of a maximum of sixteen solutions is obtained (recall that, for non-redundant robots, this is the upper bound for the number of distinct solutions associated with a given end-effector pose). This can be regarded as the addition of extra conditions in an undetermined problem. Therefore, these particular solutions conform a subset of the set of all possible solutions for a given target pose of the end-effector.

Following this approach, the geometric strategies introduced and developed in section 5.4 are extended to 7 DOF serial robots with spherical wrist. Here, the extra information is given in the form of extra points P_i that allow the definition of the geometric entities involved in the resolution. The inverse orientation problem is solved as in the section 5.4.2. As it will be seen in the following cases, the addition of these extra points entails the evaluation of one of the joint variables. Thus, the approach presented in this section is equivalent to the strategy introduced in chapter 4 (restricted to 7 DOF serial robots with spherical wrist). Even more, if the identification of the redundant joints developed in chapter 4 is applied to these manipulators, it is possible to

know exactly which points P_i are needed to be determined in order to solve the inverse position problem using conformal geometric algebra.

For each one of the cases studied in section 5.4.1, an extra degree of freedom – that corresponds either to a prismatic or revolute joint – is added. Several distinct combinations arise, but as in section 5.4.1, only the most relevant are fully developed in order not to repeat the already used geometric reasonings. In particular, the cases to be considered are: PPPP, PPRP, RRPR and RRRR.

5.5.1 PPPP

The objective is to find P_1, P_2 and P_3 to obtain the joint variables d_1, d_2, d_3 and d_4. Since all the joints are prismatic, the joint axes $\boldsymbol{z}_2, \boldsymbol{z}_3$ and $\boldsymbol{z}_4$ can be calculated as in (5.19). Now, two distinct planes:

$$\begin{aligned} \pi_1^* &= -(\boldsymbol{z}_1 \wedge \boldsymbol{z}_2)e_{123} \\ \pi_2^* &= -(\boldsymbol{z}_3 \wedge \boldsymbol{z}_4)e_{123} + d(P_0, P_w)n \end{aligned} \tag{5.92}$$

and two distinct lines are defined:

$$\begin{aligned} \ell_1^* &= \boldsymbol{z}_1 e_{123} - (\boldsymbol{z}_1 \wedge \overline{n})e_{123}n \\ \ell_2^* &= \boldsymbol{z}_4 e_{123} - (\boldsymbol{z}_4 \wedge \boldsymbol{p}_w)e_{123}n \end{aligned} \tag{5.93}$$

The intersection of π_1 and π_2 is a line containing the point P_2:

$$\ell_2 = \pi_1 \vee \pi_2 \tag{5.94}$$

To determine uniquely P_2 another plane is needed. Such a plane contains the joint axes $\boldsymbol{z}_2$ and $\boldsymbol{z}_3$. However, it also requires an extra point for setting its distance to P_0. Let define P_1 as the point that verifies:

$$P_1 \in \ell_1 \quad \text{and} \quad d(P_0, P_1) = d_1 \tag{5.95}$$

Notice that the definition of P_1 is equivalent to set d_1 at a particular instance. Now, the new plane can be fully defined as:

$$\pi_3^* = -(\boldsymbol{z}_2 \wedge \boldsymbol{z}_3)e_{123} + d_1 n \tag{5.96}$$

and, therefore, P_2 can be extracted from the intersection bivector $\pi_3 \vee \ell_2$ (using (A.67)).

Once P_0, P_1 and P_2 have been obtained, P_3 is found as the intersection of lines ℓ_3 and ℓ_4, where:

$$\ell_3^* = \boldsymbol{z}_3 e_{123} - (\boldsymbol{z}_3 \wedge \boldsymbol{p}_2)e_{123}n \tag{5.97}$$

Again, $\boldsymbol{p}_2$ represents the three dimensional vector whose null vector is P_2. Such vector is recovered using equation (5.28). Finally, the remaining joint variables d_2, d_3 and d_4 are calculated as in (5.30).

5.5.2 PPRP

Again, the joint axes $\boldsymbol{z}_2$ and $\boldsymbol{z}_3$ are calculated as in (5.19). However, since the third joint is revolute, R_{θ_3} is not a constant rotor when computing $\boldsymbol{z}_4$ and, thus, it cannot be obtained. The line ℓ_1 and the plane π_1 are defined as in (5.92) and (5.93). Now, an extra point is needed to completely describe the position of $\boldsymbol{z}_4$. Let denote as P_3 the point that verifies:

$$\ell_3^* = \boldsymbol{z}_3 e_{123} - (\boldsymbol{z}_3 \wedge \boldsymbol{p}_3) e_{123} n \quad \text{and} \quad \angle(\pi_1, \ell_3) = \theta_3 \tag{5.98}$$

The definition of the point P_3 is equivalent to set a particular value to the joint variable θ_3. Now, P_3 is translated along $\boldsymbol{z}_3$:

$$P_2 = T_{\boldsymbol{z}_3} P_3 \widetilde{T}_{\boldsymbol{z}_3} \tag{5.99}$$

where

$$T_{\boldsymbol{z}_3} = 1 - a_3 \frac{n \boldsymbol{z}_3}{2} \tag{5.100}$$

Finally, the line ℓ_2 is defined as in section 5.4.1 and point P_1 is found as the intersection point $\ell_1 \vee \ell_2$ (that can be obtained by means of (A.83)). Once the points P_0, P_1, P_2 and P_3 have been obtained, the joint variables d_1, d_2 and d_4 can be calculated as in equation (5.30).

5.5.3 RRPR

Point P_0 is translated along the joint axis $\boldsymbol{z}_1$ an amount equal to the length of the first link as in (5.57). The translated point is P_1 so the remaining unknown points are P_2 and P_3.

Now, a sphere is defined:

$$S_1^* = P_w - \frac{1}{2} a^2 n \tag{5.101}$$

where a corresponds to the length of the fourth link (either $a = a_4$ or $a = d_4$, where a_4 and d_4 are two D-H parameters). To continue, an extra point is needed. Let denote by P_3 the point that satisfies:

$$P_3 \in S_1 \quad \text{and} \quad d(P_1, P_3) = d \tag{5.102}$$

Since the second and third joint axes belong to the same plane, their links can be regarded as the sides of a triangle where, besides, the third side is given by the line segment defined by P_1 and P_3. As shown in section 5.4.1, the law of cosines can be applied in this situation to deduce the expression for the joint variable d_3. The length of both sides, as well as the angle between the joint axes, are known: a_2, d and α_3. Therefore:

$$d^2 = a_2^2 + d_3^2 - 2 a_2 d_3 \cos(\alpha_3) \tag{5.103}$$

where, as explained in section 5.4.1, there is only one positive solution for d_3. This proves the equivalence between the extra point P_3 and the joint variable d_3. Once d_3 has been determined,

the point P_2 is extracted from the intersection bivector defined by the following two spheres and one plane:

$$\begin{aligned} S_2^* &= P_1 - \frac{1}{2}a_2^2 n \\ S_3^* &= P_3 - \frac{1}{2}d_3^2 n \\ \pi_1 &= P_0 \wedge P_1 \wedge P_3 \wedge n \end{aligned} \tag{5.104}$$

Once all the points have been obtained, it is easy to recover the joint variables θ_1, θ_2 and θ_4 following the same steps as in the sections 5.4.1 and 5.4.1.

5.5.4 RRRR

As in the previous case, the point P_1 is obtained as the translation of the point P_0 along $\boldsymbol{z}_1$ (as in (5.57)). Thus, the points that remain to be found are P_2 and P_3. Now, as stated in section 5.4.1, two spheres and one plane are required to calculated P_3. One of such spheres is defined as in (5.101). For the other, a triangle whose sides are the links two and three is considered. This triangle is similar to the one defined in the previous case: the side lengths are a_2 and a_3, respectively, and the angle between both sides is α_3. The law of cosines allows to compute easily the length of the third side d as:

$$d^2 = a_3^2 + a_2^2 - 2a_2 a_3 \cos(\alpha_3) \tag{5.105}$$

where only the positive solution for d is taken. Now, the other sphere can be defined as:

$$S_2^* = P_1 - \frac{1}{2}d^2 n \tag{5.106}$$

On the other hand, the plane π_1 is defined as in (5.59). Clearly, P_3 can be extracted, using (A.67), from the intersection bivector defined by these three geometric entities.

Once P_3 have been obtained, two new spheres should be defined to calculate P_2:

$$\begin{aligned} S_3^* &= P_1 - \frac{1}{2}a_2^2 n \\ S_4^* &= P_3 - \frac{1}{2}a_3^2 n \end{aligned} \tag{5.107}$$

Again, the intersection of these two new spheres with π_1 is computed:

$$B_3 = S_3 \vee S_4 \vee \pi_1 \tag{5.108}$$

where the point P_2 is extracted from the bivector B_3. Finally, the joint variables $\theta_1, \theta_2, \theta_3$ and θ_4 are found in a similar way to which it is done in 5.4.1 by means of P_0, P_1, P_2, P_3 and P_w (with all their possible combinations).

Chapter 6

Identification of Singularities based on Geometric Algebra

Geometry is not true, it is advantageous

Henri Poincare

This chapter addresses a novel singular analysis of serial robot manipulators. Such analysis is based on the six-dimensional and three-dimensional geometric algebras and consists of identifying which configurations $\boldsymbol{q} \in \mathcal{C}$ vanish the exterior product of the lines defined from the joint axes. Moreover, since rotors are used to describe rotations and translations between arbitrary geometric entities, a distance function $d : \mathcal{C} \times \mathcal{C} \rightarrow [0, +\infty)$ can be defined in the configuration space $\mathcal{C}$ such as its restriction to $d : \mathcal{C} \times \mathcal{S} \rightarrow [0, +\infty)$ allows to compute the distance of any configuration $\boldsymbol{q} \in \mathcal{C}$ to a given singularity $\boldsymbol{q}_s \in \mathcal{S}$.

6.1 Problem statement

As shown in section 2.2, one of the main problems in robot kinematics is the identification and handling of kinematic singularities. For the identification, the most extended method consists of solving the nonlinear equations (B.22). However, the formulation of either $\det(J_G(\boldsymbol{q})) = 0$ or $\det(J_G(\boldsymbol{q})J_G^T(\boldsymbol{q})) = 0$ is not computationally efficient. Moreover, since each one of these equations is nonlinear, the seeking of closed-form solutions is difficult. In this context, geometric algebra turns to be very useful.

There is not much literature regarding the identification of singularities using geometric algebra and the majority of the contributions focuses on parallel mechanisms. For serial robots, in (Corrochano and Sobczyk, 2001), the authors extend the bracket (or Lie product) of two vectors defined in any Lie algebra to what they call the *superbracket* of the lines $\ell_1, \ldots, \ell_6$, $[\ell_1, \ldots, \ell_6]$, where the line ℓ_i denotes the axis of joint $\mathcal{R}_i$. For serial robots of 6 DOF, the main idea is to split the superbracket into small superbrackets, called bracket monomials, that are equated to zero. The singularities are the solutions of these bracket monomial equations. Following the same idea, in (Kanaan et al., 2009) the superbracket is defined in a Grassmann-Caley algebra. Since the Lie product is well defined in every Grassmann-Caley algebra, the superbracket is also well defined. However, split the superbracket into the bracket monomials in this context is not intuitive and, as a consequence, is not always realizable.

For parallel mechanisms, the works (Tanev, 2006; Chai and Xiang, 2016; Yao et al., 2017; Chai and Li, 2017) focus on approaches developed for some particular parallel robots. The main idea consists of computing, for each leg of the mechanism, the outer product of the screws defined by its joints and equating it to zero. For those legs with less than six actuated joints, combinations of two, three or more legs are considered. The main problem of these approaches rely on its lack of generality. Each approach is designed for the specific parallel robot the authors work with.

By their side, Huo et al. (2017) present a mobility analysis applying conformal geometric algebra, and a singularity analysis using an idea similar to the ones presented in the above-mentioned contributions. Finally, in (Kim et al., 2015a), conformal geometric algebra is applied to the identification of the singularities of the SPS-parallel manipulator. Several lines and planes are defined in $\mathcal{G}_{4,1}$ using the different joint axes. Then, the relative position of different combinations of these geometric entities is studied to geometrically find out the singularities. However, this method cannot be extended to other classes of parallel or serial robots nor can it be implemented as an algorithm due to its geometrical nature.

In this chapter, a novel approach for singularity identification based on the six-dimensional and three-dimensional geometric algebras is introduced. This method can be applied to arbitrary redundant and non-redundant serial robots. It consists of manipulating the exterior product of the screw axes defined by the joints. These axes can be described as generalized lines using the Plücker coordinates in order to distinguish between the lines associated with revolute joint axes to the ones associated with prismatic joint axes. Besides, this method can be simplified for serial robots with spherical wrist. Once the singularities have been identify, since rotors describe the transformations of arbitrary multivectors in geometric algebra, a distance function d can be defined in the configuration space $\mathcal{C}$ that can be used to determine the distance of any arbitrary configuration $\boldsymbol{q} \in \mathcal{C}$ to a given singularity $\boldsymbol{q}_s$.

6.2 Identification of singularities using geometric algebra

Since the degrees of freedom required to describe the position and orientation of a rigid body in the three-dimensional space are six, the more natural way of formulating the singularity problem is through the six-dimensional geometric algebra $\mathcal{G}_6$, that extends naturally the three-dimensional algebra $\mathcal{G}_3$ introduced in section A.3. Screw theory (Murray et al., 1994; Davidson and Hunt, 2004) provides an intuitive and geometrical description of the differential kinematics of serial and parallel manipulators using six-dimensional vectors. Because of this, throughout this chapter some concepts taken from this theory will be employed. This will provide the initial framework to completely understand the approach introduced in this section. First, a classical theorem of the screw theory is needed.

Theorem 6.2.1 (Chasles, 1830)**.** *Every rigid motion $f \in SE(3)$ is equivalent to a screw motion, that is, a rotation about a line followed (preceded) by a translation along that line. Such line is known as the screw axis and is denoted by S.*

Particular cases of screw motions are the pure rotations (pure translations) where the translation (rotation) is the identity. The screw axis S can be compactly represented by means of the Plücker coordinates.

Definition 6.2.2. A line ℓ in the three-dimensional space can be fully specified by two three-dimensional vectors: its direction vector $\boldsymbol{u}$ and its position vector $\boldsymbol{p}$. The *Plücker coordinates* of ℓ conforms a six-dimensional vector $[\boldsymbol{u}\ \boldsymbol{u}\times\boldsymbol{p}]^T$ where $\boldsymbol{u}\times\boldsymbol{p}$ denotes the moment vector of ℓ.

Thus, given a screw motion of a rigid body, its screw axis S is just a line ℓ (the rotational and translational axis) together with a scalar $h \in \mathbb{R}$, called the *pitch*, that satisfies:

$$S = \begin{bmatrix} \boldsymbol{u} \\ \boldsymbol{u}\times\boldsymbol{p} + h\boldsymbol{u} \end{bmatrix} \tag{6.1}$$

For the particular case of a pure rotation or a pure translation, the screw axis becomes:

$$\begin{aligned} S &= \begin{bmatrix} \boldsymbol{u} \\ \boldsymbol{u}\times\boldsymbol{p} \end{bmatrix} \quad \text{for a pure rotation } (h=0) \\ S &= \begin{bmatrix} \boldsymbol{0} \\ \boldsymbol{u} \end{bmatrix} \quad \text{for a pure translation } (h=\infty) \end{aligned} \tag{6.2}$$

Definition 6.2.3. Let S denote the screw axis of a screw motion of a rigid body B. Then, the rotational component of such motion has angular velocity $\boldsymbol{w}$, while its translational component has linear velocity $\boldsymbol{v}$. The *twist* $\boldsymbol{t}$ of the screw motion is a six-dimensional vector of the form:

$$\boldsymbol{t} = \begin{bmatrix} \boldsymbol{w} \\ \boldsymbol{v} \end{bmatrix} = \alpha S = \alpha \begin{bmatrix} \boldsymbol{u} \\ \boldsymbol{u}\times\boldsymbol{p} + h\boldsymbol{u} \end{bmatrix} \tag{6.3}$$

where α is the *amplitude* of the twist.

Again, for the particular case of pure rotations (pure translations), the twist has the form:

$$\begin{aligned} \boldsymbol{t} &= \dot{\theta} \begin{bmatrix} \boldsymbol{u} \\ \boldsymbol{u} \times \boldsymbol{p} \end{bmatrix} \quad \text{for a pure rotation} \\ \boldsymbol{t} &= \dot{d} \begin{bmatrix} \mathbf{0} \\ \boldsymbol{u} \end{bmatrix} \quad \text{for a pure translation} \end{aligned} \tag{6.4}$$

where $\theta : \mathbb{R} \to [-\pi, +\pi]$ and $d : \mathbb{R} \to [a, b]$ (with $a, b \in \mathbb{R}$) are two time-dependent functions whose image are, respectively, the angle of rotation and the displacement.

Now, let consider a serial robot $\mathcal{R}$ with n DOF where $\boldsymbol{\omega}, \boldsymbol{v}$ denote the angular and linear velocity vectors of its end-effector. If equation (B.20) is expanded, the following is obtained:

$$\begin{bmatrix} \boldsymbol{v} \\ \boldsymbol{\omega} \end{bmatrix} = J_1(\boldsymbol{q})\dot{q}_1 + \cdots + J_n(\boldsymbol{q})\dot{q}_n \tag{6.5}$$

where J_i denotes the i-th column of the geometric Jacobian J_G. Notice that the right side of equation (6.5) can be seen as the addition of the twists associated with the joints of $\mathcal{R}$ where the linear and angular parts are interchanged. Indeed, if J_i is seen as a screw axis, $\dot{q}_i$ plays the role of the twist amplitude. However, for the sake of formality, let consider the screw axis associated with the joint i of $\mathcal{R}$ and denote it by S_i. Then, for each screw axis S_i, there is a twist $\boldsymbol{t}_i$ of the form:

$$\boldsymbol{t}_i(\boldsymbol{q}) = S_i(\boldsymbol{q})\dot{q}_i = \begin{cases} \begin{bmatrix} \boldsymbol{z}_i \\ \boldsymbol{z}_i \times (\boldsymbol{o}_n - \boldsymbol{o}_i) \end{bmatrix} \dot{q}_i & \text{for a pure rotation} \\ \begin{bmatrix} \mathbf{0} \\ \boldsymbol{z}_i \end{bmatrix} \dot{q}_i & \text{for a pure translation} \end{cases} \tag{6.6}$$

where $\boldsymbol{z}_i$ is the direction vector of the joint axis and $\boldsymbol{o}_n$ ($\boldsymbol{o}_i$) is the origin of the frame attached to the end-effector (i-th joint). The following is a key result:

Theorem 6.2.4 (Tsai (1999))**.** *Let $\mathcal{R}$ be a serial robot with n DOF. Then:*

$$\begin{bmatrix} \boldsymbol{\omega} \\ \boldsymbol{v} \end{bmatrix} = S_1(\boldsymbol{q})\dot{q}_1 + \cdots + S_n(\boldsymbol{q})\dot{q}_n = [S_1(\boldsymbol{q}) \ \cdots \ S_n(\boldsymbol{q})]\dot{\boldsymbol{q}} \tag{6.7}$$

where $\dot{\boldsymbol{q}} = (\dot{q}_1, \ldots, \dot{q}_n)$.

The main advantage of the screw-based Jacobian matrix defined in equation (6.7) is that allows a geometrical identification of the singularities. Moreover, if an approach based on geometric algebra or conformal geometric algebra is used, a geometrical or algebraic identification of the singularities can be performed. For that purpose, let consider the geometric algebra $\mathcal{G}_6$ where for every $i = 1, \ldots, n$, the screw axis $S_i(\boldsymbol{q})$ is simply a vector.

The following is the main result of this section.

Theorem 6.2.5. *Let $S_i(\boldsymbol{q})$ denote the screw axis defined by the i-th joint axis expressed as a vector of $\mathcal{G}_6$. Then:*

$$S_1(\boldsymbol{q}) \wedge \cdots \wedge S_6(\boldsymbol{q}) = \det(S_1(\boldsymbol{q}) \ \cdots \ S_6(\boldsymbol{q}))\boldsymbol{e}_1 \wedge \cdots \wedge \boldsymbol{e}_6 \tag{6.8}$$

where $\boldsymbol{e}_1, \ldots, \boldsymbol{e}_6$ are the basis vectors of $\mathcal{G}_6$.

Theorem 6.2.5 can be seen as a particular case of a more general result:

Theorem 6.2.6. *Let $\boldsymbol{a}_1, \ldots, \boldsymbol{a}_n$ be a set of n vectors of $\mathcal{G}_n$. Then:*

$$\boldsymbol{a}_1 \wedge \cdots \wedge \boldsymbol{a}_n = \det(\boldsymbol{a}_1 \ \cdots \ \boldsymbol{a}_n)\boldsymbol{e}_1 \wedge \cdots \wedge \boldsymbol{e}_n \tag{6.9}$$

Proof. Let start with two vectors $\boldsymbol{a}_1, \boldsymbol{a}_2$ of $\mathcal{G}_2$. Therefore, $\boldsymbol{a}_1 = a_{11}\boldsymbol{e}_1 + a_{12}\boldsymbol{e}_2 = (a_{11}, a_{12})$ and $\boldsymbol{a}_2 = a_{21}\boldsymbol{e}_1 + a_{22}\boldsymbol{e}_2 = (a_{21}, a_{22})$ for some $a_{ij} \in \mathbb{R}$ with $1 \leq i, j \leq 2$. The exterior product of both vectors is computed as follows:

$$\begin{aligned} \boldsymbol{a}_1 \wedge \boldsymbol{a}_2 &= (a_{11}\boldsymbol{e}_1 + a_{12}\boldsymbol{e}_2) \wedge (a_{21}\boldsymbol{e}_1 + a_{22}\boldsymbol{e}_2) = \\ &= (a_{11}a_{22} - a_{21}a_{12})\boldsymbol{e}_1 \wedge \boldsymbol{e}_2 = \\ &= \det(\boldsymbol{a}_1 \ \boldsymbol{a}_2)\boldsymbol{e}_1 \wedge \boldsymbol{e}_2 \end{aligned} \tag{6.10}$$

Hence, by the properties of the determinant and the linearity and anticommutativity of the outer product, it is easy to extend equation (6.10) to a set of n vectors of $\mathcal{G}_n$:

$$\boldsymbol{a}_1 \wedge \cdots \wedge \boldsymbol{a}_n = \det(\boldsymbol{a}_1 \ \cdots \ \boldsymbol{a}_n)\boldsymbol{e}_1 \wedge \cdots \wedge \boldsymbol{e}_n \tag{6.11}$$

□

In particular, equation (6.11) is true for any set of six vectors $\boldsymbol{a}_1, \ldots, \boldsymbol{a}_6$ of $\mathcal{G}_6$, which proves theorem 6.2.5.

The following corollary of theorem 6.2.5 allows to characterize the singularities of any serial robot of 6 DOF.

Corollary 6.2.7. *Let $\mathcal{R}$ denotes a serial robot of 6 DOF and $S_1(\boldsymbol{q}), \ldots, S_6(\boldsymbol{q})$, the screws associated with its joints. Then, if $\mathcal{S}$ denotes the set of all singular configurations (clearly, $\mathcal{S} \subset \mathcal{C}$), then $\boldsymbol{q} \in \mathcal{S}$ if, and only if, $S_1(\boldsymbol{q}) \wedge \cdots \wedge S_6(\boldsymbol{q}) = 0$.*

Proof. Taking the dual of equation (6.8), the following identity is obtained:

$$(S_1(\boldsymbol{q}) \wedge \cdots \wedge S_6(\boldsymbol{q}))^* = \det(S_1(\boldsymbol{q}) \ \cdots \ S_6(\boldsymbol{q})) \tag{6.12}$$

and, therefore, the singularities of $\mathcal{R}$ are those configurations $\boldsymbol{q} \in \mathcal{C}$ that verify

$$(S_1(\boldsymbol{q}) \wedge \cdots \wedge S_6(\boldsymbol{q}))^* = 0 \tag{6.13}$$

Moreover, since for a given non-zero multivector $M \in \mathcal{G}_n$, $M^* = 0$ if, and only if, $M = 0$, equation (6.13) can be simplified to:

$$S_1(\boldsymbol{q}) \wedge \cdots \wedge S_6(\boldsymbol{q}) = 0 \tag{6.14}$$

Thus, $\boldsymbol{q} \in \mathcal{S}$ if, and only if, $S_1(\boldsymbol{q}) \wedge \cdots \wedge S_6(\boldsymbol{q}) = 0$. □

In addition, corollary 6.2.7 allows to re-define the singular set as:

$$\mathcal{S} = \{\boldsymbol{q} \in \mathcal{C} \ : \ (S_1(\boldsymbol{q}) \wedge \cdots \wedge S_6(\boldsymbol{q})) = 0\} \tag{6.15}$$

Example 6.2.8. What theorem 6.2.5 states is that, for instance, if two screw axes S_1 and S_2 verify that $S_1 \wedge S_2 = 0$ then they represent the same screw, and hence, the same generalized line. This means that if the associated screw is a translation, then the translational axes are parallel or coincident, while if the associated screw is a rotation, the rotational axes are coincident (since for rotational screws the screw axis contains the term $(\boldsymbol{z}_1 \times (\boldsymbol{o}_6 - \boldsymbol{o}_1))$, they cannot be parallel). Regarding the kinematic singularities of serial robots, this implies that two prismatic joints whose axes are either parallel or coincident give rise to a singularity and, equivalently, that two revolute joints whose axes are coincident give rise to a singularity. This is, in fact, coherent with what it is known about kinematic singularities since two parallel revolute joint axes do not give rise to a singularity.

Obviously, the same geometrical interpretation can be made for three, four or more screw axes verifying that its outer product is zero (though the number of different cases depending on the nature of the joints involved increases exponentially).

With respect to redundant serial robots, it is clear that, for $n > 6$, $S_1(\boldsymbol{q}) \wedge \cdots \wedge S_n(\boldsymbol{q}) = 0$ for any $\boldsymbol{q} \in \mathcal{C}$. Hence, corollary 6.2.7 by its own does not allow to characterize the singularities of redundant robots. However, this problem can be easily overcome by studying all the possible combinations of six screws contained in $S_1(\boldsymbol{q}) \wedge \cdots \wedge S_n(\boldsymbol{q})$.

Theorem 6.2.9. *Let $\mathcal{R}$ denotes a serial robot of n DOF and $S_1(\boldsymbol{q}), \ldots, S_n(\boldsymbol{q})$, the screws associated with its joints. Then $\boldsymbol{q} \in \mathcal{S}$ if, and only if, for each $1 \leq i \leq C(n,6)$, where $C(n,6) = \binom{n}{6}$.*

$$S_{i_1}(\boldsymbol{q}) \wedge \cdots \wedge S_{i_6}(\boldsymbol{q}) = 0 \tag{6.16}$$

Proof. It follows that, for $\boldsymbol{q} \in \mathcal{C}$:

$$\begin{aligned} & S_{i_1}(\boldsymbol{q}) \wedge \cdots \wedge S_{i_6}(\boldsymbol{q}) = 0 \text{ for every } 1 \leq i \leq C(n,6) \iff \\ & \overset{(1)}{\iff} \det(S_{i_1}(\boldsymbol{q}) \ \cdots \ S_{i_6}(\boldsymbol{q})) = 0 \text{ for every } 1 \leq i \leq C(n,6) \iff \\ & \overset{(2)}{\iff} \rho([S_1(\boldsymbol{q}) \ \cdots \ S_n(\boldsymbol{q})]) < 6 \end{aligned} \tag{6.17}$$

where (1) uses equation (6.12) and (2) uses that all the minors of order 6 of $[S_1(\boldsymbol{q}) \ \cdots \ S_n(\boldsymbol{q})]$ have null determinant. Clearly, $\rho([S_1(\boldsymbol{q}) \ \cdots \ S_n(\boldsymbol{q})]) < 6$ if, and only if, $\rho(J_G(\boldsymbol{q})) < 6$ which, in turn, is equivalent to $\boldsymbol{q} \in \mathcal{S}$ (by definition B.2.9). □

6.2.1 Special case: serial robots with a spherical wrist

The computation of either equation (6.14) for non-redundant robots or equation (6.16) for redundant ones is computationally more efficient than the computation of either $\det J_G(\boldsymbol{q}) = 0$ or $\det(J_G(\boldsymbol{q})J_G^T(\boldsymbol{q})) = 0$. The main reason relies in the complexity of the operations needed to obtain the expressions (6.14) or (6.16) with respect to the complexity of the operations needed for obtaining $\det J_G(\boldsymbol{q}) = 0$ or $\det(J_G(\boldsymbol{q})J_G^T(\boldsymbol{q})) = 0$. It is clear that the outer product of n vectors of $\mathcal{G}_n$ behaves like the product of real numbers and, hence, it has complexity $O(n^2)$, while the determinant has complexity $O(n^3)$ or $O(n^4)$ depending on the algorithm used. In addition, for redundant robots, there are two main operations: the product between $J_G(\boldsymbol{q})$ and $J_G^T(\boldsymbol{q})$ and the determinant of the product matrix. This implies that, for this case, the complexity increases to $O(n^3) + O(n^4)$.

However, the application of the approach presented in this chapter for redundant robots implies the computation of $C(n, 6)$ equations to find out the complete set of singular configurations. Nevertheless, similarly to what happens with the geometric Jacobian matrix J_G, a simplification can be done for the robots that have a spherical wrist, i.e., the robots whose last three joint axes are revolute and intersect at a single point. As stated in section 2.2.1, the singularities of those robots can be decoupled into position and orientation singularities. Position singularities involves the first $n-3$ joints and are computed by studying the rank of the following matrix:

$$J_p = \begin{bmatrix} \boldsymbol{z}_1 \times (\boldsymbol{o}_n - \boldsymbol{o}_1) & \cdots & \boldsymbol{z}_{n-3} \times (\boldsymbol{o}_n - \boldsymbol{o}_{n-3}) \end{bmatrix} \tag{6.18}$$

while orientation singularities involves the last three joints and are computed through the determinant of the following matrix:

$$J_o = \begin{bmatrix} \boldsymbol{z}_{n-2} & \boldsymbol{z}_{n-1} & \boldsymbol{z}_n \end{bmatrix} \tag{6.19}$$

Hence, this simplification is specially useful for redundant robots with spherical wrist. Now, let consider the three-dimensional geometric algebra $\mathcal{G}_3$. As proven in theorem 6.2.6 for $n = 3$, $\boldsymbol{a}_1 \wedge \boldsymbol{a}_2 \wedge \boldsymbol{a}_3 = \det(\boldsymbol{a}_1\ \boldsymbol{a}_2\ \boldsymbol{a}_3)\boldsymbol{e}_1 \wedge \boldsymbol{e}_2 \wedge \boldsymbol{e}_3$ for any three vectors $\boldsymbol{a}_1, \boldsymbol{a}_2, \boldsymbol{a}_3 \in \mathbb{R}^3$. Hence, analogously to what has been done before, the following characterization for the position and orientation singularities can be deduced.

Theorem 6.2.10. *Let denote by $\mathcal{R}$ a serial robot of n DOF with a spherical wrist. If $\boldsymbol{z}_i \times (\boldsymbol{o}_n - \boldsymbol{o}_i)$ is denoted by $\boldsymbol{s}_i$ for $i = 1, \ldots, n-3$, then:*

- *$\boldsymbol{q} \in \mathcal{C}$ is a position singularity if, and only if, $s_{i_1}(\boldsymbol{q}) \wedge s_{i_2}(\boldsymbol{q}) \wedge s_{i_3}(\boldsymbol{q}) = 0$ for each $1 \leq i \leq C(n-3, 3)$.*
- *$\boldsymbol{q} \in \mathcal{C}$ is an orientation singularity if, and only if, $\boldsymbol{z}_{n-2}(\boldsymbol{q}) \wedge \boldsymbol{z}_{n-1}(\boldsymbol{q}) \wedge \boldsymbol{z}_n(\boldsymbol{q}) = 0$.*

Proof. The proof is completely analogous to the proof of corollary 6.2.7. □

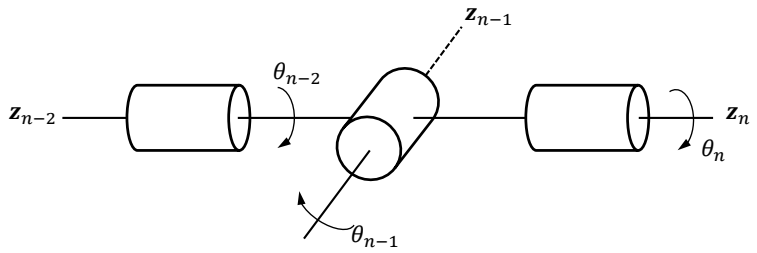

Figure 6.1: Schematic representation of the wrist singularity.

Remark 6.2.11. Since the last three joint axes intersect at a single point, there is only one orientation singularity, namely when these three joint axes are coplanar. A schematic representation of such singularity, also called *wrist singularity*, is depicted in figure 6.1.

6.3 Distance to singularities

Let $\boldsymbol{q}_1, \boldsymbol{q}_2 \in \mathcal{C}$ be two arbitrary configurations of a serial robot $\mathcal{R}$ with n DOF and let $S_1, \dots, S_n$ be the screws associated with its joints. Then, there exist $R_1(\boldsymbol{q}_1, \boldsymbol{q}_2), \dots, R_n(\boldsymbol{q}_1, \boldsymbol{q}_2)$ where for each $1 \leq i \leq n$, $R_i(\boldsymbol{q}_1, \boldsymbol{q}_2)$ is a configuration-dependent rotor in the six-dimensional geometric algebra $\mathcal{G}_6$ such that (figure 6.2):

$$S_i(\boldsymbol{q}_2) = R_i(\boldsymbol{q}_1, \boldsymbol{q}_2) S_i(\boldsymbol{q}_1) \widetilde{R}_i(\boldsymbol{q}_1, \boldsymbol{q}_2) \tag{6.20}$$

The reason why these rotors exist is simple: screws can be seen as lines and, thus, since they are geometric entities, there is always a rotor relating each pair of them. In particular, there is always a rotor relating the same screw S in two different configurations $\boldsymbol{q}_1, \boldsymbol{q}_2$.

Remark 6.3.1. Since the wedge product of $p \geq 1$ screws is also a geometric entity $O = S_{i_1} \wedge \cdots \wedge S_{i_p}$, there exists a rotor R such that $O = R S_k \widetilde{R}$ for any screw S_k. Note that, if $S_k = S_{j_i}$ for some $1 \leq i \leq p$, then $R = 1$.

Now, let $\boldsymbol{q}_s \in \mathcal{S}$ be an arbitrary singularity of $\mathcal{R}$. As explained in the previous section, if $\mathcal{R}$ has a spherical wrist, then $\boldsymbol{q}_s$ only involves a maximum of two or three joints and, therefore, two or three screw axes. If, conversely, $\mathcal{R}$ has not a spherical wrist, then it can involve a maximum of six joints. Let suppose, without loss of generality, that a given singularity $\boldsymbol{q}_s$ involve the screw axes $S_{i_1}(\boldsymbol{q}_s), \dots, S_{i_r}(\boldsymbol{q}_s)$ with $2 \leq r \leq 6$. Then, for any configuration $\boldsymbol{q} \in \mathcal{C}$, there exist $R_{i_1}(\boldsymbol{q}, \boldsymbol{q}_s), \dots, R_{i_r}(\boldsymbol{q}, \boldsymbol{q}_s) \in \mathcal{G}_6$ (or $\mathcal{G}_3$) such that:

$$S_{i_j}(\boldsymbol{q}_s) = R_{i_j}(\boldsymbol{q}, \boldsymbol{q}_s) S_{i_j}(\boldsymbol{q}) \widetilde{R}_{i_j}(\boldsymbol{q}, \boldsymbol{q}_s) \quad \forall j = 1, \dots, r \tag{6.21}$$

The notation chosen for these rotors express a configuration dependence that is not a functional dependency, i.e., there is not an analytical expression for these rotors (with $\boldsymbol{q}$ as a variable).

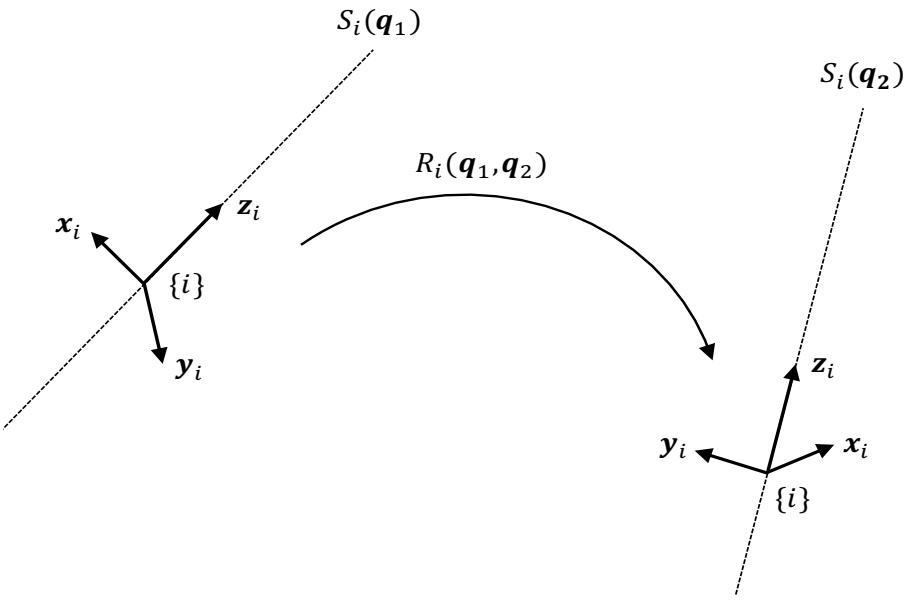

Figure 6.2: Rotor R_i relating the screw S_i in two different configurations $\boldsymbol{q}_1$ and $\boldsymbol{q}_2$.

Now, it is clear that $R_{i_j}(\boldsymbol{q}, \boldsymbol{q}_s) = 1$ if, and only if, $\boldsymbol{q} = \boldsymbol{q}_s$ for every $j = 1, \dots, r$. However, since for each j, $R_{i_j}(\boldsymbol{q}, \boldsymbol{q}_s)$ is not a function depending on $\boldsymbol{q}$, a distance function cannot be defined. But, the measure of how close is a given configuration $\boldsymbol{q}$ to a singularity can be set as:

$$\boldsymbol{q} \approx \boldsymbol{q}_s \iff R_{i_j}(\boldsymbol{q}) \approx 1 \text{ for every } j = 1, \dots, r \tag{6.22}$$

Example 6.3.2. Let $\boldsymbol{q}_s \in \mathcal{S}$ be a singularity of $\mathcal{R}$ that only involves joints $\mathcal{R}_2$ and $\mathcal{R}_3$ (with screw axes $S_2(\boldsymbol{q})$ and $S_3(\boldsymbol{q})$). Then, there exist $R_2(\boldsymbol{q}, \boldsymbol{q}_s), R_3(\boldsymbol{q}, \boldsymbol{q}_s)$ such that:

$$\begin{aligned} S_2(\boldsymbol{q}_s) &= R_2(\boldsymbol{q}, \boldsymbol{q}_s) S_2(\boldsymbol{q}) \widetilde{R}_2(\boldsymbol{q}, \boldsymbol{q}_s) \\ S_3(\boldsymbol{q}_s) &= R_3(\boldsymbol{q}, \boldsymbol{q}_s) S_3(\boldsymbol{q}) \widetilde{R}_3(\boldsymbol{q}, \boldsymbol{q}_s) \end{aligned} \tag{6.23}$$

Therefore, an arbitrary configuration $\boldsymbol{q}$ is close to $\boldsymbol{q}_s$ if, and only if:

$$\left.\begin{aligned} R_2(\boldsymbol{q}, \boldsymbol{q}_s) &\approx 1 \\ R_3(\boldsymbol{q}, \boldsymbol{q}_s) &\approx 1 \end{aligned}\right\} \tag{6.24}$$

and is singular if, and only if:

$$\left.\begin{aligned} R_2(\boldsymbol{q}, \boldsymbol{q}_s) &= 1 \\ R_3(\boldsymbol{q}, \boldsymbol{q}_s) &= 1 \end{aligned}\right\} \tag{6.25}$$

where, in general, $R_2(\boldsymbol{q}, \boldsymbol{q}_s) \neq R_3(\boldsymbol{q}, \boldsymbol{q}_s)$.

These rotors can be constructed in many different ways. The easiest way consists of considering, for each $1 \leq i \leq n$, the frame $\{i\}$ associated with each joint $\mathcal{R}_i$. Then, given a reference frame

$\{U\}$ and as stated in section 5.3, one can recover the rotor R_i that relates $\{U\}$ with $\{i\}$. Since each frame $\{i\}$ depends on the configuration $\boldsymbol{q}$, rotor $R_i(\boldsymbol{q})$ is a continuous function defined as follows:

$$\begin{aligned} R_i : \mathcal{C} &\to \langle \mathcal{G}_6 \rangle_0 + \langle \mathcal{G}_6 \rangle_2 \\ \boldsymbol{q} &\mapsto R_i(\boldsymbol{q}) \end{aligned} \tag{6.26}$$

where, as stated in A.3.10, rotors are constructed with the even-grade elements of $\mathcal{G}_n$ for $n \leq 5$ and, hence, $\langle \mathcal{G}_6 \rangle_0 + \langle \mathcal{G}_6 \rangle_2$ can be replaced by $\mathcal{G}_3^+$. Thus, these configuration-dependent rotors exhibit a functional dependency, which allows the definition of a distance function. Such distance is based on the norm of a multivector $X \in \mathcal{G}_n$, defined by the relation:

$$\|X\| = \left\langle X\widetilde{X} \right\rangle_0 \tag{6.27}$$

To prove that $\|\cdot\|$ is a norm, the following two lemmas are necessary.

Lemma 6.3.3. *For any given multivector $X \in \mathcal{G}_n$, $\left\langle X\widetilde{X} \right\rangle_0 \in \mathbb{R}^+ = [0, +\infty)$.*

Proof. According to equation (A.42), it follows that:

$$\widetilde{X} = \widetilde{\langle X \rangle_0} + \widetilde{\langle X \rangle_1} + \cdots + \widetilde{\langle X \rangle_n} \tag{6.28}$$

Then:

$$X\widetilde{X} = \sum_{i=0}^{n} \sum_{j=0}^{n} \langle X \rangle_i \widetilde{\langle X \rangle_j} \tag{6.29}$$

Note that, for each $i = 1, \ldots, n$, $\langle X \rangle_i$ is a i-vector, i.e., it only contains terms of grade i. The geometric product of two k-vectors (with different k) is stated as follows (Doran and Lasenby, 2003, pp. 93):

$$A_r B_s = \langle A_r B_s \rangle_{|r-s|} + \langle A_r B_s \rangle_{|r-s|+2} + \cdots + \langle A_r B_s \rangle_{r+s} \tag{6.30}$$

Therefore, it is clear that $\left\langle \langle X \rangle_i \widetilde{\langle X \rangle_j} \right\rangle_0 = 0$ for $i \neq j$. Thus:

$$\left\langle X\widetilde{X} \right\rangle_0 = \sum_{i=0}^{n} \left\langle \langle X \rangle_i \widetilde{\langle X \rangle_i} \right\rangle_0 \tag{6.31}$$

Now, each $\langle X \rangle_i$ can be expanded as follows:

$$\langle X \rangle_i = \sum_{j=1}^{C(n,i)} \alpha_j(i) e_{j_1} \cdots e_{j_i} \tag{6.32}$$

where, for every $1 \leq j \leq C(n,i) = \binom{n}{i}$, $\alpha_j(i) \in \mathbb{R}$ and $e_{j_1} \cdots e_{j_i}$ are the basis elements of $\langle \mathcal{G}_n \rangle_i$ (as defined in section A.3). Therefore:

$$\widetilde{\langle X \rangle_i} = \sum_{j=1}^{C(n,i)} \alpha_j(i) e_{j_i} \cdots e_{j_1} \tag{6.33}$$

and, thus:

$$\begin{aligned}\langle X\rangle_i \widetilde{\langle X\rangle}_i &= \sum_{j=1}^{C(n,i)} \alpha_j(i) e_{j_1}\cdots e_{j_i} \sum_{j=1}^{C(n,i)} \alpha_j(i) e_{j_i}\cdots e_{j_1} = \\ &= \sum_{j=1}^{C(n,i)}\sum_{k=1}^{C(n,i)} \alpha_j(i)\alpha_k(i) e_{j_1}\cdots e_{j_i} e_{k_i}\cdots e_{k_1}\end{aligned} \tag{6.34}$$

where, clearly, $\langle e_{j_1}\cdots e_{j_i} e_{k_i}\cdots e_{k_1}\rangle_0 = \delta_{jk}$ with δ_{jk} the Kronecker delta. Then:

$$\left\langle \langle X\rangle_i \widetilde{\langle X\rangle}_i \right\rangle_0 = \sum_{j=1}^{C(n,i)} \alpha_j^2 \tag{6.35}$$

that, for every $1 \leq i \leq n$, is a positive scalar. This implies that the sum of equation (6.31) is also a positive scalar. □

Lemma 6.3.4. *Given three strictly positive real numbers $a_1, a_2, a_3 \in \mathbb{R}^+ \setminus \{0\}$, the following properties hold:*

- $\sqrt{a_1 + a_2 - a_3} \leq \sqrt{a_1} + \sqrt{a_2}$.
- $\sqrt{a_1 + a_2 + a_3} \leq \sqrt{a_1} + \sqrt{a_2}$ *if, and only if,* $a_3 \leq 2\sqrt{a_1 a_2}$.

Proof. Both properties can be obtained by a straightforward computation. □

Proposition 6.3.5. *The function $\|\cdot\| : \mathcal{G}_n \to \mathbb{R}^+$ defined by the identity $\|X\|^2 = \left\langle X\widetilde{X}\right\rangle_0$ is a norm in $\mathcal{G}_n$, i.e.,:*

(i) $\|X\| \geq 0$ *for all* $X \in \mathcal{G}_n$. *In particular,* $\|X\| = 0$ *if, and only if,* $X = 0$.

(ii) $\|\lambda X\| = |\lambda|\|X\|$ *for all* $X \in \mathcal{G}_n$ *and* $\lambda \in \mathbb{R}$.

(iii) $\|X + Y\| \leq \|X\| + \|Y\|$ *for all* $X, Y \in \mathcal{G}_n$ *(usually known as the triangle inequality).*

Proof.

(i) Given a multivector X, identity $\|X\|^2 = \left\langle X\widetilde{X}\right\rangle_0$ is equivalent to:

$$\|X\| = \pm\sqrt{\left\langle X\widetilde{X}\right\rangle_0} \tag{6.36}$$

Thus, it is clear by lemma 6.3.3 that the positive branch of equation (6.36) is well defined and that $\|X\| \geq 0$. In particular, if $\|X\| = 0$, then:

$$\sqrt{\left\langle X\widetilde{X}\right\rangle_0} = 0 \Longrightarrow \left\langle X\widetilde{X}\right\rangle_0 = 0 \Longrightarrow \sum_{i=0}^{n} \left\langle \langle X\rangle_i \widetilde{\langle X\rangle}_i \right\rangle_0 = 0 \tag{6.37}$$

where all the addends of the last equation are positive by lemma 6.3.3 and, thus, all of them are equal to zero. Now, note that each addend is the geometric product of a i-vector with its reverse. Therefore, if such product is zero, the corresponding i-vector must be zero. Since all the addends are zero, all the i-vectors that conform X are zero and, thus, X is zero.

(ii) If $\lambda \in \mathbb{R}$ and $X \in \mathcal{G}_n$, then:

$$\begin{aligned} \|\lambda X\| &= \sqrt{\left\langle (\lambda X)(\lambda \widetilde{X}) \right\rangle_0} = \sqrt{\left\langle \lambda^2 X \widetilde{X} \right\rangle_0} \overset{(1)}{=} \\ &= \sqrt{\lambda^2 \left\langle X \widetilde{X} \right\rangle_0} = |\lambda| \sqrt{\left\langle X \widetilde{X} \right\rangle_0} = |\lambda| \|X\| \end{aligned} \tag{6.38}$$

where (1) uses the linearity of the grade-0 projection operator (as stated in section A.3).

(iii) Given two different multivectors X and Y, they can be expanded as linear combinations of the basis elements of $\mathcal{G}_n$ as follows:

$$\begin{aligned} X &= \sum_{i=0}^{2^n} \alpha_i e_{j_1} \cdots e_{j_i} \\ Y &= \sum_{i=0}^{2^n} \beta_i e_{j_1} \cdots e_{j_i} \end{aligned} \tag{6.39}$$

Now, it follows that:

$$X + Y = \sum_{i=0}^{2^n} (\alpha_i + \beta_i) e_{j_1} \cdots e_{j_i} \tag{6.40}$$

and, hence:

$$\begin{aligned} \|X + Y\| &= \sqrt{\left\langle (X + Y)\, \widetilde{(X + Y)} \right\rangle_0} \overset{(1)}{=} \sqrt{\sum_{i=0}^{2^n} (\alpha_i + \beta_i)^2} = \\ &= \sqrt{\underbrace{\boxed{\sum_{i=0}^{2^n} \alpha_i^2}}_{A} + \underbrace{\boxed{\sum_{i=0}^{2^n} \beta_i^2}}_{B} + 2 \underbrace{\boxed{\sum_{i=0}^{2^n} \alpha_i \beta_i}}_{C}} \end{aligned} \tag{6.41}$$

where (1) uses lemma 6.3.3, while A, B and C are just a notation given to simplify the different manipulations. Since $A, B > 0$ (if either A, B or C are equal to zero, then either $X = 0$ or $Y = 0$, which will make the condition $\|X + Y\| \leq \|X\| + \|Y\|$ trivial):

$$\sqrt{A + B + C} \overset{(1)}{\leq} \sqrt{A} + \sqrt{B} = \sqrt{\sum_{i=0}^{2^n} \alpha_i^2} + \sqrt{\sum_{i=0}^{2^n} \beta_i^2} = \|X\| + \|Y\| \tag{6.42}$$

where (1) uses the first or second property of lemma 6.3.4 depending on whether $C < 0$ or $C > 0$. It only remains to check that, if $C > 0$, $2C \leq 2\sqrt{AB}$. Indeed, to prove the

previous inequality is equivalent to prove that $C^2 \leq AB$. But:

$$\begin{aligned} AB &= \sum_{i=0}^{2^n} \alpha_i^2 \sum_{i=0}^{2^n} \beta_i^2 = \sum_{i=0}^{2^n} \sum_{j=0}^{2^n} \alpha_i^2 \beta_j^2 = \sum_{i=0}^{2^n} \alpha_i^2 \beta_i^2 + \sum_{i=0}^{2^n} \sum_{\substack{j=0 \\ j \neq i}}^{2^n} \alpha_i^2 \beta_j^2 \\ C^2 &= \left(\sum_{i=0}^{2^n} \alpha_i \beta_i \right)^2 = \sum_{i=0}^{2^n} \alpha_i^2 \beta_i^2 + \sum_{i=0}^{2^n} \sum_{\substack{j=0 \\ j \neq i}}^{2^n} \alpha_i \beta_i \alpha_j \beta_j \end{aligned} \tag{6.43}$$

and, thus, $C^2 \leq AB$ turns to:

$$\sum_{i=0}^{2^n} \alpha_i^2 \beta_i^2 + \sum_{i=0}^{2^n} \sum_{\substack{j=0 \\ j \neq i}}^{2^n} \alpha_i \beta_i \alpha_j \beta_j \leq \sum_{i=0}^{2^n} \alpha_i^2 \beta_i^2 + \sum_{i=0}^{2^n} \sum_{\substack{j=0 \\ j \neq i}}^{2^n} \alpha_i^2 \beta_j^2 \tag{6.44}$$

that is equivalent to:

$$\sum_{i=0}^{2^n} \sum_{\substack{j=0 \\ j \neq i}}^{2^n} \alpha_i \beta_i \alpha_j \beta_j \leq \sum_{i=0}^{2^n} \sum_{\substack{j=0 \\ j \neq i}}^{2^n} \alpha_i^2 \beta_j^2 \tag{6.45}$$

which, in turn, is equivalent to:

$$\begin{aligned} 0 &\leq \sum_{i=0}^{2^n} \sum_{\substack{j=0 \\ j \neq i}}^{2^n} \alpha_i^2 \beta_j^2 - \sum_{i=0}^{2^n} \sum_{\substack{j=0 \\ j \neq i}}^{2^n} \alpha_i \beta_i \alpha_j \beta_j = \\ &= \frac{1}{2} \sum_{i=0}^{2^n} \sum_{\substack{j=0 \\ j \neq i}}^{2^n} \alpha_i^2 \beta_j^2 + \frac{1}{2} \sum_{i=0}^{2^n} \sum_{\substack{j=0 \\ j \neq i}}^{2^n} \alpha_i^2 \beta_j^2 - \sum_{i=0}^{2^n} \sum_{\substack{j=0 \\ j \neq i}}^{2^n} \alpha_i \beta_i \alpha_j \beta_j = \\ &= \frac{1}{2} \sum_{i=0}^{2^n} \sum_{\substack{j=0 \\ j \neq i}}^{2^n} (\alpha_i \beta_j - \alpha_j \beta_i)^2 \end{aligned} \tag{6.46}$$

Since this last inequality is always true, the triangle inequality is also true.

□

Now, a distance function d can be defined in the rotor group $\mathfrak{R}$ (recall that, as stated in section A.3, the group $\mathfrak{R} = \{R \in \mathcal{G}_n^+ \ : \ R\widetilde{R} = 1\}$ is a rotor group if, and only if, $n \leq 5$ (lemma A.3.10), which is, indeed, the case, since for each i, $R_i \in \mathcal{G}_3^+$).

Theorem 6.3.6. *The function $d : \mathfrak{R} \times \mathfrak{R} \to \mathbb{R}^+$ defined by the identity $d(R_1, R_2) = \|R_1 - R_2\|$ is a distance in $\mathfrak{R}$, i.e.,:*

(i) $d(R_1, R_2) \geq 0$ *for all* $R_1, R_2 \in \mathfrak{R}$. *In particular,* $d(R_1, R_2) = 0$ *if, and only if,* $R_1 = R_2$.

(ii) $d(R_1, R_2) = d(R_2, R_1)$ *for all* $R_1, R_2 \in \mathfrak{R}$.

(iii) $d(R_1, R_3) \leq d(R_1, R_2) + d(R_2, R_3)$ *for all* $R_1, R_2, R_3 \in \mathfrak{R}$.

Proof. The proof is straightforward and uses the fact that $\|\cdot\|$ is a norm. Given two different rotors R_1 and R_2:

(i) $d(R_1, R_2) = \|R_1 - R_2\| \geq 0$. In particular:

$$d(R_1, R_2) = 0 \iff \|R_1 - R_2\| = 0 \overset{(1)}{\iff} R_1 - R_2 = 0 \iff R_1 = R_2 \tag{6.47}$$

where (1) uses the first property of a norm.

(ii)

$$\begin{aligned} d(R_1, R_2) = \|R_1 - R_2\| &= \sqrt{\left\langle (R_1 - R_2)\widetilde{(R_1 - R_2)} \right\rangle_0} = \\ &= \sqrt{\left\langle R_1\widetilde{R}_1 - R_1\widetilde{R}_2 - R_2\widetilde{R}_1 + R_2\widetilde{R}_2 \right\rangle_0} = \\ &= \sqrt{\left\langle R_1\widetilde{R}_1 \right\rangle_0 - \left\langle R_1\widetilde{R}_2 \right\rangle_0 - \left\langle R_2\widetilde{R}_1 \right\rangle_0 + \left\langle R_2\widetilde{R}_2 \right\rangle_0} = \\ &= \sqrt{\left\langle R_2\widetilde{R}_2 \right\rangle_0 - \left\langle R_2\widetilde{R}_1 \right\rangle_0 - \left\langle R_1\widetilde{R}_2 \right\rangle_0 + \left\langle R_1\widetilde{R}_1 \right\rangle_0} = \\ &= \sqrt{\left\langle R_2\widetilde{R}_2 - R_2\widetilde{R}_1 - R_1\widetilde{R}_2 + R_1\widetilde{R}_1 \right\rangle_0} = \\ &= \sqrt{\left\langle (R_2 - R_1)\widetilde{(R_2 - R_1)} \right\rangle_0} = \|R_2 - R_1\| = d(R_2, R_1) \end{aligned} \tag{6.48}$$

(iii) Given a rotor R_3:

$$\begin{aligned} d(R_1, R_3) = \|R_1 - R_3\| = \|R_1 - R_2 + R_2 - R_3\| &\overset{(1)}{\leq} \\ \leq \|R_1 - R_2\| + \|R_2 - R_3\| &= d(R_1, R_2) + d(R_2, R_3) \end{aligned} \tag{6.49}$$

where (1) uses the third property of a norm.

□

As stated before, the end-effector pose of $\mathcal{R}$ and the pose each joint $\mathcal{R}_i$ are described by the configuration-dependent rotors $R(\boldsymbol{q})$ and $R_i(\boldsymbol{q})$ respectively. Thus, one can be tempted to extend the distance function d to $\mathcal{C}$ as follows:

$$\begin{aligned} &d : \mathcal{C} \times \mathcal{C} \to \mathbb{R}^+ \\ &d(\boldsymbol{q}_1, \boldsymbol{q}_2) = \|R(\boldsymbol{q}_1) - R(\boldsymbol{q}_2)\| \end{aligned} \tag{6.50}$$

This function verifies all the axioms of a distance function with the exception of:

$$d(\boldsymbol{q}_1, \boldsymbol{q}_2) = 0 \Longleftrightarrow \boldsymbol{q}_1 = \boldsymbol{q}_2 \tag{6.51}$$

The reason is simple: since, in general, the inverse kinematics problem has not a unique solution, more than one different configurations can have associated the same end-effector pose and, thus, the same rotor R. However, this problem can be overcome as follows:

- For each joint $\mathcal{R}_i$, let denote by $\mathcal{C}_i$ the configuration space of the subchain conformed by the first i joints, i.e., $\mathcal{R}_1, \ldots, \mathcal{R}_i$. It is clear that, if $\mathcal{R}$ has m degrees of freedom, $\mathcal{C}_i \subset \mathcal{C}$ for every $1 \leq i \leq m$. Then, the following set of functions can be defined:

$$\begin{aligned} &d_i : \mathcal{C}_i \times \mathcal{C}_i \to \mathbb{R}^+ \\ &d_i(\boldsymbol{q}_1, \boldsymbol{q}_2) = \|R_i(\boldsymbol{q}_1) - R_i(\boldsymbol{q}_2)\| \end{aligned} \tag{6.52}$$

  where, as stated before, R_i is the rotor that describes the pose of joint $\mathcal{R}_i$. Again, these functions are not distance functions for the same reason as d (equation (6.50)) is not a distance function.

- The function:

$$\begin{aligned} &d : \mathcal{C} \times \mathcal{C} \to [0, +\infty) \\ &d(\boldsymbol{q}_1, \boldsymbol{q}_2) = d_1(\boldsymbol{q}_{1_1}\boldsymbol{q}_{2_1}) + \cdots + d_m(\boldsymbol{q}_{1_m}, \boldsymbol{q}_{2_m}) \end{aligned} \tag{6.53}$$

  where $\boldsymbol{q}_{1_i}$ ($\boldsymbol{q}_{2_i}$) denotes the first i coordinates of the configuration vector $\boldsymbol{q}_1$ ($\boldsymbol{q}_2$), defines a distance function in $\mathcal{C}$.

  Proof. Since, for each $1 \leq i \leq m$, d_i verifies axioms (ii) and (iii), it is clear that d also verifies axioms (ii) and (iii). In addition, $d_i(\boldsymbol{q}_1, \boldsymbol{q}_2) \geq 0$ for each $1 \leq i \leq m$ and $\boldsymbol{q}_1, \boldsymbol{q}_2 \in \mathcal{C}_i$. Therefore, $d(\boldsymbol{q}_1, \boldsymbol{q}_2) \geq 0$ for arbitrary $\boldsymbol{q}_1, \boldsymbol{q}_2 \in \mathcal{C}$. Finally, if $d(\boldsymbol{q}_1, \boldsymbol{q}_2) = 0$, then, since any addend of equation (6.53) is a positive scalar, it can be deduced that $d_i(\boldsymbol{q}_{1_i}, \boldsymbol{q}_{2_i}) = 0$ for every $1 \leq i \leq m$. Thus, $\boldsymbol{q}_1$ and $\boldsymbol{q}_2$ has associated, not only the same end-effector pose, but the pose of each of its joints, which clearly implies that $\boldsymbol{q}_1 = \boldsymbol{q}_2$. □

This distance function can be restricted to $\mathcal{S}$ just by considering the joints involved in a given singularity $\boldsymbol{q}_s$.

Definition 6.3.7. Let $\boldsymbol{q}_s \in \mathcal{S}$ be a singularity of $\mathcal{R}$ that involves joints $i_1, \ldots, i_r$. Then, the function $d : \mathcal{C} \times \mathcal{S} \to \mathbb{R}^+$ defined by the expression:

$$d(\boldsymbol{q}, \boldsymbol{q}_s) = d_{i_1}(\boldsymbol{q}_{i_1}, \boldsymbol{q}_{s_{i_1}}) + \cdots + d_{i_r}(\boldsymbol{q}_{i_r}, \boldsymbol{q}_{s_{i_r}}) \tag{6.54}$$

where, for each $i_1 \leq k \leq i_r$, d_k is the function defined in (6.52), is a distance function in $\mathcal{C}$.

6.4 Application to the serial robot Kuka LWR 4+

To show the advantages of the proposed method, an illustrative example is developed in this section, making use of the Kuka LWR 4+, an anthropomorphic arm with seven degrees of freedom described in detail in section B.3.1. The computations with the vectors of $\mathcal{G}_3$ have been carried out using the *Clifford Multivector Toolbox* of MATLAB (Sangwine and Hitzer, 2017).

Since the Kuka LWR 4+ has spherical wrist, its singularities can be decoupled into position and orientation singularities. Hence, theorem 6.2.10 can be applied in order to find out such singularities.

With respect to the position singularities, the following system of $C(4,3) = 4$ equations should be solved:

$$(\boldsymbol{z}_1 \times (\boldsymbol{o}_7 - \boldsymbol{o}_1)) \wedge (\boldsymbol{z}_2 \times (\boldsymbol{o}_7 - \boldsymbol{o}_2)) \wedge (\boldsymbol{z}_3 \times (\boldsymbol{o}_7 - \boldsymbol{o}_3)) = 0 \tag{6.55}$$
$$(\boldsymbol{z}_1 \times (\boldsymbol{o}_7 - \boldsymbol{o}_1)) \wedge (\boldsymbol{z}_2 \times (\boldsymbol{o}_7 - \boldsymbol{o}_2)) \wedge (\boldsymbol{z}_4 \times (\boldsymbol{o}_7 - \boldsymbol{o}_4)) = 0 \tag{6.56}$$
$$(\boldsymbol{z}_1 \times (\boldsymbol{o}_7 - \boldsymbol{o}_1)) \wedge (\boldsymbol{z}_3 \times (\boldsymbol{o}_7 - \boldsymbol{o}_3)) \wedge (\boldsymbol{z}_4 \times (\boldsymbol{o}_7 - \boldsymbol{o}_4)) = 0 \tag{6.57}$$
$$(\boldsymbol{z}_2 \times (\boldsymbol{o}_7 - \boldsymbol{o}_2)) \wedge (\boldsymbol{z}_3 \times (\boldsymbol{o}_7 - \boldsymbol{o}_3)) \wedge (\boldsymbol{z}_4 \times (\boldsymbol{o}_7 - \boldsymbol{o}_4)) = 0 \tag{6.58}$$

Using the expressions given for $\boldsymbol{z}_i, \boldsymbol{o}_i$ $(i = 1, \ldots, 4)$ in section B.3.1, the computation of each one of these equations can be performed. However, in order to simplify the expressions, the system of equations (6.55-6.58) is expressed with respect to the frame attached to the fourth joint of the Kuka LWR 4+. For doing so, an analogous of equation (B.23) is applied. Here, instead of pre-multiplying by the corresponding rotation matrix, the system of equations (6.55-6.58) is multiplied by the rotor R that performs the rotation between the frame attached to the end-effector and the frame attached to the fourth joint. For instance, equation (6.55) turns to:

$$R(\boldsymbol{z}_1 \times (\boldsymbol{o}_7 - \boldsymbol{o}_1)) \wedge (\boldsymbol{z}_2 \times (\boldsymbol{o}_7 - \boldsymbol{o}_2)) \wedge (\boldsymbol{z}_3 \times (\boldsymbol{o}_7 - \boldsymbol{o}_3))\widetilde{R} = 0 \tag{6.59}$$

which, using the geometric covariance property introduced in section A.3, becomes:

$$R(\boldsymbol{z}_1 \times (\boldsymbol{o}_7 - \boldsymbol{o}_1))\widetilde{R} \wedge R(\boldsymbol{z}_2 \times (\boldsymbol{o}_7 - \boldsymbol{o}_2))\widetilde{R} \wedge R(\boldsymbol{z}_3 \times (\boldsymbol{o}_7 - \boldsymbol{o}_3))\widetilde{R} = 0 \tag{6.60}$$

Therefore, the system of equations (6.55-6.58) turns to:

$$a_1 \wedge a_2 \wedge a_3 = 0 \tag{6.61}$$
$$a_1 \wedge a_2 \wedge a_4 = 0 \tag{6.62}$$
$$a_1 \wedge a_3 \wedge a_4 = 0 \tag{6.63}$$
$$a_2 \wedge a_3 \wedge a_4 = 0 \tag{6.64}$$

with

$$\begin{aligned} a_1 &= -10c_2s_3(40c_4 + 39)\boldsymbol{e}_1 + 400c_2s_3s_4\boldsymbol{e}_2 + (400c_2c_3 + 390s_2s_4 + 390c_2c_3c_4)\boldsymbol{e}_3 \\ a_2 &= 10c_3(40c_4 + 39)\boldsymbol{e}_1 + -400c_3s_4\boldsymbol{e}_2 + 10s_3(40c_4 + 39)\boldsymbol{e}_3 \\ a_3 &= 390s_4\boldsymbol{e}_3 \\ a_4 &= -390\boldsymbol{e}_1 \end{aligned} \tag{6.65}$$

where $s_i = \sin(q_i)$, $c_i = \cos(q_i)$ and $\boldsymbol{e}_1, \boldsymbol{e}_2, \boldsymbol{e}_3$ are basis vectors of $\mathcal{G}_3$. Now, the system of equations (6.61-6.64) turns to:

$$\left.\begin{aligned} 0 &= 0 \\ 40c_2s_4 + 39s_2c_3s_4^2 + 39c_2c_4s_4 &= 0 \\ c_2s_3s_4^2 &= 0 \\ c_3s_4^2 &= 0 \end{aligned}\right\} \tag{6.66}$$

Clearly, this system has two different solutions:

- $s_4 = 0$ or, equivalently, $q_4 = 0$.
- $c_2 = c_3 = 0$ or, equivalently, $q_2 = \pm\frac{\pi}{2}$ and $q_3 = \pm\frac{\pi}{2}$.

These two solutions correspond to the position singularities of the Kuka LWR 4+.

With respect to the orientation singularities, there is only one equation to solve:

$$\boldsymbol{z}_5 \wedge \boldsymbol{z}_6 \wedge \boldsymbol{z}_7 = 0 \tag{6.67}$$

Again, the expression of each $\boldsymbol{z}_i$ for $i = 5, 6, 7$ can be simplified by expressing those vectors with respect to the frame attached to the fourth joint. Thus, equation (6.67) becomes:

$$\begin{aligned} &\boldsymbol{e}_2 \wedge (-s_5\boldsymbol{e}_1 - c_5\boldsymbol{e}_3) \wedge (c_5s_6\boldsymbol{e}_1 + c_6\boldsymbol{e}_2 - s_5s_6\boldsymbol{e}_3) = \\ &= (-s_5\boldsymbol{e}_2 \wedge \boldsymbol{e}_1 - c_5\boldsymbol{e}_2 \wedge \boldsymbol{e}_3) \wedge (c_5s_6\boldsymbol{e}_1 + c_6\boldsymbol{e}_2 - s_5s_6\boldsymbol{e}_3) \overset{(1)}{=} \\ &= \cancel{-s_5c_5s_6\boldsymbol{e}_2 \wedge \boldsymbol{e}_1 \wedge \boldsymbol{e}_1} + \cancel{-s_5c_6\boldsymbol{e}_2 \wedge \boldsymbol{e}_1 \wedge \boldsymbol{e}_2} + s_5^2s_6\boldsymbol{e}_2 \wedge \boldsymbol{e}_1 \wedge \boldsymbol{e}_3 - \\ &- c_5^2s_6\boldsymbol{e}_2 \wedge \boldsymbol{e}_3 \wedge \boldsymbol{e}_1 - \cancel{c_5c_6\boldsymbol{e}_2 \wedge \boldsymbol{e}_3 \wedge \boldsymbol{e}_2} + \cancel{c_5s_5s_6\boldsymbol{e}_2 \wedge \boldsymbol{e}_3 \wedge \boldsymbol{e}_3} \overset{(2)}{=} \\ &= -s_5^2s_6\boldsymbol{e}_1 \wedge \boldsymbol{e}_2 \wedge \boldsymbol{e}_3 - c_5^2s_6\boldsymbol{e}_1 \wedge \boldsymbol{e}_2 \wedge \boldsymbol{e}_3 = -s_6\boldsymbol{e}_1 \wedge \boldsymbol{e}_2 \wedge \boldsymbol{e}_3 = 0 \end{aligned} \tag{6.68}$$

where (1) uses that, for a vector $\boldsymbol{x}$, $\boldsymbol{x} \wedge \boldsymbol{x} = 0$ and (2) uses the anticommutativity of the outer product.

Clearly, the last expression of equation (6.68) is zero if, and only if, $s_6 = 0$ or, equivalently, if, and only if, $q_6 = 0$. Thus, the Kuka LWR 4+ only has one orientation singularity (the wrist singularity, as explained in remark 6.2.11).

Finally, the distance function defined in 6.3.7 can be applied to any of the already obtained singular configurations. Let consider, for instance, the position singularity $q_4 = 0$. Then, the distance between an arbitrary configuration $\boldsymbol{q} \in \mathcal{C}$ and such singularity is given by the expression:

$$d(\boldsymbol{q}, \boldsymbol{q}_s) = \|R_4(\boldsymbol{q}) - R_4(\boldsymbol{q}_s)\| \tag{6.69}$$

where $\boldsymbol{q}_s$ denotes the singular configuration $q_4 = 0$ and R_4 is the rotor defining the pose of the fourth joint of the Kuka LWR 4+.

In particular, R_4 can be found using the equation (5.16) of section 5.3. Indeed, $\{\boldsymbol{e}_1, \boldsymbol{e}_2, \boldsymbol{e}_3\}$ denotes the orthonormal basis of $\mathbb{R}^3$, while $\{\boldsymbol{f}_1, \boldsymbol{f}_2, \boldsymbol{f}_3\}$ denotes the orthogonal basis defined by the frame attached to the fourth joint. Hence,

$$R_4 = \alpha(1 + \boldsymbol{e}^1\boldsymbol{f}_1 + \boldsymbol{e}^2\boldsymbol{f}_2 + \boldsymbol{e}^3\boldsymbol{f}_3) \tag{6.70}$$

where $\alpha \in \mathbb{R}$ and $\{\boldsymbol{e}^1, \boldsymbol{e}^2, \boldsymbol{e}^3\}$ is the reciprocal frame of $\{\boldsymbol{e}_1, \boldsymbol{e}_2, \boldsymbol{e}_3\}$. For an orthonormal basis, such reciprocal frame is:

$$\begin{aligned} \boldsymbol{e}^1 &= \boldsymbol{e}_1 \\ \boldsymbol{e}^2 &= -\boldsymbol{e}_2 \\ \boldsymbol{e}^3 &= \boldsymbol{e}_3 \end{aligned} \tag{6.71}$$

Thus, equation (6.70) turns to:

$$R_4 = \alpha(1 + \boldsymbol{e}_1\boldsymbol{f}_1 - \boldsymbol{e}_2\boldsymbol{f}_2 + \boldsymbol{e}_3\boldsymbol{f}_3) \tag{6.72}$$

Evaluating equation (6.72) in $\boldsymbol{q}$ and $\boldsymbol{q}_s$, the following expressions are obtained:

$$\begin{aligned} R_4(\boldsymbol{q}) &= \alpha(a_1 + a_2\boldsymbol{e}_1 \wedge \boldsymbol{e}_2 + a_3\boldsymbol{e}_1 \wedge \boldsymbol{e}_3 + a_4\boldsymbol{e}_2 \wedge \boldsymbol{e}_3) \\ R_4(\boldsymbol{q}_s) &= \alpha(b_1 + b_2\boldsymbol{e}_1 \wedge \boldsymbol{e}_2 + b_3\boldsymbol{e}_1 \wedge \boldsymbol{e}_3 + b_4\boldsymbol{e}_2 \wedge \boldsymbol{e}_3) \end{aligned} \tag{6.73}$$

where $\{\boldsymbol{e}_1 \wedge \boldsymbol{e}_2, \boldsymbol{e}_1 \wedge \boldsymbol{e}_3, \boldsymbol{e}_2 \wedge \boldsymbol{e}_3\}$ are the basis bivectors of $\mathcal{G}_3$ and

$$\begin{aligned} a_1 &= c_2s_3 + c_4s_1s_3 - c_4c_3c_1s_2 + s_3s_4c_1 + s_4s_1s_2c_3 + s_4c_1c_2 + c_2c_4s_1 \\ a_2 &= c_2s_1s_4 - c_4c_1s_3 - c_4c_3s_1s_2 - c_1c_2c_4 + s_4s_1s_3 - s_4s_2c_1c_3 \\ a_3 &= s_2s_4 + c_2c_3c_4 + c_3s_1 + c_1s_2s_3 \\ a_4 &= c_4s_2 - c_2c_3s_4 - c_1c_3 + s_1s_2s_3 \\ b_1 &= c_2s_3 + s_1s_3 - c_3c_1s_2 + c_2s_1 \\ b_2 &= -c_1s_3 - c_3s_1s_2 - c_1c_2 \\ b_3 &= c_2c_3 + c_3s_1 + c_1s_2s_3 \\ b_4 &= s_2 - c_1c_3 + s_1s_2s_3 \end{aligned} \tag{6.74}$$

Therefore, by proposition 6.3.5 and the decomposition used in the proof of lemma 6.3.3, the distance of an arbitrary configuration $\boldsymbol{q}$ to the position singularity $q_4 = 0$ is given by:

$$d(\boldsymbol{q}, \boldsymbol{q}_s) = \alpha\sqrt{(a_1 - b_1)^2 + (a_2 - b_2)^2 + (a_3 - b_3)^2 + (a_4 - b_4)^2} \tag{6.75}$$

6.5 Handling of singularities

Once the set of singular configurations $\mathcal{S}$ has been identify, several methods can be applied to handle the singularities. The detailed treatment of this topic is beyond the scope of this work. However, in order to show the possibilities of the distance function proposed in the previous section to deal with it, three different situations are commented, namely motion planning, motion control and bilateral teleoperation. In each one of these situations, the distance function defined in 6.3.7 plays an important role for handling the singularities.

6.5.1 Singularity handling in motion planning

Motion planning consists of programming collision-free motions for a given robotic manipulator from a start position to a goal one among a collection of static obstacles. The subset of robot configurations that do not cause collision with such obstacles is termed *free-of-obstacles configuration space* and it is denoted by $\mathcal{C}_{\text{free}}$. The main methods used for motion planning can be grouped in three categories:

- Potential field methods, where a differentiable real-valued function $U : \mathcal{C} \to \mathbb{R}$, called the potential function, is defined. Such function has an attractive component that pulls the trajectory towards the goal configuration and a repulsive component that pushes the trajectory away from the start configuration and from the obstacles.
- Sampling-based multi-query methods, where a roadmap is constructed over $\mathcal{C}_{\text{free}}$. The nodes represent free-of-obstacles configurations, while the edges represent feasible local paths between those configurations. Once the roadmap is constructed, a search algorithm finds out the best solution trajectory by selecting and joining the local paths through an optimization process.
- Sampling-based single-query methods, where a tree-structure data is constructed by searching new configurations (nodes) in $\mathcal{C}_{\text{free}}$ and connecting them through local paths (edges). Its main difference with respect to the multi-query methods is that, while the multi-query methods work in two times (construction of the roadmap and searching of a solution trajectory), in the single-query methods both steps are taken together. Each new configuration added to the set of nodes is connected by a local path and evaluated in order to check its feasibility.

For any method of these three categories, the distance function d defined in 6.3.7 can be applied to construct solution trajectories that avoids the singularities. Indeed:

- For a potential field method, it is enough with adding a repulsive component that pushes the trajectory, not only away from obstacles, but also away from singularities. To do so, the most efficient way is to define, for each singularity $\boldsymbol{q}_s$, a quadratic repulsive component as follows:

$$U_{r,\boldsymbol{q}_s}(\boldsymbol{q}) = \begin{cases} \dfrac{\kappa}{2}\left(\dfrac{1}{d(\boldsymbol{q},\boldsymbol{q}_s)} - \dfrac{1}{d_0}\right)^2 & \text{if } d(\boldsymbol{q},\boldsymbol{q}_s) \leq d_0 \\ 0 & \text{if } d(\boldsymbol{q},\boldsymbol{q}_s) > d_0 \end{cases} \tag{6.76}$$

  where d_0 is set as a threshold for the distance d and $\kappa \in \mathbb{R}$.
- For a sampling-based method with multiple queries, it is sufficient with removing from the roadmap those nodes associated with singular configurations. During the construction of the roadmap, each configuration $\boldsymbol{q} \in \mathcal{C}$ is evaluated to determine whether $\boldsymbol{q}$ is free-of-obstacles or not. Similarly, the idea is to evaluate each $\boldsymbol{q} \in \mathcal{C}$ in order to determine

whether $\boldsymbol{q}$ is close to a singularity or not. To speed up the process, both evaluations can be carried out together:

1) Select a value $d_0 > 0$ that will work as a threshold.
2) Given a discretization of the configuration space $\mathcal{C}$, each $\boldsymbol{q}$ of such discretization is evaluated to check whether:
   * Is free-of-obstacles.
   * Is far from any singularity. This can be done simply by evaluating whether $d(\boldsymbol{q}, \boldsymbol{q}_s) > d_0$ or $d(\boldsymbol{q}, \boldsymbol{q}_s) \leq d_0$.
3) If $\boldsymbol{q}$ is free-of-obstacles and far from any singularity, then it can be added to the set of nodes of the roadmap.

- For a sampling-based method with a single query, the approach is completely analogous to the one used for methods with multiple-queries due to the similarities between both categories.

6.5.2 Singularity handling in motion control

Motion control consists of making the end-effector of a robot to follow a time-varying trajectory specified within the manipulator workspace. A typical Inverse Dynamics Control scheme (depicted as a block diagram in figure 6.3a) can be described as:

- An input, i.e., the desired or target configuration $\boldsymbol{q}_d$ together with its velocity $\dot{\boldsymbol{q}}_d$.
- A controller based on the dynamical model of the robot:

$$\boldsymbol{\tau} = M(\boldsymbol{q})\ddot{\boldsymbol{q}} + C(\boldsymbol{q}, \dot{\boldsymbol{q}})\dot{\boldsymbol{q}} + g(\boldsymbol{q}) \tag{6.77}$$

  where $M(\boldsymbol{q})$ denotes the inertia matrix of the robot, $C(\boldsymbol{q}, \dot{\boldsymbol{q}})$ denotes the matrix of Coriolis and centrifugal forces and $g(\boldsymbol{q})$, the gravity vector.
- An output, i.e., the vector of torques $\boldsymbol{\tau}$, that is sent to the robot to perform the desired motion.
- The robot executes the motion and updates the vectors $\boldsymbol{q}$ and $\dot{\boldsymbol{q}}$.
- The robot sends such updated vectors to the controller (also know as *feedback* of the system).

To handle the singularities, a restriction can be defined inside the controller:

1) The target configuration $\boldsymbol{q}_d$ enters in the controller.
2) $\boldsymbol{q}_d$ is checked in order to determine whether is close or not to a singularity:

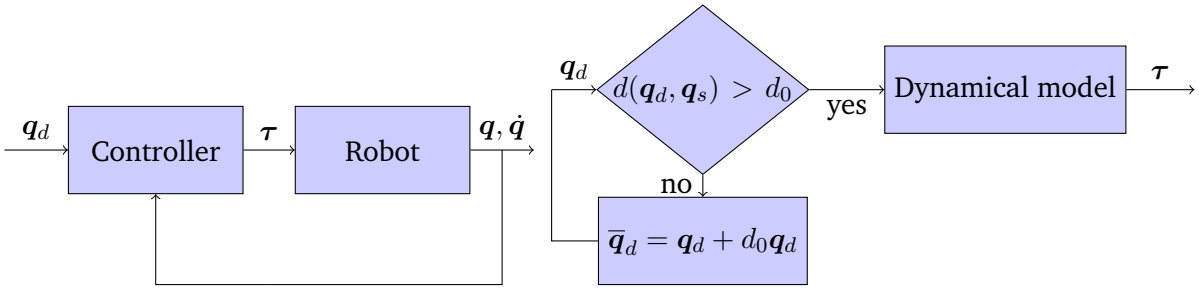

(a) General motion control scheme. **(b)** Control scheme in presence of singularities.

Figure 6.3: Motion control schemes

- Select a threshold value $d_0 > 0$.
- Evaluate the condition $d(\boldsymbol{q}_d, \boldsymbol{q}_s) > d_0$ for each singularity $\boldsymbol{q}_s$.
- If the evaluation returns yes, then $\boldsymbol{\tau}$ can be computed from $\boldsymbol{q}_d$ using the dynamical model (equation (6.77)) and sent to the robot. Otherwise, $\boldsymbol{q}_d$ is substituted by $\boldsymbol{q}_d + d_0 \boldsymbol{q}_d$ and evaluated again.

A block diagram of the above-explained scheme is depicted in figure 6.3b.

6.5.3 Singularity handling in bilateral teleoperation

Teleoperated robotic systems are characterized by a robot that executes the movements/actions commanded by a human operator. Any high-level or planning decision is made by a human user, while a robot is responsible for their mechanical implementation (Basañez and Suárez, 2009). Teleoperation systems are often, at least conceptually, split into two parts: a local manipulator and a remote manipulator. The first one refers to the device moved by the human operator, while the second refers to the robot or robot system that perform the action.

According to the information flow direction, the teleoperation may be unilateral or bilateral. In unilateral teleoperation, the local manipulator sends position or force data to the remote manipulator and only receives, as feedback, visual information from the remote scene. But, in bilateral teleoperation, position or force data are also sent from the remote manipulator in addition to the visual information.

In a bilateral teleoperation system, some strategies for handling of kinematic singularities can make use of the distance function d defined in 6.3.7. For instance, the following scheme could be applied:

1) Select a value $d_0 > 0$ that will work as a threshold.

2) The local manipulator sends a pose (force) $\boldsymbol{p}$ ($\boldsymbol{f}$) to the remote manipulator.

3) The controller of the remote manipulator obtains the associated configuration $\boldsymbol{q}$.

4) The distance $d(\boldsymbol{q}, \boldsymbol{q}_s)$ is computed for each $\boldsymbol{q}_s \in \mathcal{S}$.

5) If, for some $\boldsymbol{q}_s$, $d(\boldsymbol{q}, \boldsymbol{q}_s) < d_0$, then the remote manipulator controller computes a reaction force $\boldsymbol{f}_s$ in the same direction of the motion but with inverse sense.

6) The remote manipulator sends such force $\boldsymbol{f}_s$ to the local manipulator.

7) The human operator will be not able to move the local manipulator in such direction due to $\boldsymbol{f}_s$ and, thus, the singularity $\boldsymbol{q}_s$ will never be reached.

Chapter 7

Conclusions

7.1 Conclusions and contributions

This dissertation proposes new strategies for solving two important kinematic problems: the inverse kinematics for redundant and non-redundant serial robots and the singularity problem for arbitrary serial manipulators. The main contributions of the present work are:

- A novel closed-form method that solves the inverse kinematics of redundant serial robots of n DOF. This method consists of reducing a redundant robot $\mathcal{R}$ to a non-redundant one by the parametrization of a set of joints termed *redundant joints*. The identification of such joints is made by using global rank-deficiency conditions of the Jacobian matrix and an analysis of the workspace properties. For m denoting the number of rotational degrees of redundancy (definition B.2.5), such analysis also provides:
  - An upper bound of 2^m for the number of solution families, much smaller than the proposed by other authors as, for example, $C(n, r)$ in (Schrake et al., 1990, 1991), where r denotes the number of degrees of redundancy.
  - A partition of the workspace $\mathcal{W} = \overline{\mathcal{W}_1} \cup \cdots \cup \overline{\mathcal{W}_{2^m}}$ where each $\overline{\mathcal{W}_i}$ has associated one of above-mentioned solution families. Therefore, for a target pose $T \in \overline{\mathcal{W}_i}$ the closed-form family of solutions associated with $\overline{\mathcal{W}_i}$ can be used to solve the inverse kinematics for T.
- An innovative extension of the mixed method introduced by Pan et al. (2012), that allows the obtainment of efficient solutions for the inverse kinematics of serial robots without spherical wrist, through a combination of analytical and numerical methods. This mixed method has been proven to be faster than any other proposed numerical method. Besides, all the solutions associated with a given pose T are obtained.

- A novel closed-form method for solving the inverse kinematics of non-redundant serial robots with spherical wrist using *conformal geometric algebra*. This method solves separately the inverse position and the inverse orientation problems. The inverse position problem is solved geometrically, while the inverse orientation, algebraically. In both cases, the tools provided by conformal geometric algebra allow an efficient implementation that improves the performance with respect to the classical approaches.

- A new strategy for the identification of singular configurations using geometric algebra. While the classical approach needs to compute the determinant of the Jacobian matrix J_G, this strategy computes the outer product of the screws defined by the joint axes. Therefore, since screws can be represented by vectors of $\mathcal{G}_6$, this strategy is computationally more efficient than the classical one. Furthermore, in contrast to the classical approach, where the singularities of redundant robots are harder to identify, this method not only works for any serial robot but it solves the problem for redundant robots as for non-redundant ones.

- A new method to measure the distance of a given configuration $\boldsymbol{q} \in \mathcal{C}$ to a singularity using conformal geometric algebra. Since the pose of each joint i can be described by a configuration-dependent rotor $R_i(\boldsymbol{q})$, given two different configurations $\boldsymbol{q}_1, \boldsymbol{q}_2 \in \mathcal{C}$, the distance between them is defined as:

$$d(\boldsymbol{q}_1, \boldsymbol{q}_2) = \|R_1(\boldsymbol{q}_{1_1}) - R_1(\boldsymbol{q}_{2_1})\| + \cdots + \|R_n(\boldsymbol{q}_{1_n}) - R_n(\boldsymbol{q}_{2_n})\| \tag{7.1}$$

  where $\boldsymbol{q}_{1_i}$ ($\boldsymbol{q}_{2_i}$) denotes the first i components of the configuration vector $\boldsymbol{q}_1$ ($\boldsymbol{q}_2$). Then, given a singularity $\boldsymbol{q}_s \in \mathcal{S}$ involving joints $j_1, \ldots, j_r$, the distance of any configuration $\boldsymbol{q}$ to $\boldsymbol{q}_s$ is computed simply by restricting the previous distance function to the joints involved in $\boldsymbol{q}_s$:

$$d(\boldsymbol{q}, \boldsymbol{q}_s) = \|R_{j_1}(\boldsymbol{q}_{j_1}) - R_{j_1}(\boldsymbol{q}_{s_{j_1}})\| + \cdots + \|R_{j_r}(\boldsymbol{q}_{j_r}) - R_{j_r}(\boldsymbol{q}_{s_{j_r}})\| \tag{7.2}$$

  This distance function is applied to handle the singularities in three operating situations (motion planning, motion control and bilateral teleoperation). In each one of these fields, a threshold $d_0 > 0$ is defined in order to set a volume around $\mathcal{S}$. Then, several algorithms are used in order to avoid entering in such volume and, thus, to handle the singularities by avoiding to be close to them.

7.2 Future work

Some prospects for further research have been identified:

- **Degenerated serial robots:** In chapter 3 a characterization of global degenerated manipulators is developed. A natural question is whether a such characterization can be suitable for local degeneration, i.e., for singularities. Some of the geometric conditions given in theorem 3.1.1 also describe local singularities. Furthermore, in (Murray et al., 1994, pp. 150-153) other geometric conditions are proven to be singularities. However, the complete list is far from being fully described.

- **Inverse kinematics for redundant manipulators:** As stated in chapter 4, once the redundant joints are identified, the redundant manipulator is reduced to a non-redundant one. Depending on the geometry of such robotic manipulator, different closed-form solutions can be used for solving the inverse kinematics of the non-redundant reduced robot. As shown in section 4.4, the majority of the closed-form methods only work with manipulators that have spherical wrist. Therefore, the next step consists of the development of an efficient strategy and purely analytical strategy to solve the inverse kinematics of non-redundant robots without spherical wrist. As seen in chapter 5, conformal geometric algebra provides a framework where the manipulation of the offsets between different joints can be done easily. Thus, the geometric strategy introduced in chapter 5 can be the starting point to solve this open problem.

- **Singularities:** In chapter 6 geometric algebra is used for the identification of singularities of arbitrary serial robots. Furthermore, a distance d is defined in the configuration space $\mathcal{C}$ to find out the distance of an arbitrary configuration $\boldsymbol{q}$ to a singularity. Finally, such distance function is applied to three different situations (motion planning, motion control and bilateral teleoperation) in order to handle the singularities. Thus, the natural extension consists of the implementation and simulation of particular algorithms or control schemes in the of the ones presented in section 6.5 to handle these singularities in each one of the above-mentioned situations.

7.3 List of publications

The following list contains the published and to be submitted papers related to the topics covered in this dissertation and generated during the course of this research.

Journal publications:

- **Zaplana, I.**; Claret, J.A. and Basanez, L. (2017). Kinematic analysis of redundant robotic manipulators: application to Kuka LWR 4+ and ABB Yumi. *Revista Iberoamericana de Automática e Informática Industrial*, 15(2): 192 – 202.
  DOI: `https://doi.org/10.4995/riai.2017.8822`.
- **Zaplana, I.** and Basanez, L. (2018). A novel closed-form solution for the inverse kinematics of redundant manipulators through workspace analysis. *Mechanism and Machine Theory*, 121(2): 829 – 843.
  DOI: `https://doi.org/10.1016/j.mechmachtheory.2017.12.005`.
- General closed-form solutions for the inverse kinematics of serial robots using conformal geometric algebra. To be submitted.
- Singularities of serial robots: identification and distance computation using geometric algebra. To be submitted.

Refereed conference publications:

- Claret, J.A.; **Zaplana, I.** and Basanez, L. (2016). Teleoperating a mobile manipulator and a free-flying camera from a single haptic device. In: *Proceedings of the International Symposium on Safety, Security and Rescue Robotics, Lausanne, Switzerland* pp. 291-296.

Appendices

Appendix A

Mathematical Background

In this appendix, an introduction to the mathematical concepts used throughout this work is presented. The first three sections collect the results from several books like, for example, (Strang, 1980; Castellet and Llerena, 1996), while the last two sections are based on (Aristidou, 2010; Doran and Lasenby, 2003; Lasenby et al., 2004; Xambó-Descamps, 2016, 2017). An extensive and detailed treatment of these subjects can be found in those references.

A.1 Linear algebra

Let $\mathbb{K}$ denote a commutative field. A *vector space* over $\mathbb{K}$ is a non-empty set V together with:

- An operation, called the *addition*, defined as:

$$\begin{aligned} + : V \times V &\to V \\ (\boldsymbol{u}, \boldsymbol{v}) &\to \boldsymbol{u} + \boldsymbol{v} \end{aligned}$$

  with the following properties:

  - Associativity: $\boldsymbol{u} + (\boldsymbol{v} + \boldsymbol{w}) = (\boldsymbol{u} + \boldsymbol{v}) + \boldsymbol{w}$ for all $\boldsymbol{u}, \boldsymbol{v}, \boldsymbol{w} \in V$.
  - Commutativity: $\boldsymbol{u} + \boldsymbol{v} = \boldsymbol{v} + \boldsymbol{u}$ for all $\boldsymbol{u}, \boldsymbol{v} \in V$.
  - Null element: $\exists \boldsymbol{a} \in V$ such that $\boldsymbol{u} + \boldsymbol{a} = \boldsymbol{u}$ for all $\boldsymbol{u} \in V$ (usually denoted by $\mathbf{0}$).
  - Inverse element: $\exists \boldsymbol{b} \in V$ such that $\boldsymbol{u} + \boldsymbol{b} = \mathbf{0}$ for all $\boldsymbol{u} \in V$ (usually denoted by $-\boldsymbol{u}$).

- A second operation, the *multiplication by elements of* $\mathbb{K}$, defined as:

$$\begin{aligned} \cdot : \mathbb{K} \times V &\to V \\ (a, \boldsymbol{u}) &\to a\boldsymbol{u} \end{aligned}$$

with the following properties:

- Distributivity with respect to the elements of V: $a(\boldsymbol{u}+\boldsymbol{v}) = a\boldsymbol{u}+a\boldsymbol{v}$ for all $a \in \mathbb{K}$ and $\boldsymbol{u}, \boldsymbol{v} \in V$.
- Distributivity with respect to the elements of $\mathbb{K}$: $(a+b)\boldsymbol{u} = a\boldsymbol{u} + b\boldsymbol{u}$ for all $a, b \in \mathbb{K}$ and $\boldsymbol{u} \in V$.
- Compatibility: $(ab)\boldsymbol{u} = a(b\boldsymbol{u})$ for all $a, b \in \mathbb{K}$ and $\boldsymbol{u} \in V$.
- Null element: $\exists a \in \mathbb{K}$ such that $a\boldsymbol{u} = \boldsymbol{u}$ for all $\boldsymbol{u} \in V$ (usually denoted by 1).

Elements of V are commonly called *vectors*. If $\mathbb{K}$ is the field of real numbers $\mathbb{R}$, then V is said to be a real vector space and the elements of $\mathbb{R}$ are denoted as *scalars*.

Definition A.1.1. Let V be a vector space over $\mathbb{K}$ and suppose that $B = \{\boldsymbol{u}_1, \ldots, \boldsymbol{u}_n\}$ is a non-empty subset of V. Then, B is called a *basis* of V if it satisfies the following conditions:

- Linear independence property: $a_1\boldsymbol{u}_1 + \cdots + a_n\boldsymbol{u}_n = 0$ if, and only if, $a_1 = \cdots = a_n = 0$
- Spanning property: $\forall \boldsymbol{u} \in V$, $\exists a_1, \ldots, a_n \in \mathbb{K}$ such that $\boldsymbol{u} = a_1\boldsymbol{u}_1 + \cdots + a_n\boldsymbol{u}_n$

The elements $a_1, \ldots, a_n \in \mathbb{K}$ of the second condition are called the *coordinates* of $\boldsymbol{u}$ with respect to the basis B, and by the first condition they are uniquely determined. A vector space V that has a finite basis is called *finite-dimensional*. Its dimension is the number of elements of B. Real vector spaces of dimension n are usually denoted by $\mathbb{R}^n$.

Once the structure of vector spaces has been introduced, linear maps can be defined.

Definition A.1.2. Let U and V be two vector spaces. A map $f : U \to V$ is said to be a *linear map* if, for all $\boldsymbol{u}, \boldsymbol{v} \in U$ and $a \in \mathbb{K}$:

$$\begin{aligned} f(\boldsymbol{u}+\boldsymbol{v}) &= f(\boldsymbol{u}) + f(\boldsymbol{v}) \\ f(a\boldsymbol{u}) &= af(\boldsymbol{u}) \end{aligned} \tag{A.1}$$

Linear maps clearly preserves the structure of vector spaces, since they are operation preserving. An equivalent definition of linear maps can be made through the following result:

Proposition A.1.3. *Let U and V be two vector spaces. The map $f : U \to V$ is a linear map if, and only if, for all $\boldsymbol{u}_1, \ldots, \boldsymbol{u}_m$ and $a_1, \ldots, a_m \in \mathbb{K}$:*

$$f(a_1\boldsymbol{u}_1 + \cdots + a_m\boldsymbol{u}_m) = a_1 f(\boldsymbol{u}_1) + \ldots a_m f(\boldsymbol{u}_m) \tag{A.2}$$

Definition A.1.4. The *kernel* of f is a vector subspace of U defined as:

$$\ker(f) = \{\boldsymbol{u} \in U \mid f(\boldsymbol{u}) = 0\} \tag{A.3}$$

Definition A.1.5. The *image* of f is a vector subspace of V defined as:

$$\mathrm{Im}(f) = \{\boldsymbol{v} \in V \mid \exists \boldsymbol{u} \in U \text{ with } f(\boldsymbol{u}) = \boldsymbol{v}\} \tag{A.4}$$

An important notion is the *range* of a linear map f, i.e., the dimension of $\mathrm{Im}(f)$ as a vector subspace of V. As it will be shown later, this notion is related to the rank of a matrix.

Definition A.1.6. Let U and V be two vector spaces and $f : U \to V$ be a linear map. Then, if f is:

- One-to-one, then it is called a *monomorphism*.
- Onto, then it is called a *epimorphism*.
- Bijective, then it is called a *isomorphism*.

Furthermore, if $V = U$, then f is said to be an *endomorphism*. Finally, a bijective endomorphism is known as an *automorphism*.

Now, the notion of matrix can be introduced. First, an important result is needed:

Proposition A.1.7. *Let U be a vector space with basis $B = \{\boldsymbol{u}_1, \ldots, \boldsymbol{u}_n\}$ and let V be another vector space with an arbitrary set of vectors $\{\boldsymbol{v}_1, \ldots, \boldsymbol{v}_n\}$. Then, there exists a unique linear map $f : U \to V$ such that $f(\boldsymbol{u}_i) = \boldsymbol{v}_i$ for every $i = 1, \ldots, n$.*

Corollary A.1.8. *Let U and V be vector spaces with bases $B = \{\boldsymbol{u}_1, \ldots, \boldsymbol{u}_n\}$ and $B' = \{\boldsymbol{v}_1, \ldots, \boldsymbol{v}_m\}$. Then, for every linear map f there exist $a_{ij} \in \mathbb{K}$ for $1 \leq i \leq n; 1 \leq j \leq m$ such that:*

$$f(\boldsymbol{u}_i) = \sum_{j=1}^{m} a_{ij} \boldsymbol{v}_j \quad \forall i = 1, \ldots, n \tag{A.5}$$

The two-dimensional array of $\mathbb{K}$-elements:

$$A = \begin{pmatrix} a_{11} & \ldots & a_{1m} \\ \vdots & \ldots & \vdots \\ a_{n1} & \ldots & a_{nm} \end{pmatrix}$$

is said to be the *matrix representation of f*. The *order* of the matrix A, $n \times m$, corresponds to the dimension of the two vector spaces U and V, or, equivalently, the number of rows and columns of A. A matrix is said to be *square* if $n = m$.

Example A.1.9.

- Identity matrix (I):
$$a_{ij} = \begin{cases} 1 & \text{if } i = j \\ 0 & \text{if } i \neq j \end{cases} \tag{A.6}$$
- Null matrix (O): $a_{ij} = 0$ for $1 \leq i \leq n; 1 \leq j \leq m$.
- Upper (lower) triangular matrix: $a_{ij} = 0$ if $i > j$ ($a_{ij} = 0$ if $j < i$).
- Diagonal matrix: $a_{ij} = 0$ if $i \neq j$.
- Symmetric matrix: $a_{ij} = a_{ji}$ for $1 \leq i, j \leq n$.
- Skew-symmetric matrix:
$$a_{ij} = \begin{cases} -a_{ji} & \text{if } i \neq j \\ 0 & \text{if } i = j \end{cases} \tag{A.7}$$
- Partitioned matrix:
$$A = \begin{pmatrix} A_{11} & \dots & A_{1m} \\ \vdots & \dots & \vdots \\ A_{n1} & \dots & A_{nm} \end{pmatrix}$$
where A_{ij} are matrices of proper dimensions (also denoted as blocks).

The *transpose* A^T of a matrix A with order $n \times m$ is the matrix of order $m \times n$ which is obtained from A by interchanging its rows and columns. Clearly, a square matrix A is symmetric if, and only if, $A^T = A$ and skew-symmetric if, and only if, $A^T = -A$.

Definition A.1.10. Given two vector spaces U and V of dimensions n and m respectively:

- The set of all linear maps $f : U \to V$, denoted by $\mathcal{L}(U, V)$, is a vector space of dimension mn.
- The set of all matrices of order $n \times m$, denoted by $\mathcal{M}_{n\times m}(\mathbb{K})$, is a vector space of dimension mn. In addition, an extra binary operation can be defined in $\mathcal{M}_{n\times m}(\mathbb{K})$:
$$\begin{aligned} \cdot : \mathcal{M}_{n\times m}(\mathbb{K}) \times \mathcal{M}_{m\times p}(\mathbb{K}) &\to \mathcal{M}_{n\times p}(\mathbb{K}) \\ (A, B) &\to AB \end{aligned}$$
This operation is known as the *product* between matrices of compatible orders. In particular, if $C = AB$, the elements of C are:
$$c_{ij} = \sum_{k=1}^{m} a_{ik} b_{kj}$$
where $\{a_{ij}\}, \{b_{ij}\}$ are the elements of A and B respectively.

As one can naturally believe and, since each linear map f has associated a matrix M, there exists an isomorphism between $\mathcal{L}(U,V)$ and $\mathcal{M}_{n\times m}(\mathbb{K})$. This proves that every matrix M is in fact the matrix representation of a linear map f which, in turn, makes corollary A.1.8 to work as the definition of the concept *matrix*.

Definition A.1.11. Given a square matrix A of order n, the *algebraic complement* $A_{(i,j)}$ of the element a_{ij} is the matrix of order $n-1$ that is obtained by eliminating the row i and the column j from A.

Definition A.1.12. Given a square matrix A of order n, the *determinant* of A, denoted by $\det(A)$, is the scalar defined by:

$$\det(A) = \begin{cases} a_{11} & \text{if } n = 1 \\ \sum_{j=1}^{n} a_{ij}(-1)i + j \det(A_{(i,j)}) & \text{otherwise} \end{cases} \tag{A.8}$$

Equation (A.8) is valid for any row i. Some important properties of determinants are:

- $\det(I) = 1$ and $\det(O) = 0$.
- $\det(A) = \det(A^T)$.
- $\det(AB) = \det(A)\det(B)$.
- $\det(aA) = a^n \det(A)$ for $a \in \mathbb{K}$.
- For a diagonal or triangular matrix A:

$$\det(A) = \prod_{i=1}^{n} a_{ii} \tag{A.9}$$

- For a block-triangular matrix A with n blocks on the diagonal:

$$\det(A) = \prod_{i=1}^{n} \det(A_{ii}) \tag{A.10}$$

- If two rows (columns) are interchanged, then the determinant changes the sign. Hence, if there are two equal rows (columns), the determinant vanishes.
- If one row (column) can be expressed as the addition of two different vectors $\boldsymbol{u}+\boldsymbol{v}$, then the determinant can be expressed as the addition of two determinants, each one of a matrix where $\boldsymbol{u}$ and $\boldsymbol{v}$ replace $\boldsymbol{u}+\boldsymbol{v}$ respectively.
- If one row (column) is a linear combination of other rows (columns), the determinant vanishes.

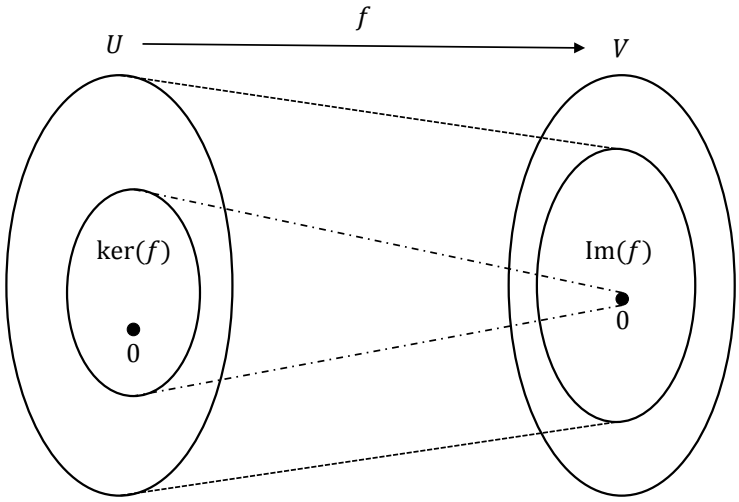

Figure A.1: Schematic representation of $\ker(f)$ and $\mathrm{Im}(f)$

Definition A.1.13. Let A be a matrix of order $n \times m$. If each column (row) of A is seen as a vector, then the *rank* of A, denoted by $\rho(A)$, is the maximum number of linearly independent columns (rows).

The following properties hold:

- $\rho(A) \leq \min\{n, m\}$. If $\rho(A) = \min\{n, m\}$, then A is said to be *full-rank*.
- $\rho(A) = \rho(A^T) = \rho(A^T A)$.

Remark A.1.14. $\ker(f)$ and $\mathrm{Im}(f)$ can be redefined using the matrix representation A of f (figure A.1):

$$\begin{aligned} \ker(f) &= \mathcal{N}(A) = \{\boldsymbol{u} \in U \mid A\boldsymbol{u} = 0\} \\ \mathrm{Im}(f) &= \mathcal{R}(A) = \{\boldsymbol{v} \in V \mid A\boldsymbol{u} = \boldsymbol{v} \text{ for some } \boldsymbol{u} \in U\} \end{aligned} \tag{A.11}$$

Then, it can be deduced that $\rho(A) = \dim(\mathrm{Im}(f))$, i.e., the range of f is the same as the rank of A.

If A is square and full-rank, then $\det(A) \neq 0$. These matrices are called *non-singular* and are of special relevance because they are invertible, i.e., there exists a square and full-rank matrix B such that:

$$BA = AB = I \tag{A.12}$$

where B is known as the *inverse* of A and it is denoted by A^{-1}. Clearly, $(A^{-1})^{-1} = A$. Furthermore, if $A^T = A^{-1}$, then A is said to be *orthogonal*. This is equivalent to:

$$A \text{ orthogonal} \iff AA^T = A^T A = I$$

Since $AA^T = I$, an orthogonal matrix A verifies that:

$$\det(A) = \pm 1 \tag{A.13}$$

Non-square and singular matrices have not inverse, but a generalized inverse, known as the *Moore-Penrose pseudoinverse*, can be defined. If $A \in \mathcal{M}_{n\times m}(\mathbb{K})$, then:

- If $n < m$ and $\rho(A) = n$, the *right pseudoinverse* of A is defined as:

$$A_r^\dagger = A^T(AA^T)^{-1} \tag{A.14}$$

- If $m < n$ and $\rho(A) = m$, the *left pseudoinverse* of A is defined as:

$$A_\ell^\dagger = (A^TA)^{-1}A^T \tag{A.15}$$

Definition A.1.15. Let A be a real square matrix of order n. Then, λ is said to be an *eigenvalue* of A if there exists a non-zero vector $\boldsymbol{v} \in \mathbb{R}^n$ such that:

$$A\boldsymbol{v} = \lambda\boldsymbol{v} \tag{A.16}$$

where $\boldsymbol{v}$ is called *eigenvector*. In general, A has n distinct eigenvalues that are the roots of the *characteristic polynomial*:

$$\det(A - \lambda I) = 0 \tag{A.17}$$

The set of all eigenvalues of a matrix A is called its *spectrum* and is denoted by $\sigma(A)$.

The matrix Δ whose columns are the eigenvectors $\boldsymbol{v}_i$ is invertible and conforms a basis for $\mathbb{R}^n$. Furthermore,

$$\Lambda = \Delta^{-1}A\Delta \tag{A.18}$$

is a diagonal matrix whose diagonal elements are the eigenvalues λ_i of A. Due to the properties of determinants, it is clear that:

$$\det(A) = \prod_{i=1}^{n} \lambda_i \tag{A.19}$$

Remark A.1.16. If A is symmetric, $\sigma(A) \subset \mathbb{R}$ and $\Lambda = \Delta^TA\Delta$. Hence, Δ is an orthogonal matrix.

The concept of eigenvalue cannot be defined for non-square matrices. However, it can be extended appropriately. Let consider a real non-square matrix A of order $n \times m$. Then:

Definition A.1.17. If $\boldsymbol{x}^TA\boldsymbol{x} \geq 0$ for every $\boldsymbol{x} \in \mathbb{R}^m$, then $A \in \mathcal{M}_n(\mathbb{R})$ is said to be *semi-definite*.

Proposition A.1.18. *A^TA is a square, symmetric and positive semi-definite matrix.*

Corollary A.1.19. *Matrix A^TA has m non-negative eigenvalues $\lambda_1 \geq \cdots \geq \lambda_m \geq 0$.*

These eigenvalues can be expressed as $\lambda_i = \sigma_i^2$ with $\sigma_i \geq 0$. Then, the scalars $\sigma_1 \geq \cdots \geq \sigma_m \geq 0$ are said to be the *singular values* of A.

Definition A.1.20. Let A be a real matrix of order $n \times m$. The *singular value decomposition* (SVD) of A is:

$$A = U\Sigma V^T \tag{A.20}$$

where U is a square orthogonal matrix of order n whose columns are the eigenvectors of AA^T; V is a square orthogonal matrix of order m whose columns are the eigenvector of A^TA; and Σ is a diagonal matrix of order $n \times m$ whose diagonal elements are σ_i. The number of non-null singular values is equal to $\rho(A)$.

Remark A.1.21. Right pseudoinverses can be computed using the singular value decomposition:

$$A^\dagger = V\Sigma^\dagger U^T \tag{A.21}$$

where $\Sigma^\dagger$ is the diagonal matrix whose diagonal elements are $1/\sigma_i$.

A.2 Euclidean Geometry

In this section, only real vector spaces are considered. Thus, let denote by $\mathbb{R}^n$ the real vector space of dimension n. First, let define the inner product between the elements of $\mathbb{R}^n$ as a tool for defining the Euclidean distance:

Definition A.2.1. Let $\boldsymbol{x}, \boldsymbol{y} \in \mathbb{R}^n$ be two vectors whose coordinates with respect to a basis of $\mathbb{R}^n$ are $(x_1, \ldots, x_n)$ and $(y_1, \ldots, y_n)$ respectively. The *inner product* between $\boldsymbol{x}$ and $\boldsymbol{y}$ is the scalar:

$$\boldsymbol{x} \cdot \boldsymbol{y} = \sum_{i=1}^{n} x_i y_i = x_1 y_1 + \cdots + x_n y_n \tag{A.22}$$

Remark A.2.2. $\boldsymbol{x} \cdot \boldsymbol{x} > 0$ for $\boldsymbol{x} \neq 0$.

Definition A.2.3. Let $\boldsymbol{x}, \boldsymbol{y} \in \mathbb{R}^n$. The *Euclidean norm* of $\boldsymbol{x}$, denoted by $\|\boldsymbol{x}\|_2$, is defined as:

$$\|\boldsymbol{x}\|_2 = \sqrt{\boldsymbol{x} \cdot \boldsymbol{x}}$$

Furthermore, the Euclidean norm allows to define the *Euclidean distance* d_2:

$$d_2(\boldsymbol{x}, \boldsymbol{y}) = \|\boldsymbol{x} - \boldsymbol{y}\|_2 \tag{A.23}$$

Definition A.2.4. A real vector space is said to be a *Euclidean space* if it is endowed with the Euclidean distance d_2

Since d_2 is uniquely determined by the inner product, many authors define the Euclidean space as a real vector space endowed with an inner product. In general, mathematicians denote the n-dimensional Euclidean space by E_n or, simply, by E, if the dimension is clear from the context.

Although E_n and $\mathbb{R}^n$ denote the same structure, throughout this section the notation E_n will be employed to emphasize the Euclidean structure provided by d_2.

The inner product also allows to define the angle between vectors:

$$\angle(\boldsymbol{x}, \boldsymbol{y}) = \arccos\left(\frac{\boldsymbol{x} \cdot \boldsymbol{y}}{\|\boldsymbol{x}\|\|\boldsymbol{y}\|}\right) \tag{A.24}$$

Remark A.2.5. In general, a vector space U over $\mathbb{K}$ can be equipped with a symmetric and non-degenerated bilinear form $q : U \times U \to \mathbb{K}$, where:

- Bilinear: $q(\cdot, \cdot)$ is linear in both arguments.
- Symmetric: $q(\boldsymbol{u}_1, \boldsymbol{u}_2) = q(\boldsymbol{u}_2, \boldsymbol{u}_1)$ for all $\boldsymbol{u}_1, \boldsymbol{u}_2 \in U$.
- Non-degenerated: $q(\boldsymbol{u}_1, \boldsymbol{u}_2) = 0$ for all $\boldsymbol{u}_2 \in U$ if, and only if, $\boldsymbol{u}_1 = 0$.

This bilinear form q is known as the *metric* of U and plays the role of the inner product (in fact, the inner product (A.22) is an example of a particular metric q). If $B = \{\boldsymbol{u}_1, \ldots, \boldsymbol{u}_n\}$ is an orthonormal basis of U, the *signature* of q is defined as the triad (p, q, r) where:

- $p + q + r = n$
- $p = \#\{\boldsymbol{e}_i \in B \mid q(\boldsymbol{e}_i, \boldsymbol{e}_i) = 1\}$
- $q = \#\{\boldsymbol{e}_i \in B \mid q(\boldsymbol{e}_i, \boldsymbol{e}_i) = 0\}$
- $r = \#\{\boldsymbol{e}_i \in B \mid q(\boldsymbol{e}_i, \boldsymbol{e}_i) = -1\}$

This concept will be useful when the conformal geometric algebra $\mathcal{G}_{n+1,1}$ of $\mathcal{R}^n$ will be introduced.

The main objective of this section is to introduce the special Euclidean group $SE(n)$ because, for $n = 3$, it describes the spatial rigid body motions. For that purposes, the following definitions and results are necessary:

Definition A.2.6. Let G be a non-empty set and let $*$ be a binary operation defined in G:

$$\begin{aligned} * : & G \times G \to G \\ & (g_1, g_2) \to g_1 * g_2 \end{aligned}$$

Then, G is a *group* with *group law* $*$ if the following statements hold:

- Closure: $g_1 * g_2 \in G$ for all $g_1, g_2 \in G$.

- Associativity: $(g_1 * g_2) * g_3 = g_1 * (g_2 * g_3)$ for all $g_1, g_2, g_3 \in G$.
- Identity element: $\exists g \in G$ such that $g_1 * g = g * g_1 = g_1$ for all $g_1 \in G$. Such element is denoted by e.
- Inverse element: For each $g \in G$ there exists $g' \in G$ such that $g * g' = g' * g = e$. Such element is denoted by g^{-1}.

Definition A.2.7. Let E be an Euclidean space. An *isometry* $f : E \to E$ is a map which preserves the Euclidean distance:

$$d_2(f(\boldsymbol{x}), f(\boldsymbol{y})) = d_2(\boldsymbol{x}, \boldsymbol{y}) \quad \forall \boldsymbol{x}, \boldsymbol{y} \in E \tag{A.25}$$

Proposition A.2.8. *If $f : E \to E$ is an isometry, then f preserves angles:*

$$|\angle(f(\boldsymbol{x}), f(\boldsymbol{y}))| = |\angle(\boldsymbol{x}, \boldsymbol{y})| \quad \forall \boldsymbol{x}, \boldsymbol{y} \in E \tag{A.26}$$

Definition A.2.9. Let E be the n-dimensional Euclidean space. The set of all isometries is a group with the composition that is known as the *Euclidean group* $E(n)$.

An isometry which also preserves the orientation is a *direct* isometry. Otherwise, the isometry is said to be an *indirect* isometry. The set of direct (indirect) isometries is a subgroup of $E(n)$ denoted by $E^+(n)$ ($E^-(n)$).

Remark A.2.10. $E^+(n)$ is also known as the *special Euclidean group* $SE(n)$ or the *rigid motions group*.

This alternative name highlights the importance of direct isometries in the description of the rigid bodies transformations, a key topic in the description of robot kinematics, which will be covered in the firsts section of next appendix.

An isometry f is said to fix at least one point if $f(\boldsymbol{p}) = \boldsymbol{p}$ for at least some $\boldsymbol{p} \in \mathbb{R}^n$. Attending to these characteristics, the isometries of $E(n)$ can be classified into four types:

- Translations: direct isometries without fixed points.
- Rotations: direct isometries with a fixed point, line or hyperplane.
- Reflections: indirect isometries with a fixed hyperplane.
- Glide reflections: indirect isometries without fixed points.

Thus, the elements of $SE(n)$ are rotations, translations and compositions of these. As explained before, these isometries are of special relevance for robot kinematics.

Definition A.2.11. The set of all isometries of an Euclidean space E with at least one fixed point is a group with the composition that is known as the *orthogonal group* $O(n)$.

Proposition A.2.12. *The orthogonal group $O(n)$ is isomorphic to the group of orthogonal matrices.*

As stated in (A.13), orthogonal matrices always have determinant ± 1. This allows to define the special orthogonal group as follows:

Definition A.2.13. The subgroup of $O(n)$ formed by the orthogonal matrices whose determinant is 1 is known as the *special orthogonal group* $SO(n)$

Obviously, the elements of $O(n)$ are rotations, reflections and compositions of these. The first ones are represented by orthogonal matrices with determinant 1, while the second ones are represented by orthogonal matrices with determinant minus -1. Hence, $SO(n)$ is made up of rotations.

Remark A.2.14. $SO(n) \subset SE(n)$

Definition A.2.15. Let $\boldsymbol{v} \in \mathbb{R}^n$ and $f \in SE(n)$. Then, f is said to be a *translation* along $\boldsymbol{v}$ if, for any vector $\boldsymbol{u} \in \mathbb{R}^n$:

$$f(\boldsymbol{u}) = \boldsymbol{u} + \boldsymbol{v} \tag{A.27}$$

Definition A.2.16. Let $\boldsymbol{v} \in \mathbb{R}^n$ and $f \in SO(n)$. Then, f is said to be a *rotation* by an angle θ around $\boldsymbol{v}$ if, for any vector $\boldsymbol{u} \in \mathbb{R}^n$:

$$f(\boldsymbol{u}) = R_{\boldsymbol{v}}(\theta)\boldsymbol{u} \tag{A.28}$$

where $R_{\boldsymbol{v}}(\theta)$ is an orthogonal matrix representing the rotation by an angle θ around $\boldsymbol{v}$. These orthogonal matrices are also known as *rotation matrices*. The plane normal to $\boldsymbol{v}$ is an invariant plane known as the *rotation plane*.

Finally, the matrix representation of an arbitrary element of $SE(n)$ is:

$$SE(n) \equiv \left\{ \begin{pmatrix} R & \boldsymbol{p} \\ 0 & 1 \end{pmatrix} \;\middle|\; R \in SO(n) \text{ and } \boldsymbol{p} \in \mathbb{R}^n \right\} \tag{A.29}$$

A.3 Geometric algebras

The main problem of vector spaces is that vectors have not inverse. Besides, the isometries of an Euclidean space are represented through matrices which entails a high computational cost when implemented. To overcome these and related problems, geometric algebra and, in particular, the conformal model of geometric algebra, provides an excellent framework. The next two sections are devoted to the introduction of both geometric algebra and its conformal model.

Definition A.3.1. Let $\mathbb{K}$ be a commutative field. A vector space A over $\mathbb{K}$ is said to be an *algebra over* $\mathbb{K}$ if it is equipped with a bilinear operation:

$$\begin{aligned} \cdot : A \times A &\to A \\ (a, b) &\to ab \end{aligned}$$

Thus, since algebras are vector spaces, all the properties studied in sections A.1 and A.2 are also true for algebras. However, the structure of algebra requires of an extra operation between vectors. First attempt is to use the *cross product*.

Definition A.3.2. Let $\boldsymbol{x}_1, \boldsymbol{x}_2 \in \mathbb{R}^3$. The cross product $\boldsymbol{x}_1 \times \boldsymbol{x}_2$ is defined as a new vector $\boldsymbol{x}_3$ that is perpendicular to both $\boldsymbol{x}_1$ and $\boldsymbol{x}_2$, with a direction given by the right-hand rule and a magnitude equal to:

$$\|\boldsymbol{x}_1 \times \boldsymbol{x}_2\|_2 = \|\boldsymbol{x}_1\|_2 \, \|\boldsymbol{x}_2\|_2 \sin(\theta)$$

where θ is the angle between $\boldsymbol{x}_1$ and $\boldsymbol{x}_2$ in the plane containing them.

Proposition A.3.3. *Let $\boldsymbol{x}_1, \boldsymbol{x}_2, \boldsymbol{x}_3 \in \mathbb{R}^3$ and $\lambda_1, \lambda_2, \lambda_3 \in \mathbb{R}$. Then, some properties of the cross product are:*

- *Anticommutativity:* $\boldsymbol{x}_1 \times \boldsymbol{x}_2 = -\boldsymbol{x}_2 \times \boldsymbol{x}_1$.
- *Bilinearity:* $\boldsymbol{x}_1 \times (\lambda_2 \boldsymbol{x}_2 + \lambda_3 \boldsymbol{x}_3) = \lambda_2(\boldsymbol{x}_1 \times \boldsymbol{x}_2) + \lambda_3(\boldsymbol{x}_1 \times \boldsymbol{x}_3)$ *and* $(\lambda_1 \boldsymbol{x}_1 + \lambda_2 \boldsymbol{x}_2) \times \boldsymbol{x}_3 = \lambda_1(\boldsymbol{x}_1 \times \boldsymbol{x}_3) + \lambda_2(\boldsymbol{x}_2 \times \boldsymbol{x}_3)$.
- *Jacobi identity:* $\boldsymbol{x}_1 \times (\boldsymbol{x}_2 \times \boldsymbol{x}_3) + \boldsymbol{x}_2 \times (\boldsymbol{x}_3 \times \boldsymbol{x}_1) + \boldsymbol{x}_3 \times (\boldsymbol{x}_1 \times \boldsymbol{x}_2) = 0$.

The major failure of the cross product is that only exists in the three-dimensional space and cannot be extended to higher dimensions. The solution to this problem was given by Grassmann (Grassmann, 2000) through the exterior product. Unlike the cross product, which results in a perpendicular vector, the exterior product of a pair of vectors $\boldsymbol{x}_1, \boldsymbol{x}_2$ results in an oriented area. In detail:

Definition A.3.4. Given two vectors $\boldsymbol{x}_1, \boldsymbol{x}_2 \in \mathbb{R}^n$, the *outer* or *exterior product* of $\boldsymbol{x}_1$ and $\boldsymbol{x}_2$, $\boldsymbol{x}_1 \wedge \boldsymbol{x}_2$, is a new element that can be seen as the oriented area of the parallelogram obtained by sweeping the vector $\boldsymbol{x}_1$ along $\boldsymbol{x}_2$ (figure A.2a).

Some properties of the exterior product are:

- Anticommutativity: $\boldsymbol{x}_1 \wedge \boldsymbol{x}_2 = -\boldsymbol{x}_2 \wedge \boldsymbol{x}_1$. In particular, $\boldsymbol{x}_1 \wedge \boldsymbol{x}_1 = 0$.
- Bilinearity:

$$\begin{aligned} &\boldsymbol{x}_1 \wedge (\lambda_2 \boldsymbol{x}_2 + \lambda_3 \boldsymbol{x}_3) = \lambda_2(\boldsymbol{x}_1 \wedge \boldsymbol{x}_2) + \lambda_3(\boldsymbol{x}_1 \wedge \boldsymbol{x}_3) \\ &\text{and} \\ &(\lambda_1 \boldsymbol{x}_1 + \lambda_2 \boldsymbol{x}_2) \wedge \boldsymbol{x}_3 = \lambda_1(\boldsymbol{x}_1 \wedge \boldsymbol{x}_3) + \lambda_2(\boldsymbol{x}_2 \wedge \boldsymbol{x}_3) \end{aligned} \tag{A.30}$$

- Associativity: $(\boldsymbol{x}_1 \wedge \boldsymbol{x}_2) \wedge \boldsymbol{x}_3 = \boldsymbol{x}_1 \wedge (\boldsymbol{x}_2 \wedge \boldsymbol{x}_3)$.

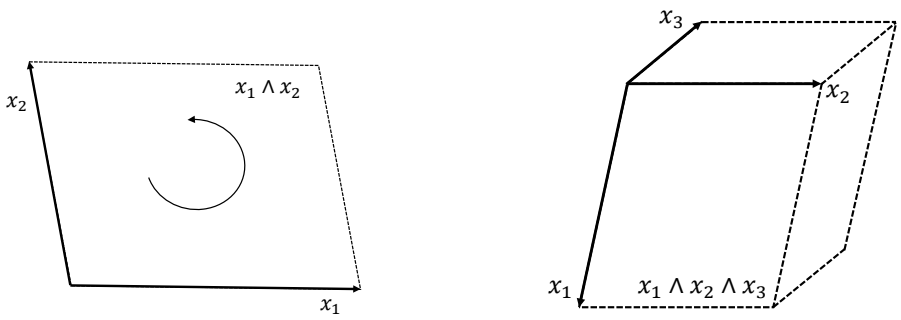

(a) Bivector **(b)** Trivector

Figure A.2: Interpretation of a bivector and a trivector

The new element defined by the exterior product is called a *bivector* and has grade two. By extension, the outer product of a bivector with a vector is known as a *trivector*, is denoted by $\boldsymbol{x}_1 \wedge \boldsymbol{x}_2 \wedge \boldsymbol{x}_3$ and has grade three. Trivectors can be seen as the oriented volume obtained by sweeping the bivector $\boldsymbol{x}_1 \wedge \boldsymbol{x}_2$ along $\boldsymbol{x}_3$ (figure A.2b).

This can be generalized to an arbitrary dimension. Thus,

$$\boldsymbol{x}_1 \wedge \boldsymbol{x}_2 \wedge \cdots \wedge \boldsymbol{x}_r \tag{A.31}$$

denotes an r-*blade*, i.e., an element of grade r. Linear combinations of r-blades are known as r-*vectors*, while linear combinations of r-vectors (for different r) are known as *multivectors*.

Later, Clifford extended the exterior product by adding the inner product. In his work (Clifford et al., 1882), Clifford defines the *geometric product* (also known as the *Clifford product*) as follows:

$$\boldsymbol{x}_1\boldsymbol{x}_2 = \boldsymbol{x}_1 \cdot \boldsymbol{x}_2 + \boldsymbol{x}_1 \wedge \boldsymbol{x}_2 \quad \boldsymbol{x}_1, \boldsymbol{x}_2 \in \mathbb{R}^n \tag{A.32}$$

Thus, the geometric product between two vectors has two components: the scalar component given by the inner product and the bivector component given by the exterior product.

Furthermore, the geometric product allows to redefine the inner and outer products in terms of the geometric one:

$$\boldsymbol{x}_1 \cdot \boldsymbol{x}_2 = \frac{1}{2}(\boldsymbol{x}_1\boldsymbol{x}_2 + \boldsymbol{x}_2\boldsymbol{x}_1) \tag{A.33}$$

$$\boldsymbol{x}_1 \wedge \boldsymbol{x}_2 = \frac{1}{2}(\boldsymbol{x}_1\boldsymbol{x}_2 - \boldsymbol{x}_2\boldsymbol{x}_1) \tag{A.34}$$

The following properties allow to extend the geometric product to an arbitrary number of vectors:

- Associativity: $(\boldsymbol{x}_1\boldsymbol{x}_2)\boldsymbol{x}_3 = \boldsymbol{x}_1(\boldsymbol{x}_2\boldsymbol{x}_3)$.

- Distributivity over the addition: $\boldsymbol{x}_1(\boldsymbol{x}_2 + \boldsymbol{x}_3) = \boldsymbol{x}_1\boldsymbol{x}_2 + \boldsymbol{x}_1\boldsymbol{x}_3$.
- Inverse element: For each $\boldsymbol{x} \in \mathbb{R}^n$ there exists $\boldsymbol{y} \in \mathbb{R}^n$ such that $\boldsymbol{xy} = 1$. Such inverse is simply:

$$\boldsymbol{x}^{-1} = \frac{\boldsymbol{x}}{\boldsymbol{x}^2} \tag{A.35}$$

Given an orthonormal basis $B = \{\boldsymbol{e}_1, \ldots, \boldsymbol{e}_n\}$ of $\mathbb{R}^n$, the definition and properties of the geometric product (A.32) allow to deduce that:

$$\boldsymbol{e}_i\boldsymbol{e}_j = \begin{cases} 1 & \text{for} \quad i = j \\ \boldsymbol{e}_i \wedge \boldsymbol{e}_j & \text{for} \quad i \neq j \end{cases} \tag{A.36}$$

Thus, for each $0 \leq k \leq n$, the set of k-vectors is spanned by:

Scalars or 0-vectors: spanned by $\{1\}$

Vectors or 1-vectors: spanned by $\{\boldsymbol{e}_1, \ldots, \boldsymbol{e}_n\}$

Bivectors: spanned by $\{\boldsymbol{e}_i \wedge \boldsymbol{e}_j\}_{1 \leq i < j \leq n}$

Trivectors: spanned by $\{\boldsymbol{e}_i \wedge \boldsymbol{e}_j \wedge \boldsymbol{e}_k\}_{1 \leq i < j < k \leq n}$

$\vdots$

r-vectors: spanned by $\{\boldsymbol{e}_{i_1} \wedge \cdots \wedge \boldsymbol{e}_{i_r}\}_{1 \leq i_1 < \cdots < i_r \leq n}$

$\vdots$

n-vector: spanned by $\{\boldsymbol{e}_1 \wedge \cdots \wedge \boldsymbol{e}_n\}$

Then, for each $0 \leq k \leq n$, there are exactly $C(n, k)$ generators for the set of k-vectors. These generators can be seen as bases of real vector spaces if the addition and the multiplication by scalars is considered. Each one of these real vector spaces has dimension $C(n, k)$.

Example A.3.5.

- 0-vectors correspond to $\mathbb{R}$, that has dimension $C(n, 0) = 1$.
- 1-vectors or, simply, vectors correspond to $\mathbb{R}^n$, that has dimension $C(n, 1) = n$.

However, none of these vector spaces is closed under the geometric product and, as a consequence, none defines an algebra. Nevertheless, the vector space spanned by all the generators defines an algebra of dimension $C(n, 0) + C(n, 1) + \cdots + C(n, n) = 2^n$.

Definition A.3.6. Let $\mathbb{R}^n$ denote the real vector space of dimension n. Then, the vector space spanned by the basis

$$\mathcal{B} = \{\boldsymbol{e}_{i_1} \wedge \cdots \wedge \boldsymbol{e}_{i_r}\}_{\substack{1 \leq i_1 < \cdots < i_r \leq n \\ 0 \leq r \leq n}} \tag{A.37}$$

endowed with the geometric product (A.32) is an algebra over $\mathbb{R}$ known as the *geometric algebra* (GA) of $\mathbb{R}^n$. Such algebra is denoted by $\mathcal{G}_n$.

Remark A.3.7. Let consider, instead of $\mathbb{R}^n$, an arbitrary vector space V of dimension n where its associated bilinear form has signature $(p, 0, q)$. This implies that, for an orthonormal basis $\{\boldsymbol{e}_1, \ldots, \boldsymbol{e}_n\}$, there are q basis elements such that $\boldsymbol{e}\boldsymbol{e} = -1$. Then, the geometric algebra of V is denoted by $\mathcal{G}_{p,q}$ and it said to have *signature* (p, q). From now on and, unless other is specified, $\mathcal{G}_n$ will denote the geometric algebra of an arbitrary vector space V where its bilinear form has signature $(p, 0, q)$ with $n = p + q$.

Since the grading structure of multivectors is a property associated with the exterior product, the elements of $\mathcal{G}_n$ can still be called r-blades, r-vectors and multivectors.

Definition A.3.8. The basis $\mathcal{B}$ of $\mathcal{G}_n$ is split in two:

$$\begin{aligned} \mathcal{B}^+ &= \{\boldsymbol{e}_{i_1} \wedge \cdots \wedge \boldsymbol{e}_{i_r}\}_{\substack{1 \leq i_1 < \cdots < i_r \leq n \\ 0 \leq r \leq n \,:\, r \text{ even}}} \\ \mathcal{B}^- &= \{\boldsymbol{e}_{i_1} \wedge \cdots \wedge \boldsymbol{e}_{i_r}\}_{\substack{1 \leq i_1 < \cdots < i_r \leq n \\ 0 \leq r \leq n \,:\, r \text{ odd}}} \end{aligned} \tag{A.38}$$

The subalgebra spanned by $\mathcal{B}^+$ ($\mathcal{B}^-$) is termed the *even subalgebra* (*odd subalgebra*) of $\mathcal{G}_n$ and is denoted by $\mathcal{G}_n^+$ ($\mathcal{G}_n^-$). Furthermore, $\mathcal{G}_n = \mathcal{G}_n^+ \oplus \mathcal{G}_n^-$.

An important family of linear operators in $\mathcal{G}_n$ are the *grade-r projection operators*, denoted by $\langle\cdot\rangle_r$ for each $0 \leq r \leq n$. Applied to an arbitrary multivector A, $\langle A\rangle_r$ projects onto the grade-r components in A, i.e., it returns the components of A that can be expressed as a linear combination of $\{\boldsymbol{e}_{i_1} \wedge \cdots \wedge \boldsymbol{e}_{i_r}\}_{1 \leq i_1 < \cdots < i_r \leq n}$. Obviously, if A_r denotes an r-vector, then $\langle A_r\rangle_r = A_r$.

Using these operators, general multivectors $A \in \mathcal{G}_n$ can be expressed as:

$$A = \langle A\rangle_0 + \langle A\rangle_1 + \cdots + \langle A\rangle_n \tag{A.39}$$

where, in addition, due to the linearity of these operators, the following properties hold:

- $\langle \lambda A\rangle_r = \lambda \langle A\rangle_r$
- $\langle A + B\rangle_r = \langle A\rangle_r + \langle B\rangle_r$

The set of all r-vectors for a given $1 \leq r \leq n$ is a vector subspace of $\mathcal{G}_n$ denoted by $\langle\mathcal{G}_n\rangle_r$ and spanned by $\mathcal{B}_r = \{\boldsymbol{e}_{i_1} \wedge \cdots \wedge \boldsymbol{e}_{i_r}\}_{1 \leq i_1 < \cdots < i_r \leq n}$. Clearly, its dimension is $C(n, r)$ but, however, since $\langle\mathcal{G}_n\rangle_r$ is not closed under the geometric product, it is not a subalgebra of $\mathcal{G}_n$.

The multivector representation (A.39) is very useful to define another important operator in $\mathcal{G}_n$. This linear operator is known as the *reversion operator*, denoted by the superscript $\sim$. The reversion is defined over the geometric product of vectors as:

$$\widetilde{\boldsymbol{a}_1 \cdots \boldsymbol{a}_m} = \boldsymbol{a}_m \cdots \boldsymbol{a}_1 \tag{A.40}$$

Identity (A.40) can be extended to r-vectors that, since they can be expressed in terms of the exterior product, have the property:

$$\widetilde{A_r} = (-1)^{\frac{r(r-1)}{2}} A_r \tag{A.41}$$

due to the anticommutativity of the exterior product. Finally, since reversion is a linear operator, the reverse of an arbitrary multivector is:

$$\widetilde{A} = \widetilde{\langle A \rangle_0} + \cdots + \widetilde{\langle A \rangle_n} \overset{(1)}{=} \langle A \rangle_0 + \langle A \rangle_1 - \langle A \rangle_2 + \cdots + (-1)^{\frac{n(n-1)}{2}} \langle A \rangle_n \tag{A.42}$$

where (1) uses equation A.41.

An interesting property of the reversion operator is that allows the definition of the inverse of an arbitrary r-blade A_r:

$$A_r^{-1} = \frac{\widetilde{A_r}}{A_r \widetilde{A_r}} \tag{A.43}$$

In particular, for 1-vectors, identity (A.43) returns (A.35).

Another operator of great interest is the *dual operator*. Every grade-n element of $\mathcal{G}_n$ is of the form $\alpha(\boldsymbol{e}_1 \wedge \cdots \wedge \boldsymbol{e}_n)$ with $\alpha \in \mathbb{R}$. For each $\alpha \in \mathbb{R}$, $\alpha(\boldsymbol{e}_1 \wedge \cdots \wedge \boldsymbol{e}_n)$ is known as the *volume element* E_α of $\mathcal{G}_n$, while the generator $\boldsymbol{e}_1 \wedge \cdots \wedge \boldsymbol{e}_n$ is known as the *pseudoscalar* of $\mathcal{G}_n$ and is usually denoted by I. Pseudoscalars allow to define the dual operator, whose action over an r-vector A_r is:

$$A_r^* = I A_r \tag{A.44}$$

where A_r^* is the orthogonal complement of A_r and, thus, is an $(n-r)$-vector.

Since chapters 5 and 6 deal with the spatial geometric algebra, the orthonormal basis of $\mathcal{G}_3$ is introduced:

$$\{1, \boldsymbol{e}_1, \boldsymbol{e}_2, \boldsymbol{e}_3, e_{12}, e_{13}, e_{23}, I\} \tag{A.45}$$

where $e_{ij} = \boldsymbol{e}_i \wedge \boldsymbol{e}_j$. Furthermore, each basis bivector squares to -1.

The effect of bivectors on vectors is illustrated in the following example:

Example A.3.9. Let consider the vector $\boldsymbol{e}_1 + \boldsymbol{e}_2$ and the bivector e_{12}, both elements of $\mathcal{G}_3$. Then:

$$\begin{aligned}(\boldsymbol{e}_1 + \boldsymbol{e}_2)e_{12} &= \boldsymbol{e}_1 e_{12} + \boldsymbol{e}_2 e_{12} = \\ &= \boldsymbol{e}_1 \boldsymbol{e}_1 \boldsymbol{e}_2 + \boldsymbol{e}_2 \boldsymbol{e}_1 \boldsymbol{e}_2 = \\ &= \boldsymbol{e}_1 \wedge \boldsymbol{e}_1 \wedge \boldsymbol{e}_2 + \boldsymbol{e}_2 \wedge \boldsymbol{e}_1 \wedge \boldsymbol{e}_2 = \\ &= \boldsymbol{e}_2 - \boldsymbol{e}_1\end{aligned} \tag{A.46}$$

Hence, bivector e_{12} rotates $\boldsymbol{e}_1 + \boldsymbol{e}_2$ counter-clockwise by 90 degrees in the plane described by it.

Since $\boldsymbol{e}_1$ and $\boldsymbol{e}_2$ are basis vectors, they generate a plane in which any vector $\boldsymbol{x}_1$ can be represented using the formula:

$$\boldsymbol{x}_1 = \|\boldsymbol{x}_1\|_2(\boldsymbol{e}_1\cos(\theta) + \boldsymbol{e}_2\sin(\theta)) = \|\boldsymbol{x}_1\|_2\,\boldsymbol{e}_1(\cos(\theta) + e_{12}\sin(\theta)) \tag{A.47}$$

where θ denotes the angle between $\boldsymbol{x}_1$ and $\boldsymbol{e}_1$.

Equation (A.47) is valid for any unit bivector B. Furthermore, it allows to define the operator that performs the rotation by an angle θ in the plane described by B:

$$\begin{aligned} R = \exp(\theta B) &= 1 + \frac{\theta B}{1!} + \frac{\theta^2 B^2}{2!} + \frac{\theta^3 B^3}{3!} + \cdots = \\ &= 1 + \frac{\theta B}{1!} - \frac{\theta^2}{2!} - \frac{\theta^3 B}{3!} + \cdots = \\ &= \cos(\theta) + B\sin(\theta) \end{aligned} \tag{A.48}$$

Operator R is termed a *rotor*. Thus, equation (A.47) can be rewritten as:

$$\boldsymbol{x}_1 = \|\boldsymbol{x}_1\|_2\,\boldsymbol{e}_1 R \tag{A.49}$$

Equation (A.49) can be seen as the rotation of $\boldsymbol{e}_1$ by an angle θ in the plane described by B. In general:

$$\boldsymbol{x}' = \boldsymbol{x}R \tag{A.50}$$

It is important to mention that the vector $\boldsymbol{x}$ lies in the plane of rotation. In a different case, the vector should be decomposed into a component that lies in the plane of rotation, $\boldsymbol{x}_\parallel$, and one normal to such plane, $\boldsymbol{x}_\perp$, such that:

$$\boldsymbol{x} = \boldsymbol{x}_\parallel + \boldsymbol{x}_\perp \tag{A.51}$$

In this situation, let consider the rotor $R = \exp(-\frac{\theta}{2}B)$ and its reverse $\widetilde{R} = \exp(\frac{\theta}{2}B)$. Then:

$$\begin{aligned} \boldsymbol{x}' &= R\boldsymbol{x}\widetilde{R} = R(\boldsymbol{x}_\parallel + \boldsymbol{x}_\perp)\widetilde{R} \overset{(1)}{=} \\ &= \left(\cos\left(\frac{\theta}{2}\right) - B\sin\left(\frac{\theta}{2}\right)\right)(\boldsymbol{x}_\parallel + \boldsymbol{x}_\perp)\left(\cos\left(\frac{\theta}{2}\right) + B\sin\left(\frac{\theta}{2}\right)\right) = \\ &= \boldsymbol{x}_\perp + \left(\cos^2\left(\frac{\theta}{2}\right) - \sin^2\left(\frac{\theta}{2}\right)\right)\boldsymbol{x}_\parallel - 2\cos\left(\frac{\theta}{2}\right)\sin\left(\frac{\theta}{2}\right)B\boldsymbol{x}_\parallel \overset{(1)}{=} \\ &= \boldsymbol{x}_\perp + \boldsymbol{x}_\parallel(\cos(\theta) + B\sin(\theta)) \end{aligned} \tag{A.52}$$

where (1) denotes the use of the following properties:

- $B\boldsymbol{x}_\perp = \boldsymbol{x}_\perp B$.

- $B\boldsymbol{x}_{\parallel} = -\boldsymbol{x}_{\parallel}B$.

These two properties can be proven easily (Doran and Lasenby, 2003, pp. 30-33).

Since in equation (A.52) the normal component of $\boldsymbol{x}$ is made up of fixed points and the component that lies in the plane described by B is rotated, it can be concluded that $R\boldsymbol{x}\widetilde{R}$ defines a rotation by an angle θ around the vector normal to the plane described by B.

In general, rotors define a group $\mathfrak{R}$ with the geometric product as group law:

$$\mathfrak{R} = \{R \in \mathcal{G}_n^+ \ : \ R\widetilde{R} = 1\} \tag{A.53}$$

Furthermore, they have the following properties:

- $\widetilde{R} = R^{-1}$
- $R\boldsymbol{x}\widetilde{R} = (-R)\boldsymbol{x}(-\widetilde{R})$
- $R\boldsymbol{x}\boldsymbol{y}\widetilde{R} = R\boldsymbol{x}\widetilde{R}R\boldsymbol{y}\widetilde{R}$
- If the signature of $\mathcal{G}_n$ is $(n, 0)$ or $(0, n)$, then R can be expressed as $R = \exp(-\frac{\theta}{2}B)$ for an angle θ and a bivector B.

The first two properties are the analogous versions of the properties that define the orthogonal matrices. The third property proves that the rotor group provides a double covering of the space of rotations while the fourth property shows the geometric covariance of rotors, i.e., that rotors preserves the structure provided by the algebra.

Remark A.3.10. The group $\mathfrak{R}$ is a rotor group only for $n \leq 5$.

As a counterexample, let consider the geometric algebra $\mathcal{G}_6$ of $\mathbb{R}^6$. The even element $R = \rho(1 + I)$, where I is the pseudoscalar of $\mathcal{G}_6$ and $\rho = \frac{1}{\sqrt{2}}$, verifies that $R\widetilde{R} = 1$. However, since it does not define a rotation, it is not a rotor (Xambó-Descamps, 2017).

Finally, let consider a reflection of the vector $\boldsymbol{x} \in \mathbb{R}^n$ in the plane orthogonal to a unit vector $\boldsymbol{m}$. In geometric algebra, reflections are formulated easily:

$$\boldsymbol{x}' = -\boldsymbol{m}\boldsymbol{x}\boldsymbol{m} \tag{A.54}$$

where $\boldsymbol{x}'$ is the reflected vector. Identity (A.54) can be extended naturally to arbitrary multivectors.

A.4 Conformal model of a geometric algebra

In this section, since n denotes a special element of the conformal geometric algebra, the dimension of an arbitrary Euclidean space will be denoted by m.

Definition A.4.1. Let $\mathbb{R}^m$ denote the m-dimensional real vector space. The *conformal closure* of $\mathbb{R}^m$ is defined as the space

$$\mathbb{R}^{m+1,1} = \mathbb{R}^m \perp \mathbb{R}^{1,1}$$

where $\perp$ denotes the orthogonal sum between two vector spaces, i.e., the direct sum where, besides, both spaces are mutually orthogonal. On the other hand, $\mathbb{R}^{1,1}$ is a hyperbolic plane, that is, a 2-dimensional vector space with signature $(1, 0, 1)$.

Definition A.4.2. The geometric algebra of $\mathbb{R}^{m+1,1}$ is said to be the *conformal geometrical algebra* (CGA) of $\mathbb{R}^m$. This algebra is denoted by $\mathcal{G}_{m+1,1}$.

If $\{e, \overline{e}\}$ denote the basis of the hyperbolic plane $\mathbb{R}^{1,1}$, then $e^2 = 1$ and $\overline{e}^2 = -1$. These two basis vectors allow to define two special vectors as follows:

$$\begin{aligned} n &= e + \overline{e} \\ \overline{n} &= e - \overline{e} \end{aligned} \tag{A.55}$$

where, by definition, $n^2 = \overline{n}^2 = 0$. Thus, these two vectors are *null vectors*. Furthermore, n is associated with the point at infinity, while $\overline{n}$, with the origin.

Three basic properties of these null vectors are:

$$n \cdot \overline{n} = 2 \tag{A.56}$$

$$\boldsymbol{x} \cdot n = \boldsymbol{x} \cdot \overline{n} = 0 \quad \forall \boldsymbol{x} \in \mathbb{R}^m \tag{A.57}$$

$$(n \wedge \overline{n})^2 = 4 \tag{A.58}$$

Arbitrary vectors of $\mathbb{R}^m$ can be represented as null vectors of $\mathcal{G}_{m+1,1}$. If $\boldsymbol{x} \in \mathbb{R}^m$, its null vector representation is given by:

$$X = H(\boldsymbol{x}) = \frac{1}{2}(\boldsymbol{x}^2 n + 2\boldsymbol{x} - \overline{n}) \tag{A.59}$$

where the map $H : \mathbb{R}^m \to \mathcal{G}_{m+1,1}$ is known as the *Hestenes' embedding*.

Using (A.56-A.58), the following relation can be deduced:

$$\begin{aligned} X_1 \cdot X_2 &= H(\boldsymbol{x}_1) \cdot H(\boldsymbol{x}_2) = \\ &= \frac{1}{4}(\boldsymbol{x}_1^2 n + 2\boldsymbol{x}_1 - \overline{n}) \cdot (\boldsymbol{x}_2^2 n + 2\boldsymbol{x}_2 - \overline{n}) = \\ &= -\frac{1}{2}\boldsymbol{x}_1^2 + \boldsymbol{x}_1 \cdot \boldsymbol{x}_2 - \frac{1}{2}\boldsymbol{x}_2^2 = \\ &= -\frac{1}{2}(\boldsymbol{x}_1 - \boldsymbol{x}_2)^2 = -\frac{1}{2}\|\boldsymbol{x}_1 - \boldsymbol{x}_2\|_2^2 = \\ &= -\frac{1}{2}d_2^2(\boldsymbol{x}_1, \boldsymbol{x}_2) \end{aligned} \tag{A.60}$$

As a consequence, the distance between two null vectors of $\mathcal{G}_{m+1,1}$ can be defined extending the Euclidean distance (A.23) as follows:

$$d(X_1, X_2) = \sqrt{-2(X_1 \cdot X_2)} \tag{A.61}$$

Given a null vector $X \in \mathcal{G}_{m+1,1}$, it can be rotated by sandwiching it with the rotor R that describes the desired rotation. Indeed, $X' = RX\widetilde{R}$ where R is defined as the exponential of a bivector (A.48).

In $\mathcal{G}_m$, the only bivectors that squares to zero are $\boldsymbol{x} \wedge \boldsymbol{x}$ (with $\boldsymbol{x} \in \mathbb{R}^m$). In this situation, since $R = \exp\left(-\frac{\theta}{2}(\boldsymbol{x} \wedge \boldsymbol{x})\right)$, $R = 1$ and the rotation defined is the identity. However, in $\mathcal{G}_{m+1,1}$ the bivectors of the form $\boldsymbol{x} \wedge n$ also squares to zero. These bivectors define a family $\mathrm{B} = \{\boldsymbol{x} \wedge n \ : \ \boldsymbol{x} \in \mathcal{G}_{m+1,1}\}$ which, in turn, define a special class of rotors, the *translators* $T_{\boldsymbol{x}}$:

$$T_{\boldsymbol{x}} = \exp\left(\frac{n \wedge \boldsymbol{x}}{2}\right) = 1 + \frac{n \wedge \boldsymbol{x}}{2} + \frac{1}{2}\left(\frac{n \wedge \boldsymbol{x}}{2}\right)^2 + \cdots \overset{(1)}{=} 1 + \frac{n\boldsymbol{x}}{2} \tag{A.62}$$

where (1) uses the property (A.57). Translator $T_{\boldsymbol{x}}$ defines a translation along $\boldsymbol{x} \in \mathbb{R}^m$ of length $\|\boldsymbol{x}\|$. As rotors, translators are applied to an element $A \in \mathcal{G}_{m+1,1}$ by sandwiching it as follows:

$$A' = T_{\boldsymbol{x}} A \widetilde{T}_{\boldsymbol{x}} \tag{A.63}$$

So, rigid motions are easily described in conformal geometric algebra. Furthermore, the manipulation of such transformations become very easy due to their simple formulation.

Another advantage of conformal geometric algebra relies on its simple description of the different geometric objects. Henceforth, the conformal geometric algebra $\mathcal{G}_{4,1}$ of the three-dimensional space will be considered. There, the different geometric entities are described by blades. For a given geometric entity O, this is referred as the *primal representation* of O.

The following is an important and intuitive property of primal representations:

Theorem A.4.3. *Let O denote the primal representation of a geometric entity defined in the conformal geometric algebra $\mathcal{G}_{4,1}$. A null vector X lies in O if, and only if, $X \wedge O = 0$.*

An additional constraint that simplifies the formulation of the following results is that, for any null vector X, $X \cdot n = -1$.

A.4.1 Bivectors

Definition A.4.4. Let $\boldsymbol{x}, \boldsymbol{y} \in \mathbb{R}^m$ with $\boldsymbol{x} \neq \boldsymbol{y}$. Then, $X \wedge Y$ is the null vector representation of the *point pair* $\{\boldsymbol{x}, \boldsymbol{y}\}$.

Given a bivector of the form $X \wedge Y \neq 0$, it can be split into a pair of null vectors that are unique up to a scale.

Let

$$F = \frac{1}{\beta} X \wedge Y \tag{A.64}$$

where $\beta^2 = (X \wedge Y)^2$, so that $F^2 = 1$. Now, a projector operator is defined:

$$P = \frac{1}{2}(1 + F) \tag{A.65}$$

while its reverse is:

$$\widetilde{P} = \frac{1}{2}(1 - F) \tag{A.66}$$

Some easy to prove properties of these operators are:

- $PP = P$.
- $\widetilde{P}\widetilde{P} = \widetilde{P}$.
- $P\widetilde{P} = \widetilde{P}P = 0$.
- $PX = 0$ and $\widetilde{P}X = X$.
- $PY = Y$ and $\widetilde{P}Y = 0$.

Proposition A.4.5. *A bivector $X \wedge Y \in \mathcal{G}_{4,1}$ verifies that $(X \wedge Y) \cdot n = Y - X$*

Thus, by proposition A.4.5 and the above-mentioned properties of the projector operator, it follows that:

$$\begin{aligned} X &= -\widetilde{P}[(X \wedge Y) \cdot n]P \\ Y &= P[(X \wedge Y) \cdot n]\widetilde{P} \end{aligned} \tag{A.67}$$

However, equation (A.67) does not work for bivectors of the form $X \wedge n$ or $n \wedge X$. For these bivectors, the approach followed in (Cameron, 2008) turns to be useful. There, instead of using the projector operator (A.65), the following expressions are used:

$$\begin{aligned} \boldsymbol{x} &= \frac{1}{4}(n \wedge X \wedge \overline{n}) \cdot (n \wedge \overline{n}) \quad \text{if the bivector is } n \wedge X \\ \boldsymbol{x} &= \frac{1}{4}(\overline{n} \wedge X \wedge n) \cdot (n \wedge \overline{n}) \quad \text{if the bivector is } X \wedge n \end{aligned} \tag{A.68}$$

where $\boldsymbol{x}$ is the real vector whose null vector representation is X.

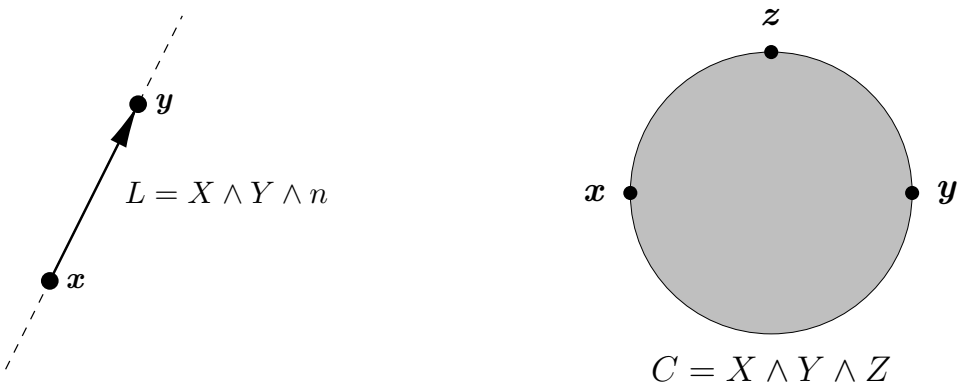

(a) Line passing through null vectors X and Y **(b)** Circle passing through null vectors X, Y and Z

Figure A.3: Line and circle

A.4.2 Trivectors

Trivectors represent lines and circles. In this section, the *primal representation* of both is given first and then, their *dual representations* are introduced.

Definition A.4.6. Let X and Y be two different null vectors. Then, the trivector $L = X \wedge Y \wedge n$ represents the line passing through the points $\boldsymbol{x}, \boldsymbol{y}$ with direction $\boldsymbol{x}$ to $\boldsymbol{y}$, X, Y being the null vector representations of $\boldsymbol{x}, \boldsymbol{y}$, respectively (figure A.3a).

Clearly, the line with opposite direction is represented by $L' = Y \wedge X \wedge n$ and fulfils $L' = -L$.

Definition A.4.7. Let X, Y and Z be the null vector representations of three different points $\boldsymbol{x}, \boldsymbol{y}$ and $\boldsymbol{z}$. Then, the trivector $C = X \wedge Y \wedge Z$ represents the circle passing through the points $\boldsymbol{x}, \boldsymbol{y}$ and $\boldsymbol{z}$ (figure A.3b).

Theorem A.4.3 applied to circles states that a null vector X lies in C if $X \wedge C = 0$. Since circles live in a two-dimensional space, the conformal geometric algebra $\mathcal{G}_{3,1}$ of $\mathcal{G}_2$ is used instead of $\mathcal{G}_{4,1}$. Thus, the dual operator applied to C returns a vector, C^*. Hence, an alternative but useful representation of the circle is given by the equation $X \cdot C^* = 0$.

Let consider a null vector X lying in the circle C^* and let $\overline{C}$ denote its center. Then, the radius r is calculated through equation (A.60):

$$X \cdot \overline{C} = -\frac{1}{2} d_2^2(\boldsymbol{x}, \overline{\boldsymbol{c}}) = -\frac{1}{2} r^2 \tag{A.69}$$

where $\boldsymbol{x}, \overline{\boldsymbol{c}}$ are the vectors whose null vectors are X and $\overline{C}$, respectively. Thus, for a normalised

null vector X, identity (A.69) implies that:

$$X \cdot \left(\overline{C} - \frac{1}{2} r^2 n \right) = 0 \tag{A.70}$$

and, therefore, the dual representation of C is deduced:

$$C^* = \overline{C} - \frac{1}{2} r^2 n \tag{A.71}$$

Applying a similar reasoning, the dual representation of a line L is also deduced:

$$L^* = \boldsymbol{v} e_{123} + (\boldsymbol{v} \times \boldsymbol{p}) e_{123} n \tag{A.72}$$

where $\boldsymbol{v}$ denotes the direction vector and $\boldsymbol{p}$ a point of the line.

A.4.3 4-vectors

General 4-vectors represent planes and spheres. Again, their primal representations are presented first and, then, the dual ones are introduced.

Definition A.4.8. Let X, Y and Z be three different null vectors. Then, the 4-vector $P = X \wedge Y \wedge Z \wedge n$ represents the plane passing through the points $\boldsymbol{x}, \boldsymbol{y}$ and $\boldsymbol{z}$.

Definition A.4.9. Let W, X, Y and Z be the null vector representations of four different points $\boldsymbol{w}, \boldsymbol{x}, \boldsymbol{y}$ and $\boldsymbol{z}$. Then, the 4-vector $S = W \wedge X \wedge Y \wedge Z$ represents the sphere that passes through the four points $\boldsymbol{w}, \boldsymbol{x}, \boldsymbol{y}$ and $\boldsymbol{z}$.

As in the case of trivectors, a dual representation based on the inner product can be defined for both geometric entities. For the plane, such representation is:

$$P^* = \boldsymbol{v} + dn \tag{A.73}$$

where $\boldsymbol{v}$ denotes the vector normal to P and d, its perpendicular distance from the origin.

For the sphere, the dual representation is:

$$S^* = C - \frac{1}{2} r^2 n \tag{A.74}$$

where C is the null vector representation of the centre and r, its radius.

A.4.4 Intersections between geometric entities

The *intersection* or *meet* between any two geometric entities O_1 and O_2 is denoted by $O_1 \vee O_2$ and is governed by the formula:

$$O_1 \vee O_2 = \left[\langle O_1 O_2 \rangle_{2m-p-r} \right]^* \tag{A.75}$$

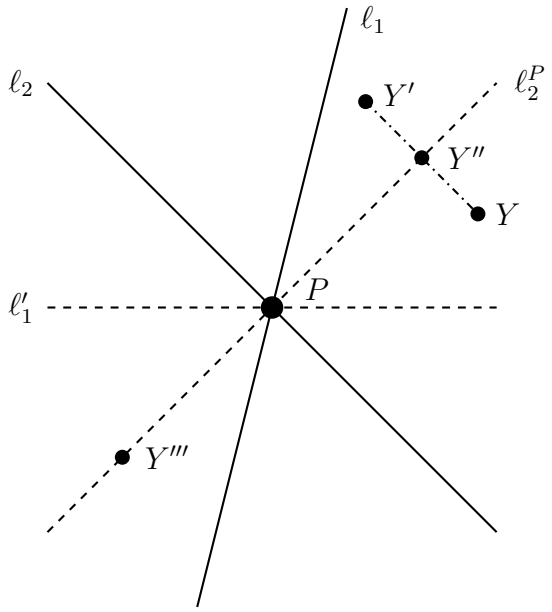

Figure A.4: Intersection point of ℓ_1 and ℓ_2

where m denotes the dimension of the space spanned by O_1 and O_2, while r and p are the grades of the geometric entities O_1 and O_2 respectively.

Different cases are listed and studied:

- O_1 and O_2 are lines:

  If ℓ_1 and ℓ_2 denote those lines, equation (A.75) remains as follows:

  $$\left[\langle \ell_1 \ell_2 \rangle_{2\cdot 5-3-3}\right]^* = [\langle \ell_1 \ell_2 \rangle_4]^* \tag{A.76}$$

  Thus, $[\langle \ell_1 \ell_2 \rangle_4]^*$ is a grade-one element, i.e., a vector. Vectors do not represent any geometric entity in conformal geometric algebra. Therefore, an alternative method to obtain the intersection point is required (Aristidou, 2010; Lasenby et al., 2004).

  Let assume that the lines ℓ_1 and ℓ_2 intersect at point P. Then, the reflection (as defined in (A.54)) of the line ℓ_1 in the line ℓ_2 is considered:

  $$\ell_1' = -\ell_2 \ell_1 \ell_2 \tag{A.77}$$

  Then, a line perpendicular to ℓ_2 that passes through the point P is found:

  $$\ell_2^P = \ell_1 - \ell_1' \tag{A.78}$$

  Let consider an arbitrary null vector Y and reflect it in ℓ_2^P:

  $$Y' = -\ell_2^P Y \ell_2^P \tag{A.79}$$

Then, the midpoint of Y and Y' is calculated:

$$Y'' = \frac{1}{2}(Y + Y') \tag{A.80}$$

Such point lies on the line ℓ_2^P. Thereafter, point Y'' is reflected in ℓ_2:

$$Y''' = -\ell_2 Y'' \ell_2 \tag{A.81}$$

to take the midpoint:

$$P' = \frac{1}{2}(Y'' + Y''') \tag{A.82}$$

The intersection point P can be extracted as follows:

$$P = \frac{-(P'nP')}{2(P' \cdot n)^2} \tag{A.83}$$

- O_1 and O_2 are circles:

  If C_1 and C_2 denote those circles, equation (A.75) becomes:

  $$C_1 \vee C_2 = [\langle C_1 C_2 \rangle_4]^* \tag{A.84}$$

  Again, the intersection is a grade-one element and, therefore, it does not return the intersection points (two circles always have a maximum of two intersection points). In this case, it is enough with considering the plane π that contains C_1: $\pi = C_1 \wedge n$. Now, the intersection between π and C_2 is performed:

  $$\pi \vee C_2 = [\langle \pi C_2 \rangle_3]^* \tag{A.85}$$

  This intersection is a grade two element, i.e., a bivector. If B denotes such bivector, then:

  - If $B^2 = 0$, then $B = X \wedge n$ for some null vector X. This null vector can be extracted using the identity (A.68).
  - If $B^2 > 0$, then $B = X \wedge Y$ for some null vectors X and Y. These null vectors can be extracted using the identity (A.67).
  - If $B^2 < 0$, then, since bivectors that squares to negative numbers do not contain any null vector, the intersection is empty.

- O_1 is a circle and O_2 is a line:

  If C denotes that circle and ℓ, the line, equation (A.75) becomes:

  $$C \vee \ell = [\langle C \ell \rangle_4]^* \tag{A.86}$$

  Since the meet is again a grade-one element, the plane π that contains C is considered. Thus, the intersection between π and ℓ is a grade-two element. If B denotes such intersection, then $B = X \wedge n$ for some null vector X (the intersection between a plane and a line is a single point at the most). Clearly, X can be extracted from B using equation (A.68).

- O_1 and O_2 are planes:

  If π_1 and π_2 denote those planes, equation (A.75) becomes:

  $$\pi_1 \vee \pi_2 = [\langle \pi_1 \pi_2 \rangle_2]^* \tag{A.87}$$

  Thus, the intersection is a grade-three element, i.e., a trivector. Trivectors represent lines and circles and in this case, since the intersection between two planes is a line, (A.87) represents a line ℓ. Then:

  - If $\ell^2 = 0$, the intersection does not exist.
  - If $\ell^2 \neq 0$, the intersection is the line $\ell = X \wedge Y \wedge n$ where X and Y are the null vector representations of two points $\boldsymbol{x}$ and $\boldsymbol{y}$, respectively.

  Given the intersection line ℓ, its direction vector can be recovered by calculating the dual line ℓ^*.

- O_1 is a plane and O_2 is a circle or a line:

  These two cases have already been treated in the cases where the intersection of two circles or a circle and a line have been considered.

- O_1 and O_2 are spheres:

  If S_1 and S_2 denote those spheres, equation (A.75) becomes:

  $$S_1 \vee S_2 = [\langle S_1 S_2 \rangle_2]^* \tag{A.88}$$

  Then, the intersection is a grade-three element, i.e., a trivector. Let denote this trivector by T. Since the intersection of two spheres is always a circle or a point, trivector T verifies that:

  - If $T^2 > 0$, then $T = X \wedge Y \wedge Z$ for some null vectors X, Y and Z. Taking the dual representation of such circle, its center and radius can be found.
  - If $T^2 = 0$, then T is a circle whose dual representation has zero radius. Its centre is the intersection point of S_1 and S_2. Hence, the two spheres are tangent.
  - If $T^2 < 0$, then the intersection is empty.

- O_1 is a sphere and O_2 is a circle or a line:

  If S denotes that sphere and C, the circle (it is completely analogous if, instead of a circle, a line is considered), equation (A.75) becomes:

  $$S \vee C = [\langle SC \rangle_3]^* \tag{A.89}$$

  Then, the intersection is a grade-two element, i.e., a bivector. Let denote by B such bivector. As in the precedent cases, the sign of B^2 provides information on whether the intersection exists:

  - If $B^2 = 0$, then $B = X \wedge n$ for some null vector X. This null vector can be extracted using identity (A.68).

  - If $B^2 > 0$, then $B = X \wedge Y$ for some null vectors X and Y. These null vectors can be extracted using identity (A.67).
  - If $B^2 < 0$, then the intersection is empty.

- O_1 is a sphere and O_2 is a plane:

  This case is exactly the same as the case of two spheres. The intersection, when exists, is a circle or a point. The sign of the trivector's square indicates whether the two geometric entities intersect, are tangent, or do not intersect at all.

Finally, in conformal geometric algebra, the angle between two geometric entities O_1 and O_2 is calculated as follows:

$$\theta = \arccos\left(\frac{O_1 \cdot O_2}{|O_1||O_2|}\right) \tag{A.90}$$

that remembers the expression used to calculate the angle between two vectors (A.24).

Appendix B

Robotics Background

In this appendix, an introduction to robot kinematics is presented. The first section describes the kinematics of rigid bodies, while the second section applies such description to the study of kinematic chains. Finally, third section presents the kinematics of some redundant serial robots. The main references followed throughout this appendix are (Murray et al., 1994; Siciliano et al., 2008; Spong et al., 2006).

B.1 Rigid Body Kinematics

Definition B.1.1. A *rigid body* B in an n-dimensional Euclidean space is a set of points constrained so that the distance between any two of them remains constant for all time regardless of external forces exerted on it.

The concept of rigid body is an idealization of a solid whose deformations associated with its flexibility are neglected (José and Saletan, 1998).

B.1.1 Position and orientation of a rigid body

A rigid body B is completely described in a three-dimensional space by its *configuration* or *pose*, i.e, its *position* and *orientation*, with respect to a reference frame.

Let denote the reference frame by $\{\boldsymbol{o}, \boldsymbol{x}, \boldsymbol{y}, \boldsymbol{z}\}$. A suitable point $\boldsymbol{o}'$ on the body is selected and an orthonormal frame $\{\boldsymbol{x}', \boldsymbol{y}', \boldsymbol{z}'\}$ is attached to the body at $\boldsymbol{o}'$. The position of B with respect to the reference frame is given by the position vector $\boldsymbol{p} = \boldsymbol{o}' - \boldsymbol{o}$, while its orientation is given by

the system:

$$\begin{aligned} \boldsymbol{x}' &= \alpha_1 \boldsymbol{x} + \alpha_2 \boldsymbol{y} + \alpha_3 \boldsymbol{z} \\ \boldsymbol{y}' &= \beta_1 \boldsymbol{x} + \beta_2 \boldsymbol{y} + \beta_3 \boldsymbol{z} \\ \boldsymbol{z}' &= \gamma_1 \boldsymbol{x} + \gamma_2 \boldsymbol{y} + \gamma_3 \boldsymbol{z} \end{aligned} \tag{B.1}$$

where $\alpha_i, \beta_i, \gamma_i \in \mathbb{R}$ for $i = 1, 2, 3$. The system (B.1) is the result of expressing $\{\boldsymbol{x}', \boldsymbol{y}', \boldsymbol{z}'\}$ in terms of $\{\boldsymbol{x}, \boldsymbol{y}, \boldsymbol{z}\}$.

Since $\{\boldsymbol{o}, \boldsymbol{x}, \boldsymbol{y}, \boldsymbol{z}\}$ and $\{\boldsymbol{o}', \boldsymbol{x}', \boldsymbol{y}', \boldsymbol{z}'\}$ are orthonormal frames, the matrix

$$R = \begin{pmatrix} \alpha_1 & \beta_1 & \gamma_1 \\ \alpha_2 & \beta_2 & \gamma_2 \\ \alpha_3 & \beta_3 & \gamma_3 \end{pmatrix} \tag{B.2}$$

is an orthogonal matrix. Thus, R can be seen as the matrix representation of a rotation $f \in SO(3) \subset SE(3)$. In particular, f defines the rotation required to transform $\{\boldsymbol{x}, \boldsymbol{y}, \boldsymbol{z}\}$ into $\{\boldsymbol{x}', \boldsymbol{y}', \boldsymbol{z}'\}$. Furthermore, the position vector $\boldsymbol{p}$ can be seen as the translation of the origin $\boldsymbol{o}$. Indeed, $\boldsymbol{o}' = g(\boldsymbol{o}) = \boldsymbol{o} + \boldsymbol{p}$ for $g \in SE(3)$. Therefore, the composition $f \circ g$ is also an isometry of $SE(3)$ that represents the pose of B. Such isometry can be expressed, using the matrix representation (A.29), as:

$$T = \begin{pmatrix} R & \boldsymbol{p} \\ 0 & 1 \end{pmatrix}$$

where T is also known as the *pose matrix* of B – if seen as describing the position and orientation of B – or the *homogeneous transformation matrix* between frames $\{\boldsymbol{o}, \boldsymbol{x}, \boldsymbol{y}, \boldsymbol{z}\}$ and $\{\boldsymbol{o}', \boldsymbol{x}', \boldsymbol{y}', \boldsymbol{z}'\}$ – if seen as an element of $SE(3)$. That is the reason why $SE(3)$ is also known as the group of *rigid motions*.

Given a vector $\boldsymbol{v}'$, expressed with respect to $\{\boldsymbol{o}', \boldsymbol{x}', \boldsymbol{y}', \boldsymbol{z}'\}$, it is expressed with respect to the reference frame as follows:

$$\boldsymbol{v} = \boldsymbol{p} + R\boldsymbol{v}' \tag{B.3}$$

or, equivalently, as:

$$\boldsymbol{v} = T\boldsymbol{v}' \tag{B.4}$$

The inverse transformations are:

$$\boldsymbol{v}' = -R^T \boldsymbol{p} + R^T \boldsymbol{v} \tag{B.5}$$

$$\boldsymbol{v}' = T^{-1} \boldsymbol{v} \tag{B.6}$$

Now, the *degrees of freedom* (DOF) of the rigid body B are the number of independent scalar variables that are required to completely determine its configuration. In (LaValle, 2006, chapter 4) is shown that the number of degrees of freedom for $SE(n)$ – and consequently for an unconstrained rigid body in $\mathbb{R}^n$ – is:

$$\#\text{DOF} = \frac{n(n+1)}{2} \tag{B.7}$$

Then, since the three-dimensional kinematics of B are considered, $n = 3$ and, therefore, B has six degrees of freedom: three for describing its position and three for describing its orientation.

Since rotation matrices have nine elements, this description of the orientation has nine parameters. A description of the orientation that uses more that three parameters (only three parameters) is said to be a *non-minimal representation* (*minimal representation*) of the orientation. An example of a minimal representation are the Euler angles.

Euler angles

The Euler angles are three angles of rotation (φ, θ, ψ) where each rotation is taken about one axis of $\{\boldsymbol{x}', \boldsymbol{y}', \boldsymbol{z}'\}$. For the first rotation, any of the three axes can be chosen as the axis of revolution, and the two successive rotations must have different axes of revolution, so there are only two alternatives for the second and the third rotations. This means that there are twelve different conventions for the Euler angles (Craig, 1989). The most used conventions are the ZYZ Euler angles and the ZYX Euler angles. The ZYZ angles convention is developed as an illustrative example. The overall rotation described by the ZYZ Euler angles is obtained as composition of the following rotations:

- Rotation by an angle φ about $\boldsymbol{z}'$ (described by the rotation matrix $R_{\boldsymbol{z}'}(\varphi)$). The current frame is denoted by $\{\boldsymbol{x}'_1, \boldsymbol{y}'_1, \boldsymbol{z}'_1\}$.
- Rotation by an angle θ about $\boldsymbol{y}'_1$ (described by the rotation matrix $R_{\boldsymbol{y}'_1}(\theta)$). The current frame is denoted by $\{\boldsymbol{x}'_2, \boldsymbol{y}'_2, \boldsymbol{z}'_2\}$.
- Rotation by an angle ψ about $\boldsymbol{z}'_2$ (described by the rotation matrix $R_{\boldsymbol{z}'_2}(\psi)$). The current frame is denoted by $\{\boldsymbol{x}'_3, \boldsymbol{y}'_3, \boldsymbol{z}'_3\}$.

The composition of these rotations is described by the rotation matrix:

$$\begin{aligned} R_{ZYZ} &= R_{\boldsymbol{z}'}(\varphi) R_{\boldsymbol{y}'_1}(\theta) R_{\boldsymbol{z}'_2}(\psi) = \\ &= \begin{pmatrix} \mathrm{c}_\varphi \mathrm{c}_\theta \mathrm{c}_\psi - \mathrm{s}_\varphi \mathrm{s}_\psi & -\mathrm{c}_\varphi \mathrm{c}_\theta \mathrm{s}_\psi - \mathrm{s}_\varphi \mathrm{c}_\psi & \mathrm{c}_\varphi \mathrm{s}_\theta \\ \mathrm{s}_\varphi \mathrm{c}_\theta \mathrm{c}_\psi + \mathrm{c}_\varphi \mathrm{s}_\psi & -\mathrm{s}_\varphi \mathrm{c}_\theta \mathrm{s}_\psi + \mathrm{c}_\varphi \mathrm{c}_\psi & \mathrm{s}_\varphi \mathrm{s}_\theta \\ -\mathrm{s}_\theta \mathrm{c}_\psi & \mathrm{s}_\theta \mathrm{s}_\psi & \mathrm{c}_\theta \end{pmatrix} \end{aligned} \tag{B.8}$$

where $\mathrm{c}_\varphi = \cos(\varphi), \mathrm{c}_\theta = \cos(\theta), \mathrm{c}_\psi = \cos(\psi)$, etc. The solution for the inverse problem, that consists of determining the Euler angles from a given rotation matrix $R = (r_{ij})_{1 \leq i,j \leq 3} \in SO(3)$, is:

$$\left.\begin{aligned} \varphi &= \operatorname{atan2}(r_{23}, r_{13}) \\ \theta &= \operatorname{atan2}\left(\sqrt{r_{13}^2 + r_{23}^2}, r_{33}\right) \\ \psi &= \operatorname{atan2}(r_{32}, -r_{31}) \end{aligned}\right\} \qquad \text{for } \theta \in (0, \pi)$$

$$\left.\begin{aligned}\varphi &= \operatorname{atan2}(-r_{23}, -r_{13}) \\ \theta &= \operatorname{atan2}\left(-\sqrt{r_{13}^2 + r_{23}^2}, r_{33}\right) \\ \psi &= \operatorname{atan2}(-r_{32}, r_{31})\end{aligned}\right\} \qquad \text{for } \theta \in (-\pi, 0)$$

where $\operatorname{atan2}(y, x)$ computes $\arctan(y/x)$ but using the sign of both x and y to decide the quadrant in which the resulting angle lies. The above equations are not determined for the values of θ such that $\mathrm{s}_\theta = 0$. This situation is known as *gimbal lock*, a particular case of a *representation singularity*, i.e., those configurations where one of the three degrees of freedom that describes the orientation is lost. This means that the three parameters of this representation are not enough for a fully description of the orientation. Every minimal representation of the orientation has representation singularities. These singularities are not related to the motion capabilities of $\mathcal{R}$ because they can be avoided if a non-minimal representation of the orientation is adopted. Because of that, a useful and non-minimal representation of the orientation is needed. Unit quaternions are a good example of a such representation.

Unit quaternions

As stated in section A.3, any geometric algebra $\mathcal{G}_n$ can be expressed as the direct sum $\mathcal{G}_n^+ \oplus \mathcal{G}_n^-$. In particular, $\mathcal{G}_3 = \mathcal{G}_3^+ \oplus \mathcal{G}_3^-$ where:

$$\begin{aligned}\mathcal{G}_3^+ &= \operatorname{span}\{1, e_{12}, e_{13}, e_{23}\} \\ \mathcal{G}_3^- &= \operatorname{span}\{\boldsymbol{e}_1, \boldsymbol{e}_2, \boldsymbol{e}_3, I\}\end{aligned} \tag{B.9}$$

The subalgebra $\mathcal{G}_3^+$ is also called the *quaternion algebra* over $\mathbb{R}$ and is usually denoted by $\mathbb{H}$. Quaternions are an extension of complex numbers where the imaginary unit is replaced by three units (given by the three basis bivectors). Then, an arbitrary $\boldsymbol{q} \in \mathbb{H}$ can be expressed as

$$\boldsymbol{q} = \underbrace{\alpha}_{\text{Scalar part}} + \underbrace{e_x e_{12} + e_y e_{13} + e_z e_{23}}_{\text{Vector part}} \tag{B.10}$$

where $\alpha \in \mathbb{R}$ and $\boldsymbol{\varepsilon} = (e_x, e_y, e_z) \in \mathbb{R}^3$. Furthermore, since they can be expressed as the addition of a scalar and a bivector, they naturally define rotations in space. A quaternion $\boldsymbol{q}$ is said to be a *unit quaternion* if $\boldsymbol{q}\tilde{\boldsymbol{q}} = 1$. Given a rotation matrix $R = (r_{ij})_{1 \le i,j \le 3} \in SO(3)$, the quaternion that defines the same rotation is given by:

$$\begin{aligned}\alpha &= \frac{1}{2}\sqrt{r_{11} + r_{22} + r_{33} + 1} \\ e_x &= \frac{1}{2}\operatorname{sgn}(r_{32} - r_{23})\sqrt{r_{11} - r_{22} - r_{33} + 1} \\ e_y &= \frac{1}{2}\operatorname{sgn}(r_{13} - r_{31})\sqrt{r_{22} - r_{33} - r_{11} + 1} \\ e_z &= \frac{1}{2}\operatorname{sgn}(r_{21} - r_{12})\sqrt{r_{33} - r_{11} - r_{22} + 1}\end{aligned} \tag{B.11}$$

while, for the inverse problem, the rotation matrix associated with a given unit quaternion $\boldsymbol{q}$ is:

$$R = \begin{pmatrix} 2(\alpha^2 + e_x^2) - 1 & 2(e_x e_y - \alpha e_z) & 2(e_x e_z + \alpha e_y) \\ 2(e_x e_y + \alpha e_z) & 2(\alpha^2 + e_y^2) - 1 & 2(e_y e_z - \alpha e_x) \\ 2(e_x e_z - \alpha e_y) & 2(e_y e_z + \alpha e_x) & 2(\alpha^2 + e_z^2) - 1 \end{pmatrix} \tag{B.12}$$

More properties and applications of quaternions and, in particular, of unit quaternions can be found in (Favieri, 2008; Sariyildiz and Temeltas, 2009).

B.2 Kinematics of serial chains

Definition B.2.1. A *rigid serial robotic manipulator* $\mathcal{R}$ is an open kinematic chain made up of a sequence of rigid bodies, called links, connected by means of actuated kinematic pairs, called joints, that provide relative motion between consecutive links.

Only two types of joints are considered throughout this work: revolute joints, that only perform rotations and prismatic joints, that only perform translations. At the end of the last link, there is a tool or device, termed the *end-effector*. Similarly, the beginning of the chain is constrained to a fixed base. Hence, for a robot $\mathcal{R}$ with n links, there are n joints increasingly numbered from the base to the end-effector.

Since each link is a rigid body, an orthonormal frame can be attached to it. In particular, such frame is placed at the joint that moves the corresponding link. So, the frame $\{\boldsymbol{o}_i, \boldsymbol{x}_i, \boldsymbol{y}_i, \boldsymbol{z}_i\}$ is attached to joint i for describing the pose of link i (figure B.1a). Each joint frame is obtained from the previous one through the composition of rigid motions that can be expressed by homogeneous transformation matrices constructed using the *Denavit-Hartenberg convention* (Denavit and Hartenberg, 1965). The Denavit-Hartenberg convention consists of the use of four parameters, the *D-H parameters* (figure B.1b):

- a_i, the perpendicular distance between the joint axes $\boldsymbol{z}_{i-1}$ and $\boldsymbol{z}_i$.
- α_i, the angle between the joint axes $\boldsymbol{z}_{i-1}$ and $\boldsymbol{z}_i$.
- θ_i, the angle between $\boldsymbol{x}_{i-1}$ and $\boldsymbol{x}_i$.
- d_i, the distance between $\boldsymbol{o}'_{i-1}$ and $\boldsymbol{o}_i$, where $\boldsymbol{o}'_{i-1}$ is the projection of $\boldsymbol{o}_{i-1}$ over the joint axis $\boldsymbol{z}_i$.

Depending on the nature of the i-th joint, either the angle θ_i or the displacement d_i acts as a *joint variable*, while the other three parameters act as constants – length a_i, angle α_i and d_i or θ_i depending on which one describes the joint variable.

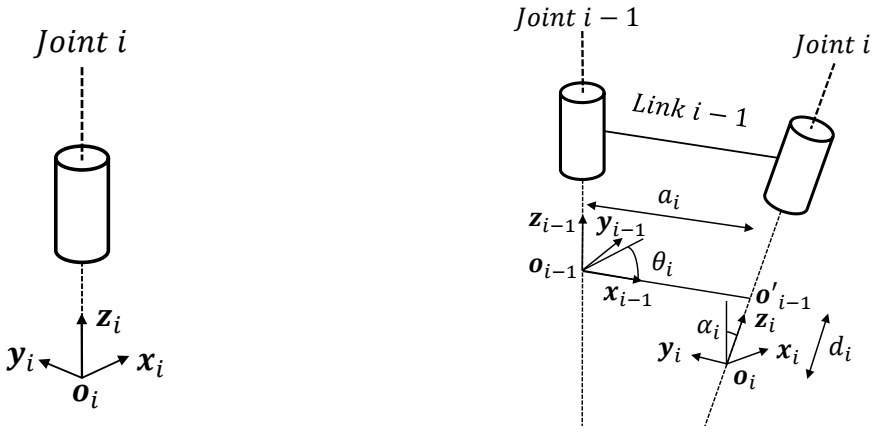

(a) Frame attached to joint i **(b)** Relation between consecutive joints

Figure B.1: The D-H convention

Therefore, each joint frame is related to the preceding one by a homogeneous transformation matrix A_i^{i-1} that describes the pose of joint i with respect to joint $i-1$ (the first joint frame is related to the world reference frame). Hence, the pose of every joint of $\mathcal{R}$ determines the end-effector pose and the homogeneous transformation matrix T_n^0 relating the end-effector frame with the reference frame will be:

$$T_n^0 = A_1^0 \cdot A_2^1 \cdots A_n^{n-1} \tag{B.13}$$

where:

$$A_i^{i-1} = \begin{pmatrix} \cos(\theta_i) & -\sin(\theta_i) & 0 & a_i \\ \sin(\theta_i)\cos(\alpha_i) & \cos(\theta_i)\cos(\alpha_i) & -\sin(\alpha_i) & -\sin(\alpha_i)d_i \\ \sin(\theta_i)\sin(\alpha_i) & \cos(\theta_i)\sin(\alpha_i) & \cos(\alpha_i) & \cos(\alpha_i)d_i \\ 0 & 0 & 0 & 1 \end{pmatrix} \tag{B.14}$$

In general, if the nature of joint i is not specified, its joint variable is denoted by q_i. The vector of all joint variables for a serial robot $\mathcal{R}$ is denoted by $\boldsymbol{q} = (q_1, \ldots, q_n)$ and is known as the *configuration*.

Definition B.2.2. The set of all possible configurations $\boldsymbol{q}$ for a serial robot $\mathcal{R}$ is a vector subspace of $\mathbb{R}^n$ known as the *configuration space* $\mathcal{C}$.

Definition B.2.3. A serial robot $\mathcal{R}$ is said to have n *degrees of freedom* (DOF) if its configuration can be minimally specified by n variables.

Proposition B.2.4. *For a serial robot $\mathcal{R}$, the number and nature of the joints determine the number of DOF. Thus, a serial robot $\mathcal{R}$ with n revolute or prismatic joints has n DOF. Furthermore, the number degrees of freedom determines the dimension of $\mathcal{C}$.*

For the task of positioning and orientating its end-effector in the space, the manipulators with more than 6 DOF are called *redundant* while the rest are *non-redundant*.

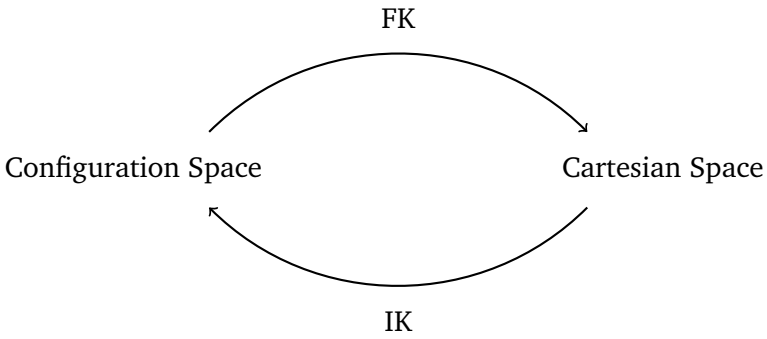

Figure B.2: Relation between configuration and Cartesian space

Definition B.2.5. A redundant robot $\mathcal{R}$ has $r = n - 6$ *degrees of redundancy*. Furthermore, if p denotes the number of prismatic joints of $\mathcal{R}$, then it has $m = r - p$ *rotational degrees of redundancy*, i.e., the degrees of redundancy associated with the revolute joints of $\mathcal{R}$.

Remark B.2.6. If $\mathcal{R}$ only has revolute joints, then $r = m$.

If a minimal representation of the orientation is chosen, the end-effector pose can be expressed as a six-dimensional vector $\boldsymbol{x} \in \mathbb{R}^6$, where the three first coordinates of $\boldsymbol{x}$ describe the end-effector position while the last three, its orientation.

Definition B.2.7. The set of all poses $\boldsymbol{x}$ of the end-effector with respect to a reference frame is a vector subspace of $\mathbb{R}^6$ known as the *operational space* $\mathcal{X}$.

With reference to the operational space $\mathcal{X}$, an index of robot performance is the so-called *workspace* $\mathcal{W}$, i.e., the total volume swept out by the origin of the end-effector frame as the robot $\mathcal{R}$ executes all possible motions.

Thus, identity (B.13) can be expressed as a function

$$\begin{aligned} f &: \mathcal{C} \to \mathcal{X} \\ f(\boldsymbol{q}) &= \boldsymbol{x} \end{aligned} \tag{B.15}$$

that relates $\mathcal{C}$ to $\mathcal{X}$. Such function is known as the *kinematic* or *forward kinematics function* of $\mathcal{R}$.

Hence, the *forward kinematic problem* consists of obtaining the pose of the end-effector given the value of the joint variables. On the other hand, the *inverse kinematic problem* consists of recovering the joint variables that provides a given end-effector pose. In other words, the forward kinematics relates the configuration space $\mathcal{C}$ to the operational space $\mathcal{X}$, while the inverse kinematics gives the reverse relation (figure B.2).

If f is differentiated with respect to time, the following relation is obtained:

$$\dot{\boldsymbol{x}} = J(\boldsymbol{q})\dot{\boldsymbol{q}} \tag{B.16}$$

where $\dot{\boldsymbol{x}}$ denotes the end-effector velocity vector; $\dot{\boldsymbol{q}}$, the vector of the joint velocities; and J, the *Jacobian matrix* of f. If

$$f(\boldsymbol{q}) = (f_1(\boldsymbol{q}), \ldots, f_6(\boldsymbol{q})) \tag{B.17}$$

then

$$J = \left(\frac{\partial f_i(\boldsymbol{q})}{\partial q_j} \right)_{\substack{1 \leq i \leq 6 \\ 1 \leq j \leq n}} \tag{B.18}$$

In robot kinematics, the Jacobian matrix (B.18) is also known as the *analytical* or *task Jacobian* and is usually denoted by $J_A(\boldsymbol{q})$.

However, the components of $\dot{\boldsymbol{x}}$ relative to the end-effector orientation express the rate of change of the parameters characterizing the minimal representation chosen, i.e., they are not the components of the end-effector angular velocity vector. If $\boldsymbol{v}$ denotes the end-effector linear velocity vector and $\boldsymbol{\omega}$, its angular velocity vector, the following relation is obtained:

$$\dot{\boldsymbol{x}} = T(\boldsymbol{x})\boldsymbol{v} \tag{B.19}$$

where $\boldsymbol{v}$ is:

$$\boldsymbol{v} = \begin{pmatrix} \boldsymbol{v} \\ \boldsymbol{\omega} \end{pmatrix}$$

and where $T(\boldsymbol{x})$ is a transformation matrix of the form:

$$T(\boldsymbol{x}) = \begin{pmatrix} I & 0 \\ 0 & R(\boldsymbol{x}) \end{pmatrix}$$

where $R(\boldsymbol{x})$ is a matrix that specifically depends on the minimal representation of the orientation adopted.

Now, the following relation can be established:

$$\boldsymbol{v} = J_G(\boldsymbol{q})\dot{\boldsymbol{q}} \tag{B.20}$$

where $J_G(\boldsymbol{q})$ denotes the *geometric Jacobian* matrix of $\mathcal{R}$. If $J_G = (J_1, \ldots, J_n)$, then:

$$J_i = \begin{cases} \begin{bmatrix} \boldsymbol{z}_i \times (\boldsymbol{o}_n - \boldsymbol{o}_i) \\ \boldsymbol{z}_i \end{bmatrix} & \text{if } i \text{ is revolute} \\ \begin{bmatrix} \boldsymbol{z}_i \\ 0 \end{bmatrix} & \text{if } i \text{ is prismatic} \end{cases} \tag{B.21}$$

In robotics, the geometric Jacobian J_G is the most used because, computationally speaking, it is easier to calculate and more efficient if implemented in different algorithms.

Proposition B.2.8. $J_A(\boldsymbol{q}) = T(\boldsymbol{x})J_G(\boldsymbol{q})$

Definition B.2.9. Let $\mathcal{R}$ be a serial robot of n DOF. Then, a configuration $\boldsymbol{q} \in \mathcal{C}$ is said to be a *singularity* of $\mathcal{R}$ if $\rho(J_A(\boldsymbol{q})) < \min\{n, 6\}$.

As stated in proposition B.2.8, if $J_A(\boldsymbol{q})$ is rank-deficient, then either $T(\boldsymbol{x})$ or $J_G(\boldsymbol{q})$ is rank-deficient. If $T(\boldsymbol{x})$ is rank-deficient, then $\boldsymbol{q}$ is a representation singularity. As mentioned in section B.1, these singularities are always associated with minimal representations of the orientation and do not correspond to mechanical limitations of $\mathcal{R}$. If, conversely, $J_G(\boldsymbol{q})$ is rank-deficient, then $\boldsymbol{q}$ is said to be a *kinematic singularity*. Kinematic singularities are related to the motion of the end-effector. Thus, the relation B.20 allows to deduce that a kinematic singularity is also a configuration where:

- $\mathcal{R}$ looses one or more degrees of freedom.
- $\mathcal{R}$ cannot translate or rotate its end-effector around one or more Cartesian directions.
- $\mathcal{R}$ requires unbounded joint velocities to generate finite end-effector linear and angular velocities.

As mentioned above, kinematic singularities can be identified using the geometric Jacobian $J_G(\boldsymbol{q})$. Indeed, $\boldsymbol{q} \in \mathcal{C}$ is a singularity if, and only if

$$\begin{aligned} \det(J_G(\boldsymbol{q})) &= 0 \quad \text{if } \mathcal{R} \text{ is non-redundant.} \\ \det(J_G^T(\boldsymbol{q})J_G(\boldsymbol{q})) &= 0 \quad \text{if } \mathcal{R} \text{ is redundant.} \end{aligned} \tag{B.22}$$

The geometric Jacobian $J_G(\boldsymbol{q})$ is represented with respect to the world frame (usually located in the base of $\mathcal{R}$). To represent $J_G(\boldsymbol{q})$ in a different frame $\mathcal{B}$, the following identity is used:

$$J_G(\boldsymbol{q})^{\mathcal{B}} = BJ_G(\boldsymbol{q}) \tag{B.23}$$

where

$$B = \begin{pmatrix} R_0^{\mathcal{B}} & 0 \\ 0 & R_0^{\mathcal{B}} \end{pmatrix}$$

with $R_0^{\mathcal{B}} = (R_{\mathcal{B}}^0)^T$ and where $R_{\mathcal{B}}^0$ denotes the rotation matrix that relates the orientation of $\mathcal{B}$ with respect to the orientation of the world frame.

Using the principle of virtual work, the following relation is obtained:

$$\boldsymbol{\tau} = J_G(\boldsymbol{q})\boldsymbol{f} \tag{B.24}$$

where $\boldsymbol{\tau}$ denotes the vector of joint torques and $\boldsymbol{f}$, the vector of Cartesian forces applied to the end-effector of $\mathcal{R}$. In particular,

$$\boldsymbol{f} = \begin{pmatrix} \boldsymbol{f} \\ \boldsymbol{m} \end{pmatrix}$$

where $\boldsymbol{f}$ is the vector of linear forces and $\boldsymbol{m}$, the vector of moments, both applied to the end-effector.

To conclude this section, an important class of serial robots is introduced. These manipulators are those that possesses *spherical wrist*. For these robots, the axes of their last three joints intersect at a common point, denoted as the *wrist center point*, or are parallel, i.e., the intersection is the point at the infinity. In this context, the origin of the end-effector frame is moved to the wrist center point (or the point at the infinity) by a fixed transformation – fixed in the sense that it does not depend on any joint variable. Therefore, the last three joints only contribute to the orientation of the end-effector, while the rest contribute to its position and orientation. For these robots, some kinematic problems can be simplified.

B.3 Kinematics of some redundant robots

In this section a kinematic description of the serial redundant robots used throughout this dissertation is introduced. In particular, the homogeneous transformation matrices constructed with the D-H parameters; the forward kinematics and the geometric Jacobian of the *Kuka LWR 4+*, the *Stäubli TX90 mounted on a translational motion unit* and the *ABB Yumi* are presented.

B.3.1 Kuka LWR 4+

The Kuka LWR 4+ is an anthropomorphic arm with seven degrees of freedom that possesses spherical wrist (figure B.3a and picture B.3b). Its D-H parameters are shown in table B.1. With these D-H parameters, the following transformation matrices are obtained:

$$A_1^0 = \begin{pmatrix} \cos(\theta_1) & -\sin(\theta_1) & 0 & 0 \\ \sin(\theta_1) & \cos(\theta_1) & 0 & 0 \\ 0 & 0 & 1 & 310 \\ 0 & 0 & 0 & 1 \end{pmatrix} \qquad A_2^1 = \begin{pmatrix} \sin(\theta_2) & \cos(\theta_2) & 0 & 0 \\ 0 & 0 & -1 & 0 \\ -\cos(\theta_2) & \sin(\theta_2) & 0 & 0 \\ 0 & 0 & 0 & 1 \end{pmatrix}$$

$$A_3^2 = \begin{pmatrix} \cos(\theta_3) & -\sin(\theta_3) & 0 & 0 \\ 0 & 0 & 1 & 400 \\ -\sin(\theta_3) & -\cos(\theta_3) & 0 & 0 \\ 0 & 0 & 0 & 1 \end{pmatrix} \qquad A_4^3 = \begin{pmatrix} -\cos(\theta_4) & \sin(\theta_4) & 0 & 0 \\ 0 & 0 & 1 & 0 \\ \sin(\theta_4) & \cos(\theta_4) & 0 & 0 \\ 0 & 0 & 0 & 1 \end{pmatrix}$$

$$A_5^4 = \begin{pmatrix} -\cos(\theta_5) & \sin(\theta_5) & 0 & 0 \\ 0 & 0 & 1 & 390 \\ \sin(\theta_5) & \cos(\theta_5) & 0 & 0 \\ 0 & 0 & 0 & 1 \end{pmatrix} \qquad A_6^5 = \begin{pmatrix} \cos(\theta_6) & -\sin(\theta_6) & 0 & 0 \\ 0 & 0 & -1 & 0 \\ \sin(\theta_6) & \cos(\theta_6) & 0 & 0 \\ 0 & 0 & 0 & 1 \end{pmatrix}$$

$$A_7^6 = \begin{pmatrix} \cos(\theta_7) & -\sin(\theta_7) & 0 & 0 \\ 0 & 0 & 1 & 78 \\ -\sin(\theta_7) & -\cos(\theta_7) & 0 & 0 \\ 0 & 0 & 0 & 1 \end{pmatrix}$$

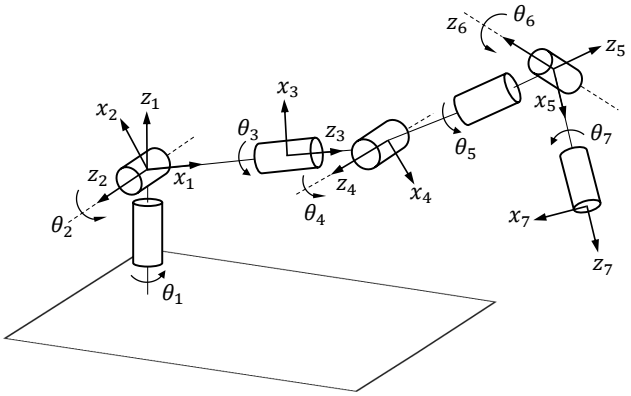

(a) Schematic representation of the Kuka LWR 4+

(b) Picture of the Kuka LWR 4+

Figure B.3: The Kuka LWR 4+

	α_i	a_i	d_i	θ_i	offset
1	0	0	310	θ_1	0
2	90	0	0	θ_2	-90
3	-90	0	400	θ_3	0
4	-90	0	0	θ_4	180
5	-90	0	390	θ_5	180
6	90	0	0	θ_6	0
7	-90	0	78	θ_7	0

Table B.1: D-H parameters of Kuka LWR 4+

With these matrices, the pose matrix T_7^0 can be constructed. Its elements are:

$$
\begin{aligned}
n_1 &= s_7(s_5(c_4(s_1s_3 - c_1c_3s_2) + c_1c_2s_4) - c_5(c_3s_1 + c_1s_2s_3)) - c_7(s_6(s_4(s_1s_3 - c_1c_3s_2) - \\
&\quad - c_1c_2c_4) + c_6(c_5(c_4(s_1s_3 - c_1c_3s_2) + c_1c_2s_4) + s_5(c_3s_1 + c_1s_2s_3))) \\
n_2 &= c_7(s_6(s_4(c_1s_3 + c_3s_1s_2) + c_2c_4s_1) + c_6(c_5(c_4(c_1s_3 + c_3s_1s_2) - c_2s_1s_4) + s_5(c_1c_3 - \\
&\quad - s_1s_2s_3))) - s_7(s_5(c_4(c_1s_3 + c_3s_1s_2) - c_2s_1s_4) - c_5(c_1c_3 - s_1s_2s_3)) \\
n_3 &= s_7(s_5(s_2s_4 + c_2c_3c_4) + c_2c_5s_3) - c_7(c_6(c_5(s_2s_4 + c_2c_3c_4) - c_2s_3s_5) - s_6(c_4s_2 - c_2c_3s_4)) \\
s_1 &= s_7(s_6(s_4(s_1s_3 - c_1c_3s_2) - c_1c_2c_4) + c_6(c_5(c_4(s_1s_3 - c_1c_3s_2) + c_1c_2s_4) + s_5(c_3s_1 + \\
&\quad + c_1s_2s_3))) + c_7(s_5(c_4(s_1s_3 - c_1c_3s_2) + c_1c_2s_4) - c_5(c_3s_1 + c_1s_2s_3)) \\
s_2 &= -s_7(s_6(s_4(c_1s_3 + c_3s_1s_2) + c_2c_4s_1) + c_6(c_5(c_4(c_1s_3 + c_3s_1s_2) - c_2s_1s_4) + s_5(c_1c_3 - \\
&\quad - s_1s_2s_3))) - c_7(s_5(c_4(c_1s_3 + c_3s_1s_2) - c_2s_1s_4) - c_5(c_1c_3 - s_1s_2s_3)) \\
s_3 &= c_7(s_5(s_2s_4 + c_2c_3c_4) + c_2c_5s_3) + s_7(c_6(c_5(s_2s_4 + c_2c_3c_4) - c_2s_3s_5) - s_6(c_4s_2 - c_2c_3s_4))
\end{aligned}
$$

$$
\begin{aligned}
a_1 &= s_6(c_5(c_4(s_1s_3 - c_1c_3s_2) + c_1c_2s_4) + s_5(c_3s_1 + c_1s_2s_3)) - c_6(s_4(s_1s_3 - c_1c_3s_2) - c_1c_2c_4)\\
a_2 &= c_6(s_4(c_1s_3 + c_3s_1s_2) + c_2c_4s_1) - s_6(c_5(c_4(c_1s_3 + c_3s_1s_2) - c_2s_1s_4) + s_5(c_1c_3 - s_1s_2s_3))\\
a_3 &= s_6(c_5(s_2s_4 + c_2c_3c_4) - c_2s_3s_5) + c_6(c_4s_2 - c_2c_3s_4)\\
p_1 &= 400c_1c_2 - 390s_4(s_1s_3 - c_1c_3s_2) + 390c_1c_2c_4\\
p_2 &= 400c_2s_1 + 390s_4(c_1s_3 + c_3s_1s_2) + 390c_2c_4s_1\\
p_3 &= 400s_2 + 390c_4s_2 - 390c_2c_3s_4 + 310
\end{aligned}
$$

Finally, the geometric Jacobian matrix of the Kuka LWR 4+, $J_G(\boldsymbol{q})$, is calculated using (B.21). Since the Kuka LWR 4+ has spherical wrist, the submatrix formed by the first three rows with the last three columns is a block of zeros. Therefore, the elements of $J_G(\boldsymbol{q})$ (with the exception of the block of zeros) are:

$$
\begin{aligned}
J_{11} &= -400c_2s_1 - 390s_4(c_1s_3 + c_3s_1s_2) - 390c_2c_4s_1\\
J_{12} &= -c_1(400s_2 + 390c_4s_2 - 390c_2c_3s_4)\\
J_{13} &= c_2s_1(390c_4s_2 - 390c_2c_3s_4) - s_2(390s_4(c_1s_3 + c_3s_1s_2) + 390c_2c_4s_1)\\
J_{14} &= (390c_4s_2 - 390c_2c_3s_4)(c_1c_3 - s_1s_2s_3) - c_2s_3(390s_4(c_1s_3 + c_3s_1s_2) + 390c_2c_4s_1)\\
J_{21} &= 400c_1c_2 - 390s_4(s_1s_3 - c_1c_3s_2) + 390c_1c_2c_4\\
J_{22} &= -s_1(400s_2 + 390c_4s_2 - 390c_2c_3s_4)\\
J_{23} &= -s_2(390s_4(s_1s_3 - c_1c_3s_2) - 390c_1c_2c_4) - c_1c_2(390c_4s_2 - 390c_2c_3s_4)\\
J_{24} &= (390c_4s_2 - 390c_2c_3s_4)(c_3s_1 + c_1s_2s_3) - c_2s_3(390s_4(s_1s_3 - c_1c_3s_2) - 390c_1c_2c_4)\\
J_{31} &= 0\\
J_{32} &= c_1(400c_1c_2 - 390s_4(s_1s_3 - c_1c_3s_2) + 390c_1c_2c_4) + s_1(400c_2s_1 + 390s_4(c_1s_3 + c_3s_1s_2) +\\
&\quad + 390c_2c_4s_1)\\
J_{33} &= c_1c_2(390s_4(c_1s_3 + c_3s_1s_2) + 390c_2c_4s_1) + c_2s_1(390s_4(s_1s_3 - c_1c_3s_2) - 390c_1c_2c_4)\\
J_{34} &= (c_1c_3 - s_1s_2s_3)(390s_4(s_1s_3 - c_1c_3s_2) - 390c_1c_2c_4) - (390s_4(c_1s_3 + c_3s_1s_2) +\\
&\quad + 390c_2c_4s_1)(c_3s_1 + c_1s_2s_3)\\
J_{41} &= 0\\
J_{42} &= s_1\\
J_{43} &= c_1c_2\\
J_{44} &= -c_3s_1 - c_1s_2s_3\\
J_{45} &= c_1c_2c_4 - s_4(s_1s_3 - c_1c_3s_2)\\
J_{46} &= c_5(c_3s_1 + c_1s_2s_3) - s_5(c_4(s_1s_3 - c_1c_3s_2) + c_1c_2s_4)\\
J_{47} &= s_6(c_5(c_4(s_1s_3 - c_1c_3s_2) + c_1c_2s_4) + s_5(c_3s_1 + c_1s_2s_3)) - c_6(s_4(s_1s_3 - c_1c_3s_2) - c_1c_2c_4)\\
J_{51} &= 0\\
J_{52} &= -c_1\\
J_{53} &= c_2s_1\\
J_{54} &= c_1c_3 - s_1s_2s_3\\
J_{55} &= s_4(c_1s_3 + c_3s_1s_2) + c_2c_4s_1
\end{aligned}
$$

$$J_{56} = s_5(c_4(c_1s_3 + c_3s_1s_2) - c_2s_1s_4) - c_5(c_1c_3 - s_1s_2s_3)$$
$$J_{57} = c_6(s_4(c_1s_3 + c_3s_1s_2) + c_2c_4s_1) - s_6(c_5(c_4(c_1s_3 + c_3s_1s_2) - c_2s_1s_4) + s_5(c_1c_3 - s_1s_2s_3))$$
$$J_{61} = 1$$
$$J_{62} = 0$$
$$J_{63} = s_2$$
$$J_{64} = c_2s_3$$
$$J_{65} = c_4s_2 - c_2c_3s_4$$
$$J_{66} = -s_5(s_2s_4 + c_2c_3c_4) - c_2c_5s_3$$
$$J_{67} = s_6(c_5(s_2s_4 + c_2c_3c_4) - c_2s_3s_5) + c_6(c_4s_2 - c_2c_3s_4)$$

B.3.2 Stäubli TX90 mounted on a translational motion unit

The Stäubli TX90 is an industrial manipulator with six degrees of freedom and spherical wrist. This robot has been mounted on a linear track, that can be seen as an additional prismatic joint (figure B.4a, picture B.4b and table B.2). With the D-H parameters, the following transformation matrices are obtained:

$$A_1^0 = \begin{pmatrix} 1 & 0 & 0 & 0 \\ 0 & 0 & 1 & d_1 \\ 0 & -1 & 0 & 0 \\ 0 & 0 & 0 & 1 \end{pmatrix} \qquad A_2^1 = \begin{pmatrix} \cos(\theta_2) & -\sin(\theta_2) & 0 & 0 \\ 0 & 0 & -1 & -478 \\ \sin(\theta_2) & \cos(\theta_2) & 0 & 0 \\ 0 & 0 & 0 & 1 \end{pmatrix}$$

$$A_3^2 = \begin{pmatrix} \sin(\theta_3) & \cos(\theta_3) & 0 & 50 \\ 0 & 0 & 1 & 50 \\ \cos(\theta_3) & -\sin(\theta_3) & 0 & 0 \\ 0 & 0 & 0 & 1 \end{pmatrix} \qquad A_4^3 = \begin{pmatrix} -\sin(\theta_4) & -\cos(\theta_4) & 0 & 425 \\ \cos(\theta_4) & -\sin(\theta_4) & 0 & 0 \\ 0 & 0 & 1 & 0 \\ 0 & 0 & 0 & 1 \end{pmatrix}$$

$$A_5^4 = \begin{pmatrix} \cos(\theta_5) & -\sin(\theta_5) & 0 & 0 \\ 0 & 0 & -1 & -425 \\ \sin(\theta_5) & \cos(\theta_5) & 0 & 0 \\ 0 & 0 & 0 & 1 \end{pmatrix} \qquad A_6^5 = \begin{pmatrix} \cos(\theta_6) & -\sin(\theta_6) & 0 & 0 \\ 0 & 0 & 1 & 0 \\ -\sin(\theta_6) & -\cos(\theta_6) & 0 & 0 \\ 0 & 0 & 0 & 1 \end{pmatrix}$$

$$A_7^6 = \begin{pmatrix} \cos(\theta_7) & -\sin(\theta_7) & 0 & 0 \\ 0 & 0 & -1 & 0 \\ \sin(\theta_7) & \cos(\theta_7) & 0 & 0 \\ 0 & 0 & 0 & 1 \end{pmatrix}$$

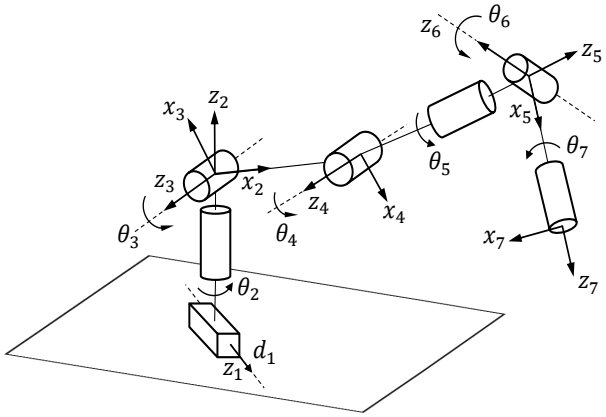

(a) Schematic representation of the Stäubli TX90 mounted on a translational motion unit

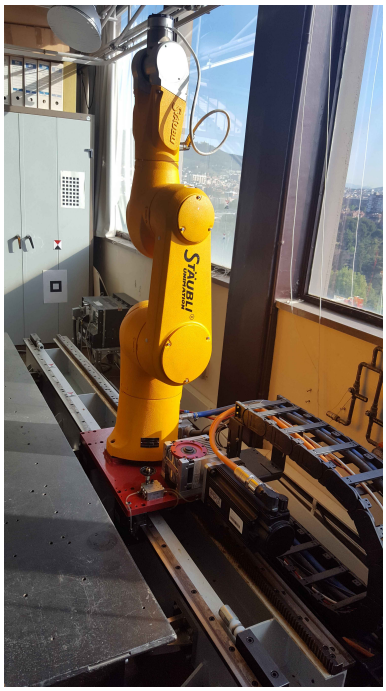

(b) Picture of the Stäubli TX90 mounted on a translational motion unit

Figure B.4: The Stäubli TX90 mounted on a translational motion unit

	α_i	a_i	d_i	θ_i	offset
1	-90	0	d_1	0	0
2	90	0	478	θ_2	0
3	-90	50	50	θ_3	-90
4	0	425	0	θ_4	90
5	90	0	425	θ_5	0
6	-90	0	0	θ_6	0
7	90	0	0	θ_7	0

Table B.2: D-H parameters of the Stäubli TX90 mounted on a translational motion unit

Again, the pose matrix T_7^0 is depicted:

$$
\begin{aligned}
n_1 &= -s_7(c_5s_2 + s_5(c_2c_3c_4 - c_2s_3s_4)) - c_7(c_6(s_2s_5 - c_5(c_2c_3c_4 - c_2s_3s_4)) + s_6(c_2c_3s_4 + c_2c_4s_3))\\
n_2 &= s_7(c_2c_5 + s_5(s_2s_3s_4 - c_3c_4s_2)) + c_7(c_6(c_2s_5 - c_5(s_2s_3s_4 - c_3c_4s_2)) - s_6(c_3s_2s_4 + c_4s_2s_3))\\
n_3 &= s_5s_7(c_3s_4 + c_4s_3) - c_7(s_6(c_3c_4 - s_3s_4) + c_5c_6(c_3s_4 + c_4s_3))\\
s_1 &= s_7(c_6(s_2s_5 - c_5(c_2c_3c_4 - c_2s_3s_4)) + s_6(c_2c_3s_4 + c_2c_4s_3)) - c_7(c_5s_2 + s_5(c_2c_3c_4 - c_2s_3s_4))\\
s_2 &= c_7(c_2c_5 + s_5(s_2s_3s_4 - c_3c_4s_2)) - s_7(c_6(c_2s_5 - c_5(s_2s_3s_4 - c_3c_4s_2)) - s_6(c_3s_2s_4 + c_4s_2s_3))\\
s_3 &= s_7(s_6(c_3c_4 - s_3s_4) + c_5c_6(c_3s_4 + c_4s_3)) + c_7s_5(c_3s_4 + c_4s_3)
\end{aligned}
$$

$$
\begin{aligned}
a_1 &= \mathrm{c}_6(\mathrm{c}_2\mathrm{c}_3\mathrm{s}_4 + \mathrm{c}_2\mathrm{c}_4\mathrm{s}_3) - \mathrm{s}_6(\mathrm{s}_2\mathrm{s}_5 - \mathrm{c}_5(\mathrm{c}_2\mathrm{c}_3\mathrm{c}_4 - \mathrm{c}_2\mathrm{s}_3\mathrm{s}_4)) \\
a_2 &= \mathrm{s}_6(\mathrm{c}_2\mathrm{s}_5 - \mathrm{c}_5(\mathrm{s}_2\mathrm{s}_3\mathrm{s}_4 - \mathrm{c}_3\mathrm{c}_4\mathrm{s}_2)) + \mathrm{c}_6(\mathrm{c}_3\mathrm{s}_2\mathrm{s}_4 + \mathrm{c}_4\mathrm{s}_2\mathrm{s}_3) \\
a_3 &= \mathrm{c}_6(\mathrm{c}_3\mathrm{c}_4 - \mathrm{s}_3\mathrm{s}_4) - \mathrm{c}_5\mathrm{s}_6(\mathrm{c}_3\mathrm{s}_4 + \mathrm{c}_4\mathrm{s}_3) \\
p_1 &= 50\mathrm{c}_2 - 50\mathrm{s}_2 + 425\mathrm{c}_2\mathrm{s}_3 + 425\mathrm{c}_2\mathrm{c}_3\mathrm{s}_4 + 425\mathrm{c}_2\mathrm{c}_4\mathrm{s}_3 \\
p_2 &= d_1 + 50\mathrm{c}_2 + 50\mathrm{s}_2 + 425\mathrm{s}_2\mathrm{s}_3 + 425\mathrm{c}_3\mathrm{s}_2\mathrm{s}_4 + 425\mathrm{c}_4\mathrm{s}_2\mathrm{s}_3 \\
p_3 &= 425\mathrm{c}_3 + 425\mathrm{c}_3\mathrm{c}_4 - 425\mathrm{s}_3\mathrm{s}_4 + 478
\end{aligned}
$$

Finally, the geometric Jacobian matrix $J_G(\boldsymbol{q})$ is calculated using (B.21). As the Kuka LWR 4+, the Stäubli TX90 has spherical wrist, so there is a block of zeros in $J_G(\boldsymbol{q})$. Therefore, the elements of $J_G(\boldsymbol{q})$ (with the exception of that block of zeros) are the following:

$$
\begin{aligned}
J_{11} &= 425\mathrm{c}_3 + 425\mathrm{c}_3\mathrm{c}_4 - 425\mathrm{s}_3\mathrm{s}_4 + 478 \\
J_{12} &= -50\mathrm{c}_2 - 50\mathrm{s}_2 - 425\mathrm{s}_2\mathrm{s}_3 - 425\mathrm{c}_3\mathrm{s}_2\mathrm{s}_4 - 425\mathrm{c}_4\mathrm{s}_2\mathrm{s}_3 \\
J_{13} &= \mathrm{c}_2(425\mathrm{c}_3 + 425\mathrm{c}_3\mathrm{c}_4 - 425\mathrm{s}_3\mathrm{s}_4) \\
J_{14} &= \mathrm{c}_2(425\mathrm{c}_3\mathrm{c}_4 - 425\mathrm{s}_3\mathrm{s}_4) \\
J_{21} &= 0 \\
J_{22} &= 50\mathrm{c}_2 - 50\mathrm{s}_2 + 425\mathrm{c}_2\mathrm{s}_3 + 425\mathrm{c}_2\mathrm{c}_3\mathrm{s}_4 + 425\mathrm{c}_2\mathrm{c}_4\mathrm{s}_3 \\
J_{23} &= \mathrm{s}_2(425\mathrm{c}_3 + 425\mathrm{c}_3\mathrm{c}_4 - 425\mathrm{s}_3\mathrm{s}_4) \\
J_{24} &= \mathrm{s}_2(425\mathrm{c}_3\mathrm{c}_4 - 425\mathrm{s}_3\mathrm{s}_4) \\
J_{31} &= 50\mathrm{s}_2 - 50\mathrm{c}_2 - 425\mathrm{c}_2\mathrm{s}_3 - 425\mathrm{c}_2\mathrm{c}_3\mathrm{s}_4 - 425\mathrm{c}_2\mathrm{c}_4\mathrm{s}_3 \\
J_{32} &= 0 \\
J_{33} &= -\mathrm{c}_2(425\mathrm{c}_2\mathrm{s}_3 + 425\mathrm{c}_2\mathrm{c}_3\mathrm{s}_4 + 425\mathrm{c}_2\mathrm{c}_4\mathrm{s}_3) - \mathrm{s}_2(425\mathrm{s}_2\mathrm{s}_3 + 425\mathrm{c}_3\mathrm{s}_2\mathrm{s}_4 + 425\mathrm{c}_4\mathrm{s}_2\mathrm{s}_3) \\
J_{34} &= -\mathrm{c}_2(425\mathrm{c}_2\mathrm{c}_3\mathrm{s}_4 + 425\mathrm{c}_2\mathrm{c}_4\mathrm{s}_3) - \mathrm{s}_2(425\mathrm{c}_3\mathrm{s}_2\mathrm{s}_4 + 425\mathrm{c}_4\mathrm{s}_2\mathrm{s}_3) \\
J_{41} &= 0 \\
J_{42} &= 0 \\
J_{43} &= -\mathrm{s}_2 \\
J_{44} &= -\mathrm{s}_2 \\
J_{45} &= \mathrm{c}_2\mathrm{c}_3\mathrm{s}_4 + \mathrm{c}_2\mathrm{c}_4\mathrm{s}_3 \\
J_{46} &= -\mathrm{c}_5\mathrm{s}_2 - \mathrm{s}_5(\mathrm{c}_2\mathrm{c}_3\mathrm{c}_4 - \mathrm{c}_2\mathrm{s}_3\mathrm{s}_4) \\
J_{47} &= \mathrm{c}_6(\mathrm{c}_2\mathrm{c}_3\mathrm{s}_4 + \mathrm{c}_2\mathrm{c}_4\mathrm{s}_3) - \mathrm{s}_6(\mathrm{s}_2\mathrm{s}_5 - \mathrm{c}_5(\mathrm{c}_2\mathrm{c}_3\mathrm{c}_4 - \mathrm{c}_2\mathrm{s}_3\mathrm{s}_4)) \\
J_{51} &= 1 \\
J_{52} &= 0 \\
J_{53} &= \mathrm{c}_2 \\
J_{54} &= \mathrm{c}_2 \\
J_{55} &= \mathrm{c}_3\mathrm{s}_2\mathrm{s}_4 + \mathrm{c}_4\mathrm{s}_2\mathrm{s}_3 \\
J_{56} &= \mathrm{c}_2\mathrm{c}_5 + \mathrm{s}_5(\mathrm{s}_2\mathrm{s}_3\mathrm{s}_4 - \mathrm{c}_3\mathrm{c}_4\mathrm{s}_2) \\
J_{57} &= \mathrm{s}_6(\mathrm{c}_2\mathrm{s}_5 - \mathrm{c}_5(\mathrm{s}_2\mathrm{s}_3\mathrm{s}_4 - \mathrm{c}_3\mathrm{c}_4\mathrm{s}_2)) + \mathrm{c}_6(\mathrm{c}_3\mathrm{s}_2\mathrm{s}_4 + \mathrm{c}_4\mathrm{s}_2\mathrm{s}_3)
\end{aligned}
$$

$$
\begin{aligned}
J_{61} &= 0 \\
J_{62} &= 1 \\
J_{63} &= 0 \\
J_{64} &= 0 \\
J_{65} &= c_3c_4 - s_3s_4 \\
J_{66} &= s_5(c_3s_4 + c_4s_3) \\
J_{67} &= c_6(c_3c_4 - s_3s_4) - c_5s_6(c_3s_4 + c_4s_3)
\end{aligned}
$$

B.3.3 ABB Yumi

The ABB Yumi is a manipulator that possesses two anthropomorphic arms connected to a fixed torso (figure B.5, picture B.6 and table B.3). Each arm has seven degrees of freedom but, unlike the Kuka LWR 4+, they have not spherical wrist. Moreover, there are not three consecutive joints whose axes intersect at a single point.

Again, the transformation matrices based on the D-H parameters are listed:

$$
A_1^0 = \begin{pmatrix} \cos(\theta_1) & -\sin(\theta_1) & 0 & 0 \\ \sin(\theta_1) & \cos(\theta_1) & 0 & 0 \\ 0 & 0 & 1 & 166 \\ 0 & 0 & 0 & 1 \end{pmatrix} \qquad A_2^1 = \begin{pmatrix} \cos(\theta_2) & -\sin(\theta_2) & 0 & 30 \\ 0 & 0 & -1 & 0 \\ \sin(\theta_2) & \cos(\theta_2) & 0 & 0 \\ 0 & 0 & 0 & 1 \end{pmatrix}
$$

$$
A_3^2 = \begin{pmatrix} \cos(\theta_3) & -\sin(\theta_3) & 0 & -30 \\ 0 & 0 & 1 & 251.5 \\ -\sin(\theta_3) & -\cos(\theta_3) & 0 & 0 \\ 0 & 0 & 0 & 1 \end{pmatrix} \qquad A_4^3 = \begin{pmatrix} \cos(\theta_4) & -\sin(\theta_4) & 0 & 40.5 \\ 0 & 0 & -1 & 0 \\ \sin(\theta_4) & \cos(\theta_4) & 0 & 0 \\ 0 & 0 & 0 & 1 \end{pmatrix}
$$

$$
A_5^4 = \begin{pmatrix} \cos(\theta_5) & -\sin(\theta_5) & 0 & -40.5 \\ 0 & 0 & 1 & 265 \\ -\sin(\theta_5) & -\cos(\theta_5) & 0 & 0 \\ 0 & 0 & 0 & 1 \end{pmatrix} \qquad A_6^5 = \begin{pmatrix} \cos(\theta_6) & -\sin(\theta_6) & 0 & 27 \\ 0 & 0 & -1 & 0 \\ \sin(\theta_6) & \cos(\theta_6) & 0 & 0 \\ 0 & 0 & 0 & 1 \end{pmatrix}
$$

$$
A_7^6 = \begin{pmatrix} \cos(\theta_7) & -\sin(\theta_7) & 0 & -27 \\ 0 & 0 & 1 & 36 \\ -\sin(\theta_7) & -\cos(\theta_7) & 0 & 0 \\ 0 & 0 & 0 & 1 \end{pmatrix}.
$$

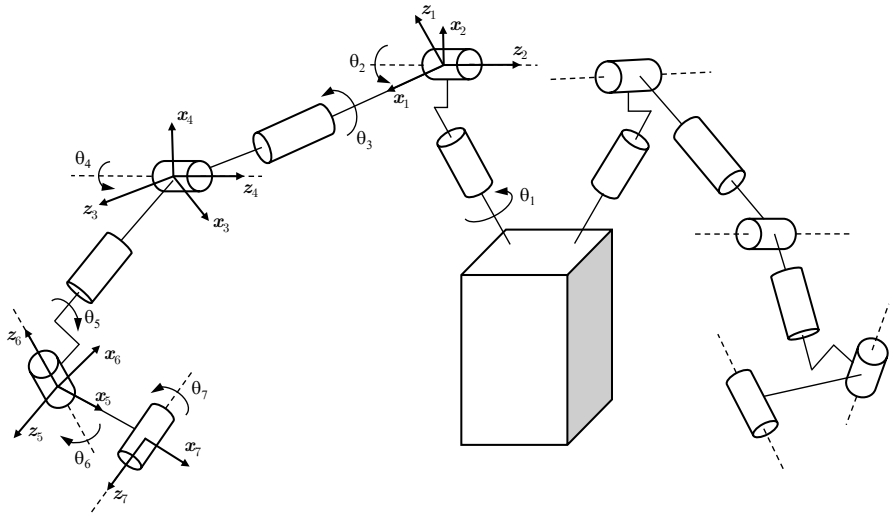

Figure B.5: Schematic representation of the ABB Yumi

Now, the elements of the forwards kinematics matrix T_7^0 are depicted:

$$
\begin{aligned}
n_1 &= \mathrm{c}_7(\mathrm{s}_6(\mathrm{s}_4(\mathrm{s}_1\mathrm{s}_3 - \mathrm{c}_1\mathrm{c}_2\mathrm{c}_3) - \mathrm{c}_1\mathrm{c}_4\mathrm{s}_2) - \mathrm{c}_6(\mathrm{c}_5(\mathrm{c}_4(\mathrm{s}_1\mathrm{s}_3 - \mathrm{c}_1\mathrm{c}_2\mathrm{c}_3) + \mathrm{c}_1\mathrm{s}_2\mathrm{s}_4) + \\
&+ \mathrm{s}_5(\mathrm{c}_3\mathrm{s}_1 + \mathrm{c}_1\mathrm{c}_2\mathrm{s}_3))) + \mathrm{s}_7(\mathrm{s}_5(\mathrm{c}_4(\mathrm{s}_1\mathrm{s}_3 - \mathrm{c}_1\mathrm{c}_2\mathrm{c}_3) + \mathrm{c}_1\mathrm{s}_2\mathrm{s}_4) - \mathrm{c}_5(\mathrm{c}_3\mathrm{s}_1 + \mathrm{c}_1\mathrm{c}_2\mathrm{s}_3)) \\
n_2 &= -\mathrm{c}_7(\mathrm{s}_6(\mathrm{s}_4(\mathrm{c}_1\mathrm{s}_3 + \mathrm{c}_2\mathrm{c}_3\mathrm{s}_1) + \mathrm{c}_4\mathrm{s}_1\mathrm{s}_2) - \mathrm{c}_6(\mathrm{c}_5(\mathrm{c}_4(\mathrm{c}_1\mathrm{s}_3 + \mathrm{c}_2\mathrm{c}_3\mathrm{s}_1) - \mathrm{s}_1\mathrm{s}_2\mathrm{s}_4) + \\
&+ \mathrm{s}_5(\mathrm{c}_1\mathrm{c}_3 - \mathrm{c}_2\mathrm{s}_1\mathrm{s}_3))) - \mathrm{s}_7(\mathrm{s}_5(\mathrm{c}_4(\mathrm{c}_1\mathrm{s}_3 + \mathrm{c}_2\mathrm{c}_3\mathrm{s}_1) - \mathrm{s}_1\mathrm{s}_2\mathrm{s}_4) - \mathrm{c}_5(\mathrm{c}_1\mathrm{c}_3 - \mathrm{c}_2\mathrm{s}_1\mathrm{s}_3)) \\
n_3 &= \mathrm{c}_7(\mathrm{c}_6(\mathrm{c}_5(\mathrm{c}_2\mathrm{s}_4 + \mathrm{c}_3\mathrm{c}_4\mathrm{s}_2) - \mathrm{s}_2\mathrm{s}_3\mathrm{s}_5) + \mathrm{s}_6(\mathrm{c}_2\mathrm{c}_4 - \mathrm{c}_3\mathrm{s}_2\mathrm{s}_4)) - \mathrm{s}_7(\mathrm{s}_5(\mathrm{c}_2\mathrm{s}_4 + \mathrm{c}_3\mathrm{c}_4\mathrm{s}_2) + \mathrm{c}_5\mathrm{s}_2\mathrm{s}_3) \\
s_1 &= \mathrm{c}_7(\mathrm{s}_5(\mathrm{c}_4(\mathrm{s}_1\mathrm{s}_3 - \mathrm{c}_1\mathrm{c}_2\mathrm{c}_3) + \mathrm{c}_1\mathrm{s}_2\mathrm{s}_4) - \mathrm{c}_5(\mathrm{c}_3\mathrm{s}_1 + \mathrm{c}_1\mathrm{c}_2\mathrm{s}_3)) - \mathrm{s}_7(\mathrm{s}_6(\mathrm{s}_4(\mathrm{s}_1\mathrm{s}_3 - \mathrm{c}_1\mathrm{c}_2\mathrm{c}_3) - \\
&- \mathrm{c}_1\mathrm{c}_4\mathrm{s}_2) - \mathrm{c}_6(\mathrm{c}_5(\mathrm{c}_4(\mathrm{s}_1\mathrm{s}_3 - \mathrm{c}_1\mathrm{c}_2\mathrm{c}_3) + \mathrm{c}_1\mathrm{s}_2\mathrm{s}_4) + \mathrm{s}_5(\mathrm{c}_3\mathrm{s}_1 + \mathrm{c}_1\mathrm{c}_2\mathrm{s}_3))) \\
s_2 &= \mathrm{s}_7(\mathrm{s}_6(\mathrm{s}_4(\mathrm{c}_1\mathrm{s}_3 + \mathrm{c}_2\mathrm{c}_3\mathrm{s}_1) + \mathrm{c}_4\mathrm{s}_1\mathrm{s}_2) - \mathrm{c}_6(\mathrm{c}_5(\mathrm{c}_4(\mathrm{c}_1\mathrm{s}_3 + \mathrm{c}_2\mathrm{c}_3\mathrm{s}_1) - \mathrm{s}_1\mathrm{s}_2\mathrm{s}_4) + \mathrm{s}_5(\mathrm{c}_1\mathrm{c}_3 - \\
&- \mathrm{c}_2\mathrm{s}_1\mathrm{s}_3))) - \mathrm{c}_7(\mathrm{s}_5(\mathrm{c}_4(\mathrm{c}_1\mathrm{s}_3 + \mathrm{c}_2\mathrm{c}_3\mathrm{s}_1) - \mathrm{s}_1\mathrm{s}_2\mathrm{s}_4) - \mathrm{c}_5(\mathrm{c}_1\mathrm{c}_3 - \mathrm{c}_2\mathrm{s}_1\mathrm{s}_3)) \\
s_3 &= -\mathrm{c}_7(\mathrm{s}_5(\mathrm{c}_2\mathrm{s}_4 + \mathrm{c}_3\mathrm{c}_4\mathrm{s}_2) + \mathrm{c}_5\mathrm{s}_2\mathrm{s}_3) - \mathrm{s}_7(\mathrm{c}_6(\mathrm{c}_5(\mathrm{c}_2\mathrm{s}_4 + \mathrm{c}_3\mathrm{c}_4\mathrm{s}_2) - \mathrm{s}_2\mathrm{s}_3\mathrm{s}_5) + \mathrm{s}_6(\mathrm{c}_2\mathrm{c}_4 - \mathrm{c}_3\mathrm{s}_2\mathrm{s}_4)) \\
a_1 &= \mathrm{c}_6(\mathrm{s}_4(\mathrm{s}_1\mathrm{s}_3 - \mathrm{c}_1\mathrm{c}_2\mathrm{c}_3) - \mathrm{c}_1\mathrm{c}_4\mathrm{s}_2) + \mathrm{s}_6(\mathrm{c}_5(\mathrm{c}_4(\mathrm{s}_1\mathrm{s}_3 - \mathrm{c}_1\mathrm{c}_2\mathrm{c}_3) + \mathrm{c}_1\mathrm{s}_2\mathrm{s}_4) + \mathrm{s}_5(\mathrm{c}_3\mathrm{s}_1 + \mathrm{c}_1\mathrm{c}_2\mathrm{s}_3)) \\
a_2 &= -\mathrm{c}_6(\mathrm{s}_4(\mathrm{c}_1\mathrm{s}_3 + \mathrm{c}_2\mathrm{c}_3\mathrm{s}_1) + \mathrm{c}_4\mathrm{s}_1\mathrm{s}_2) - \mathrm{s}_6(\mathrm{c}_5(\mathrm{c}_4(\mathrm{c}_1\mathrm{s}_3 + \mathrm{c}_2\mathrm{c}_3\mathrm{s}_1) - \mathrm{s}_1\mathrm{s}_2\mathrm{s}_4) + \mathrm{s}_5(\mathrm{c}_1\mathrm{c}_3 - \mathrm{c}_2\mathrm{s}_1\mathrm{s}_3)) \\
a_3 &= \mathrm{c}_6(\mathrm{c}_2\mathrm{c}_4 - \mathrm{c}_3\mathrm{s}_2\mathrm{s}_4) - \mathrm{s}_6(\mathrm{c}_5(\mathrm{c}_2\mathrm{s}_4 + \mathrm{c}_3\mathrm{c}_4\mathrm{s}_2) - \mathrm{s}_2\mathrm{s}_3\mathrm{s}_5) \\
p_1 &= 30\mathrm{c}_1 - 30\mathrm{c}_1\mathrm{c}_2 - (503\mathrm{c}_1\mathrm{s}_2)/2 - (81\mathrm{s}_1\mathrm{s}_3)/2 - 27\mathrm{c}_5(\mathrm{c}_4(\mathrm{s}_1\mathrm{s}_3 - \mathrm{c}_1\mathrm{c}_2\mathrm{c}_3) + \mathrm{c}_1\mathrm{s}_2\mathrm{s}_4) + \\
&+ 36\mathrm{c}_6(\mathrm{s}_4(\mathrm{s}_1\mathrm{s}_3 - \mathrm{c}_1\mathrm{c}_2\mathrm{c}_3) - \mathrm{c}_1\mathrm{c}_4\mathrm{s}_2) - 27\mathrm{s}_6(\mathrm{s}_4(\mathrm{s}_1\mathrm{s}_3 - \mathrm{c}_1\mathrm{c}_2\mathrm{c}_3) - \mathrm{c}_1\mathrm{c}_4\mathrm{s}_2) + \\
&+ 27\mathrm{c}_6(\mathrm{c}_5(\mathrm{c}_4(\mathrm{s}_1\mathrm{s}_3 - \mathrm{c}_1\mathrm{c}_2\mathrm{c}_3) + \mathrm{c}_1\mathrm{s}_2\mathrm{s}_4) + \mathrm{s}_5(\mathrm{c}_3\mathrm{s}_1 + \mathrm{c}_1\mathrm{c}_2\mathrm{s}_3)) + 36\mathrm{s}_6(\mathrm{c}_5(\mathrm{c}_4(\mathrm{s}_1\mathrm{s}_3 - \mathrm{c}_1\mathrm{c}_2\mathrm{c}_3) + \\
&+ \mathrm{c}_1\mathrm{s}_2\mathrm{s}_4) + \mathrm{s}_5(\mathrm{c}_3\mathrm{s}_1 + \mathrm{c}_1\mathrm{c}_2\mathrm{s}_3)) + (81\mathrm{c}_4(\mathrm{s}_1\mathrm{s}_3 - \mathrm{c}_1\mathrm{c}_2\mathrm{c}_3))/2 + 265\mathrm{s}_4(\mathrm{s}_1\mathrm{s}_3 - \mathrm{c}_1\mathrm{c}_2\mathrm{c}_3) - \\
&- 27\mathrm{s}_5(\mathrm{c}_3\mathrm{s}_1 + \mathrm{c}_1\mathrm{c}_2\mathrm{s}_3) + (81\mathrm{c}_1\mathrm{c}_2\mathrm{c}_3)/2 - 265\mathrm{c}_1\mathrm{c}_4\mathrm{s}_2 + (81\mathrm{c}_1\mathrm{s}_2\mathrm{s}_4)/2
\end{aligned}
$$

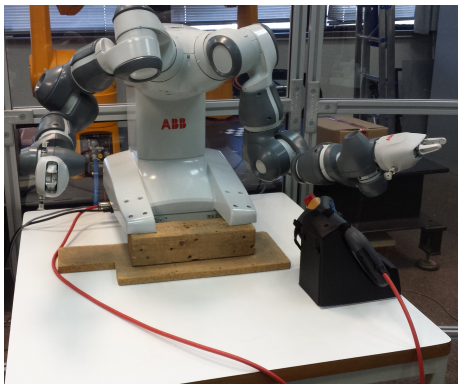

Figure B.6: Picture of the ABB Yumi

	α_i	a_i	d_i	θ_i
1	0.0	0.0	166.0	θ_1
2	90.0	30.0	0.0	θ_2
3	-90.0	-30.0	251.5	θ_3
4	90.0	40.5	0.0	θ_4
5	-90.0	-40.5	265.0	θ_5
6	90.0	27.0	0.0	θ_6
7	-90.0	-27.0	36.0	θ_7

Table B.3: D-H parameters of the ABB Yumi

$$
\begin{aligned}
p_2 = {} & 30s_1 - 30c_2s_1 + (81c_1s_3)/2 - (503s_1s_2)/2 + 27c_5(c_4(c_1s_3 + c_2c_3s_1) - s_1s_2s_4) - \\
& - 36c_6(s_4(c_1s_3 + c_2c_3s_1) + c_4s_1s_2) + 27s_6(s_4(c_1s_3 + c_2c_3s_1) + c_4s_1s_2) - 27c_6(c_5(c_4(c_1s_3 + \\
& + c_2c_3s_1) - s_1s_2s_4) + s_5(c_1c_3 - c_2s_1s_3)) - 36s_6(c_5(c_4(c_1s_3 + c_2c_3s_1) - s_1s_2s_4) + \\
& + s_5(c_1c_3 - c_2s_1s_3)) - (81c_4(c_1s_3 + c_2c_3s_1))/2 - 265s_4(c_1s_3 + c_2c_3s_1) + 27s_5(c_1c_3 - c_2s_1s_3) + \\
& + (81s_1s_2s_4)/2 + (81c_2c_3s_1)/2 - 265c_4s_1s_2 \\
p_3 = {} & (503c_2)/2 - 30s_2 + 265c_2c_4 + (81c_3s_2)/2 - (81c_2s_4)/2 - 27c_6(c_5(c_2s_4 + c_3c_4s_2) - s_2s_3s_5) - \\
& - 36s_6(c_5(c_2s_4 + c_3c_4s_2) - s_2s_3s_5) + 27c_5(c_2s_4 + c_3c_4s_2) + 36c_6(c_2c_4 - c_3s_2s_4) - 27s_6(c_2c_4 - \\
& - c_3s_2s_4) - 27s_2s_3s_5 - (81c_3c_4s_2)/2 - 265c_3s_2s_4 + 166
\end{aligned}
$$

Finally, the elements of the geometric Jacobian matrix $J_G(\boldsymbol{q})$ are given. In this case, since the ABB Yumi has not a spherical wrist, there is not a block of zeros in $J_G(\boldsymbol{q})$:

$$
\begin{aligned}
J_{11} &= 0 \\
J_{12} &= s_1 \\
J_{13} &= -c_1s_2 \\
J_{14} &= c_3s_1 + c_1c_2s_3 \\
J_{15} &= s_4(s_1s_3 - c_1c_2c_3) - c_1c_4s_2 \\
J_{16} &= c_5(c_3s_1 + c_1c_2s_3) - s_5(c_4(s_1s_3 - c_1c_2c_3) + c_1s_2s_4) \\
J_{17} &= c_6(s_4(s_1s_3 - c_1c_2c_3) - c_1c_4s_2) + s_6(c_5(c_4(s_1s_3 - c_1c_2c_3) + c_1s_2s_4) + s_5(c_3s_1 + c_1c_2s_3)) \\
J_{21} &= 0 \\
J_{22} &= -c_1 \\
J_{23} &= -s_1s_2 \\
J_{24} &= c_2s_1s_3 - c_1c_3 \\
J_{25} &= -s_4(c_1s_3 + c_2c_3s_1) - c_4s_1s_2 \\
J_{26} &= s_5(c_4(c_1s_3 + c_2c_3s_1) - s_1s_2s_4) - c_5(c_1c_3 - c_2s_1s_3) \\
J_{27} &= -c_6(s_4(c_1s_3 + c_2c_3s_1) + c_4s_1s_2) - s_6(c_5(c_4(c_1s_3 + c_2c_3s_1) - s_1s_2s_4) + s_5(c_1c_3 - c_2s_1s_3))
\end{aligned}
$$

$$
\begin{aligned}
J_{31} &= 1\\
J_{32} &= 0\\
J_{33} &= c_2\\
J_{34} &= s_2 s_3\\
J_{35} &= c_2 c_4 - c_3 s_2 s_4\\
J_{36} &= s_5(c_2 s_4 + c_3 c_4 s_2) + c_5 s_2 s_3\\
J_{37} &= c_6(c_2 c_4 - c_3 s_2 s_4) - s_6(c_5(c_2 s_4 + c_3 c_4 s_2) - s_2 s_3 s_5)\\
J_{41} &= 0\\
J_{42} &= -166 c_1\\
J_{43} &= -2 s_1(15 c_2 + 83 s_2 - 15)\\
J_{44} &= (503 s_1 s_3)/2 - (81 c_1 s_2)/2 - 166 c_1 c_3 - 30 s_1 s_2 s_3 - (503 c_1 c_2 c_3)/2 + 30 c_1 c_3 s_2 + 166 c_2 s_1 s_3\\
J_{45} &= (81 c_3 s_1)/2 + 30 c_4 s_1 + (81 c_1 c_2 s_3)/2 - 30 c_2 c_4 s_1 - (81 c_3 c_4 s_1)/2 - 166 c_4 s_1 s_2 - 166 c_1 s_3 s_4 -\\
&\quad - (503 c_3 s_1 s_4)/2 - (81 c_1 c_2 c_4 s_3)/2 - (503 c_1 c_2 s_3 s_4)/2 - 166 c_2 c_3 s_1 s_4 + 30 c_1 s_2 s_3 s_4 + 30 c_3 s_1 s_2 s_4\\
J_{46} &= 27 s_1 s_3 s_4 + 30 s_1 s_4 s_5 - 166 c_1 c_3 c_5 - 27 c_1 c_4 s_2 - (81 c_1 c_5 s_2)/2 + 265 c_3 s_1 s_5 + (503 c_5 s_1 s_3)/2 -\\
&\quad - (503 c_1 c_2 c_3 c_5)/2 - 27 c_1 c_2 c_3 s_4 + 30 c_1 c_3 c_5 s_2 + (81 c_1 c_4 c_5 s_2)/2 + 265 c_1 c_2 s_3 s_5 +\\
&\quad + 166 c_2 c_5 s_1 s_3 + 265 c_1 c_5 s_2 s_4 + 166 c_1 c_4 s_3 s_5 + (503 c_3 c_4 s_1 s_5)/2 +\\
&\quad + 265 c_4 c_5 s_1 s_3 - 30 c_5 s_1 s_2 s_3 - 30 c_2 s_1 s_4 s_5 - (81 c_3 s_1 s_4 s_5)/2 - (81 c_5 s_1 s_3 s_4)/2 -\\
&\quad - 166 s_1 s_2 s_4 s_5 - 265 c_1 c_2 c_3 c_4 c_5 + (81 c_1 c_2 c_3 c_5 s_4)/2 + (503 c_1 c_2 c_4 s_3 s_5)/2 + 166 c_2 c_3 c_4 s_1 s_5 -\\
&\quad - (81 c_1 c_2 s_3 s_4 s_5)/2 - 30 c_1 c_4 s_2 s_3 s_5 - 30 c_3 c_4 s_1 s_2 s_5\\
J_{47} &= 27 c_3 c_5 s_1 + (81 c_3 c_6 s_1)/2 + 30 c_4 c_6 s_1 + 27 c_1 c_2 c_5 s_3 + (81 c_1 c_2 c_6 s_3)/2 - 30 c_2 c_4 c_6 s_1 -\\
&\quad - (81 c_3 c_4 c_6 s_1)/2 - 27 c_3 c_5 c_6 s_1 - 166 c_4 c_6 s_1 s_2 - 166 c_1 c_6 s_3 s_4 - (503 c_3 c_6 s_1 s_4)/2 -\\
&\quad - 166 c_1 c_3 s_5 s_6 - 265 c_3 c_5 s_1 s_6 - 27 c_1 s_2 s_4 s_5 - 27 c_4 s_1 s_3 s_5 - (81 c_1 s_2 s_5 s_6)/2 - 30 c_5 s_1 s_4 s_6 +\\
&\quad + (503 s_1 s_3 s_5 s_6)/2 + 27 c_1 c_2 c_3 c_4 s_5 - (81 c_1 c_2 c_4 c_6 s_3)/2 - 27 c_1 c_2 c_5 c_6 s_3 - (503 c_1 c_2 c_6 s_3 s_4)/2 -\\
&\quad - 166 c_2 c_3 c_6 s_1 s_4 - (503 c_1 c_2 c_3 s_5 s_6)/2 - 265 c_1 c_2 c_5 s_3 s_6 - 166 c_1 c_4 c_5 s_3 s_6 - (503 c_3 c_4 c_5 s_1 s_6)/2 +\\
&\quad + 30 c_1 c_6 s_2 s_3 s_4 + 30 c_3 c_6 s_1 s_2 s_4 + 30 c_1 c_3 s_2 s_5 s_6 + (81 c_1 c_4 s_2 s_5 s_6)/2 + 27 c_1 c_6 s_2 s_4 s_5 +\\
&\quad + 30 c_2 c_5 s_1 s_4 s_6 + (81 c_3 c_5 s_1 s_4 s_6)/2 + 27 c_4 c_6 s_1 s_3 s_5 + 166 c_2 s_1 s_3 s_5 s_6 + 265 c_1 s_2 s_4 s_5 s_6 +\\
&\quad + 166 c_5 s_1 s_2 s_4 s_6 + 265 c_4 s_1 s_3 s_5 s_6 - 30 s_1 s_2 s_3 s_5 s_6 - (81 s_1 s_3 s_4 s_5 s_6)/2 - 27 c_1 c_2 c_3 c_4 c_6 s_5 -\\
&\quad - 265 c_1 c_2 c_3 c_4 s_5 s_6 - (503 c_1 c_2 c_4 c_5 s_3 s_6)/2 - 166 c_2 c_3 c_4 c_5 s_1 s_6 + (81 c_1 c_2 c_3 s_4 s_5 s_6)/2 +\\
&\quad + (81 c_1 c_2 c_5 s_3 s_4 s_6)/2 + 30 c_1 c_4 c_5 s_2 s_3 s_6 + 30 c_3 c_4 c_5 s_1 s_2 s_6\\
J_{51} &= 0\\
J_{52} &= -166 s_1\\
J_{53} &= 2 c_1(15 c_2 + 83 s_2 - 15)\\
J_{54} &= 30 c_1 s_2 s_3 - 166 c_3 s_1 - (81 s_1 s_2)/2 - 166 c_1 c_2 s_3 - (503 c_2 c_3 s_1)/2 - (503 c_1 s_3)/2 + 30 c_3 s_1 s_2\\
J_{55} &= 30 c_1 c_2 c_4 - 30 c_1 c_4 - 166 s_1 s_3 s_4 - (81 c_1 c_3)/2 + (81 c_1 c_3 c_4)/2 + 166 c_1 c_4 s_2 + (503 c_1 c_3 s_4)/2 +\\
&\quad + (81 c_2 s_1 s_3)/2 + 166 c_1 c_2 c_3 s_4 - 30 c_1 c_3 s_2 s_4 - (81 c_2 c_4 s_1 s_3)/2 - (503 c_2 s_1 s_3 s_4)/2 + 30 s_1 s_2 s_3 s_4
\end{aligned}
$$

$$
\begin{aligned}
J_{56} = {} & 30c_1c_5s_2s_3 - (503c_1c_5s_3)/2 - 166c_3c_5s_1 - 27c_4s_1s_2 - 27c_1s_3s_4 - (81c_5s_1s_2)/2 - 30c_1s_4s_5 - \\
& - 166c_1c_2c_5s_3 - (503c_2c_3c_5s_1)/2 - (503c_1c_3c_4s_5)/2 - 265c_1c_4c_5s_3 - 27c_2c_3s_1s_4 - 265c_1c_3s_5 + \\
& + 30c_3c_5s_1s_2 + 30c_1c_2s_4s_5 + (81c_4c_5s_1s_2)/2 + (81c_1c_3s_4s_5)/2 + \\
& + (81c_1c_5s_3s_4)/2 + 265c_2s_1s_3s_5 + 166c_1s_2s_4s_5 + 265c_5s_1s_2s_4 + 166c_4s_1s_3s_5 - 166c_1c_2c_3c_4s_5 - \\
& - 265c_2c_3c_4c_5s_1 + 30c_1c_3c_4s_2s_5 + (81c_2c_3c_5s_1s_4)/2 + (503c_2c_4s_1s_3s_5)/2 - (81c_2s_1s_3s_4s_5)/2 - \\
& - 30c_4s_1s_2s_3s_5 \\
J_{57} = {} & 30c_1c_2c_4c_6 - (81c_1c_3c_6)/2 - 30c_1c_4c_6 - 27c_1c_3c_5 + (81c_1c_3c_4c_6)/2 + 27c_1c_3c_5c_6 + \\
& + 166c_1c_4c_6s_2 + (503c_1c_3c_6s_4)/2 + 265c_1c_3c_5s_6 + 27c_2c_5s_1s_3 + \\
& + (81c_2c_6s_1s_3)/2 + 27c_1c_4s_3s_5 + 30c_1c_5s_4s_6 - 166c_6s_1s_3s_4 - \\
& - (503c_1s_3s_5s_6)/2 - 166c_3s_1s_5s_6 - 27s_1s_2s_4s_5 - (81s_1s_2s_5s_6)/2 + \\
& + 166c_1c_2c_3c_6s_4 + (503c_1c_3c_4c_5s_6)/2 + 27c_2c_3c_4s_1s_5 - 30c_1c_3c_6s_2s_4 - \\
& - (81c_2c_4c_6s_1s_3)/2 - 27c_2c_5c_6s_1s_3 - 30c_1c_2c_5s_4s_6 - (81c_1c_3c_5s_4s_6)/2 - \\
& - 27c_1c_4c_6s_3s_5 - (503c_2c_6s_1s_3s_4)/2 - 166c_1c_2s_3s_5s_6 - (503c_2c_3s_1s_5s_6)/2 - \\
& - 265c_2c_5s_1s_3s_6 - 166c_1c_5s_2s_4s_6 - 265c_1c_4s_3s_5s_6 - 166c_4c_5s_1s_3s_6 + \\
& + 30c_6s_1s_2s_3s_4 + 30c_1s_2s_3s_5s_6 + 30c_3s_1s_2s_5s_6 + (81c_4s_1s_2s_5s_6)/2 + \\
& + 27c_6s_1s_2s_4s_5 + (81c_1s_3s_4s_5s_6)/2 + 265s_1s_2s_4s_5s_6 + 166c_1c_2c_3c_4c_5s_6 - \\
& - 30c_1c_3c_4c_5s_2s_6 - 27c_2c_3c_4c_6s_1s_5 - 265c_2c_3c_4s_1s_5s_6 - (503c_2c_4c_5s_1s_3s_6)/2 + \\
& + (81c_2c_3s_1s_4s_5s_6)/2 + (81c_2c_5s_1s_3s_4s_6)/2 + 30c_4c_5s_1s_2s_3s_6 \\
J_{61} = {} & 0 \\
J_{62} = {} & 30 \\
J_{63} = {} & 0 \\
J_{64} = {} & (81c_2)/2 + 30c_3 - 30c_2c_3 - (503c_3s_2)/2 \\
J_{65} = {} & -(s_3(60c_2s_4 - 60s_4 - 81s_2 + 81c_4s_2 + 503s_2s_4))/2 \\
J_{66} = {} & 27c_2c_4 + (81c_2c_5)/2 + 30c_3c_5 + 265s_2s_3s_5 - 30c_2c_3c_5 - (81c_2c_4c_5)/2 - (503c_3c_5s_2)/2 - \\
& - 265c_2c_5s_4 - 27c_3s_2s_4 - 30c_4s_3s_5 - 265c_3c_4c_5s_2 + 30c_2c_4s_3s_5 + (81c_3c_5s_2s_4)/2 + \\
& + (503c_4s_2s_3s_5)/2 - (81s_2s_3s_4s_5)/2 \\
J_{67} = {} & 27c_5s_2s_3 + 27c_2s_4s_5 + (81c_6s_2s_3)/2 + (81c_2s_5s_6)/2 + 30c_6s_3s_4 + 30c_3s_5s_6 + 27c_3c_4s_2s_5 - \\
& - 30c_2c_6s_3s_4 - (81c_4c_6s_2s_3)/2 - 30c_2c_3s_5s_6 - 27c_5c_6s_2s_3 - \\
& - (81c_2c_4s_5s_6)/2 - 27c_2c_6s_4s_5 + 30c_4c_5s_3s_6 - (503c_6s_2s_3s_4)/2 - \\
& - (503c_3s_2s_5s_6)/2 - 265c_5s_2s_3s_6 - 265c_2s_4s_5s_6 - 30c_2c_4c_5s_3s_6 - \\
& - 27c_3c_4c_6s_2s_5 - 265c_3c_4s_2s_5s_6 - (503c_4c_5s_2s_3s_6)/2 + (81c_3s_2s_4s_5s_6)/2 + (81c_5s_2s_3s_4s_6)/2
\end{aligned}
$$

Figure B.7: Picture of Barcelona Mobile Manipulator (BMM)

B.3.4 Barcelona Mobile Manipulator

The Barcelona Mobile Manipulator (BMM) is an omnidirectional mobile platform with spherical wheels carrying a standard arm manipulator (figure B.7). The platform possesses three degrees of freedom in the plane: two independent translations and a rotation around itself. The arm manipulator used is a Kuka LWR 4+ and, as a result, BMM has ten degrees of freedom. Due to the omnidirectonality of the platform, its Jacobian is a constant matrix. The kinematic description of the platform can be found in (Clos Costa and Martínez Miralles, 2007), while the kinematic description of the Kuka LWR 4+ robot has been developed in section B.3.1.

Appendix C

Prototype Trigonometric Equations

The following list shows the main prototype trigonometric equations used in this paper. A more complete list of such kind of equations can be found in (Paul, 1981; Rieseler et al., 1990):

$$\sin(\theta) = a \Longrightarrow \theta = \text{atan2}\left(a, \pm\sqrt{1-a^2}\right) \tag{C.1}$$

$$\cos(\theta) = a \Longrightarrow \theta = \text{atan2}\left(\pm\sqrt{1-a^2}, a\right) \tag{C.2}$$

$$\left.\begin{array}{r}\sin(\theta) = a \\ \cos(\theta) = b\end{array}\right\} \Longrightarrow \theta = \text{atan2}(a, b) \tag{C.3}$$

$$a\cos(\theta) + b\sin(\theta) = 0 \Longrightarrow \left\{\begin{array}{c}\theta = \text{atan2}(-a, b) \\ \text{or} \\ \theta = \text{atan2}(a, -b)\end{array}\right. \tag{C.4}$$

$$a\cos(\theta) + b\sin(\theta) = c \Longrightarrow \theta = \text{atan2}(c, \pm\alpha) - \text{atan2}(a, b) \tag{C.5}$$
$$\text{where } \alpha = \sqrt{a^2 + b^2 - c^2}$$

$$\left.\begin{array}{r}a\cos(\theta_1) + b\cos(\theta_2) = e \\ a\sin(\theta_1) + b\sin(\theta_2) = f\end{array}\right\} \Longrightarrow \theta_1 = \text{atan2}\left(\beta, \pm\sqrt{e^2 + f^2 - \beta^2}\right) \tag{C.6}$$
$$\text{where } \beta = \frac{a^2 + e^2 + f^2 - b^2}{2a}$$

Bibliography

Abdel-Malek, K. and Othman, S. (1999). Multiple sweeping using the Denavit-Hartenberg representation method. *Computer-Aided Design*, 31(9):567 – 583.

Abdel-Malek, K., Yeh, H., and Khairallah, N. (1999). Workspace, void, and volume determination of the general 5DOF manipulator. *Mechanics of Structures and Machines*, 27(1):89 – 115.

Aboaf, E. and Paul, R. (1987). Living with the singularity of robot wrist. In *IEEE International Conference on Robotics and Automation (ICRA), Raleigh, NC, USA*, pages 1713 – 1717.

Ahuactzin, J. and Gupta, K. (1999). The kinematic roadmap: A motion planning based global approach for inverse kinematics of redundant robots. *IEEE Transactions on Robotics and Automation*, 15(4):653 – 669.

Angeles, J. (2007). *Fundamentals of Robotic and Mechanical Systems: Theory, Methods, and Algorithms*. Springer-Verlag.

Aristidou, A. (2010). *Tracking and Modelling Motion for Biomechanical Analysis*. PhD thesis, Department of Engineering – University of Cambridge.

Aristidou, A. and Lasenby, J. (2011). FABRIK: A fast, iterative solver for the Inverse Kinematics problem. *Graphical Models*, 73(5):243 – 260.

Aspragathos, A. and Dimitros, J. (1998). A comparative study of three methods for robots kinematics. *IEEE Transactions on Systems, Man, and Cybernetics*, 28(2):135 – 145.

Baillieul, J. (1986). Avoiding obstacles and resolving kinematic redundancy. In *IEEE International Conference on Robotics and Automation (ICRA), San Francisco, CA, USA*, pages 1698 – 1704.

Basañez, L. and Suárez, R. (2009). *Teleoperation*, pages 449 – 468. Springer Berlin Heidelberg.

Bayro-Corrochano, E. and Kähler, D. (2000). Motor algebra approach for computing the kinematics of robot manipulators. *Journal of Robotic Systems*, 17(9):495 – 516.

Bayro-Corrochano, E. and Kähler, D. (2001). Kinematics of robot manipulators in the motor algebra. In Sommer, G., editor, *Geometric Computing with Clifford Algebras: Theoretical Foundations and Applications in Computer Vision and Robotics*, pages 471 – 488. Springer Berlin Heidelberg, Berlin, Heidelberg.

Bedrossian, N. (1990). Classification of singular configurations for redundant manipulators. In *IEEE International Conference on Robotics and Automation (ICRA), Cincinnati, OH, USA*, pages 818 – 823.

Bedrossian, N. and Flueckiger, K. (1991). Characterizing spatial redundant manipulator singularities. In *IEEE International Conference on Robotics and Automation (ICRA), Sacramento, CA, USA*, pages 714 – 719.

Bohigas, O. (2013). *Numerical Computation and Avoidance of Manipulator Singularities*. PhD thesis, Institute of Robotics and Industrial Informatics – Universitat Politècnica de Catalunya - BarcelonaTech.

Bruyninckx, H. (2010). *Robot Kinematics and Dynamics*. Katholieke Universiteit Leuven, Belgium.

Buhmiler, S., Krejic, N., and Luzanin, Z. (2010). Practical quasi-Newton algorithms for singular nonlinear systems. *Numerical Algorithms*, 55(4):481 – 502.

Burdick, J. (1989). On the inverse kinematics of redundant manipulators: Characterization of the self-motion manifolds. In *IEEE International Conference on Robotics and Automation (ICRA), Scottsdale, AZ, USA*, pages 264 – 270.

Buss, S. (2009). *Introduction to inverse kinematics with Jacobian transpose, pseudoinverse and Damped Least Squares methods.* Technical report, University of California, San Diego.

Buss, S. and Kim, J. (2005). Selectively Damped Least Squares for inverse kinematics. *Journal of Graphics Tools*, 10(3):37 – 49.

Cameron, J. (2008). *Aspects of Conformal Geometric Algebra with Applications in Motion Capture*. PhD thesis, Department of Engineering – University of Cambridge.

Campos-Macías, L., Carbajal-Espinosa, O., Loukianov, A., and Bayro-Corrochano, E. (2017). Inverse kinematics for a 6-DOF walking humanoid robot leg. *Advances in Applied Clifford Algebras*, 27(1):581 – 597.

Castellet, M. and Llerena, I. (1996). *Álgebra lineal y geometría*. Reverté.

Chai, X. and Li, Q. (2017). Analytical mobility analysis of Bennett linkage using geometric algebra. *Advances in Applied Clifford Algebras*, 27(3):2083 – 2095.

Chai, X. and Xiang, J. (2016). Mobility analysis of limited-degrees-of-freedom parallel mechanisms in the framework of geometric algebra. *ASME Journal of Mechanisms and Robotics*, 8(4):41005 – 41005/9.

Chang, K. and Khatib, O. (1995). Manipulator control at kinematic singularities: A dynamically consistent strategy. In *IEEE/RSJ International Conference on Intelligent Robots and Systems (IROS), Pittsburgh, PA, USA*, pages 84 – 88.

Chang, P. (1987). A closed-form solution for inverse kinematics of robot manipulators with redundancy. *IEEE Journal on Robotics and Automation*, 3(5):393 – 403.

Cheng, F., Chen, T., and Kung, F. (1998). Study and resolution of singularities for a 7DoF redundant manipulator. *IEEE Transactions on Industrial Electronics*, 45(3):469 – 480.

Cheng, F., Hour, T., Sun, Y., and Chen, T. (1997). Study and resolution of singularities for a 6DoF PUMA manipulator. *IEEE Transactions on Systems, Man, and Cybernetics*, 27(2):332 – 343.

Cheng, Y., Huang, Q., and Zhang, W. (2010). Kinematic analysis and solution of the natural posture of 7DoF humanoid manipulator. In *International Conference on Automation and Logistics (ICAL), Hong Kong and Macau, China*, pages 156 – 162.

Chevallereau, C. (1996). Feasible trajectories for a nonredundant robot at a singularity. In *IEEE International Conference on Robotics and Automation (ICRA), Minneapolis, MN, USA*, pages 1871 – 1876.

Chiaverini, S. and Egeland, O. (1990). A solution to the singularity problem for six-joint manipulators. In *IEEE International Conference on Robotics and Automation (ICRA), Cincinnati, OH, USA*, pages 644 – 649.

Clifford, W., Smith, H., and Tucker, R. (1882). *Mathematical Papers by William Kingdon Clifford – Edited*. Macmillan London.

Clos Costa, D. and Martínez Miralles, J. (2007). *Plataforma Mòbil amb Rodes Esfèriques per al Robot "Lightweight Robot 4" de Kuka Roboter*. Technical report, Institute of Industrial and Control Engineering – Universitat Politècnica de Catalunya - BarcelonaTech.

Corrochano, E. B. and Sobczyk, G. (2001). Applications of lie algebras and the algebra of incidence. In Corrochano, E. and Sobczyk, G., editors, *Geometric Algebra with Applications in Science and Engineering*, pages 252 – 277. Birkhäuser Boston, Boston, MA.

Craig, J. (1989). *Introduction to Robotics: Mechanics and Control*. Addison-Wesley Longman Publishing Company.

Davidson, J. and Hunt, K. (2004). *Robots and Screw Theory: Applications of Kinematics and Statics to Robotics*. Oxford University Press.

De Luca, A. and Oriolo, G. (1991a). The reduced gradient method for solving redundancy in robot arms. *RoboterSysteme*, 7:117 – 122.

De Luca, A. and Oriolo, G. (1991b). Reduced gradient method for solving redundancy in robot arms. In *Triennial World Congres of the International Federation of Automatic Control (IFAC), Tallinn, USSR*, pages 133 – 138.

De Luca, A., Oriolo, G., and Giordano, P. R. (2006). Kinematic modeling and redundancy resolution for nonholonomic mobile manipulators. In *IEEE International Conference on Robotics and Automation (ICRA), Orlando, FL, USA*, pages 1867 – 1873.

Denavit, J. and Hartenberg, R. S. (1965). A kinematic notation for lower-pair mechanisms based on matrices. *Journal of Applied Mechanics*, 22(2):215 – 221.

Diankov, R. (2010). *Automated Construction of Robotics Manipulation Programs*. PhD thesis, Robotics Institute, Carnegie Mellon University.

Dong, H., Du, Z., and Chirikjian, G. (2013). Workspace density and inverse kinematics for planar serial revolute manipulators. *Mechanism and Machine Theory*, 70:508 – 522.

Doran, C. and Lasenby, A. (2003). *Geometric Algebra for Physicists*. Cambridge University Press.

Drexler, D. (2016). Solution of the closed-loop inverse kinematics algorithm using the Crank-Nicolson method. In *IEEE International Symposium on Applied Machine Intelligence and Informatics (SAMI), Herlany, Slovakia*, pages 351 – 356.

Edwards, C. (1973). *Advanced Calculus of Several Variables*. Dover Books on Mathematics Series. Dover Publications.

Fang, Y. and Tsai, L. (2003). Feasible motion solutions for serial manipulators at singular configurations. *Journal of Mechanical Design*, 125(1):61 – 69.

Favieri, L. (2008). *Introducción a los Cuaterniones*. Technical report, Creative Commons.

Fratu, A., Vermeiren, L., and Dequidt, A. (2010). Using the redundant inverse kinematics system for collision avoidance. In *International Symposium on Electrical and Electronics Engineering (ISEEE), Galati, Romania*, pages 88 – 93.

Freund, E. and Weber, H. (1985). *Robotertechnologie I*. Vorlensungsskript.

Gottlieb, D. (1986). Robots and topology. In *IEEE International Conference on Robotics and Automation (ICRA), San Francisco, CA, USA*, pages 1689 – 1691.

Goyal, K. and Sethi, D. (2010). An analytical method to find workspace of a robotic manipulator. *Journal of Mechanical Engineering*, 41(1):25 – 30.

Grassmann, H. (2000). *Ausdehnungslehre – English Reedition*. American Mathematical Society.

Gupta, K. and Roth, B. (1982). Design considerations for manipulator workspace. *ASME. Journal of Mechanical Design*, 104(4):704 – 711.

Haug, E., Luh, C., Adkins, F., and Wang, J. (2000). Numerical algorithms for mapping boundaries of manipulator workspaces. *Journal of Mechanical Design*, 118(2):228 – 234.

Heiss, H. (1985). *Die explizite Lösung der Kinematischen Gleichung für eine Klasse von Industrierobotern*. PhD thesis, Technische Universität München (TUM).

Heiss, H. (1993). Redundancy resolution for an eight-axis manipulator. In *Computational Kinematics, Scholss Dagstuhl, Germany*, pages 55 – 66. Springer Netherlands.

Hemami, A. (1988). A more general closed-form solution to the inverse kineamatics of mechanical arms. *Advanced Robotics of the Robotics Society of Japan*, 2(4):315 – 325.

Hijazi, A., Bretheé, J., and Lefebvre, D. (2016). Singularity analysis of a planar robotic manipulator: Application to an XY-Theta platform. *Mechanism and Machine Theory*, 100:104 – 119.

Hildenbrand, D., Zamora, J., and Bayro-Corrochano, E. (2008). Inverse kinematics computation in computer graphics and robotics using conformal geometric algebra. *Advances in Applied Clifford Algebras*, 18(3):699–713.

Hollerbach, J. (1985). Optimum kinematic design for a seven degree of freedom manipulator. In *Robotics Research: The Second International Symposium, Yyoto, Japan*, pages 215 – 222. MIT Press.

Hrdina, J., Návrat, A., and Vašík, P. (2017). CGA-based robotic snake control. *Advances in Applied Clifford Algebras*, 27(1):621 – 632.

Hsu, P., Hauser, J., and Sastry, S. (1988). Dynamic control of redundant manipulators. In *American Control Conference, Atlanta, GA, USA*, pages 2135 – 2139.

Huang, L. and Jiang, R. (2013). A new method of inverse kinematics solution for industrial 7DoF robot. In *32nd Chinese Control Conference (CCC), Xi'an, China*, pages 6063 – 6065.

Huang, Y., Yong, Y. S., Chiba, R., Arai, T., Ueyama, T., and Ota, J. (2016). Kinematic control with singularity avoidance for teaching-playback robot manipulator system. *IEEE Transactions on Automation Science and Engineering*, 13(2):729–742.

Hueso, J., Martínez, E., and Torregrosa, J. (2009). Modified Newton's method for systems of nonlinear equations with singular Jacobian. *Journal of Computational and Applied Mathematics*, 224(1):77 – 83.

Huo, X., Sun, T., and Song, Y. (2017). A geometric algebra approach to determine motion/-constraint, mobility and singularity of parallel mechanism. *Mechanism and Machine Theory*, 116:273 – 293.

Ivlev, O. and Gräser, A. (1997). An analytical method for the inverse kinematics of redundant robots. In *International Conference Advanced Robotics, Intelligent Automation and Active Systems, Bremen, Germany*, pages 416 – 421.

Ivlev, O. and Gräser, A. (1998). Resolving redundancyof series kinematic chains through imaginary links. In *International Conference on Computational Engineering in Systems Applications (CESA98), Nabeul- Hammamet, Tunisia*, pages 477 – 482.

José, J. and Saletan, E. J. (1998). *Classical Dynamics: A Contemporary Approach*. Cambridge University Press.

Judd, R. and Van Til, R. (1985). A perfomance measure for computing the reverse kinematic solution for robots with redundant degrees of freedom. In *International Conference on Decision and Control, Fort Lauderdale, FL, USA*, pages 360 – 361.

Jung, D., Yoo, Y., Koo, J., Song, M., and Won, S. (2011). A novel redundancy resolution method to avoid joint limits and obstacles on anthropomorphic manipulator. In *Society of Instrument and Control Engineers (SICE) Annual Conference, Tokyo, Japan*, pages 924 – 929.

Kanaan, D., Wenger, P., Caro, S., and Chablat, D. (2009). Singularity analysis of lower mobility parallel manipulators using Grassmann–Cayley algebra. *IEEE Transactions on Robotics*, 25(5):995 – 1004.

Kauschke, M. (1996). Closed form solutions applied to redundant serial link manipulators. *Mathematics and Computers in Simulation*, 41(5):509 – 516.

Khatib, O. (1987). A unified approach for motion and force control of robot manipulators: The operational space formulation. *International Journal of Robotics and Automation*, 3(1):43 – 51.

Kieffer, J. (1994). Differential analysis of bifurcations and isolated singularities for robots and mechanisms. *IEEE Transactions on Robotics and Automation*, 10(1):1 – 10.

Kim, J. S., Jeong, J. H., and Park, J. H. (2015a). Inverse kinematics and geometric singularity analysis of a 3-SPS/S redundant motion mechanism using conformal geometric algebra. *Mechanism and Machine Theory*, 90:23 – 36.

Kim, J. S., Jeong, J. H., and Park, J. H. (2015b). Inverse kinematics of a redundant manipulator based on conformal geometry using geometric approach. In *12th International Conference on Informatics in Control, Automation and Robotics (ICINCO), Colmar, France*, pages 179 – 185.

Kircanski, M. (1993). Symbolical singular value decomposition for 7DoF manipulator and its application to robot control. In *IEEE International Conference on Robotics and Automation (ICRA), Atlanta, GA, USA*, pages 895 – 900.

Kircanski, M. and Petrovic, T. (1991). Inverse kinematic solution for a 7DOF robot with minimal computational complexity and singularity avoidance. In *IEEE International Conference on Robotics and Automation (ICRA), Sacramento, CA, USA*, pages 2664 – 2669.

Kleppe, A. and Egeland, O. (2016). Inverse kinematics for industrial robots using conformal geometric algebra. *Modeling, Identification and Control*, 37(1):63 – 75.

Kucuck, S. and Bingul, Z. (2005). The inverse kinematics solutions of fundamental robot manipulators with offset wrist. In *IEEE International Conference on Mechatronics (ICM), Taipei, Taiwan*, pages 197 – 202.

Kucuk, S. and Bingul, Z. (2014). Inverse kinematics solutions for industrial robot manipulators with offset wrists. *Applied Mathematical Modelling*, 38(7):1983 – 1999.

Lasenby, A., Lasenby, J., and Wareham, R. (2004). *A covariant approach to geometry using geometric algebra*. Technical report, Department of Engineering – University of Cambridge.

Lau, H. and Wai, L. (2002). A Jacobian-based redundant control strategy for 7DOF WAM. In *Proceedings of the Conference on Control, Automation, Robotics and Vision (ICARV), Singapore*, pages 1060 – 1065.

LaValle, S. M. (2006). *Planning Algorithms*. Cambridge University Press.

Lee, S. and Bejczy, A. (1991). Redundant arm kinematic control based on parametrization. In *IEEE International Conference on Robotics and Automation, Sacramento, CA, USA*, pages 458 – 465.

Lee, T. and Yang, D. (1983). On the evaluation of manipulator workspace. *ASME Journal of Mechanisms, Transmissions, and Automation in Design*, 105(1):70 – 77.

Lin, Y. and Min, H. (2015). Inverse kinematics of modular manipulator robot with shoulder offset based on geometric method mixed with analytical method algorithm. In *IEEE International Conference on Cyber Technology in Automation, Control, and Intelligent Systems (CYBER), Shenyang, China*, pages 1198 – 1203.

Liu, Y., Wang, D., Sun, J., Chang, L., Ma, C., Ge, Y., and Gao, L. (2015). Geometric approach for inverse kinematics analysis of 6-DOF serial robot. In *IEEE International Conference on Information and Automation, Lijiang, China*, pages 852 – 855.

Lloyd, J. (1998). Removing singularities of serial manipulators by transforming the workspace. In *IEEE International Conference on Robotics and Automation (ICRA), Leuven, Belgium*, pages 2935 – 2940.

Lovass-Nagy, V. and Schilling, R. (1987). Control of kinematically redundant robots using {1}-inverses. *IEEE Transactions on Systems, Man, and Cybernetics*, 17(4):644 – 649.

Luh, J. and Gu, Y. (1985). Industrial robots with seven joints. In *IEEE International Conference on Robotics and Automation (ICRA), St. Louis, MO, USA*, pages 1010–1015.

Manocha, D. and Canny, J. (1994). Efficient inverse kinematics for general 6R manipulators. *IEEE Transactions on Robotics and Automation*, 10(5):648 – 657.

Munkres, J. (2000). *Topology*. Featured Titles for Topology Series. Prentice Hall, Incorporated.

Murray, R., Li, Z., and Shankar Sastry, S. (1994). *A Mathematical Introduction to Robotic Manipulation*. CRC Press.

Nakamura, Y. and Hanafusa, H. (1986). Inverse kinematic solutions with singularity robustness for robot manipulator control. *Journal of Dynamic Systems, Measurement, and Control*, 108(3):163 – 171.

Nenchev, D. (1989). Redundancy resolution through local optimization: A review. *Journal of Robotics Systems*, 6(6):769 – 798.

Nenchev, D. and Uchiyama, M. (1995). Singularity-consistent path tracking: A null space based approach. In *IEEE International Conference on Robotics and Automation (ICRA), Nagoya, Japan*, pages 2482 – 2489.

Oetomo, D. (2004). *Singularity Analysis and Handling Towards Mobile Manipulation*. PhD thesis, National University of Singapore.

Oetomo, D. and Ang Jr, M. (2009). Singularity robust algorithm in serial manipulators. *Robotics and Computer-Integrated Manufacturing*, 25(1):122 – 134.

Oetomo, D., Ang Jr, M., and Lim, T. (2002). Singularity robust manipulator control using virtual joints. In *IEEE International Conference on Robotics and Automation (ICRA), Washington DC, USA*, pages 2418 – 2423.

Oetomo, D. and Lim, S. (2001). Singularity handling on PUMA in operational space formulation. *Experimental Robotics VII: Lecture Notes in Control and Information Sciences*, 271:491 – 500.

O'Neil, K., Chen, Y., and Seng, J. (1997). Removing singularities of resolved motion rate control of mechanisms, including self-motion. *IEEE Transactions on Robotics and Automation*, 13(5):741 – 751.

Pan, H., Fu, B., Chen, L., and Feng, J. (2012). The inverse kinematics solutions of robot manipulators with offset wrist using the offset modification method. In *Selected Papers from the International Conference on Automation and Robotics (ICAR 2011): Advances in Automation and Robotics, Vol.1*, pages 655 – 663. Springer Berlin Heidelberg.

Paul, R. (1981). *Robot Manipulators: Mathematics, Programming and Control*. The MIT Press.

Pieper, D. (1968). *The Kinematics of Manipulation under Computer Control*. PhD thesis, Stanford Artificial Intelligence Laboratory – Stanford University.

Podhorodeski, R., Goldenberg, A., and Fenton, R. (1991). Resolving redundant manipulator joint rates and indentifying special arm configurations using Jacobian null-space bases. *IEEE Transactions on Robotics and Automation*, 7(5):607 – 618.

Porges, O., Stouraitis, T., Borst, C., and Roa, M. (2013). Reachability and capability analysis for manipulation tasks. In *ROBOT2013: First Iberian Robotics Conference: Advances in Robotics*, pages 703 – 718. Springer International.

Pozna, C., Horváth, E., and Hollósi, J. (2016). The inverse kinematics problem, a heuristical approach. In *IEEE International Symposium on Applied Machine Intelligence and Informatics (SAMI), Herlany, Slovakia*, pages 299 – 304.

Qingmei, M., Pengcheng, W., Jiaming, D., Huiping, S., and Minzhou, L. (2015). An algorithm of inverse kinematics for manipulator with redundancy. In *IEEE International Conference on Cyber Technology in Automation, Control, and Intelligent Systems (CYBER), Shenyang, China*, pages 54 – 58.

Rieseler, H., Schrake, H., and Wahl, F. (1990). Symbolic computation of closed form solutions with prototype equations. In *International Workshop on Advances in Robot Kinematics, Linz, Austria*, pages 343 – 351.

Sangwine, S. and Hitzer, E. (2017). Clifford Multivector Toolbox (for MATLAB). *Advances in Applied Clifford Algebras*, 27(1):539 – 558.

Sariyildiz, E. and Temeltas, H. (2009). Solution of inverse kinematic problem for serial robot using quaternions. In *IEEE/ASME International Conference on Advanced Intelligent Mechatronics (AIM), Singapore*, pages 26 – 31.

Schinstock, D. (1998). Approximate solutions to unreachable commands in teleoperation of a robot. *Robotics and Computer-Integrated Manufacturing*, 14(3):219 – 227.

Schrake, H., Rieseler, H., and Wahl, F. (1990). Symbolic kinematics inversion of redundant robots. In *International Symposium on Foundations of Robotics, Berlin, Germany*, pages 1 – 10.

Schrake, H., Rieseler, H., and Wahl, F. (1991). Manipulator classification by means of a kinematics description language. In *International Conference on Advanced Robotics (ICAR), Pisa, Italy*, pages 678 – 682.

Schwartz, E. and Doty, K. (1988). Derivation of redundant wrist manipulators to avoid interior workspace singularities. In *International Conference SouthEastCon, Knoxville, TN, USA*, pages 403 – 407.

Selig, J. M. (2001). Robot kinematics and flags. In Corrochano, E. and Sobczyk, G., editors, *Geometric Algebra with Applications in Science and Engineering*, pages 211 – 234. Birkhäuser Boston, Boston, MA.

Seng, J., O'Neil, K., and Chen, Y. (1995). Escapability of singular configuration for redundant manipulators via self-motion. In *IEEE/RSJ International Conference on Intelligent Robots and Systems (IROS), Pittsburgh, PA, USA*, pages 78 – 83.

Shamir, T. (1990). The singularities of redundant robot arms. *The International Journal of Robotics Research*, 9(1):113 – 121.

Shimizu, M., Kakuya, H., Yoon, W., Kitagaki, K., and Kosuge, K. (2008). Analytical inverse kinematic computation for 7-DoF redundant manipulator with joint limits and its application to redundancy resolution. *IEEE Transactions on Robotics*, 24(5):1131 – 1142.

Siciliano, B. and Khatib, O. (2008). *Springer Handbook of Robotics*. Springer-Verlag.

Siciliano, B., Sciavicco, L., Villani, L., and Oriolo, G. (2008). *Robotics: Modelling, Planning and Control*. Springer Publishing Company.

Singh, G. and Claassens, J. (2010). An analytical solution for the inverse kinematics of a redundant 7DoF manipulator with link offsets. In *IEEE/RSJ International Conference on Intelligent Robots and Systems (IROS), Taipei, Taiwan*, pages 2976 – 2982.

Spong, M., Hutchinson, S., and Vidyasagar, M. (2006). *Robot Modeling and Control*. John Wiley and Sons.

Stanisic, M. and Pennock, G. (1985). A nondegenerate kinematic solution of a seven-jointed robot manipulator. *International Journal of Robotics Research*, 4(2):10 – 20.

Strang, G. (1980). *Linear Algebra and its Application*. New York: Academic.

Sung, Y., Cho, D., and Chung, M. (1996). A constrained optimization approach to resolving manipulator redundancy. *Journal of Robotics Systems*, 13(5):275 – 288.

Taki, S. and Nenchev, D. (2014). A novel singularity-consistent inverse kinematics decomposition for S-R-S type manipulators. In *IEEE International Conference on Robotics and Automation (ICRA), Hong Kong, China*, pages 5070 – 5075.

Tanev, T. K. (2006). Singularity analysis of a 4-DOF parallel manipulator using geometric algebra. In Lennarčič, J. and Roth, B., editors, *Advances in Robot Kinematics: Mechanisms and Motion*, pages 275 – 284. Springer Netherlands, Dordrecht.

Tatum, R., Lucas, D., Weaver, J., and Perkins, J. (2015). Geometrically motivated inverse kinematics for an arm with 7 degrees of freedom. In *MTS/IEEE OCEANS, Washington DC, USA*, pages 1 – 6.

Tchoń, K. and Muszyński, R. (1997). Singularities of nonredundant robot kinematics. *The International Journal of Robotics Research*, 16(1):60 – 76.

Tokarz, K. and Kieltyka, S. (2010). Geometric approach to inverse kinematics for arm manipulator. In *WSEAS International Conference on Systems: Part of the 14th WSEAS CSCC Multiconference - Volume II, Corfu Island, Greece*, pages 682 – 687.

Tørdal, S., Hovland, G., and Tyapin, I. (2017). Efficient implementation of inverse kinematics on a 6-DOF industrial robot using conformal geometric algebra. *Advances in Applied Clifford Algebras*, 27(3):2067–2082.

Tsai, L. (1999). *Robot Analysis: The Mechanics of Serial and Parallel Manipulators*. John Wiley and Sons.

Vaezi, M., Samavati, F., Jazeh, H., and Moosavian, S. (2011). Singularity analysis of 6DoF Stäubli TX40 robot. In *International Conference on Mechatronics and Automation (ICMA), Beijing, China*, pages 446 – 451.

Vahrenkamp, N., Muth, D., Kaiser, P., and Asfour, T. (2015). IK-Map: An enhanced workspace representation to support inverse kinematics solvers. In *IEEE-RAS International Conference on Humanoid Robots (Humanoids), Seoul, South Korea*, pages 785 – 790.

Wampler, C. (1986). Manipulator inverse kinematic solutions based on vector formulations and damped least-squares methods. *IEEE Transactions on Systems, Man, and Cybernetics*, 16(1):93 – 101.

Wang, W., Suga, Y., Iwata, H., and Sugano, S. (2012). Solve inverse kinematics through a new quadratic minimization technique. In *IEEE/ASME International Conference on Advanced Intelligent Mechatronics (AIM), Kachsiung, Taiwan*, pages 306 – 313.

Waziri Yusuf, M., Wah June, L., and Abu Hassan, M. (2011). Jacobian-free diagonal Newton's method for solving nonlinear systems with singular Jacobian. *Malaysian Journal of Mathematical Sciences*, 5(2):241 – 255.

Wei, Y., Jian, S., He, S., and Wang, Z. (2014). General approach for inverse kinematics of nR robots. *Mechanism and Machine Theory*, 75:97 – 106.

Wu, M., Kung, Y. S., Lee, F. C., and Chen, W. C. (2015). Inverse kinematics of robot manipulators with offset wrist. In *International Conference on Advanced Robotics and Intelligent Systems (ARIS), Taipei, Taiwan*, pages 1 – 6.

Xambó-Descamps, S. (2016). Álgebra geométrica y geometrías ortogonales. *La Gaceta de la RSME*, 19(3):559 – 588.

Xambó-Descamps, S. (2017). *Real Spinorial Groups – a Short Mathematical Introduction*. SR-MA/Springerbrief. Springer.

Xia, J., Jiang, Z., Liu, H., and Cai, H. (2014). Analytical inverse kinematic computation for anthropomorphic manipulator based on human-like motion optimization and maximum reachable region optimization. In *IEEE International Conference on Robotics and Biomimetics (ROBIO), Bali, Indonesia*, pages 2292 – 2297.

Xu, W., Zhang, J., Liang, B., and Li, B. (2016). Singularity analysis and avoidance for robot manipulators with nonspherical wrists. *IEEE Transactions on Industrial Electronics*, 63(1):277 – 290.

Yang, D. and Lee, T. (1983). On the workspace of mechanical manipulators. *ASME Journal of Mechanisms, Transmissions, and Automation in Design*, 105(1):62 – 69.

Yao, H., Chen, Q., Chai, X., and Li, Q. (2017). Singularity analysis of 3-RPR parallel manipulators using geometric algebra. *Advances in Applied Clifford Algebras*, 27(3):2097 – 2113.

Yong, Y., Huang, Y., Chiba, R., Arai, T., Ueyama, T., and Ota, J. (2013). Teaching-playback robot manipulator system in consideration of singularities. In *IEEE/ASME International Conference on Advanced Intelligent Mechatronics (AIM), Wollongong, NSW, Australia*, pages 453 – 458.

Yu, C., Jin, M., and Liu, H. (2012). An analytical solution for inverse kinematic of 7-DOF redundant manipulators with offset-wrist. In *IEEE International Conference on Mechatronics and Automation, Chengdu, China*, pages 92 – 97.

Zamora, J. and Bayro-Corrochano, E. (2004). Inverse kinematics, fixation and grasping using conformal geometric algebra. In *IEEE/RSJ International Conference on Intelligent Robots and Systems (IROS), Sendai, Japan*, pages 3841 – 3846.